



TECHNISCHE  
UNIVERSITÄT  
WIEN  
Vienna University of Technology

## **Dissertation**

# **SUGAR ALCOHOLS AND OTHER ORGANIC COMPOUNDS AS PHASE CHANGE MATERIALS**

ausgeführt zum Zwecke der Erlangung des akademischen Grades eines Doktors der  
Naturwissenschaften unter der Leitung von

**Associate Prof. Dr. Michael Schnürch**

**Institut für Angewandte Synthesechemie, E163**

eingereicht an der Technischen Universität Wien

**Fakultät für Technische Chemie**

Von

**M.Sc. Yago Magan Montoto**

Burggasse 102/6

1070 Wien

Wien, 03.09.2018

# Acknowledgements

## Abstract

The objective of this thesis was the synthesis and modification of novel phase-change materials (PCMs) which are able to absorb a high amount of energy at the time of melting and release it upon recrystallization. Organic compounds as PCMs are very interesting as a result of their high storage capacity, safety and low cost. Additionally, they are able to cover an interesting range of melting temperatures. There is a large number of PCMs that change their phase in a range of 80 °C to 200 °C. Thus, the use of latent heat storage systems using organic PCMs has a promising future for industrial applications at medium temperatures.

It was possible to obtain better organic materials for thermal storage devices and improve their melting energy and thermal stability among other properties by studying and comparing their structures and identifying trends. This resulted in an efficient design of a new class of organic Phase-change materials (PCMs) which are able to store up to 375.6 kJ/kg in the predefined temperature range of 80 °C to 200 °C. Beyond their relatively high storage capacity, these materials display advantages regarding safety and low-cost production.

Within this thesis, the melting enthalpy and melting temperature for different groups of organic PCMs was compared based on their structure. Additionally, DSC measurements combined with thermal stability TGA analysis of these compounds was carried out.

## Kurzfassung

Das Ziel dieser Arbeit war die Synthese und Modifikation von neuartigen Phase-Change-Materialien (PCMs), die in der Lage sind, eine hohe Energiemenge während des Schmelzvorgangs aufzunehmen und bei Rekristallisation wieder freizusetzen. Organische Verbindungen sind als PCMs aufgrund ihrer hohen Speicherkapazität, Sicherheit und niedrigen Kosten sehr interessant. Darüber hinaus sind sie in der Lage, einen interessanten Bereich an Schmelztemperaturen abzudecken. Es gibt eine große Anzahl von PCMs, die ihre Phase in einem Bereich von 80 °C bis 200 °C ändern. Der Einsatz von organischen PCMs für Latentwärmespeichersysteme hat daher eine vielversprechende Zukunft für industrielle Anwendungen bei mittleren Temperaturen.

Es war möglich, verbesserte organische Materialien für thermische Speicher zu erhalten. Unter anderen konnten Schmelzenergie und thermische Stabilität durch eine Analyse und einen Vergleich der chemischen Strukturen sowie die Identifizierung von Trends verbessert werden. Dadurch wurde es ermöglicht eine neue Klasse von organischen Phase-Change-Materialien (PCMs) zu designen, die bis zu 375,6 kJ/kg im vordefinierten Temperaturbereich von 80 °C bis 200 °C speichern können. Neben ihrer relativ hohen Lagerkapazität weisen diese Materialien Vorteile hinsichtlich Sicherheit und kostengünstiger Produktion auf.

Innerhalb dieser Arbeit wurde Schmelzenthalpie und Schmelztemperatur für verschiedene Gruppen von organischen PCMs basierend auf ihrer Struktur verglichen. Zusätzlich wurde für diese Verbindung DSC-Messungen in Kombination mit einer TGA-Analyse zur Bestimmung der thermischen Stabilität durchgeführt.



# Contents

Acknowledgements .....	2
Abstract .....	3
Kurzfassung .....	4
Synthetic schemes.....	10
Abbreviations .....	18
1. Introduction.....	21
1.1 Thermal energy storage systems (TES) .....	21
1.1.1 System types.....	22
1.1.1.1 Thermo-chemical heat storage (THS) .....	22
1.1.1.2 Sensible heat storage (SHS).....	23
1.1.1.3 Latent heat storage (LHS).....	24
1.2 Phase-change materials .....	26
1.2.1 Inorganic phase change materials .....	27
1.2.1.1 Salt hydrates .....	27
1.2.1.2 Other salt compositions .....	29
1.2.1.3 Metals and metal alloys .....	30
1.2.2 Eutectic mixtures .....	31
1.2.3 Organic phase change materials.....	32
1.2.3.1 Paraffins .....	32
1.2.3.2 Non-paraffins.....	34
1.2.4 Recent PCM advancements.....	35
1.2.4.1 PCM capsules.....	35
1.2.4.2 PCM Composites.....	36
1.3 Melting points and energy .....	37
1.3.1 Hydrogen bonding .....	37
1.3.2 Van der Waals forces .....	38
1.4 Thermoanalytical techniques .....	39
1.4.1 Differential scanning calorimetry (DSC).....	40
1.4.2 Thermogravimetric analysis (TGA).....	41
2. Results and discussion .....	42

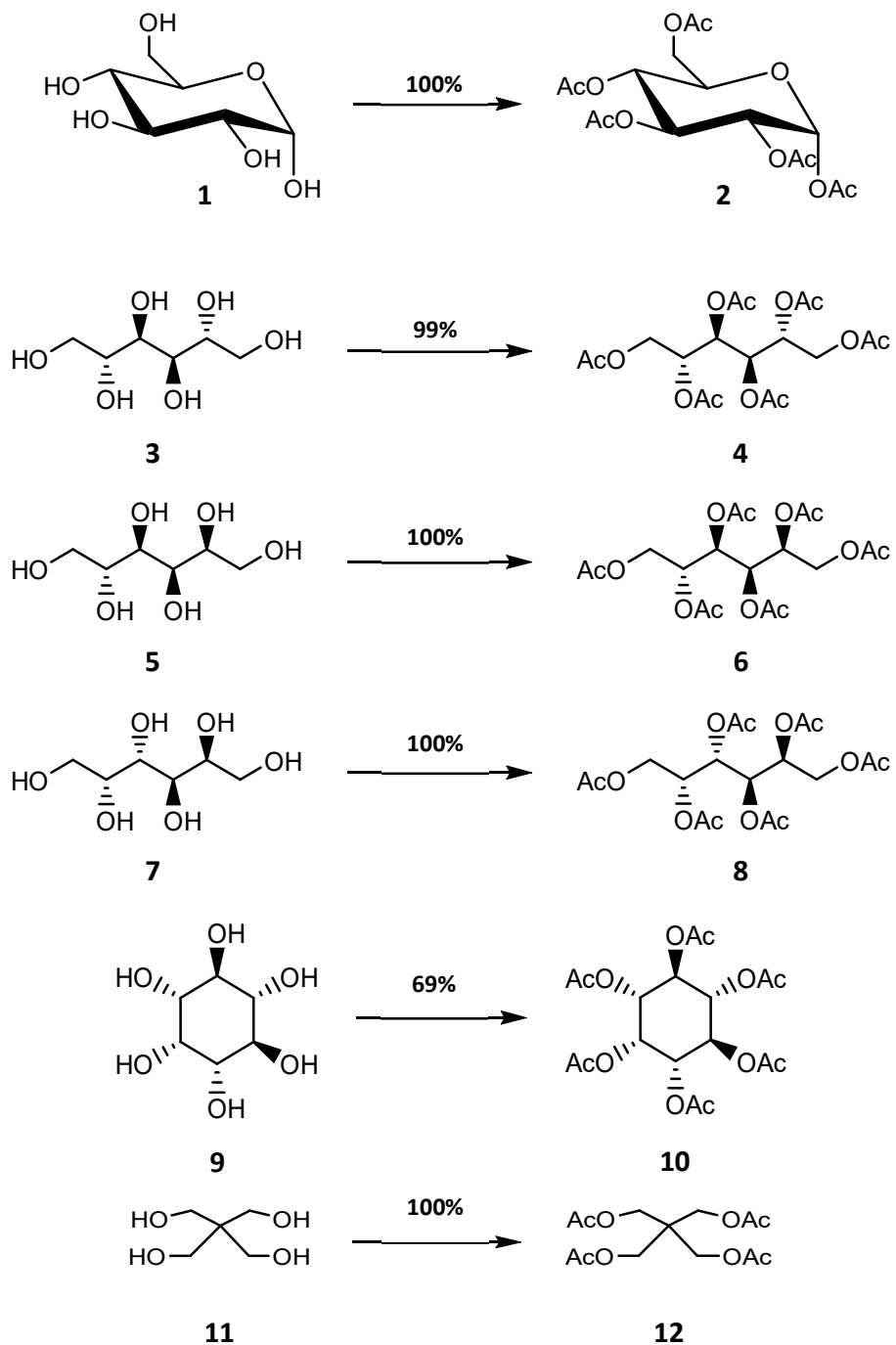
2.1	Towards sugars and derivatives .....	42
2.1.1	General considerations .....	42
2.1.2	Sugar alcohols.....	43
2.1.3	Acetylated sugars.....	53
2.1.4	Sugar acids and derivatives .....	56
2.1.5	Other sugars .....	59
2.2	Towards arenes .....	62
2.3	Towards amino acids .....	66
2.4	Towards purines and pyrimidines.....	69
2.5	Towards dyes.....	72
2.6	Towards other organic compounds .....	74
2.7	Towards fatty acids .....	76
2.8	Towards carboxylic acids and derivatives .....	79
2.8.1	Dicarboxylic acids.....	79
2.8.2	Aliphatic- $\alpha,\omega$ -diamides .....	85
2.8.3	Diamide derivatives .....	92
2.8.4	Other acids .....	97
2.9	Towards 3,6-diazaoctane-1,8-diol and derivatives.....	99
3.	Conclusions .....	110
4.	Experimental .....	112
4.1	General notes .....	112
4.2	Preparation of acetylated sugar derivatives .....	113
4.2.1	General procedure A.....	113
4.2.2	Synthesis of 1,2,3,4,6-penta-O-acetyl-D-glucopyranose <sup>[101,102,107]</sup> .....	114
4.2.3	Synthesis of 1,2,3,4,5,6-hexa-O-acetyl-D-mannitol <sup>[101,102]</sup> .....	115
4.2.4	Synthesis of 1,2,3,4,5,6-hexa-O-acetyl-D-glucitol <sup>[101,102]</sup> .....	116
4.2.5	Synthesis of 1,2,3,4,5,6-hexa-O-acetyl-D-galactitol <sup>[101,102]</sup> .....	117
4.2.6	Synthesis of 1,2,3,4,5,6-hexa-O-acetyl-myo-inositol <sup>[101,102,114]</sup> .....	118
4.2.7	Synthesis of pentaerythritol tetraacetate <sup>[101,102]</sup> .....	119
4.3	Preparation of mucic acid derivatives.....	120
4.3.1	General procedure B.....	120
4.3.2	Synthesis of dimethyl galactarate <sup>[103]</sup> .....	121
4.3.3	Synthesis of diethyl galactarate <sup>[104]</sup> .....	122

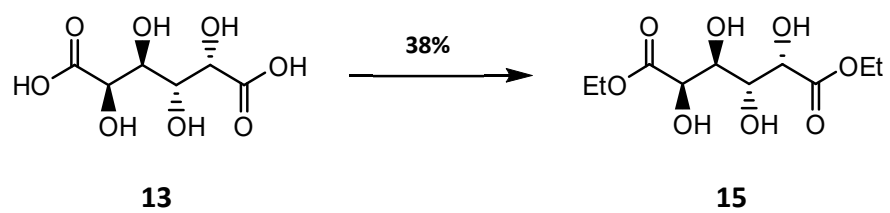
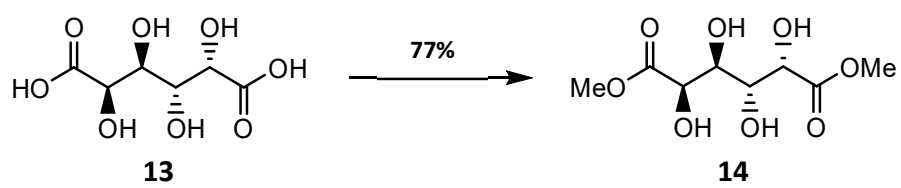
4.4	Preparation of sugar alcohols.....	123
4.4.1	Synthesis of (E/Z)-3-bromopropenyl acetate <sup>[66]</sup> .....	123
4.4.2	Synthesis of 1,2-dideoxy-L- <i>glycero</i> -D- <i>manno</i> -oct-1-enitol peracetate (crude) <sup>[66]</sup> .....	124
4.4.3	Synthesis of 1,2-dideoxy-L- <i>glycero</i> -D- <i>manno</i> -oct-1-enitol <sup>[66]</sup> .....	125
4.4.4	Synthesis of 1,2-dideoxy-L- <i>glycero</i> -D- <i>manno</i> -oct-1-enitol peracetate <sup>[67]</sup> .....	126
4.4.5	Synthesis of perseitol <sup>[67]</sup> .....	128
4.4.6	Synthesis of 1,2-dideoxy-D- <i>erythro</i> -D- <i>manno</i> -non-1-enitol peracetate <sup>[67]</sup> .....	130
4.4.7	Synthesis of 1,2-dideoxy-D- <i>erythro</i> -D- <i>manno</i> -non-1-enitol <sup>[67,105]</sup> .....	131
4.4.8	Synthesis of 1,2-dideoxy-D- <i>erythro</i> -D- <i>manno</i> -non-1-enitol peracetate <sup>[67,105]</sup> .....	132
4.4.9	Synthesis of D- <i>erythro</i> -D- <i>manno</i> -octitol <sup>[67,68,69,105]</sup> .....	134
4.4.10	Synthesis of 1,2-dideoxy-D- <i>erythro</i> -L- <i>gluco</i> -non-1-enitol peracetate <sup>[67,105]</sup> .....	136
4.4.11	Synthesis of 1,2-dideoxy-D- <i>erythro</i> -L- <i>gluco</i> -non-1-enitol <sup>[67,105]</sup> .....	138
4.4.12	Synthesis of D- <i>erythro</i> -L- <i>gluco</i> -octitol <sup>[67,68,69,105]</sup> .....	139
4.5	Preparation of aliphatic- $\alpha,\omega$ -diamides .....	141
4.5.1	General procedure C .....	141
4.5.2	General procedure D.....	141
4.5.3	Synthesis of glutaramide <sup>[72]</sup> .....	142
4.5.4	Synthesis of pimelamide <sup>[72]</sup> .....	143
4.5.5	Synthesis of suberamide <sup>[72]</sup> .....	144
4.5.6	Synthesis of azelamide <sup>[73]</sup> .....	145
4.5.7	Synthesis of sebacamide <sup>[72]</sup> .....	146
4.5.8	Synthesis of undecanediamide <sup>[72]</sup> .....	147
4.5.9	Synthesis of dodecanediamide <sup>[72,73]</sup> .....	148
4.5.10	Synthesis of tetradecanediamide <sup>[73]</sup> .....	150
4.5.11	Synthesis of hexadecanediamide <sup>[73]</sup> .....	151
4.5.12	Synthesis of octadecanediamide <sup>[73]</sup> .....	152
4.6	Preparation of substituted diamides .....	154
4.6.1	General procedure E .....	154
4.6.2	Oxalamide derivatives.....	155
4.6.2.1	N,N'-Dimethyloxalamide <sup>[75-77]</sup> .....	155
4.6.2.2	N,N'-Diethyloxalamide <sup>[75-77]</sup> .....	156
4.6.2.3	N,N'-Dipropyloxalamide <sup>[75-77]</sup> .....	157
4.6.2.4	N,N'-Dibutyloxalamide <sup>[75-77]</sup> .....	158

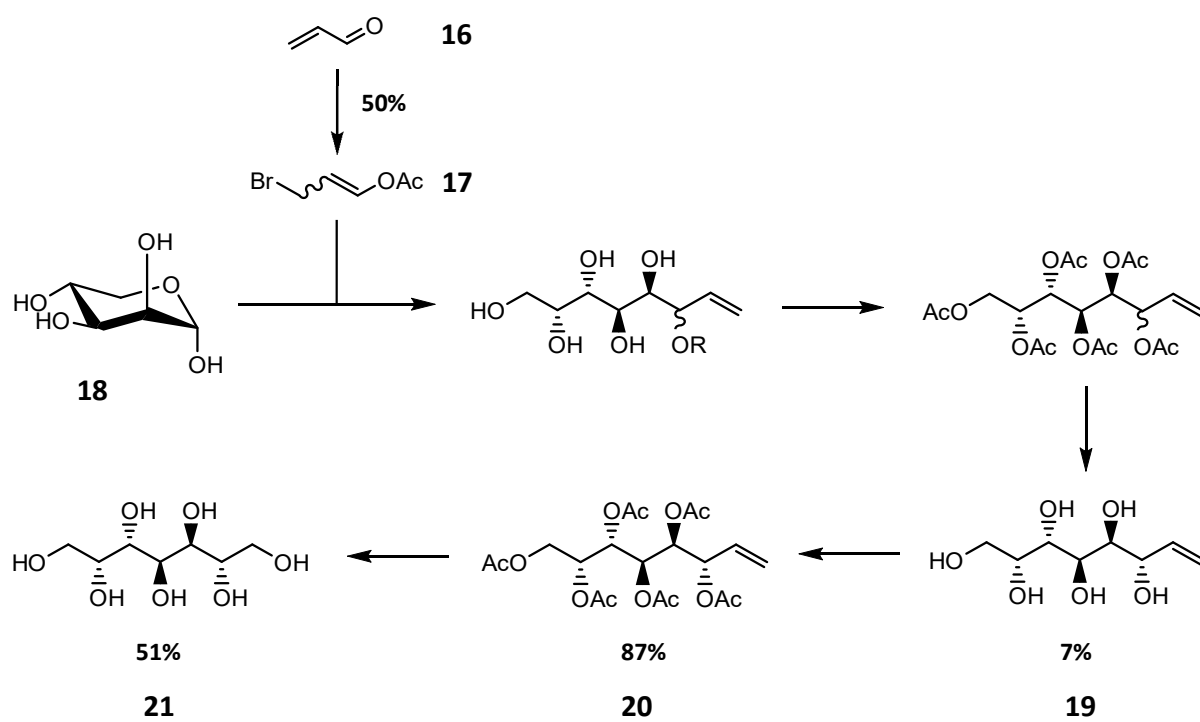
4.6.2.5 N,N'-Dioctyloxalamide <sup>[75-77]</sup> .....	159
4.6.2.6 N,N'-Didecyloxalamide <sup>[75-77]</sup> .....	160
4.6.2.7 N,N'-Dioctadecyloxalamide <sup>[75-77]</sup> .....	161
4.7 Preparation of 3,6-diazaoctane-1,8-diol derivatives .....	163
4.7.1 Synthesis of 3,6,9-triazaundecane-1,11-diol .....	163
4.7.1.1 Synthesis of 1,4,7-Tris(2-nitrobenzenesulfonyl)-1,4,7-triazaheptane <sup>[81]</sup> .....	163
4.7.1.2 Synthesis of 1,4,7-Tris(2-nitrobenzenesulfonyl)-3,6,9-triazaundecane-1,11-diol <sup>[81]</sup> .....	165
4.7.1.3 Synthesis of 3,6,9-triazaundecane-1,11-diol [82] .....	167
4.8 Preparation of 4,7-diazadecanediamide and derivatives .....	168
4.8.1 Synthesis of 4,7-diazadecanediamide <sup>[83]</sup> .....	168
4.9 Preparation of oxamides .....	169
4.9.1 General procedure F - Dinitrile formation.....	169
4.9.2 General procedure G - Dinitrile hydrolysis.....	169
4.9.3 Synthesis of 4,7-dioxa-1,10-octanedicarboxamide <sup>[87]</sup> .....	170
4.9.4 Synthesis of 4,7,10-trioxa-tridecanedinitrile <sup>[89]</sup> .....	171
4.9.5 Synthesis of 4,7,10-trioxa-1,13-undecanedicarboxamide <sup>[87]</sup> .....	172
4.9.6 Synthesis of 4,7,10,13-tetraoxahexadecanedinitrile <sup>[89]</sup> .....	173
4.9.7 Synthesis of 4,7,10,13-tetraoxa-1,16-hexadecanedicarboxamide <sup>[87]</sup> .....	174
4.10 Preparation of sulfaramides.....	175
4.10.1 Synthesis of 3-[2-(2-carbamoylethylsulfanyl)ethylsulfanyl]propionamide <sup>[90]</sup> .....	175
5. Appendix .....	176
5.1 TU STA graphics .....	176
5.1.1 Sugars and derivatives .....	176
5.1.2 Arene.....	195
5.1.3 Amino acids .....	203
5.1.4 Purines and pirimidines.....	208
5.1.5 Dyes.....	212
5.1.6 Other organic compounds.....	214
5.1.7 Fatty acids.....	221
5.1.8 Acids and derivatives .....	223
5.1.9 3,6-diazaoctane-1,8-diol and derivatives.....	246
5.2 AIT DSC graphics .....	250
5.3 References.....	266



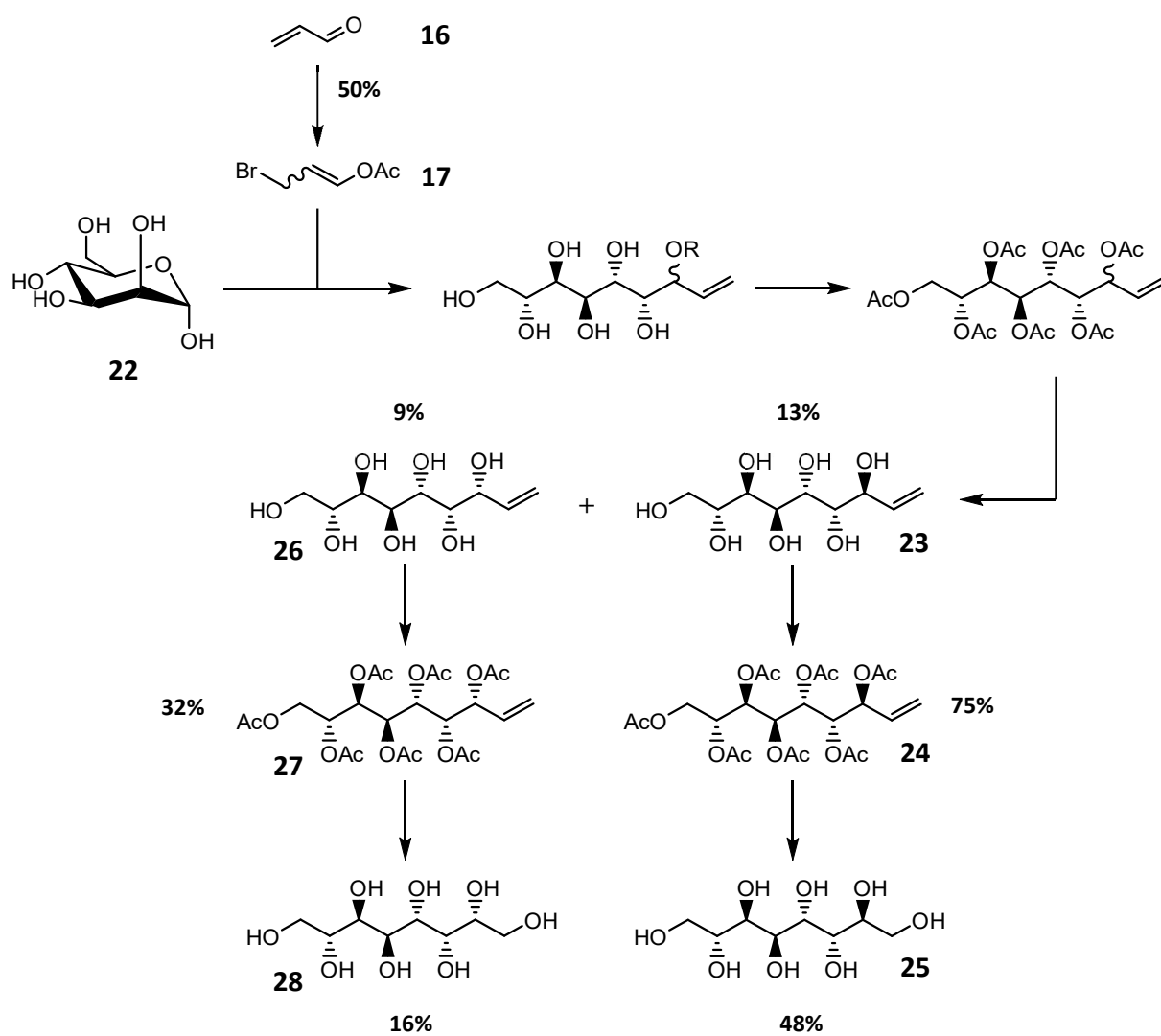
## Synthetic schemes

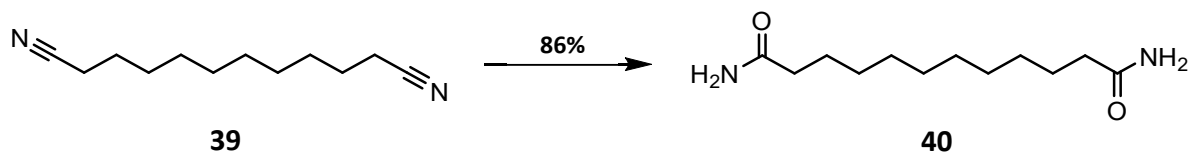
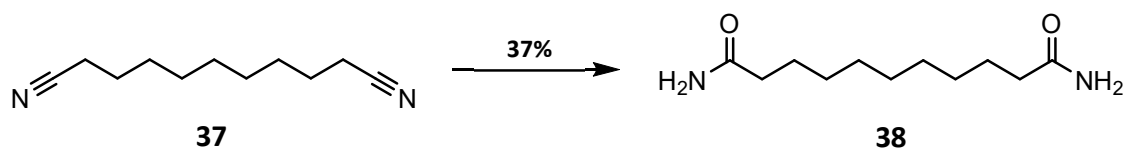
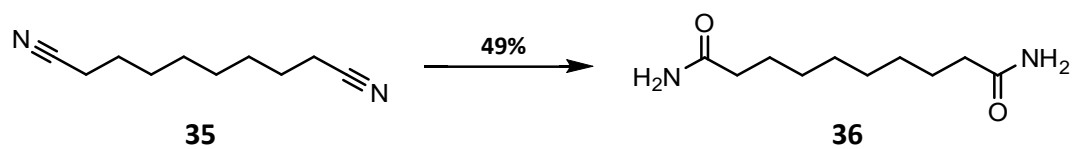
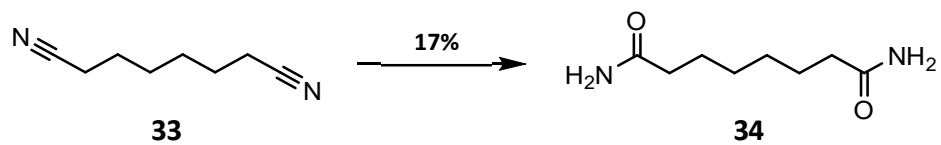
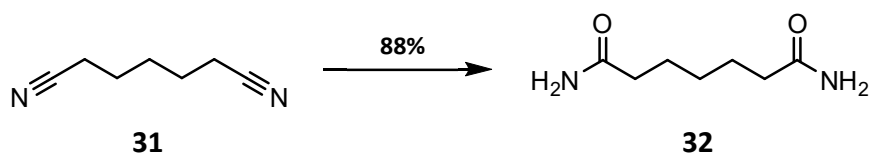
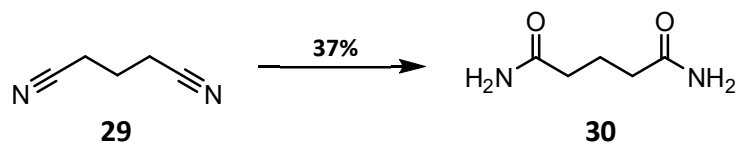


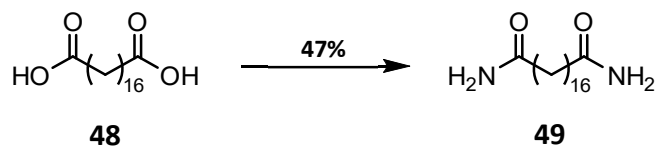
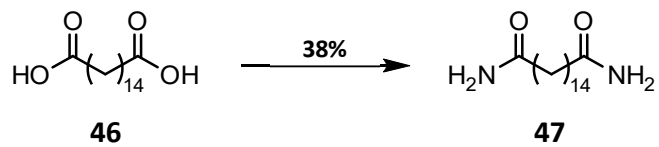
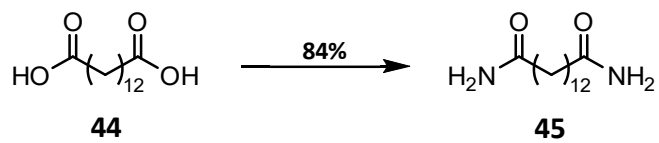
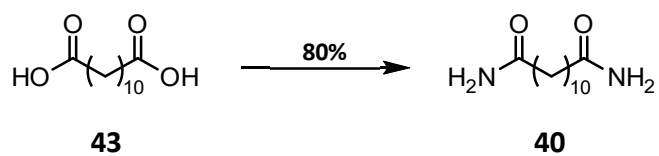
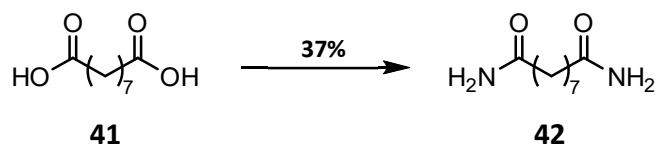


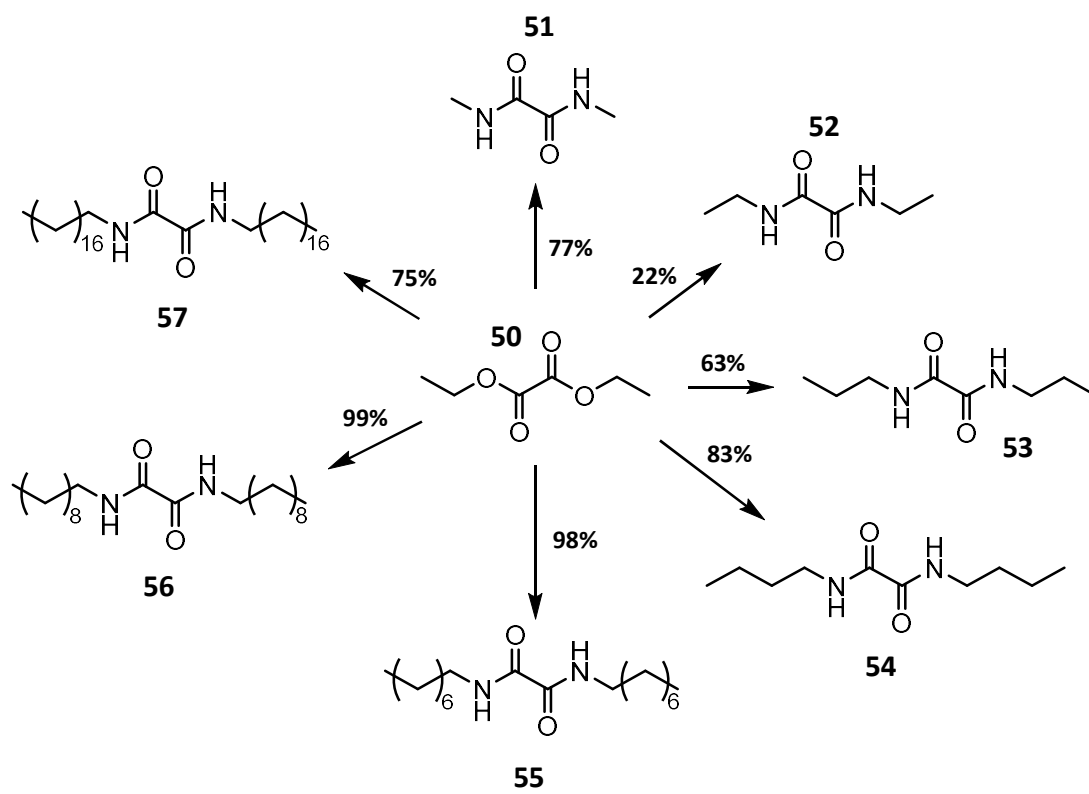


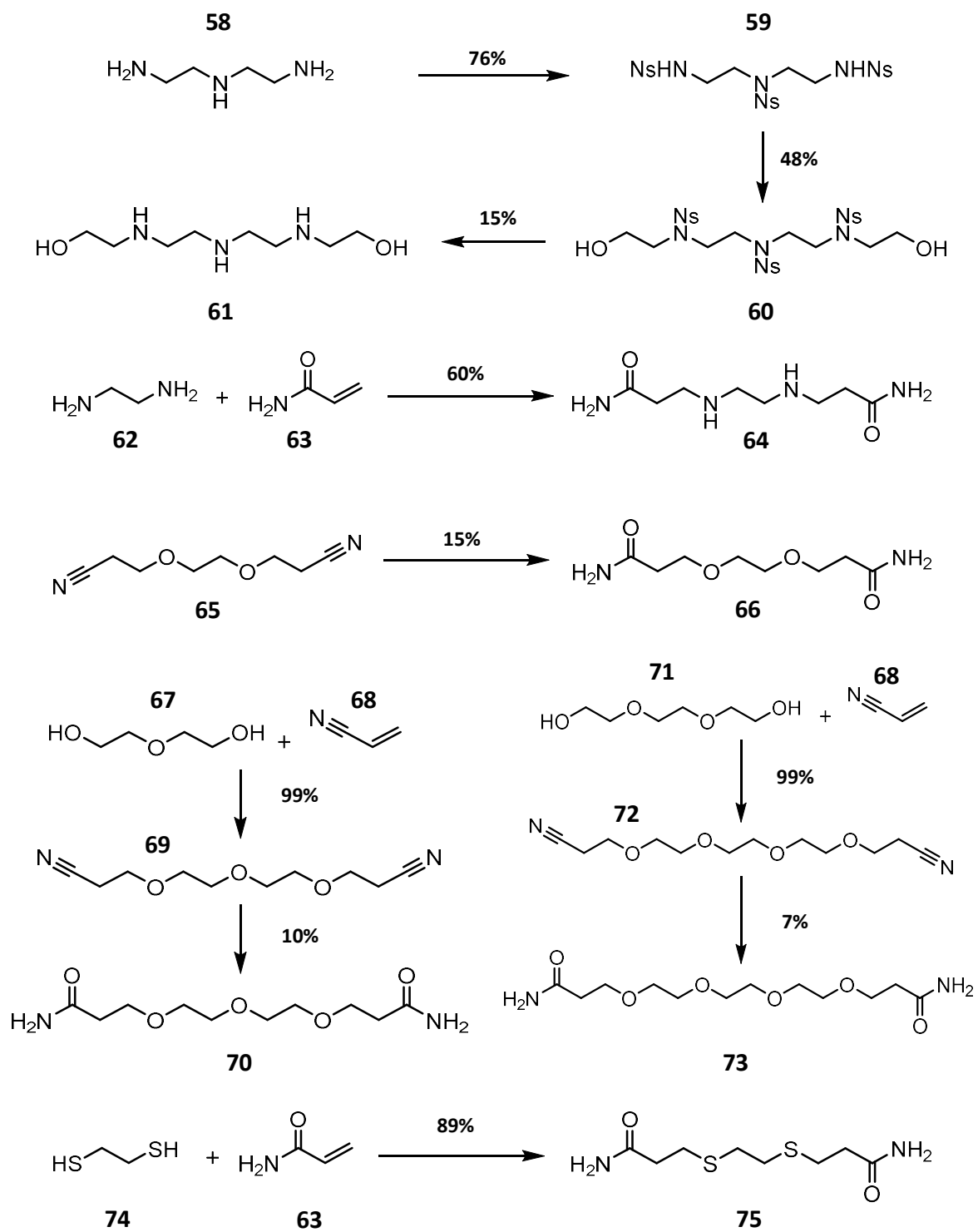












## Abbreviations

Anhyd.	Anhydride
Aq.	Aqueous
Ac <sub>2</sub> O	Acetic anhydride
BORAX	sodium tetraborate
C <sub>p</sub>	Specific heat (J/kg °K)
c	Specific heat (J/kg °C)
DCM	Dichloromethane
DIPEA	N,N-Diisopropylethylamine
DMAP	4-Dimethylaminopyridine
DMF	N,N-Dimethylformamide
DMSO	Dimethyl sulfoxide
DSC	Differential scanning calorimetry
EDC·HCL	N-(3-Dimethylaminopropyl)-N'-ethylcarbodiimide hydrochloride
EGA	Evolved gas analysis
Eq.	equivalent
EtOAc	Ethyl acetate
Et <sub>2</sub> O	Diethyl ether
Exp.	Experimental
FTIR	Fourier transform infrared spectrometer
g	gram
h	hour
H	Hydrogen
HPLC	High-performance liquid chromatography
J	Joule
L <sub>f</sub>	Latent heat
Lit.	Literature

LHS	Latent heat storage
LGLHS	Liquid-gas latent heat storage
m	Mass
Min	Minute
MP	Melting point
MPLC	Medium Pressure Liquid Chromatography
MS	Mass spectrometry
N°	Number
NN-Bis	NN'-Bis (2-hydroxyethyl)ethylenediamine
Ns	Nosyl group
NMR	Nuclear magnetic resonance
O	Oxygen
PCM	Phase change material
PE	Petroleum ether
PEG	Polyethylene glycol
ppm	Parts per million
Py	Pyridine
Q	Heat
R <sub>f</sub>	Ratio of front
R.T.	Room temperature
SHS	Sensible heat storage
SLLHS	Solid-liquid latent heat storage
SM	Starting material
SSLHS	Solid-solid latent heat storage
STA	Simultaneous thermal analysis
t	Time
T	Temperature
T <sub>i</sub>	Initial temperature
T <sub>f</sub>	Final temperature

TCM	Thermochemical materials
TES	Thermal energy storage
TGA	Thermogravimetric analysis
THF	Tetrahydrofuran
TLC	Thin-layer chromatography
W	Watt
$\Delta H$	Enthalpy of fusion



# 1. Introduction

## 1.1 Thermal energy storage systems (TES)

Energy represents one of the basic pillars of both, our daily life and progress. Following the energy crises in the seventies and early eighties, the importance of the energy sector for developing countries was highlighted and since then, an upward trend was constantly observed in the demand for energy (Figure 1.1.1) [1]. In addition, there are a number of factors such as the continuing increase in the use of fossil fuels, greenhouse gas emissions and the growing world population, among others, which require an increased energy supply and more efficient energy usage in the future [2].

In an attempt to maintain control of the situation and even revert this growth tendency; this demand must be managed in a sustainable way. To this end, it is necessary to rely on other new energy strategies. One of these strategies is based on avoiding energy losses linked, for example, to make use of residual heat of industrial processes

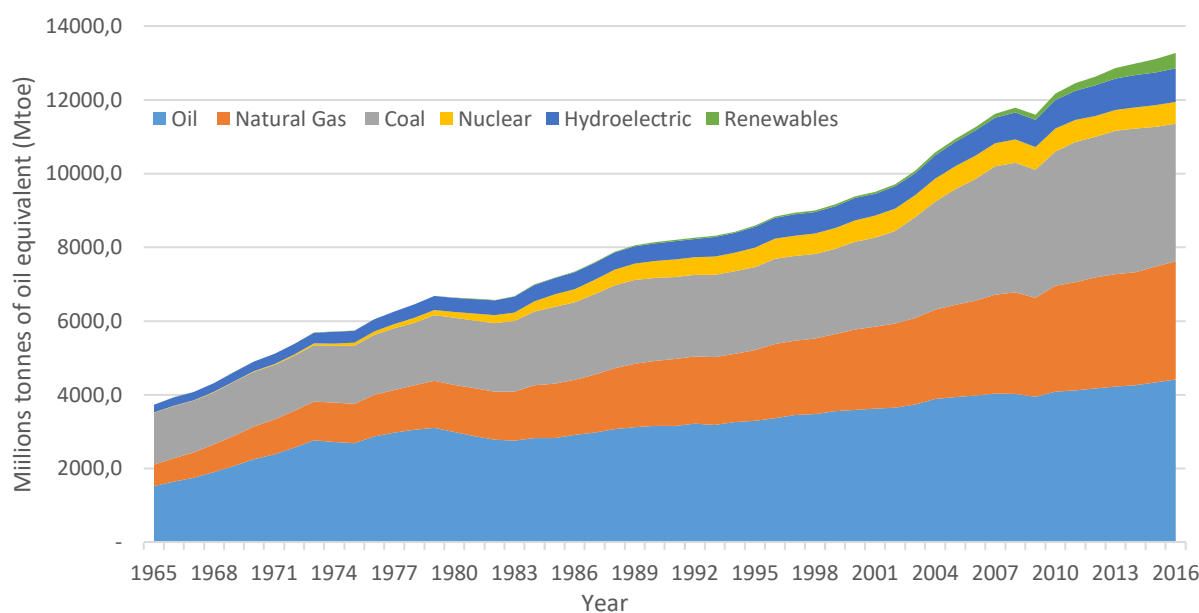
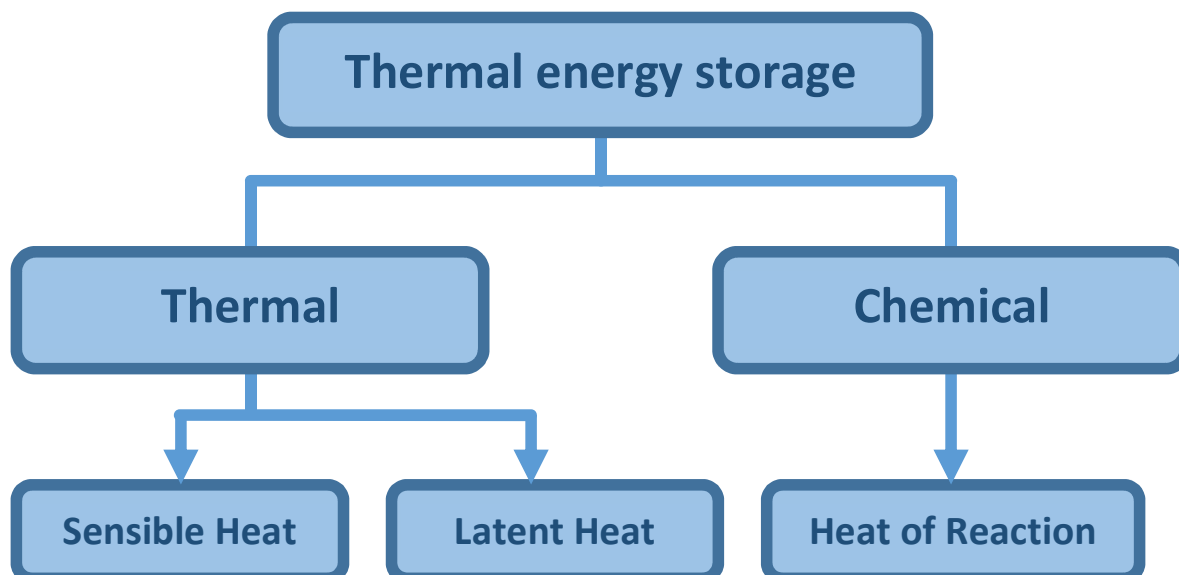


Figure 1.1.1 – World primary energy consumption by fuel type, 1965–2014 [3]

To improve the global energy management mentioned earlier, TES systems are an attractive option which allows storing waste heat instead of releasing it unused into the environment. This methodology is intended to raise the energy efficiency both in domestic as well as in industrial sectors.

### 1.1.1 System types

TES systems can be classified in three types: sensible, latent and thermo-chemical heat storages.

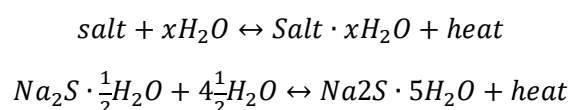


Scheme 1.1.1 – Thermal energy storage classification

#### 1.1.1.1 Thermo-chemical heat storage (THS)

Chemical heat is by definition the energy which is released once a chemical bond is broken. On this basis, reversible endothermic chemical reactions might be used to store energy. One of the most significant advantages of this method is the capability of the systems to store energy without loss of heat and the high energy density of the thermochemical materials (TCM) [2,4].

One current example are salt hydrates. Salt hydrates can be considered as both, THS and inorganic PCM. Regarding THS, this commonly used TCMs store thermal energy by drying the salt hydrate to, afterwards, store water and the dried salt separately. There is therefore a thermo-chemical reversible reaction where a dative bond between the water and the salt is formed or broken. As equation 1.1.1 shows, that energy can be recovered in the form of heat by mixing water with the dried salt.



Equation 1.1.1 – Example of a Thermo-chemical reversible reaction where a dative bond between the water and the salt is formed or broken[5]

THS systems present a storage density around 8 to 10 times larger than sensible heat storage systems and two times larger than latent heat storage systems. All this combined with the capability to conserve the heat energy at ambient temperature in long term periods without heat losses. Nevertheless, there is a limitation related to the volume of material that can be employed on a system because an efficient reaction needs efficient heat and mass transfer [2]. A lot of research is going on in this area and thermo-chemical storage is at a very early phase. Considering that this project has to develop a storage solution for industry, meaning large amounts, the volume limitation of THS is key to aiming for different technologies with no capacity constraints as for example latent and sensible heat storage. Moreover, some salt formations might release toxic gases as H<sub>2</sub>S during hydration and some others present high corrosivity, which results in a more complex and expensive container design [4]. Some of the operational temperature ranges of this salt hydrates would not fit properly with the operational temperature ranges defined for medium temperature industrial applications and only in these operating temperatures for salt hydrates is where the thermo-chemical reaction can be reversed and give the energy back [5]. Consequently, Thermo-chemical storage does not represent nowadays a suitable option for medium temperature industrial applications.

### 1.1.1.2 Sensible heat storage (SHS)

Sensible heat storage is the heat which is stored by increasing the temperature of a solid or a liquid without a change in its phase. As it is shown in equation 1.1.2 where Q is the heat, C<sub>p</sub> is the specific heat of a certain material, m is the mass, T is the temperature, C is the heat capacity and H is the enthalpy; the stored heat is going to depend on the heat capacity and the temperature rise of the storage medium [6,7].

$$Q = \int_{T_i}^{T_f} m C_p dT = m C_p (T_f - T_i)$$

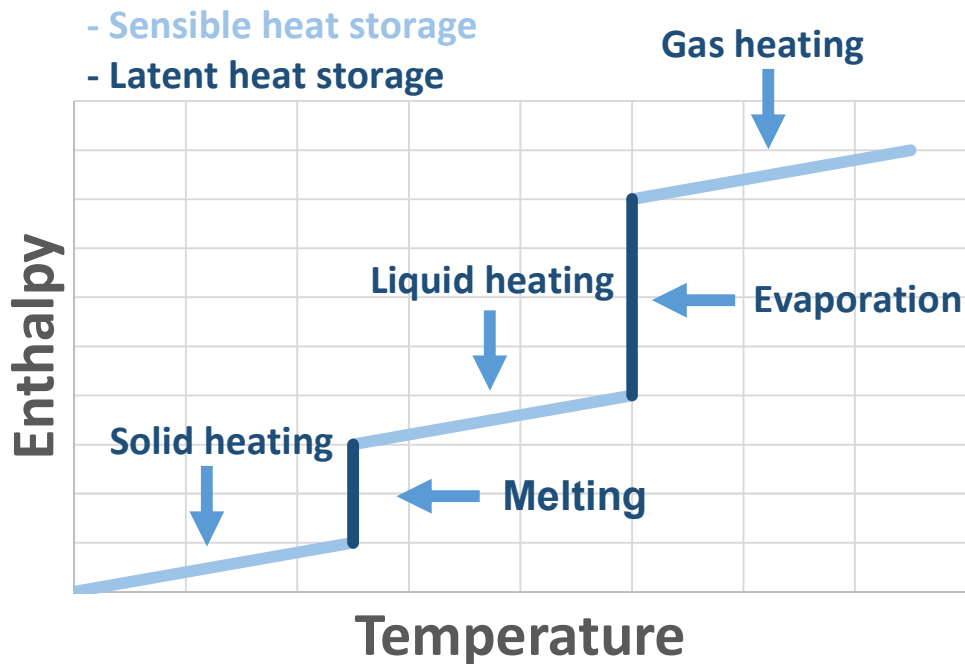
$$\Delta H = C \Delta T = m c \Delta T$$

**Equation 1.1.2** – Thermodynamic equations for Heat in SHS

Depending on the phase of the material, SHS systems can be classified in two types:

- **Liquid sensible storage.** As for example, water which is one of the best SHS materials due to its high specific heat and low cost. Once an operational temperature above 100 °C is required, oils or molten salts could be employed. Sensible heat storage through heating of a liquid is the most common method for heat storage. [6-8]
- **Solid sensible storage.** As for example rocks or metals.

Sensible heat storage is often present in latent heat storage (LHS). That could be easily observed in Figure 1.1.2 where the SHS would be only related to solid and liquid heating and LHS, as will be discussed later, is taking place during a change of phase.



**Figure 1.1.2** – Sensible heat storage (SHS) can be observed in the light blue heating transitions and latent heat storage (LHS) in the dark blue phase-change transitions related to the melting and evaporation.

### 1.1.1.3 Latent heat storage (LHS)

Latent heat storage is based on the heat which is absorbed, stored and released depending on the temperature of a material which would undergo a change in its phase. This phase change might be solid-solid, solid-liquid and liquid-vapor. Solid-solid phase change is related to the transition between different solid conformations of one compound. In this case, equation 1.1.3 for LHS would embrace the SHS of both phases, as for example solid and liquid, and particularly the latent energy of our material at the melting point [6-8]. Here  $a_m \Delta H_m$  would represent the specific latent heat ( $L_f$ ) of the material

$$Q = \int_{T_i}^{T_m} m C_p dT + m a_m \Delta H_m + \int_{T_m}^{T_f} m C_p dT$$

$$Q = m [C_{sp}(T_m - T_i) + a_m \Delta H_m + C_{lp}(T_f - T_m)]$$

**Equation 1.1.3** – Thermodynamic equations for Heat in LHS

This fact can be easily observed above in Figure 1.2 where once our solid material starts to be heated, it starts to absorb energy. Energy absorption begins with solid SHS until the melting point where thermal energy is stored because of its latent heat of fusion. At this stage, the temperature would not be raised,

and heat would favour the phase transition. Later, temperature could increase again, and it would be possible accumulating more energy because of its SHS during the liquid heating.

Therefore, LHS results in a more effective way to save energy than SHS only considering its latent heat. LHS systems present higher energy density per unit mass and per unit volume than SHS systems among other advantages. Phase change materials (PCMs) are the materials employed in LHS and they have the advantage of providing, on one hand, a high storage density for a certain storage volume, therefore, lower space and weight requirement and higher temperature stability of the system, which eventually provide containers with a more convenient design; and, on the other hand, LHS allows us to use a certain storage material in a short range of temperatures where the phase transition takes place.

As mentioned above, there are three important phase transitions:

#### **- Solid-solid latent heat storage (SSLHS)**

This latent heat storage is going to be related to the phase transition between different solid conformations of one compound. For this reason, one advantage which can be observed at first sight is the lack of need for encapsulation. Encapsulation is not necessarily due to the lack of leakage in solid-solid phase transition, therefore less production costs [9].

Some materials such as polyethylene glycol and polyurethane have been reported in the literature [10-14] as an option. These organic SSPCMs can be easily prepared and often have melting points below 100 °C but their latent energy is frequently lower than solid-liquid phase transitions.

#### **- Liquid-gas latent heat storage (LGLHS)**

Liquid-gas latent heat storage has the highest energy in terms of phase transition, but it may result in a more complex container design. This design could give problems over the time due to the big volume changes because of the expansion from a liquid to a gas [7]

#### **- Solid-liquid latent heat storage (SLLHS)**

In this case, the phase transition from solid to liquid is going to be listed in general terms the most attractive alternative for latent heat storage, thus the most widely studied [7,8]. This thesis is focused on the way of storing heat by using the latent heat of a substance and in this particular case, we are interested in solid to liquid phase transitions.

Even though the latent energy is not comparable to the high latent energy of LGLHS, the container will not present technical complications related to enormous changes in volume. Nevertheless, one disadvantage that SSLHS tend to present, could be the need of encapsulation. By using this procedure, leaking of the Liquid PCM may be prevented but it might lower the overall density storage of the LHS and increase the production cost [7,9]. Other disadvantages which have to be considered and improved are the low thermal conductivity which some PCMs have shown, the phase segregation that could be observed usually in inorganic materials such as salt hydrates and subcooling, meaning that a compound is still a liquid in a temperature below its melting point.

Anyhow, some of these problems can be avoided and the performance of this SSLHS PCMs might be enhanced by using different techniques that will be discussed in the following sections.

## 1.2 Phase-change materials

Materials used for LHS are known as phase change materials (PCMs) and they have to provide ideally 22 properties [9] that can be ranked in four different groups:

### -Thermal properties

Large latent heat, large specific heat, large thermal conductivity in both liquid and solid phases, suitable phase change temperature, rapid heat transfer

### -Kinetic or Physical Properties

Large density, small volume change during phase change, low vapour pressure, no subcooling, sufficient crystallization time, favourable phase equilibrium

### -Chemical properties

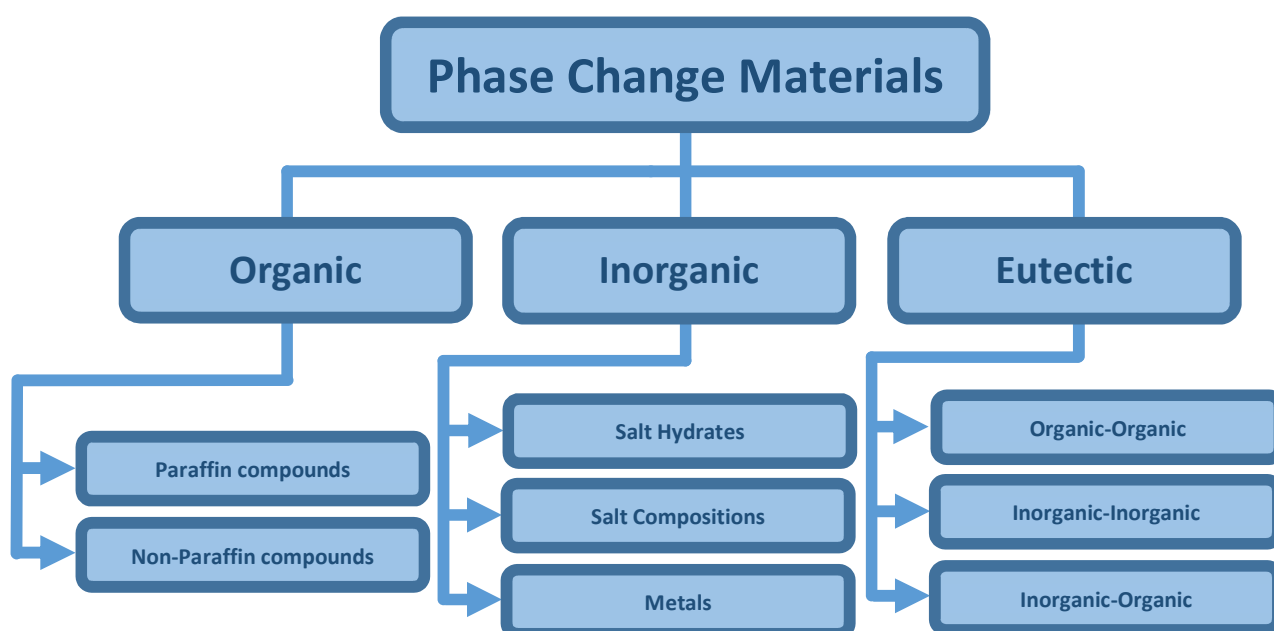
Long-term chemical stability, compatibility with construction and container materials, completely reversible freeze/melt cycle, no chemical decomposition, no fire hazard, non-toxic, non-flammable, non-explosive

### -Economic properties

Abundant, available, cost effective

As no single material currently has all the required properties for an ideal thermal storage medium, one must use the available materials and try to make up for the poor or inconvenient properties by an adequate system design.

Moreover, PCMs can be divided into two groups, organic and inorganic compounds [1]. Combination of organic and/or inorganic materials, called eutectic mixtures, can be found on the market as well.



Scheme 1.1.2 – Phase change material classification

As can be seen in Figure 1.1.3, organic and inorganic compounds cover different ranges regarding melting energy and melting points as well. Inorganics typically cover melting temperatures  $>400$  °C, whereas organic compounds melt typically below 250 °C. Hence, the two classes are complementary in their potential applications, the organics suitable for “low temperature” applications[15-17].

Typically, there is a large gap between both, organic and inorganic volumetric latent heat storage capacity. Inorganic materials tend to have double capacity than organic materials

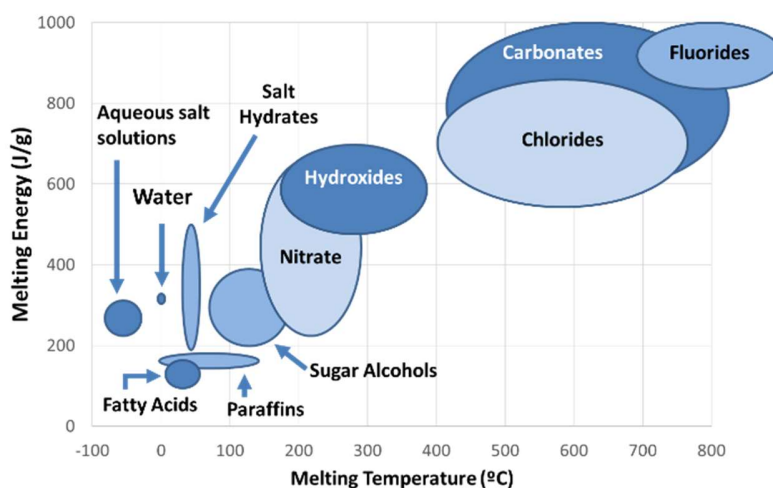


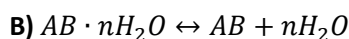
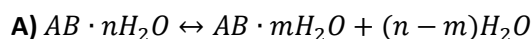
Figure 1.1.3 - Classification of PCM with their melting temperature and enthalpy (graph: ZAE Bayern)

## 1.2.1 Inorganic phase change materials

In turn, inorganic materials can be classified in three main groups too: salt hydrates, inorganic salts and metallic ones [7,8].

### 1.2.1.1 Salt hydrates

Salt hydrates basically consist of water and a salt forming a typical crystalline solid of general formula  $AB \cdot nH_2O$  and they are one of the most studied PCMs for LLS [6,18]. Even though this transition looks like a melting/crystallization process, this case is in fact a dehydration or hydration of the salt



Equation 1.2 – melting reaction for a salt hydrate with moles of water(A) or its anhydrous form (B)

They can be used either alone or in eutectic mixtures and a melting range is reported of temperatures (table 1.1.1) between 15 to 117°C [6,18,19]. These salt hydrates can undergo three different types of melting:

- **Congruent melting**, when the anhydrous salt is totally soluble in its water of hydration at the melting temperature
- **Incongruent melting**, when the salt is not totally soluble in its water of hydration at the melting temperature
- **Semi-congruent melting**, when liquid and solid phases are in equilibrium during a phase transition

Salt hydrates present several advantages such as high latent heat of fusion per unit volume, relatively high thermal conductivity and small volume changes on melting. Moreover, they are cheap and easily available. Two of these low-cost available salts are  $\text{CaCl}_2 \cdot 6\text{H}_2\text{O}$  and  $\text{Na}_2\text{SO}_4 \cdot 10\text{H}_2\text{O}$  [6]. They are not very corrosive and suitable for plastics. They only present risk of corrosion in metal containers, widely employed in TES systems.

One of the main problems in using salt hydrates is the segregation, which is the formation of different hydrates or dehydrated salts that settle out. This usually happens when salt hydrates melt incongruently and inevitably results in a reduction of the active volume available, affecting negatively the heat storage capacity. It was reported in the literature [18,11] that phase transition energy falls below 73% in  $\text{Na}_2\text{SO}_4 \cdot 10\text{H}_2\text{O}$  after 1000 melting/recrystallization cycles, but this issue can be corrected by using gelled or thickening agents. In addition, most of the salt hydrates suitable for thermal storage tend to melt incongruently. To confront the segregation problem, solutions such as mechanical stirring [20], encapsulation of the PCM to reduce the separation [21] and the aforementioned addition of thickening agents [22] were proposed among others.

Another problem that has been observed is subcooling, meaning that a compound is still a liquid in a temperature below its melting point. It has been observed that the addition of some nucleation agents can overcome this problem.

**Table 1.1.1** – melting temperatures and heat of fusion: Salt hydrates [18]

<b>Material</b>	<b>Melting temperature (°C)</b>	<b>Heat of fusion (kJ/kg)</b>	<b>Melting Behaviour</b>
$\text{LiClO}_3 \cdot 3\text{H}_2\text{O}$	8	253	c
$\text{NaCl} \cdot \text{Na}_2\text{SO}_4 \cdot 10 \text{H}_2\text{O}$	18	286	n.a.
$\text{KF} \cdot 4\text{H}_2\text{O}$	18	330	c
$\text{K}_2\text{HO}_4 \cdot 4 \text{H}_2\text{O}$	18.5	231	n.a.
$\text{Mn}(\text{NO}_3)_2 \cdot 6 \text{H}_2\text{O}$	25	148	n.a.
$\text{LiBO}_2 \cdot 8 \text{H}_2\text{O}$	25.7	289	n.a.
$\text{CaCl}_2 \cdot 6 \text{H}_2\text{O}$	29-30	170-192	lc
$\text{Na}_2\text{SO}_4 \cdot 10 \text{H}_2\text{O}$	32	251-254	ic
$\text{Na}_2\text{CO}_3 \cdot 10 \text{H}_2\text{O}$	33-36	247	lc
$\text{CaBr}_2 \cdot 6 \text{H}_2\text{O}$	34	115-138	n.a.
$\text{Na}_2\text{HPO}_4 \cdot 12 \text{H}_2\text{O}$	35	256-281	ic
$\text{Zn}(\text{NO}_3)_2 \cdot 6\text{H}_2\text{O}$	36	134-147	c
$\text{Na}_2\text{S}_2\text{O}_3 \cdot 5\text{H}_2\text{O}$	48	209	n.a.
$\text{CH}_3\text{COONa} \cdot 3 \text{H}_2\text{O}$	58	265	ic
$\text{NaOH} \cdot \text{H}_2\text{O}$	58	272	n.a.
$\text{Ba}(\text{OH})_2 \cdot 8 \text{H}_2\text{O}$	78	265-280	c
$\text{Al}_2(\text{SO}_4)_3 \cdot 18 \text{H}_2\text{O}$	88	218	lc
$\text{Sr}(\text{OH})_2 \cdot 8 \text{H}_2\text{O}$	89	370	lc
$\text{Mg}(\text{NO}_3)_2 \cdot 6 \text{H}_2\text{O}$	89.9	167	c
$(\text{NH}_4)\text{Al}(\text{SO}_4) \cdot 6 \text{H}_2\text{O}$	95	269	n.a.
$\text{LiCl} \cdot \text{H}_2\text{O}$	99	212	ic
$\text{MgCl}_2 \cdot 6 \text{H}_2\text{O}$	117	167	n.a.



### 1.2.1.2 Other salt compositions

Beyond the salt hydrates, other inorganic salts can be considered as PCMs. These are the molten salts which are salts that are solid at standard temperature and pressure (STP) but enters the liquid phase due to elevated temperatures. Some inorganic salts start melting at temperatures as low as 200 °C and some can reach melting temperatures of >1400 °C. Due to this feature, they are unsuitable for medium temperature applications, however very suitable for high temperature applications. As can be seen in table 1.1.2, they often offer higher storage capacity than other materials. Heat of fusion over 1000 kJ/kg can be reached in salts as LiF.

**Table 1.1.2** – melting temperatures and heat of fusion: Salt compositions [9]

<b>Material</b>	<b>Melting temperature (°C)</b>	<b>Heat of fusion (kJ/kg)</b>
LiNO <sub>3</sub>	253	363
NaOH-Na <sub>2</sub> NO <sub>2</sub>	265	313
NaOH-Na <sub>2</sub> NO <sub>3</sub>	271	263
Zn <sub>2</sub> Cl <sub>2</sub>	280	75
Na <sub>2</sub> NO <sub>2</sub>	282	216
Na <sub>2</sub> NO <sub>3</sub>	307	182
NaOH	318	159
KNO <sub>3</sub>	330	266
KOH	360	148
LiOH	462	875
MgCl <sub>2</sub>	714	453
KCl	770	355
NaCl	800	483
LiF	848	1037
Na <sub>2</sub> CO <sub>3</sub>	854	275
KF	858	507
K <sub>2</sub> CO <sub>2</sub>	898	200
NaF	996	796
MgF <sub>2</sub> ·KF	1008	710
Na <sub>2</sub> O	1132	770
MgF <sub>2</sub>	1263	883
CaF <sub>2</sub>	1411	393

### 1.2.1.3 Metals and metal alloys

Some low melting metals might be taken into account as PCMs for LHS as well. They show remarkable properties that other inorganic PCMs do not. Metallic materials usually present high thermal conductivity, which allows to develop simple system containers, and high latent energy density. Some other features of this group could be low heat of fusion per unit weight, low specific heat and low vapour pressures. However, one of the reasons why metals have not been seriously considered for PCM is due to their heavy weight. As we can see in table 1.1.2, most of these interesting metal PCMs are melting at temperatures of >300 °C.

**Table 1.1.2** – melting temperatures and heat of fusion: Metals [8,23-27]

<b>Material</b>	<b>Composition (wt%)</b>	<b>Melting temperature (°C)</b>	<b>Heat of fusion (kJ/kg)</b>
Zn/Mg	53.7/46.3	340	185
Zn/Mg	52/48	340	180
Zn/Al	96/4	381	138
Al/Mg/Zn	59/33/6	443	310
Al/Mg/Zn	60/34/6	450.3	329
Mg/Cu/Zn	60/25/15	452	254
Mg/Cu/Ca	52/25/23	453	184
Al/Mg	65.35/34.65	497	285
Al/Cu/Mg	60.8/33.2/6	506	365
Al/Cu/Si/Mg	64.6/28/5.2/2.2	507	374
Al/Cu/Mg/Zn	54/22/18/6	520	305
Al/Cu/Si	68.5/26.5/5	525	364
Al/Cu/Sb	64.3/34/1.7	545	331
Al/Cu	66.92/33.08	548	372
Al/Si/Mg	83.14/11.7/5.16	555	485
Al/Si	87.76/12.24	557	498
Cu/Al/Si	49.1/46.3/4.6	571	406
Al/Cu/Si	65/30/5	571	422
Al/Si/Sb	86.4/9.6/4.2	575	471
Si/Al	86/12	576	560
Si/Al	80/20	585	460
Zn/Cu/Mg	49/45/6	703	176
Cu/P	91/9	715	134
Cu/Zn/P	69/17/14	720	368
Cu/Zn/Si	74/19/7	765	125
Cu/Si/Mg	56/27/17	770	420
Mg/Ca	84/16	790	272
Mg/Si/Zn	47/38/15	800	313
Cu/Si	80/20	803	197
Cu/P/Si	83/10/7	840	92
Si/Mg/Ca	49/30/21	865	305
Si/Mg	56/44	946	757

## 1.2.2 Eutectic mixtures

An eutectic is a minimum melting composition of two or more components, each of which melts and freezes congruently, forming a mixture of the component crystals during crystallization. Eutectics tend to melt and recrystallize without showing segregation because they recrystallize to an intimate mixture of crystals, leaving little opportunity for the components to separate. On melting both components liquify at the same time thus no separation occurs [6,28].

**Table 1.1.3** – melting temperatures and heat of fusion of organic and inorganics eutectic materials

taken from the literature [6,17-19]

Material	Composition (wt %)	Melting temperature (°C)	Heat of fusion (kJ/kg)
Na <sub>2</sub> SO <sub>4</sub> + NaCl + KCl + H <sub>2</sub> O	31/13/16/40	4	234
C <sub>5</sub> H <sub>5</sub> C <sub>6</sub> H <sub>5</sub> + (C <sub>6</sub> H <sub>5</sub> ) <sub>2</sub> O	26.5/73.5	12	97.9
Triethylolethane + water + urea	38.5/31.5/30	13.4	160
C <sub>14</sub> H <sub>28</sub> O <sub>2</sub> + C <sub>10</sub> H <sub>20</sub> O <sub>2</sub>	34/66	24	147.7
CaCl <sub>2</sub> + MgCl <sub>2</sub> ·6H <sub>2</sub> O	50/50	25	95
CH <sub>3</sub> CONH <sub>2</sub> + NH <sub>2</sub> CONH <sub>2</sub>	50/50	27	163
Triethylolethane + urea	62.5/37.5	29.8	218
Ca(NO <sub>3</sub> ) <sub>2</sub> ·4H <sub>2</sub> O + Mg(NO <sub>3</sub> ) <sub>2</sub> ·6H <sub>2</sub> O	47/53	30	136
CH <sub>3</sub> COONa·3H <sub>2</sub> O + NH <sub>2</sub> CONH <sub>2</sub>	40/60	30	200.5
NH <sub>2</sub> CONH <sub>2</sub> + NH <sub>4</sub> NO <sub>3</sub>	53/47	46	95
Mg(NO <sub>3</sub> ) <sub>2</sub> ·6H <sub>2</sub> O + NH <sub>4</sub> NO <sub>3</sub>	61.5/38.5	52	125.5
Mg(NO <sub>3</sub> ) <sub>2</sub> ·6H <sub>2</sub> O + MgCl <sub>2</sub> ·6H <sub>2</sub> O	58.7/41.3	59	132.2
Mg(NO <sub>3</sub> ) <sub>2</sub> ·6H <sub>2</sub> O + MgCl <sub>2</sub> ·6H <sub>2</sub> O	50/50	59.1	144
Mg(NO <sub>3</sub> ) <sub>2</sub> ·6H <sub>2</sub> O + Al(NO <sub>3</sub> ) <sub>3</sub> ·9H <sub>2</sub> O	53/47	61	148
CH <sub>3</sub> CONH <sub>2</sub> + C <sub>17</sub> H <sub>35</sub> COOH	50/50	65	218
Mg(NO <sub>3</sub> ) <sub>2</sub> ·6H <sub>2</sub> O + MgBr <sub>2</sub> ·6H <sub>2</sub> O	59/41	66	168
Napthalene + benzoic acid	67.1/32.9	67	123.4
AlCl <sub>3</sub> + NaCl + ZrCl <sub>2</sub>	79/17/4	68	234
AlCl <sub>3</sub> + NaCl + KCl	66/20/14	70	209
NH <sub>2</sub> CONH <sub>2</sub> + NH <sub>4</sub> Br	66.6/33.4	76	151
LiNO <sub>3</sub> + NH <sub>4</sub> NO <sub>3</sub> + NaNO <sub>3</sub>	25/65/10	80.5	113
LiNO <sub>3</sub> + NH <sub>4</sub> NO <sub>3</sub> + KNO <sub>3</sub>	26.4/58.7/14.9	81.5	116
LiNO <sub>3</sub> + NH <sub>4</sub> NO <sub>3</sub> + NH <sub>4</sub> Cl	27/68/5	81.6	108
AlCl <sub>3</sub> + NaCl + KCl	60/26/14	93	213
AlCl <sub>3</sub> + NaCl	66/34	93	201

### 1.2.3 Organic phase change materials

As advantages of organic PCMs may be considered that they are typically non-corrosive and display often only low subcooling, whereas inorganic compounds typically have a larger phase enthalpy but are eventually corrosive and display problems with subcooling. Organic materials do not present phase segregation and in some cases, such as the paraffins, better cycle-stability than inorganics. Organic PCMs may be classified as paraffins and non-paraffins [7,18].

#### 1.2.3.1 Paraffins

Paraffins are a family of acyclic saturated hydrocarbons with the general chemical formula  $C_nH_{2n+2}$ . Their melting point and latent energy is related to the chain length. The longer the chain, the more Van der Waals interaction they have and therefore higher melting points and latent energies. One of the most used paraffins for LHS systems is the paraffin wax which consists of a mixture of different paraffins with a chain length between twenty and forty carbon atoms. Paraffins tend to be more expensive than salt hydrates and only technical grade paraffins can be used as PCMs [7,18].

Additional paraffin benefits include no tendency to segregate, non-corrosiveness and chemical stability. Sharma et al. [7] reported stable properties after 1500 cycles in commercial-grade paraffin wax. Moreover, paraffins do not undergo big volume changes and show congruent melting and good nucleating capacity. They are safe, non-reactive and compatible with metal LHS containers.

Even though they are chemically stable, slow oxidation due to oxygen exposure was reported in the literature [6]. This means the need for closed containers with inert atmosphere. Furthermore, they present another drawback as low thermal conductivity, incompatibility with plastic containers and they do not offer well-defined melting points. They are slightly flammable too, but all these problems can be partially fixed by modifying the wax or the design of the proper container.

Table 1.1.4 – melting temperatures and heat of fusion: Paraffins

Material	No. of "C" Atoms	Melting temperature (°C)	Heat of fusion (kJ/kg)
n - Dodecane	12	-12	n.a.
n - Tridecane	13	-6	n.a.
n - Tetradecane	14	4.5-5.6	231
n - Pentadecane	15	10	207
n - Hexadecane	16	18.2	238
n - Heptadecane	17	22	215
n - Octadecane	18	28.2	245
n - Nonadecane	19	31.9	222
n - Eicosane	20	37	247
n - Heneicosane	21	41	215
n - Docosane	22	44	249
n - Tricosane	23	47	234
n - Tetracosane	24	51	255
n - Pentacosane	25	54	238
Paraffin wax	n.a.	32	251
n - Hexacosane	26	56	257
n - Heptacosane	27	59	236
n - Octacosane	28	61	255
n - Nonacosane	29	64	240
n - Triacontane	30	65	252
n - Hentriacontane	31	n.a.	n.a.
n - Dotriacontane	32	70	n.a.
n - Tritriacontane	33	71	189

### 1.2.3.2 Non-paraffins

Non-paraffins are the largest group of candidates for PCMs for LHS and it embraces materials with very diverse chemical and physical properties. For all these reasons, it is going to constitute the subject matter of this study. Lane [6], Abhat [19] and Buddhi et al. [29] have also conducted broad research on this category of PCMs and some of the properties that they generally share are: high heat of fusion, inflammability, low thermal conductivity, low flash points, varying level of toxicity and instability at high temperatures [7].

Initially, two groups stand out in this family. On one hand, fatty acids which usually offer higher melting energies than paraffins and also present a reproducible melting-recrystallization behaviour [30, 31]. Nevertheless, fatty acids double the cost since they are around 2-2.5 times more expensive than technical grade paraffins [7]. On the other hand, polyols have been gaining the attention of several researchers for medium temperature heat storage applications [18,32-37]. For example, sugar alcohols usually show melting temperatures in a range from 100 to 170 °C and high latent energies. However, they also present as a drawback poor thermal conductivity and lack of stability in long-term tests.

**Table 1.1.5** – melting temperatures and heat of fusion: Non-paraffins

<b>Material</b>	<b>Melting temperature (°C)</b>	<b>Heat of fusion (kJ/kg)</b>
Formic acid	7.8	247
Caprilic acid	16.7	187
Acetic acid	17.9	198.7
Glycerin	21	188
Lithium chloride ethanolate	20-25	146
Polyethylene glycol 600	26	184
D-Lactic acid	29	197
Camphenilone	39	205
Docosyl bromide	40	201
Caprylone	40	259
Heptadecanone	41	201
1-Cyclohexyloctadecane	41	218
4-Heptadecanone	41	197
Cyanamide	44	209
Methyl behenate	45	230
3-Heptadecanone	48	218
2-Heptadecanone	48	218
Camphene	50	238
9-Heptadecanone	51	213
Methyl behenate	52	234
Pentadecanoic acid	52.5	178
Hypophosphoric acid	55	213
Chloroacetic acid	56	130
Trimyristin	33-561.87	201-213

Bee wax	61.8	177
Glycolic acid	63	109
Arachic acid	76.5	227
Bromcamphor	77	174
Durene	79.3	156
Acetamide	81	241
Methyl brombenzoate	81	126
Alpha naphthol	96	163
Glutaric acid	97.5	156
p-Xylene dichloride	100	138.7
Methyl Fumarate	102	242
Catechol	104.3	207
Quinone	115	171
Acetanilide	115	142
Succinic anhydride	119	204
Benzoic acid	121.7	142.8
Stibene	124	167
Benzamide	127.2	169.4
Phenacetin	137	136.7
Alpha glucose	141	174
Acetyl – p- toluidene	146	180
Phenylhydrazone benzaldehyde	155	134.8
Salicylic acid	159	199
Benzanilide	161	162
Mannitol	166	294
Hydroquinone	172.4	258
p-Aminobenzoic acid	187	153

---

## 1.2.4 Recent PCM advancements

### 1.2.4.1 PCM capsules

This technique is commonly employed in LHS between materials which undergo a solid-liquid phase transition. The encapsulation would solve problems such as leakage of the PCM in its liquid form. These capsules can be classified in macro- and microcapsules and both have to fulfil different requirements. The PCM capsules have to meet requirements of resistance, thermal stability and strength, among others. Capsules must protect the material from harmful environmental interactions and provide enough surface for heat transfer, easy handling and structural stability [9,39].

Macrocapsules are the most common ones, widely reported in the literature in different shapes (spherical and cylindrical) and different materials (metal and plastics) [40-44]. More recent is the microencapsulation which has gained prominence due to interesting features as increasing the heat

transfer area of the PCM. Moreover, this technique would protect the material from reacting with the external environment and would allow changes in the volume of the storage material during phase change. The fact that a material could undergo changes in volume during the phase transition is commonly a drawback that is often observed in liquid-gas latent heat storage. This problem can be avoided with PCM encapsulation. Some of the drawbacks are the poor thermal conductivity or the poor heat transfer features that encapsulation shows and the fact that this is a costly process [45-47].

#### **1.2.4.2 PCM Composites**

PCM composites are a mixture of several materials where encapsulation is not required and they might be an alternative for improving some of the drawbacks which PCM encapsulation presents. With this technique, the low thermal conductivity that some organic materials show can be enhanced. The fact of not needing encapsulation would lower costs and increase thermal storage density [48,9].

There are four main methods reported in the literature to prepare PCM composites: impregnation or infiltration, dispersion or kneading, compression and electro spinning.

Impregnation is the most widely studied method and it could avoid leakage of the liquid PCM due to capillarity and surface tension forces. This method can develop PCM composites for LHS with outstanding thermal properties such as great thermal conductivity and high density of heat storage once materials such as porous graphite [49,50] or porous metals [51,52] are chosen to combine with the PCM.

For the dispersion or kneading methods, a powder material such as graphite is mixed with the powder solid PCM at room temperature and then melted [53]. Similarly, the different powders are mixed for the compression method to finally compress them at room temperature [48]. The most sophisticated method is the electrospinning where nanofibers and microfibers are employed to enhance the PCM properties [54].



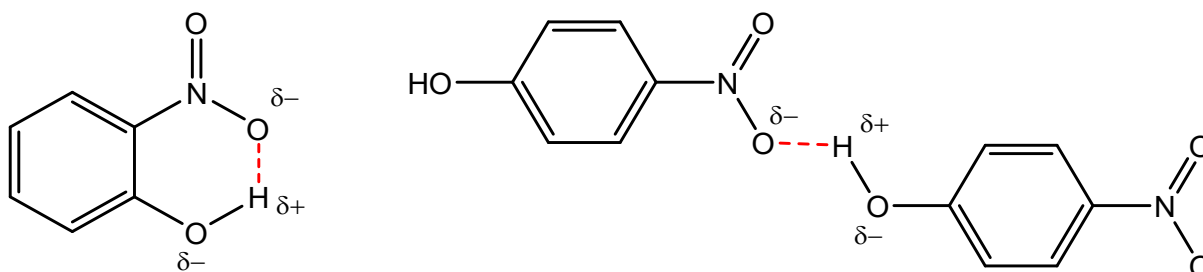
## 1.3 Melting points and energy

To understand the rationale behind different melting points and melting energies, a close look must be taken to the different functional groups, their geometric arrangement and their intermolecular interactions. In-depth knowledge of most major intermolecular interactions is required if a new class of PCMs with an improved thermal behaviour has to be synthesized.

Two intramolecular forces are going to be predominant in this study: hydrogen bonding and van der Waals forces.

### 1.3.1 Hydrogen bonding

Hydrogen bonding is defined as an electrostatic (dipole-dipole) attraction between an electronegative atom and a hydrogen atom which is, at the same time, attached to another electronegative atom. This kind of bonding always involves a hydrogen atom and is going to be grounded on the large difference in the electronegativity between hydrogen and the more electronegative atoms. Another important fact to consider is that hydrogen bonds can occur between molecules, intermolecular, or within parts of a single molecule, intramolecular.



**Figure 1.1.4** – Intramolecular hydrogen bonding in *o*-nitrophenol and intermolecular in *p*-nitrophenol

The most common example to explain hydrogen bonding is related to water molecules. As can be noted in figure 1.1.5, the difference in the electronegativity between the hydrogen and oxygen atoms of the water molecule would favour a dipole where both H would present a partial atomic charge of +0.4 and -0.8 for the O atom. This variation in the charges would affect the orientation of the water molecules, pointing the positive-charged H atoms to the negative-charged O atoms of the neighbouring molecules [55].

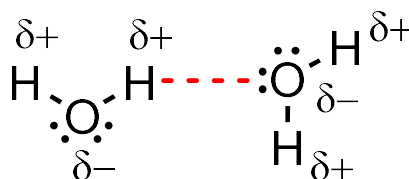


Figure 1.1.5 – Intermolecular hydrogen bonding in a water dimer

Nevertheless, Hydrogen bonding could occur not only with oxygen atoms but also with different atoms, being the most common nitrogen and fluorine. With regard to the electronegativity of the atom which is taking part in the hydrogen bonding, Different bond strengths are going to be observed [56,57].

- F–H⋯:F (161.5 kJ/mol or 38.6 kcal/mol)
- O–H⋯:N (29 kJ/mol or 6.9 kcal/mol)
- O–H⋯:O (21 kJ/mol or 5.0 kcal/mol)
- N–H⋯:N (13 kJ/mol or 3.1 kcal/mol)
- N–H⋯:O (8 kJ/mol or 1.9 kcal/mol)

One other factor which is going to affect the bond strength and energy is going to be the length of the hydrogen bond and its corresponding bonding angle [58]. This bond angle is going to depend on the hydrogen bond donor, thus a thoughtful distribution of hydrogen donor and acceptors has to be present in the future class of PCMs. Moreover, a well-design geometry and a good packing is necessary and has to be taken into consideration as well when developing new PCMs.

### 1.3.2 Van der Waals forces

Beyond covalent/ionic bonds and hydrogen bonding, a different kind of intermolecular interactions may be found in nature. Those are the Van der Waals forces. These attraction/repulsion forces between molecules, atoms and surfaces would be significantly weaker than the rest of intermolecular interactions [59].

Van der Waals forces are going to embrace some different forces as London dispersion force, Debye force and Keesom force [60]. The London dispersion forces are the ones between instantaneously induced dipoles. In the case of Debye forces, the interaction would be between a permanent dipole and an induced dipole, and regarding Keesom force, an interaction between permanent dipoles.

Despite of the previously mentioned issue concerning the weakness of the Van der Waals interactions, these forces have to be considered in long-chain alkane compounds such as paraffins, since they increase with the surface of the molecule. In these particular cases, Van der Waals interactions become increasingly important [59].

## 1.4 Thermoanalytical techniques

In order to study the properties of the candidate materials some thermal analysis was done. In this project two main techniques were fundamental, differential scanning calorimetry (DSC) and thermogravimetric analysis (TGA). Both techniques were carried out in the same machine as is the case in simultaneous thermal analysis (STA) devices which generally refers to the simultaneous application of TGA and DSC to one and the same sample in a single instrument. One advantage of this simultaneous analysis can be the identical conditions for the TGA and DSC signals (same atmosphere, gas flow rate, vapour pressure of the sample, heating rate, thermal contact to the sample crucible and sensor, etc.). Moreover, the STA machine can be improved by coupling to an Evolved Gas Analyzer (EGA) like Fourier transform infrared spectroscopy (FTIR) or mass spectrometry (MS).



**Figure 1.1.6** – STA 449 F1 JUPITER Netzsch employed in most of the STA measurement of this project

### 1.4.1 Differential scanning calorimetry (DSC)

Differential scanning calorimetry (DSC) is a thermoanalytical method where the amount of heat consumed or released by a sample after a perturbation is measured. In the particular case of the DSC, this perturbation is going to be a change in temperature.

During the experiment, two crucibles are going to be located in the same oven, one of the crucibles is empty and serves as reference and the other contains the sample. Both undergo identical conditions of pressure, atmosphere and temperature. For the temperature parameter, there would be a fixed heating rate which means a constant increase as a function of time. The rationale behind the detection of the phase transitions in this technique lies in the fact that, once the sample suffer a phase transition, a different amount of heat has to be applied exclusively to the sample in order to have in both crucibles, sample and reference, the same temperature. This amount of heat transferred to the sample would depend directly on the process, which can be exothermic or endothermic [61].

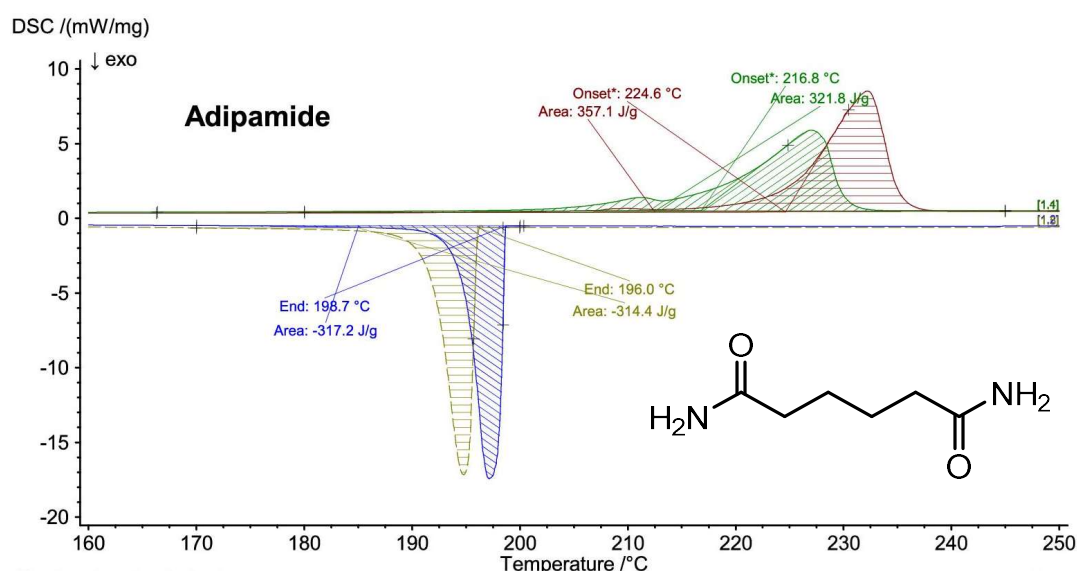


Figure 1.1.7 – Adipamide DSC graph where two cycles of melting-recrystallization were done

Figure 1.1.7 shows the common phase transitions which are going to be encountered in this study, a solid sample which upon heating melts to a liquid and once it cools down, would recrystallize again. This melting-recrystallization procedure is referred to a cycle in this thesis. An application of additional heat to the sample will be needed for the melting transition. Melting processes are endothermic transitions unlike recrystallization, which is exothermic and would require less heat than the reference. Considering all the mentioned above, the heating differences between reference and sample allows to calculate the energy released or absorbed for different PCMs at the phase transition.

### 1.4.2 Thermogravimetric analysis (TGA)

In the case of thermogravimetric analysis (TGA), the mass of the sample is going to be measured over the time as the temperature changes. This thermoanalytical method is going to deliver a valuable input in terms of physical and chemical information as phase transitions, absorption and thermal decomposition among others [62].

Several authors have been using this technique to evaluate the thermal stability of different materials [63,64]. In the particular case of this study, decomposition is going to become the key parameter to measure. Figure 1.1.8 shows in the green line the mass behaviour of the sample and how it is initially losing water and finally decomposing at melting point.

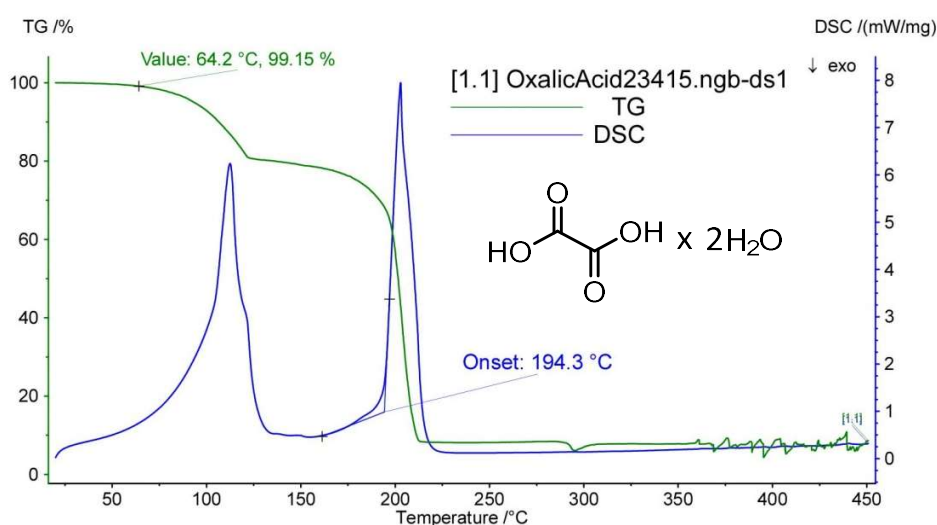


Figure 1.1.8 – Adipamide DSC graph where two cycles of melting-recrystallization were done

## 2. Results and discussion

On the basis that several industrial processes are carried out in boiling water as solvent (or heated by water steam) at ambient or elevated pressure, a target temperature range for our organic PCMs was defined, starting a bit below 100 °C. Thermal stability is paramount too since PCMs must be used in thermal energy storages (TES) devices and hence up-scaled at some point to industrial scale, where a typical volume is  $\geq 10 \text{ m}^3$ . Therefore, the material has to be cheap and stable. A facile synthesis with minimal work-up has to be used instead of synthetic modifications via multi-step routes in order to favour a low-cost product. Moreover, an intended lifetime of 10 years with a daily phase transition would end up in 3650 melting/crystallization cycles. This fact highlighted a need for developing more stable compounds since a material decomposition would negatively affect the storage capacity.

Due to all these project requirements, this study is oriented to temperatures between 80 to 300 °C where a wide range of organic compounds have their melting points. Hence, several families of compounds were analysed and chemical modifications within each family were undertaken in order to influence the melting points and ideally get to higher latent energies and favourable cycle stability. With this approach, new application temperatures within a given compound class would become available. This would be highly interesting, since then organic materials could be modified in order to fit the required temperature range for a given process. Moreover, to confirm that proper thermal behaviour, DSC and TGA measurements from all of them were done.

### 2.1 Towards sugars and derivatives

#### 2.1.1 General considerations

Amongst other organic compounds, sugars are nowadays one of the most interesting and studied candidates for PCMs [32,34-36]. They can reach high melting energies for organic materials up to 300 kJ/kg and melting temperatures in our operational range. They usually show fitting phase change temperatures for medium temperature storage and offer high melting energy capacity, favourable safety and economic conditions.

For all these reasons, they immediately become a main target group and its screening study was divided in sugar alcohols, sugar acids, other sugars and different simple modifications of the aforementioned.

## 2.1.2 Sugar alcohols

Considering all the sugars, sugar alcohols represent the most interesting group in terms of phase change material behaviour. They are able to absorb and release a big amount of energy due to their hydroxy groups which allow efficient hydrogen bonding. In a first series of experiments we conducted simultaneous thermal analysis (STA) measurements of commercially available sugar alcohols.

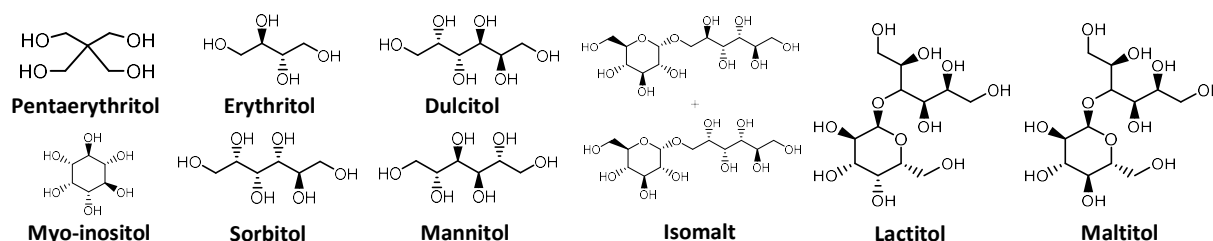


Figure 2.1.1 – Different structures of the initially tested sugar alcohols

It was found that most of the tested compounds (figure 2.1.1) have suitable melting points and they offer well-defined peaks in their DSC with a big gap between melting and degradation, as can be seen from Table 2.1.1 and Figure 2.1.2. At this stage, we observed outstanding phase energies for aliphatic sugar alcohols, such as mannitol, sorbitol and dulcitol, because of their structural symmetry. That distribution of the hydroxy groups favoured effective hydrogen bonding which results in higher latent energies. Only the complex sugar alcohols are not appropriate for the PCMs applications. Lactitol, maltitol and isomalt show a low melting energy. Moreover, isomalt could only recrystallize in the presence of water which limits its applicability in industrial settings.

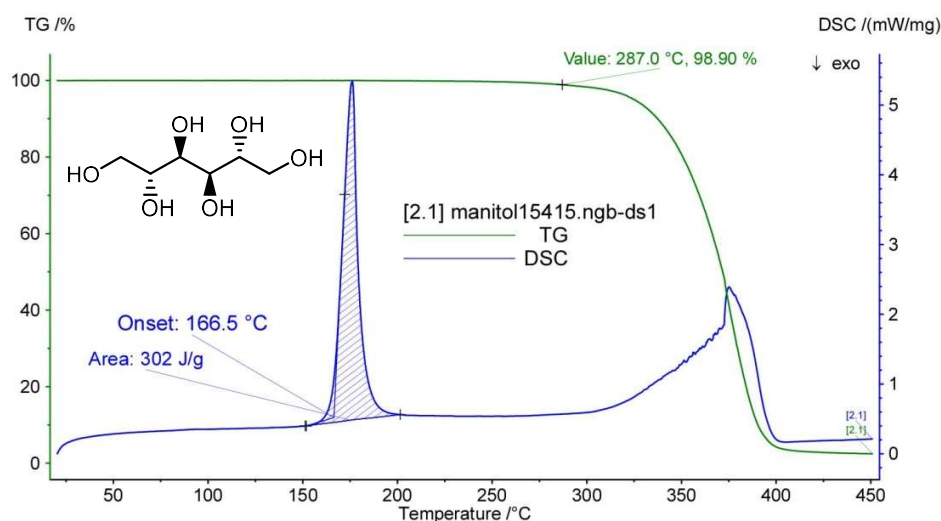


Figure 2.1.2 – Mannitol STA graph

Table 2.1.1 – Sugar Alcohols STA measurements data

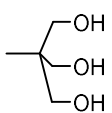
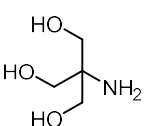
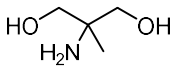
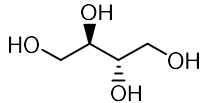
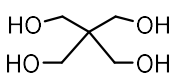
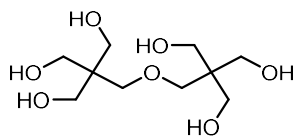
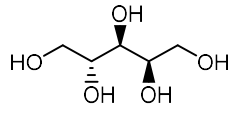
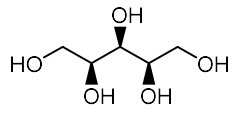
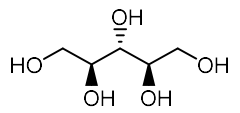
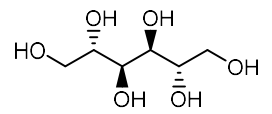
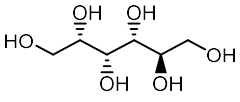
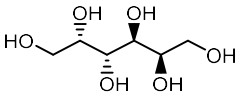
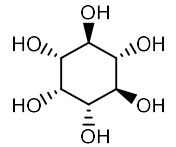
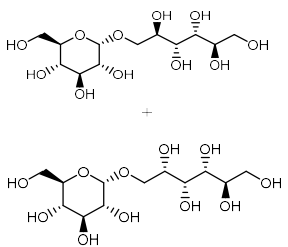
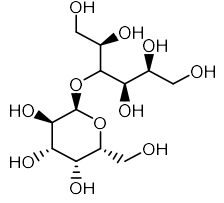
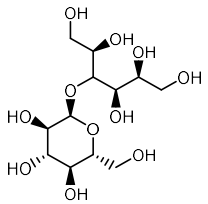
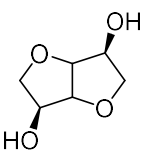
Compound	Structure	MP lit. T (°C)	MP exp. T (°C)	$\Delta H$ Exp (kJ/kg)	Degradation T(TGA)
Pentaglycerine		180	200	249	-
Tris(hydroxymethyl) aminomethane		171	136	352.8	-
Aminoglycol		110	78	-	-
Erythritol		118	119	319.6	244.6
Pentaerythritol		260	187	321.3	238.5
Dipentaerythritol		218	218	318.3	244.5
Arabitol		90	102	230 <sup>[36]</sup>	239
Xylitol		94	93	263.3 <sup>[15]</sup>	278.5
Ribitol		100	102	247 <sup>[36]</sup>	255.5
Mannitol		166	166	307	287.0

Table 2.1.1 – Sugar Alcohols STA measurements data



Compound	Structure	MP lit. T (°C)	MP exp. T (°C)	ΔH Exp (kJ/kg)	Degradation T(TGA)
Sorbitol		111	99	265.7	293.3
Dulcitol		185	187	409.2	318.5
Myo-Inositol		225	224.5	270.7	341.3
Isomalt		145	147.6	113.7	285.1
Lactitol		146	-	142(lit)	-
Maltitol		145	150	200.3	274
Dianhydro mannitol		84	84	175.5	-

It can also be seen on table 2.1.1 that different chain lengths of aliphatic sugar alcohols were measured. Erythritol was the sugar alcohol which represent the 4-carbon length and arabitol and its stereoisomers

(xylitol and ribitol) exhibited the behaviour of the 5-carbon sugar alcohols. It can also be observed that sugar alcohols with an even chain length show larger storage capacity than odd ones due to a better disposition of the hydroxyl groups and therefore a more efficient intramolecular packing. Moreover, different derivatives from erythritol were investigated as pentaerythritol and dipentarythritol. Both are attractive options since they present melting energies in the range of 320 kJ/kg and melting points higher than 200 °C.

Another interesting compound class are the cyclic sugar alcohols. Inositol (figure 2.1.3) is the most relevant and, prominent among them, and another representative is myo-inositol. This is the most common isomer, commercially available with a low price and provides a good latent energy of 270.7 kJ/kg. Considering symmetry and less steric repulsions, it would make sense to include in this study the scyllo-inositol (figure 2.1.4). Scyllo-inositol has a better disposition of the hydroxyl moieties and favourable intramolecular packing but unfortunately the material decomposes once it melts.

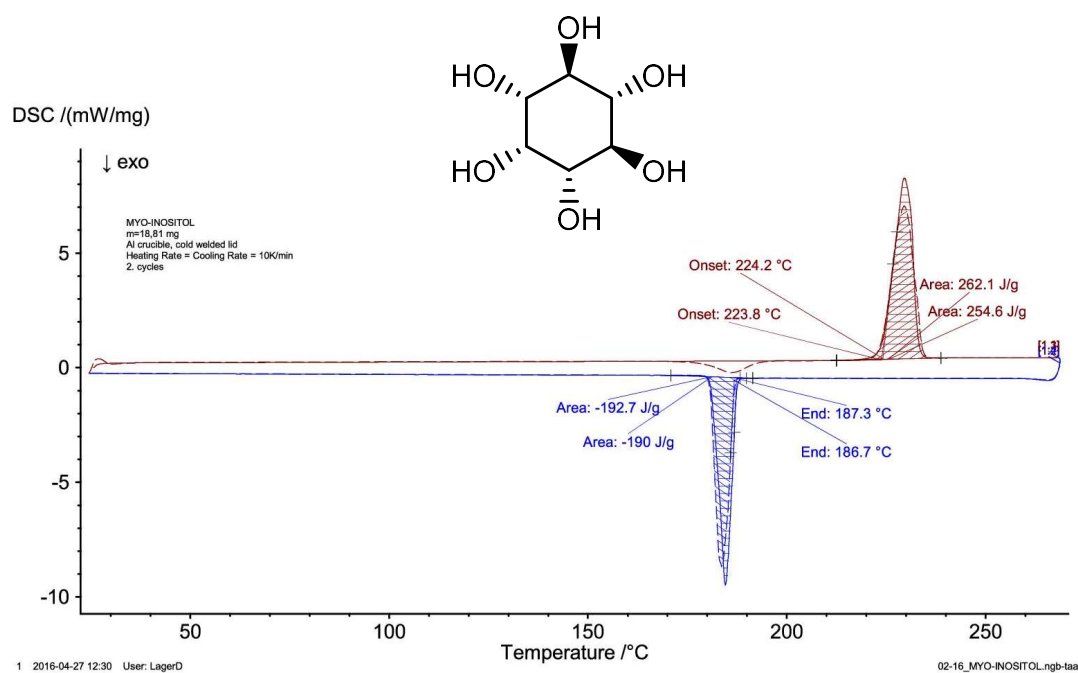
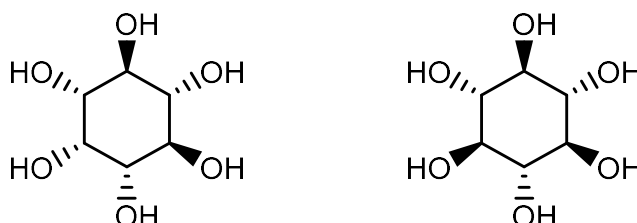


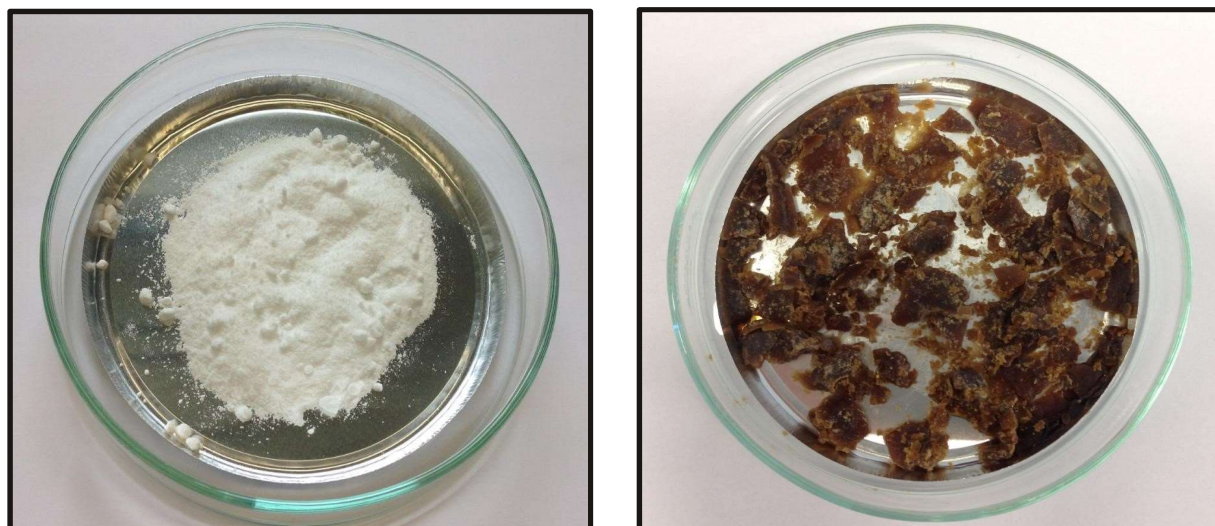
Figure 2.1.3 – Myo inositol DSC graph.



**Figure 2.1.4** – Two inositol isomers structure. Myo-inositol (left) and scyllo-inositol (right).

Finally, some other derivatives from sugar alcohols as pentaglycerine, aminoglycol or tris(hydroxymethyl)aminomethane were measured to complete the group. From them, only pentaglycerine seems to be enough stable after melting to be considered as a promising candidate but its latent energy of 249 kJ/kg is quite low in comparison with other sugar alcohols.

Even if most of these sugar alcohols fit well to the project requirements, thermal stability tests have to be done. Accordingly, mannitol experienced subcooling and degradation after several cycles because of the oxidation of the material in oxygen atmosphere [34]. A simple and effective solution to this problem might be using an inert atmosphere. However, cycle tests carried out at our project partner Südsucker reveal that even under argon atmosphere mannitol loses energy storage capacity after 100 cycles. In this case, the material underwent not only decomposition but also formation of dimers (figure 2.1.5). Something similar occurs with pentaerythritol which also gave decomposition and formation of by-products. For others, such as dulcitol, cycle stability was even less reliable [34,35].



**Figure 2.1.5** – Mannitol sample before (left) and after (right) 100 cycles under argon atmosphere

Only regular erythritol has shown a remarkable thermal behaviour and after 100 cycles it presented significant stability and no significant degradation as long as the maximum temperature reached did not exceed 150 °C (figure 2.1.6). If the temperature rises to 180 °C, some little decomposition was observed.

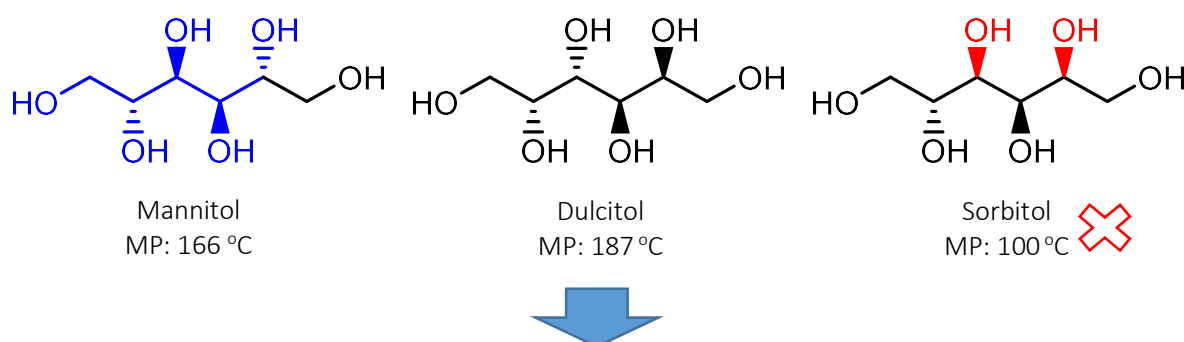
Moreover, some thickening agents such as carboxymethyl cellulose were investigated but finally did not result in higher thermal stable. Regarding the issue of subcooling in sugar alcohols, it has been observed that the addition of some nucleation agents can overcome this problem. [32]

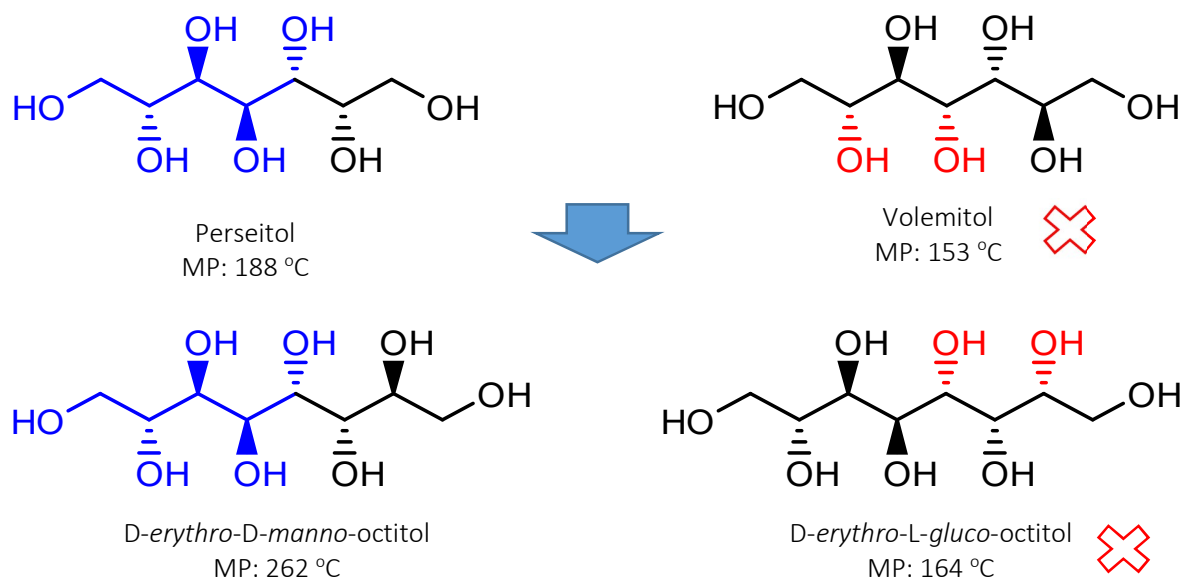


Figure 2.1.6 – Erythritol sample after (left) and before (right) 100 cycles under argon atmosphere

After compiling all the data related to most of the natural occurring aliphatic sugar alcohols, a trend can be observed (scheme 2.1.1 and table 2.1.1) where latent energy and melting point tend to increase in a direct relation with a greater number of carbons in the chain. Accordingly, T. Inagaki and T. Ishida have predicted in their computational design of long chain sugar alcohols [65] outstanding properties in terms of thermal storage. The authors expected higher latent energies for the even sugar alcohols, being C8 and C12 the most promising ones with melting energies around 450 J/g and 500 J/g respectively.

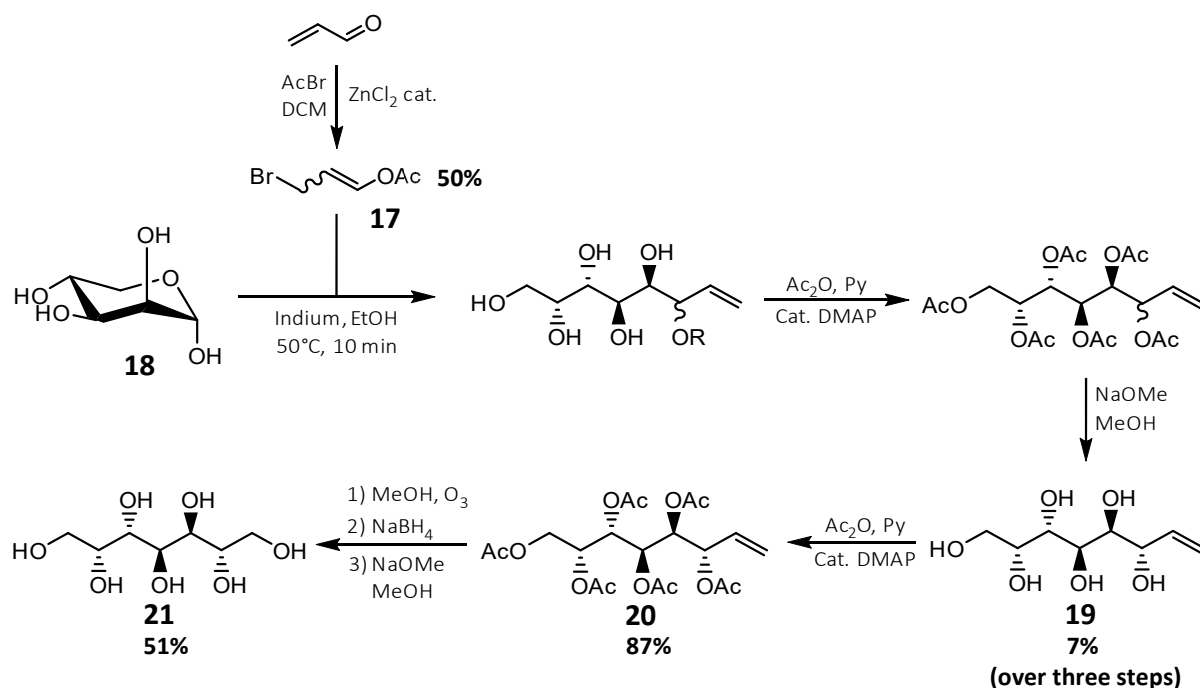
For all these reasons, a synthetic route to obtain octitols was designed, which gives on the way also access to heptitols. It is important to point out that the synthesized sugars must follow a pattern similar to Mannitol or Dulcitol (scheme 2.1.1) where 1,3 interactions of the hydroxy functional groups in anti would favour less repulsions and would impact in the thermal behaviour with higher energies and melting points than 1,3 syn compounds as sorbitol.





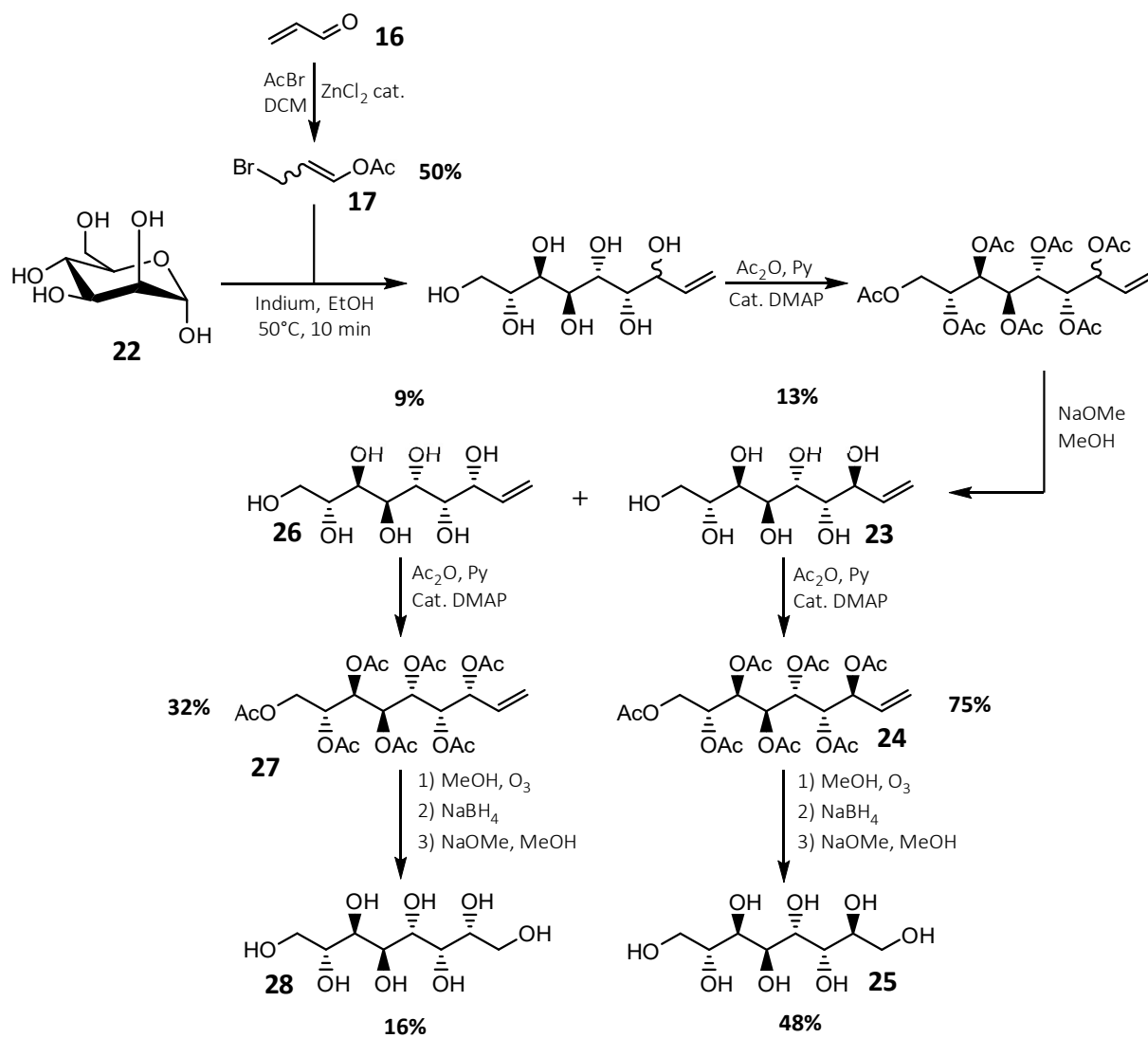
**Scheme 2.1.1** – Different 1-3 hydroxi interactions in hexitols, heptitols and octitols. Marked in red unfavoured 1,3 syn interactions and, therefore, with an X the unfavoured compounds. Marked in blue the common structure that sugar alcohols share

The correctly configured heptose for the synthesis of the perseitol was in fact available due to the methodology developed in the lab for the chain elongation of sugars by indium-mediated acyloxyallylation and ozonolysis [66]. This is the suitable method to secure the necessary configuration in heptitols and octitols for the major compound formed. In principle, only the reduction of the L-glycero-D-manno-heptose to perseitol was required, generally done by using an aqueous solution of sodium borohydride [67]. However, this reduction turned out to be more troublesome than expected and therefore the reported elongation of L-lyxose **18** was repeated and the methodology was [49] only adapted from the original text [66] in the ozonolysis step, where a reductive work-up with NaBH<sub>4</sub> [68,69] was included in order to obtain the heptitol instead of the heptose (scheme 2.1.2). Upon initial experiments, it became clear that for reliable and full reduction of sugar to sugar alcohol it was required to undertake this step at the peracetylated form (**20**). Yields were not optimized since the main objective was to have the material in hand to perform proper thermal analysis.



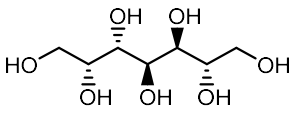
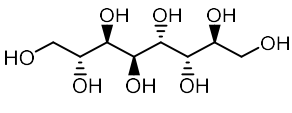
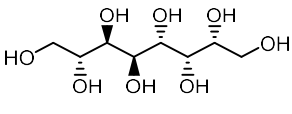
Scheme 2.1.2 – Perseitol synthetic route and yields

The same protocol was then followed for the octitol synthesis starting from D-mannose, except for the separation of the two predominant isomers at the first reaction (acetate stage) in contrast to the crystallisation of 20. The idea behind this is to obtain both *D-erythro-D-manno*-octitol (major isomer) and *D-erythro-L-gluco*-octitol (minor isomer) and compare them with the predicted data reported by T. Inagaki and T. Ishida [65]. Even though high yields are not the main target, some work-up modification was implemented in order to increase the amount of product in the final ozonolysis step for *D-erythro-L-gluco*-octitol **28**. Instead of employing a work-up with a saturated solution of ammonium chloride for a liquid-liquid extraction, a few drops of acetic acids were added and the reaction mixture was concentrated to remove the excess of boron species. Nevertheless, this new procedure could not help to improve the yield compared to the results for perseitol or *D-erythro-D-manno*-octitol (Scheme 2.1.3).



Scheme 2.1.3 – Octitol synthetic route and yields

Table 2.1.2 – Synthesized sugar alcohols STA measurements data

Compound	Structure	MP lit. T (°C)	MP exp. T (°C)	$\Delta H$ Exp (kJ/kg)	Degradation T(TGA)
Perseitol		188	184	260.8	-
D-erythro-D-manno-octitol		262	261	352.2	-
D-erythro-L-gluco-octitol		166	164	163.8	-

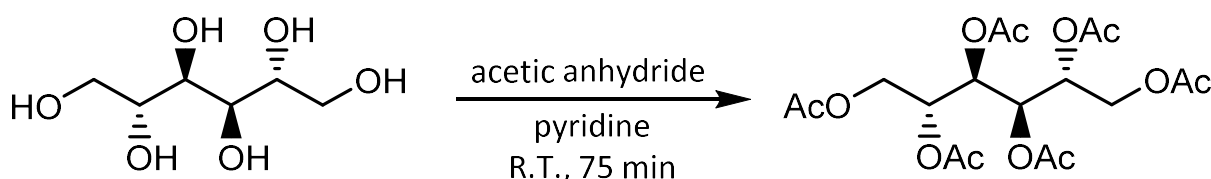
The synthesized sugar alcohols showed an uneven thermal behaviour (table 2.1.2) and showed the predicted trends although with these first samples of material the predicted values could not yet be reached. For example the herein synthesized, D-erythro-D-manno-octitol did not live up to the literature expectations with a melting energy of 352 J/g as compared to the predicted 450 J/g. This melting energy is lower than the expected one from the computational analysis but still higher than other lower-chain sugar alcohols and further is significantly higher than its epimer D-erythro-L-gluco-octitol, as predicted. Nevertheless, this synthetic route to obtain heptitols and octitols is not efficient from an economic viewpoint when ton quantities of a compound have to be prepared. The final product would cost thousands of euros, being far away from the low-cost requirement of this project. They were only synthesized to confirm the increasing trend on melting energies for higher polyols, thus, a new synthetic route would have to be developed in case of upscaling.



### 2.1.3 Acetylated sugars

In order to improve cycle stability, chemical modifications could also be beneficial in order to get to less reactive and hence more stable compounds. In this regard, acetylation reactions on sugar alcohols are the natural first choice since these reactions are typically high yielding and only use inexpensive starting materials, which is important for the large quantity application we have in mind. Additionally, these reactions are often used to block reactive hydroxy groups in sugar chemistry [38].

Acetylation leads of course to the loss of hydrogen bonding, which would lead to a (desired) decrease in melting point but also in melting energy. On the other hand, the molecular weight is significantly increased, which typically has the exact opposite effect, an increase in melting point and eventually also in melting energy. So, it had to be seen, which of the two parameters is of greater importance, possibility for hydrogen bonding or molecular weight. In our hands, all investigated acetylations have shown quantitative yields for all the sugars that were modified. A typical procedure for acetylation used the following conditions depicted in scheme 2.1.4.



**Scheme 2.1.4** – Acetylated mannitol synthetic route

With the acetylated sugars in hand again STA analyses were performed (Figure 2.1.7). The acetylation of sugars provides a product with lower melting point and lower melting energy than the starting material due to the absence of hydrogen bonding possibilities, showing that this is the dominant effect (Table 2.1.3). All the acetylated derivatives, with the only exception of the acetylated myo-inositol, are stable and provide well-defined peaks. Acetylated glucose provides a more stable compound than glucose itself but presents a very low storage capacity of 121.2 kJ/kg. In terms of melting energy, only acetylated dulcitol is able to reach 200 kJ/kg. The rest of acetylated materials (mannitol, sorbitol and pentaerythritol) show melting energies between 139 and 164 kJ/kg and these values are below the requirements of this project.

Our goal of obtaining a lower melting point was achieved but, unfortunately, once the hydroxy groups are substituted by acetyl groups the properties of the material decline regarding latent energy. Considering all these points, acetylation does not improve the overall properties of sugar alcohols as PCMs.

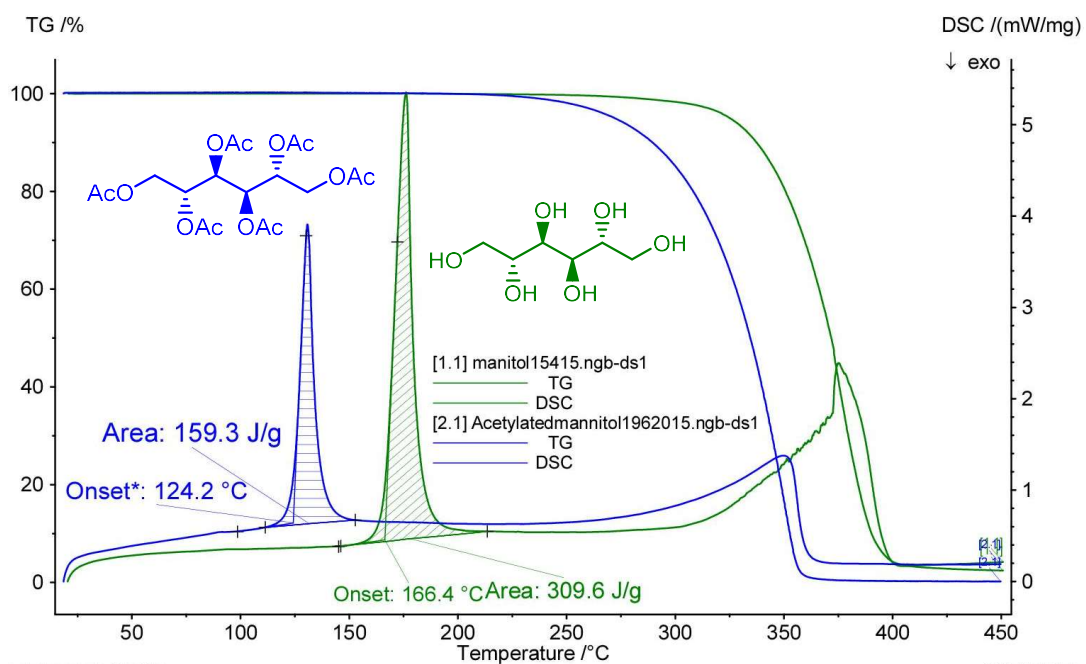
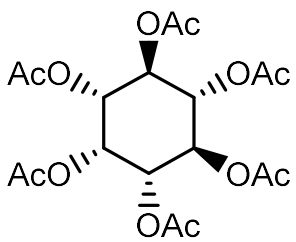
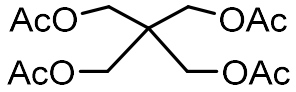


Figure 2.1.7 – Mannitol and its acetylated derivative properties comparison

Table 2.1.3 – Acetylated sugars STA measurements data

Compound	Structure	MP lit. T (°C)	MP exp. T (°C)	$\Delta H$ Exp (kJ/kg)	Degradation T(TGA)
D-galactopyranose peracetate		109	108.1	121.2	213.9
D-mannitol peracetate		120	122.7	164	232.3
D-glucitol peracetate		100	97.3	162.4	171.7
D-galactitol peracetate		171	170.4	200.7	200.7

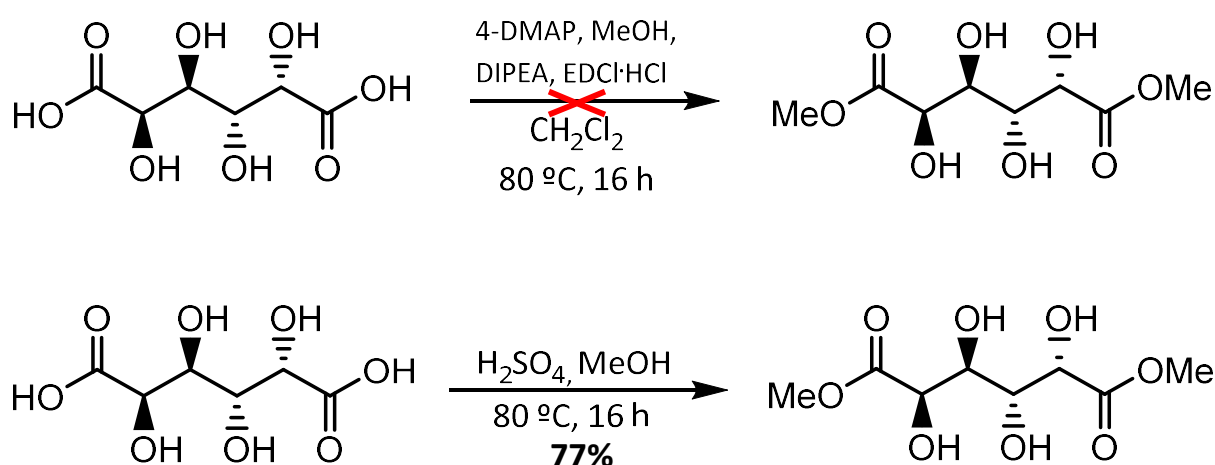
Table 2.1.3 – Acetylated sugars STA measurements data

Compound	Structure	MP lit. T (°C)	MP exp. T (°C)	$\Delta H$ Exp (kJ/kg)	Degradation T(TGA)
Myo-inositol peracetate		214	212.6	Decomposition	210.8
Pentaerythritol peracetate		80	75.3	139.9	142.9

## 2.1.4 Sugar acids and derivatives

Regarding hydrogen bonding, sugar acids seemed to be an excellent option but decomposition was observed when they melt. Carboxylic acid functional groups can undergo decarboxylation reactions upon heating, which might explain their behaviour during the phase change.

In order to confer more stability some modifications such as esterification or amidation were considered. Esterification of tartaric acid generates derivatives with melting points lower as required, with diethyl tartrate being a liquid at room temperature.



**Scheme 2.1.5** – DIPEA protocol (top) shows no conversion and Fischer protocol (bottom) present a yield of 77% for dimethyl galactarate

Meanwhile, esterification of mucic acid with methanol or ethanol gave compounds with suitable melting points between 97 and 192 °C (Table 2.1.4). To this end, dimethyl and diethyl galactarate were synthesized. Initially an esterification with *N,N*-diisopropylethylamine (DIPEA) was tried, however this was not successful. Simple Fischer esterification proved to be successful, i.e. refluxing mucic acid and the proper alcohol in the presence of H<sub>2</sub>SO<sub>4</sub> [70]. The yields using Fischer esterification were 77% for the dimethyl galactarate and 38% for the diethyl galactarate. Unfortunately, both sugar derivatives tend to decompose. The same problem was shown in another common sugar acid, sodium gluconate (Figure 2.1.8). In connection with esterification, another simple modification as amidation was considered. Nevertheless, it has been reported in the literature that amide derivatives from mucic and tartaric acids decompose at their melting point and thereby they were not measured.

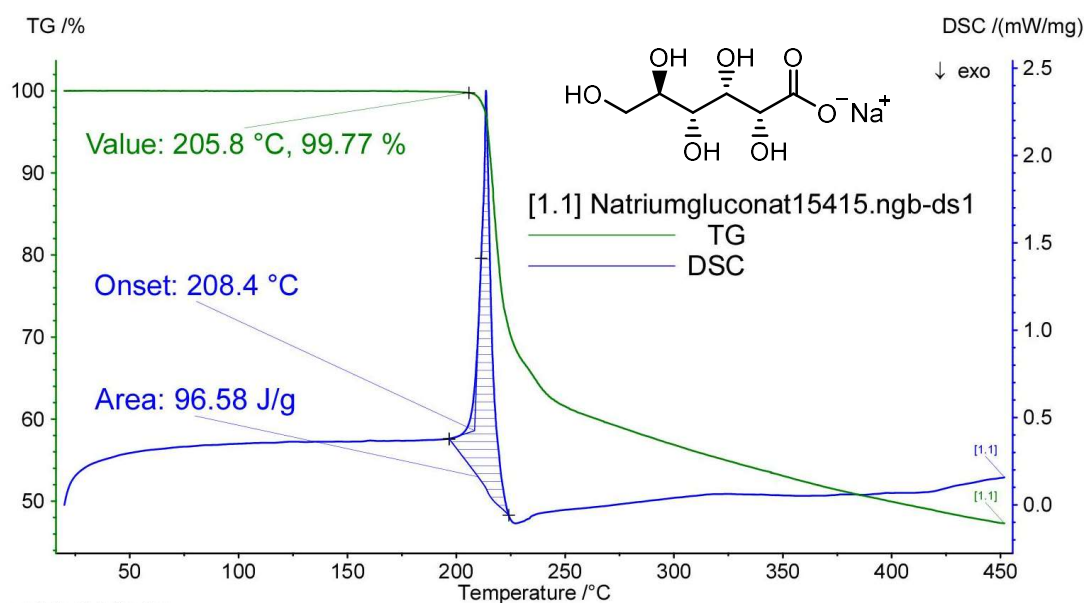
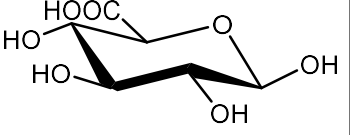
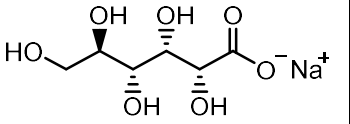


Figure 2.1.8 – Sodium gluconate STA graph

Table 2.1.4 – Sugar acids and derivatives STA measurements data

Compound	Structure	MP lit. T (°C)	MP exp. T (°C)	$\Delta H$ Exp (kJ/kg)	Degradation T(TGA)
Tartaric Acid		210	206.2	Decomposition	205.6
Mucic Acid		220	220.5	Decomposition	214.6
Dimethyl galactarate		189	192.6	Decomposition	180.3
Diethyl galactarate		158	96.9	Decomposition	96.9

Table 2.1.4 – Sugar acids and derivatives STA measurements data

Compound	Structure	MP lit. T (°C)	MP exp. T (°C)	$\Delta H$ Exp (kJ/kg)	Degradation T(TGA)
Glucuronic Acid		156	150.1	Decomposition	193.9
Sodium Gluconate		198	208.4	Decomposition	205.8

## 2.1.5 Other sugars

To get a more complete overview on the potential application of sugars as PCMs, other common sugars were studied. Some of them decompose at the melting point but even when they are stable the energy released is not as big as the sugar alcohols melting energy. Galactose, arabinose and sorbose decompose at the melting point and glucose and xylose deliver melting energies of 264.9 and 237.4 kJ/kg respectively (table 2.1.5). In these last cases, the base of the DSC peak is not really well-defined which could mean a non-reliable material (figure 2.1.9).

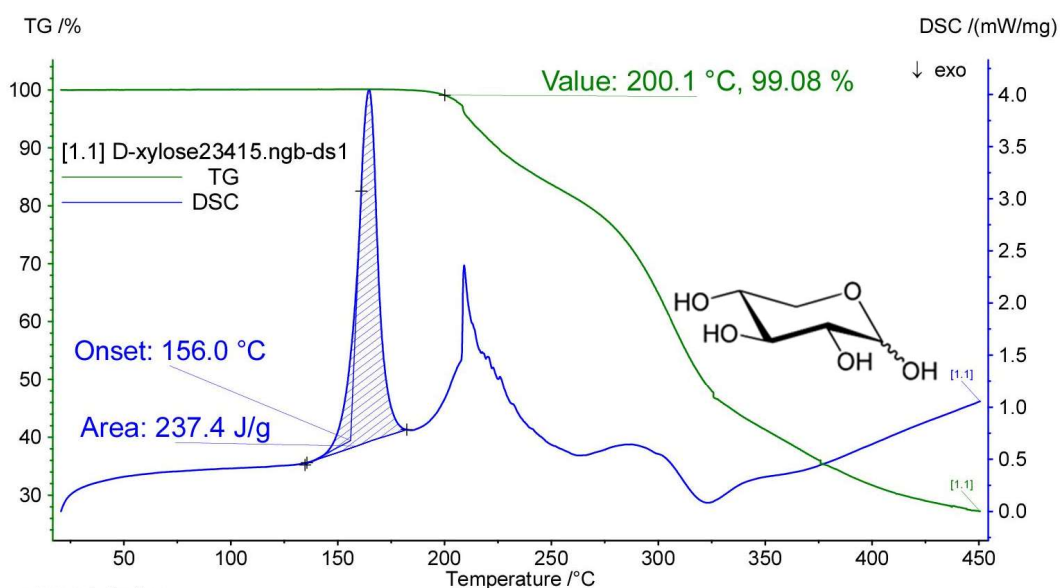


Figure 2.1.9 – Xylose STA graph

One of these compounds, Methyl- $\alpha$ -mannoside, is considered as a very stable sugar and showed a reliable melting pattern in STA measurements and DSC cycle tests (figure 2.1.10). Nevertheless, it presents a melting energy lower than 250 J/g and serious difficulties to recrystallize once the sample was cooled down to room temperature, Thus, complicating the process of releasing back the energy storage.

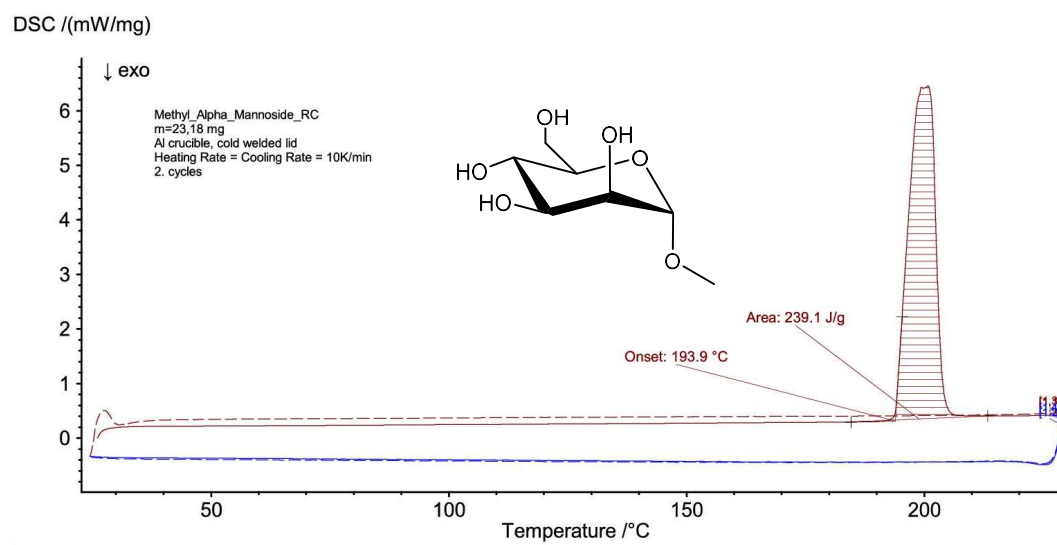
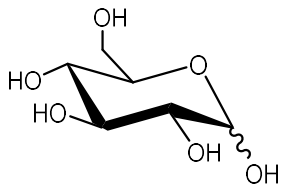
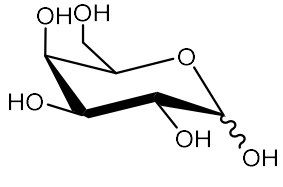
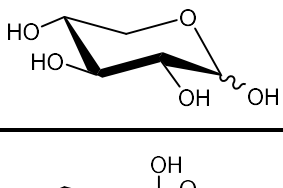
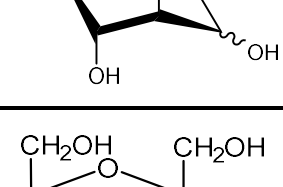
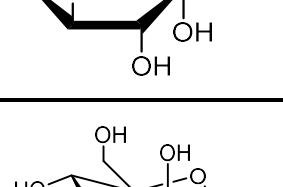
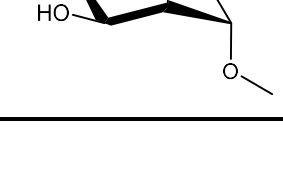


Figure 2.1.10 – Methyl- $\alpha$ -mannoside STA graph



Table 2.1.5 – Other sugars STA measurements data

Compound	Structure	MP lit. T (°C)	MP exp. T (°C)	$\Delta H$ Exp (kJ/kg)	Degradation T(TGA)
D-(+)-Glucose		152	158.1	264.9	204.8
D-(+)-Galactose		163	160.3	Decomposition	193.9
D-(+)-Xylose		154	156	237.4	200.1
D-(+)-Arabinose		164	166.4	Decomposition	190.9
L-(-)-Sorbitose		165	169.6	Decomposition	184.3
Methyl- $\alpha$ -D-mannoside			192.2	223.9	-

## 2.2 Towards arenes

Many substituted benzene derivatives are commercially available and easy to modify by electrophilic substitution reactions and to a lesser extent by nucleophilic aromatic substitutions, which will certainly bring the opportunity to include suitable functional groups and obtain a better design of the compound and therefore an improved PCM. Catechol and resorcinol are the most relevant compounds of this group with melting points close to 100 °C and melting energies of 267.2 and 288.5 kJ/kg respectively. Both generate well defined DSC graphs with a phase change in our required temperature range (figure 2.2.1). The main disadvantage is the melting energy which is lower as compared to sugar alcohols (table 2.2.1). Hydroquinone diethyl ether represents the arene with the highest latent energy, 292.5 kJ/kg. Arenes that show a more complex structure tend to present a low latent energy. Some examples are benzanilide with a melting energy of 185.4 kJ/kg and 4-acetamido benzaldehyde with the lowest storage capacity for the arenes of 172.4 kJ/kg.

In terms of stability only melamine and anthraquinone decompose when they melt but further several cycle tests need to be done to check the long-term stability. Since the melting energy was lower as compared to other compounds, these tests were not carried out.

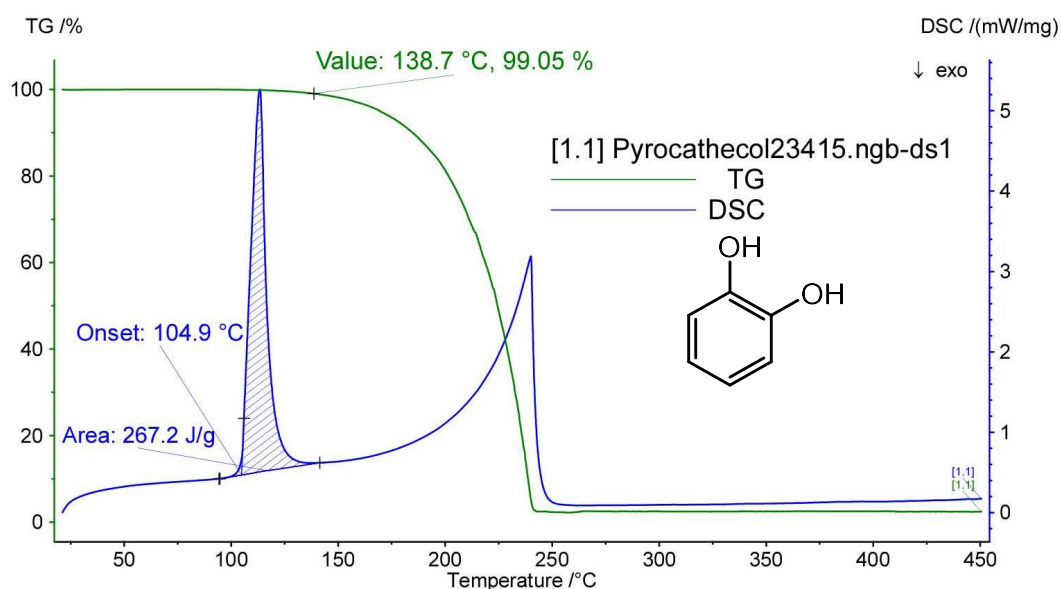


Figure 2.2.1 – Pyrocatechol STA graph

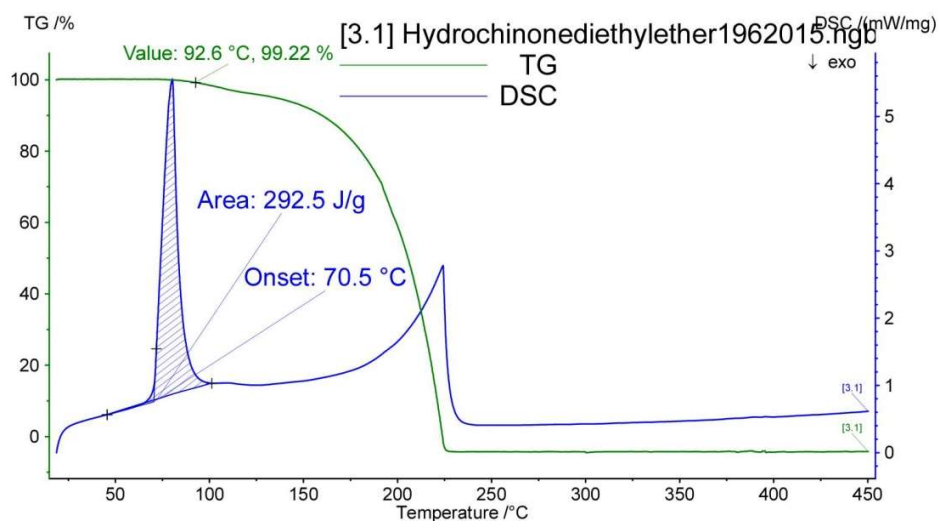


Figure 2.2.2 – Hydroquinone Diethyl ether STA graph

Table 2.2.1 – Arene STA measurements Data

Compound	Structure	MP lit. T (°C)	MP exp. T (°C)	$\Delta H$ Exp (kJ/kg)	Degradation T(TGA)
Pyrocatechol	<chem>Oc1ccccc1O</chem>	105	104.9	267.2	138.7
Resorcinol	<chem>Oc1ccc(O)cc1</chem>	110	110.1	288.5	165.2

Table 2.2.1 – Arene STA measurements Data

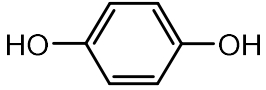
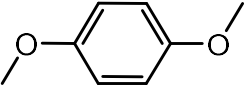
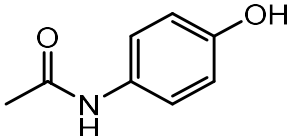
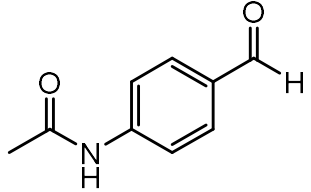
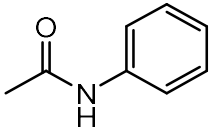
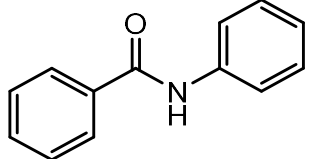
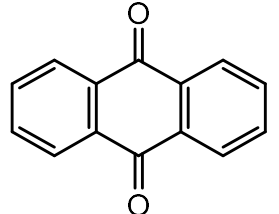
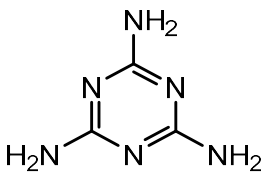
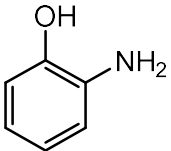
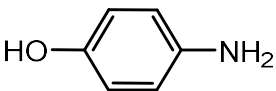
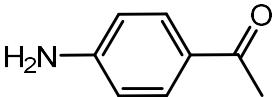
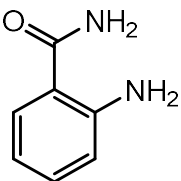
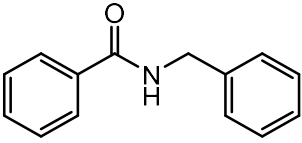
Compound	Structure	MP lit. T (°C)	MP exp. T (°C)	$\Delta H$ Exp (kJ/kg)	Degradation T(TGA)
Hydroquinone		172	173.2	265.2	180.1
Hydroquinone Diethyl ether		60	70.5	292.5	92.6
4-Acetamide phenol		175	169.4	219.2	216.9
4-Acetamido benzaldehyde		156	155.9	172.4	195.1
Acetanilide		114	115.2	217	179.5
Benzanilide		163	163.3	185.4	202.1
Anthraquinone		286	285.3	Decomposition	242.9

Table 2.2.1 – Arene STA measurements Data

Compound	Structure	MP lit. T (°C)	MP exp. T (°C)	$\Delta H$ Exp (kJ/kg)	Degradation T(TGA)
Melamine		354	362.0	Decomposition	290.8
2-Aminophenol		175	176.4	Decomposition	163
4-Aminophenol		189	189.4	270.7	179.8
4-Amino acetophenone			183.1	249.2	256
Anthranilamide		111	112.0	254	201.9
N-Benzyl benzamide		104	106.4	197.7	186.4

## 2.3 Towards amino acids

At first sight, amino acids might seem an interesting group because of their functional groups which can take part in hydrogen bonding. Alanylglycine was reported as the organic compound with the highest melting energy (387 J/g) in this class (figure 2.3.1). All the amino acids measured were purchased or obtained from the university stock (table 2.3.1) and, unfortunately, with no exceptions decompose when they melt. Even when amino acids tend to decompose when they melt, it is possible to obtain their energy data by calculating the area below the DSC peak but in this case that energy is going to be enhanced due to the degradation process. Moreover this group has to be discarded because of the proper degradation itself.

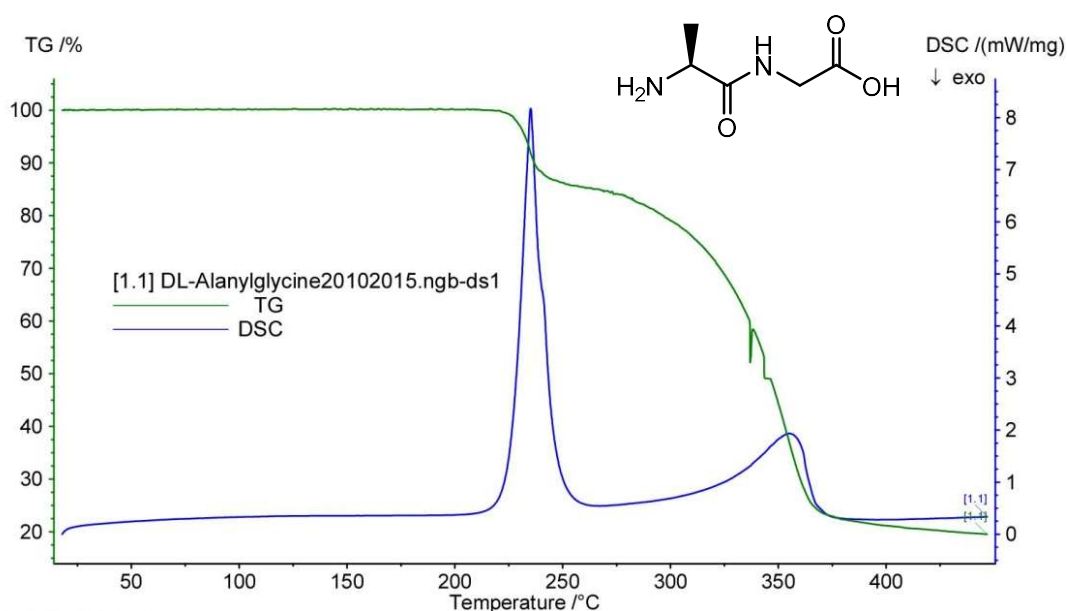


Figure 2.3.1 – Alanylglycine STA graph

Table 2.3.1 – Amino acids STA measurements data

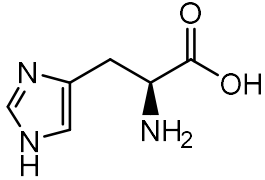
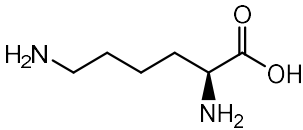
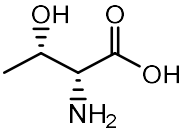
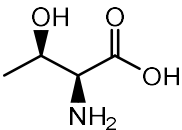
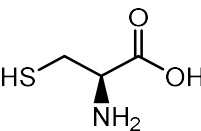
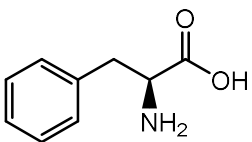
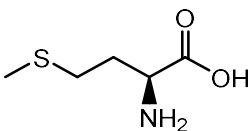
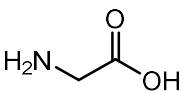
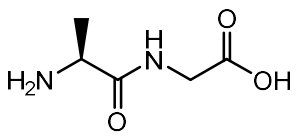
Compound	Structure	MP lit. T (°C)	MP exp. T (°C)	$\Delta H$ Exp (kJ/kg)	Degradation T(TGA)
L-Histidine		287	283.9	Decomposition	281.4
Lysine		224	221.6	Decomposition	219.4
D-Threonine		255	253.4	Decomposition	244.5
L-Threonine		255	255.8	Decomposition	252.0
L-Cysteine		240	217.5	Decomposition	213.3
Phenylalanine		275	276.9	Decomposition	273.3
Methionine		281	281.9	Decomposition	270.3
Glycine		233	251.8	Decomposition	246.6

Table 2.3.1 – Amino acids STA measurements data

Compound	Structure	MP lit. T (°C)	MP exp. T (°C)	$\Delta H$ Exp (kJ/kg)	Degradation T(TGA)
Alanylglycine		228	223.7	Decomposition	-



## 2.4 Towards purines and pyrimidines

Purines and pyrimidines are another group of organic compounds abundant in nature which present a good number of hydrogen donors and acceptors. It is for these two reasons that they were initially considered for an initial screening measurement. Nevertheless, most of the purines and pyrimidines analysed in this project, just as amino acids, used to decompose when they change the phase (table 2.4.1). Only caffeine is relatively stable (figure 2.4.1) and even in this case, the melting energy is far from our energy requirements (110.1 kJ/kg). For all these reasons, the group was discarded.

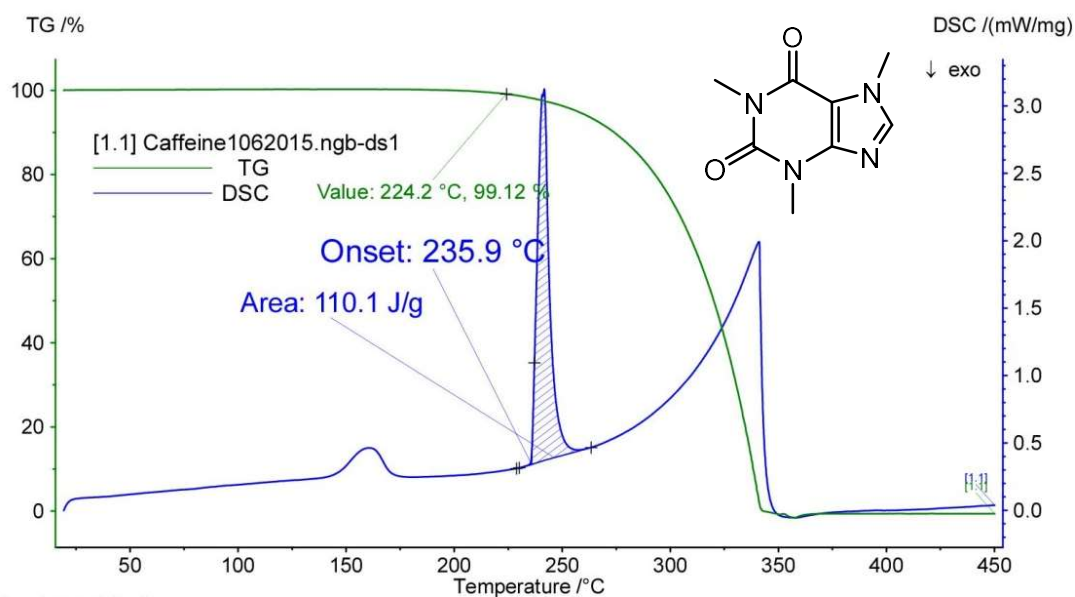


Figure 2.4.1. – Caffeine STA graph

Table 2.4.1. – Purines and pyrimidines STA measurements data

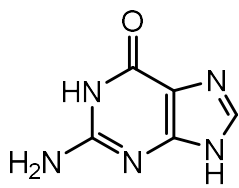

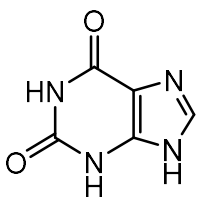
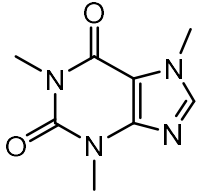
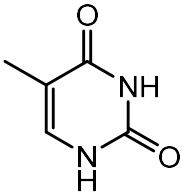
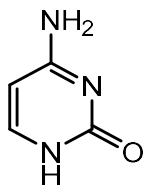
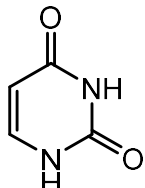
Compound	Structure	MP lit. T (°C)	MP exp. T (°C)	$\Delta H$ Exp (kJ/kg)	Degradation T(TGA)
Guanine		360	-	-	-
Adenine		360	360	Decomposition	265
Xanthine		300	413.4	Decomposition	370.9
Caffeine		235	235.9	110.1	224.9
Thymine		317	320.2	Decomposition	248.8

Table 2.4.1. – Purines and pyrimidines STA measurements data

Compound	Structure	MP lit. T (°C)	MP exp. T (°C)	$\Delta H$ Exp (kJ/kg)	Degradation T(TGA)
Cytosine		300 - 325	314.8	Decomposition	317.1
Uracil		335	339.9	Decomposition	300.3

## 2.5 Towards dyes

Due to the fact that one important requirement which must be considered beyond the melting point and melting energy is the cost of the material, different organic compounds from industrial applications were analysed. Dyes are widely employed in the textile industry and will offer bulk discounts when a set amount is purchased.

Taking into consideration the above discussion, the first dye included in this list (table 2.5.1) was indigo. Indigo is a natural dye extracted from the leaves of certain plants which is also well known for his contribution to the colour of denim cloth and blue jeans in the textile industry. To complete the group, three azo dyes were measured as well. Para red is the first azo dye discovered in 1880 that dyes cellulose fibers with a red colour and, on the other hand, methyl orange and methyl red are both azo dyes which are widely employed as pH indicators.

Nevertheless, none of these dyes have shown appropriate properties. Generally, the materials decompose at the melting point (figure 2.5.1). In case a decomposition was not observed, the energy released is lower than our minimum melting energy target, >150 °C (figure 2.5.2). In all cases, dyes are not an interesting group for PCMs applications.

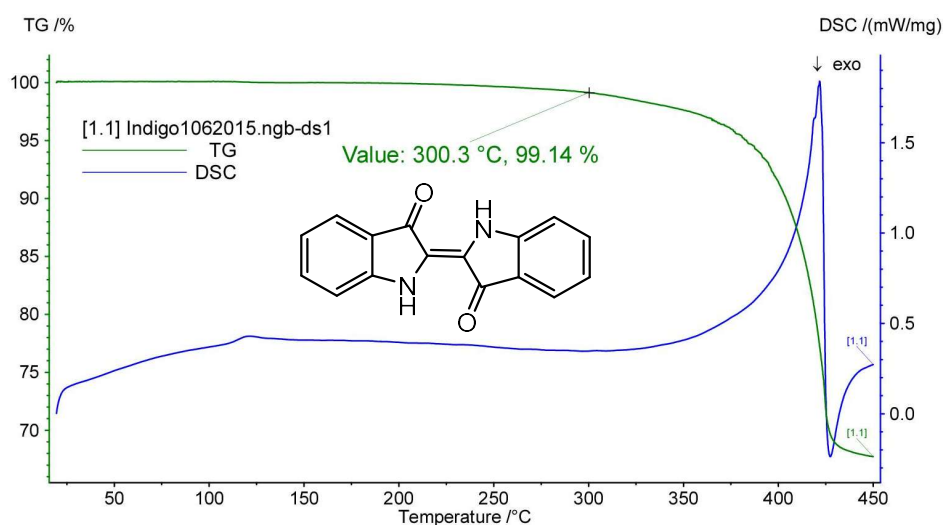


Figure 2.5.1 – Indigo STA measurement

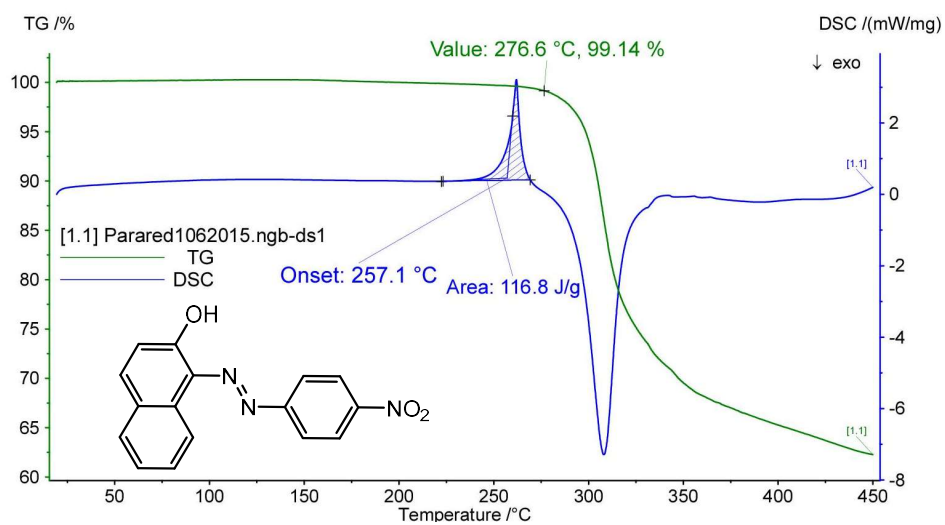


Figure 2.5.2 – Para red STA measurement

Table 2.5.1 – Dyes STA measurements data

Compound	Structure	MP lit. T (°C)	MP exp. T (°C)	$\Delta H$ Exp (kJ/kg)	Degradation T(TGA)
Indigo		390	390	Decomposition	300
Para Red		248	257.1	116.8	276
Methyl orange		300	374.6	Decomposition	153.2 / 351.8
Methyl red		179	179.1	Decomposition	114.1 / 179.3

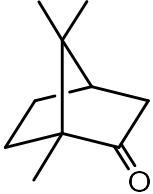
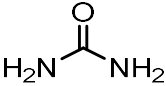
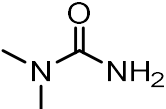
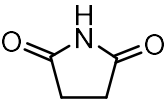
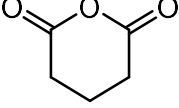
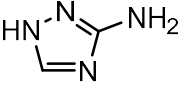
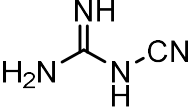
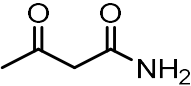
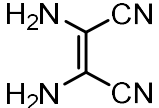
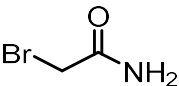
## 2.6 Towards other organic compounds

Beyond the main groups, some other compounds were tested which are summarized in this chapter. Some remarkable addition might be, on one hand, acetamide which shows a large melting energy with a melting point lower than the water boiling point. Some other derivatives from acetamide, as acetoacetamide, diethylacetoamido malonate and 2-bromoacetamide, were considered. Acetoacetamide has a melting point of 54 °C, which is far from the minimum 80 °C required. By contrast, 2-bromoacetamida and diethylacetoamido malonate have a melting point of 87 °C and 95°C but only a storage capacity of 228.7 and 227.4 kJ/kg respectively. Other small organic compounds with similar structure would also be interesting. Urea and its derivative, dimethylurea were tested but both decompose at their melting temperatures 135.2 and 183.2 °C respectively. Dicyandiamide and Diaminomaleonitrile are structure-related to urea too and they present the same thermal behaviour by decomposing at melting. A very common terpenoid as camphor was also tested and decomposed at the melting transition. 3-amino-1,2,4-triazol, for instance, do not decompose but its melting energy, 237.5 kJ/kg, is below the minimum requirements. On the other hand, succinic and glutaric anhydride, both in the requirement range of the project. Thus, these three compounds might be considered for further tests. However, there are more promising candidates in other groups as sugar or acids and therefore these three compounds were relegated to a secondary level. Succinimide present a close structure to succinic anhydride but less storage capacity, 239.9 kJ/kg, below the melting energy required in this project.

The rest were not fitting due to some of our requirements and that is why they were discarded.

**Table 2.6.1** – Other organic compounds STA measurements data

Compound	Structure	MP lit. T (°C)	MP exp. T (°C)	$\Delta H$ Exp (kJ/kg)	Degradation T(TGA)
Acetamide		80	80.4	372.2	128.2
Diethylacetamido malonate		95	96.5	227.4	170.1
Succinic anhydride		118	116.9	252	154.9

Camphor		175	-	Decomposition	-
Urea		132	135.2	Decomposition	-
1,1-Dimethylurea		180	183.2	Decomposition	163.6
Succinimide		123	125.5	239.9	177.8
Glutaric anhydride		55	97.6	295.8	188.1
3-amino-1,2,4-triazol		151	149.6	237.5	196.4
Dicyandiamide		209	200.7	350.2	-
Acetoacetamide		54	-	Decomposition	-
Diamino maleonitrile		182	-	Decomposition	-
2-bromoacetamide		87	81.2	228.7	125.3

## 2.7 Towards fatty acids

Fatty acids are one of the most commonly used phase change materials for technical applications [7,15,18,96]. However, they were initially ruled out due to their low melting points, which are below our predefined requirements.

Another interesting option would be the amides of this fatty acids. They show higher melting points than their respective acids (table 2.7.1) and they can be prepared easily or obtained at low cost.

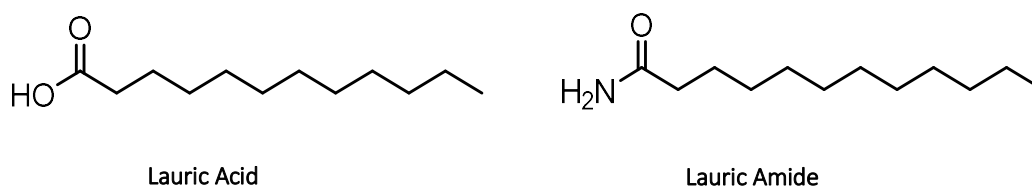


Figure 2.7.1 – Fatty acids and amides structure

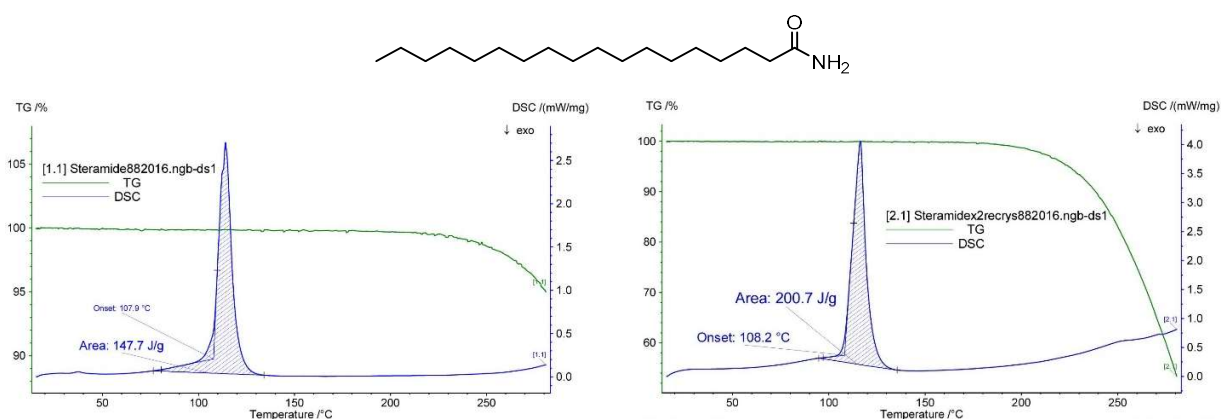
Table 2.7.1 – Fatty acids and amides melting points comparison

Name	Number of C	Acid Melting point	Amide Melting point
Lauric Acid	12	43	100
Myristic Acid	14	54	102
Palmitic Acid	16	63	103
Stearic Acid	18	69	107
Arachidic Acid	20	75	109
Behenic Acid	22	80	111

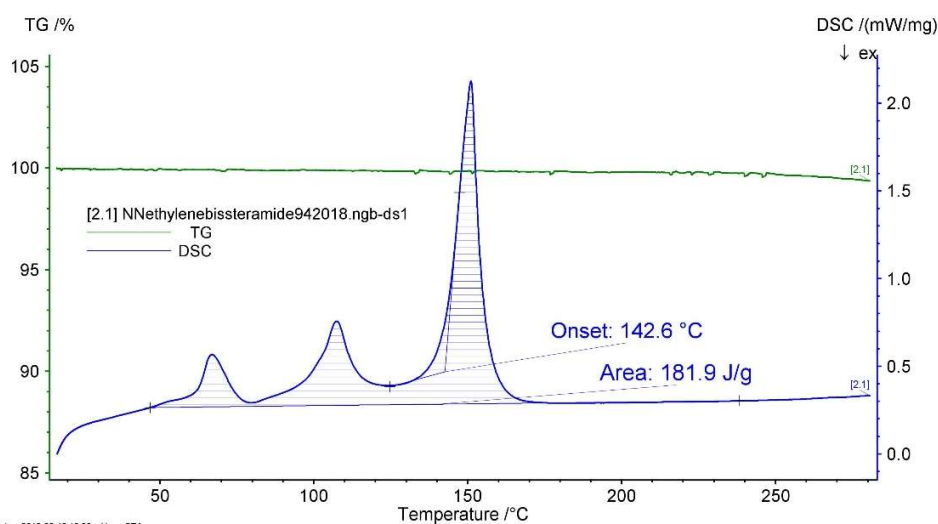
Due to these considerations, commercial stearamide was purchased from Sigma-Aldrich in order to obtain first DSC data from a fatty acids amide. The initial batch had an 85% purity and as it could be observed in figure 2.7.2 below, the melting energy was far from our minimum requirements. Given this fact and in order to have a realistic overview from the amides of fatty acids, two recrystallizations in ethanol of the stearamide were done. A pure product was obtained for new STA measurements and it was observed that, even though there is an increase in the phase transition energy with regard to the first stearamide sample, the melting energy is still far from our best materials. Still, the goal to increase the melting point was reached and pure stearamide gave a melting point of 108 °C.



Finally, a last compound was measured to close the fatty acids chapter. The *N,N'*-ethylenebis(stearamide) is a compound obtained from the reaction of ethylenediamine and stearic acid and it was expected some improvement in the melting energy because of the long aliphatic chain and the presence of hydrogen bonding donors and acceptors. However, figure 2.7.3 showed two solid-solid phase transitions and a STA graph where the melting energy is below 200 J/g. These solid-solid phase transitions are common too in the oxalamides which present long aliphatic chains at both sides.

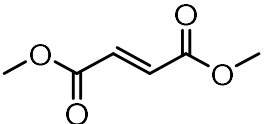
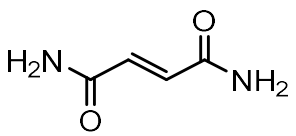
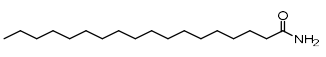
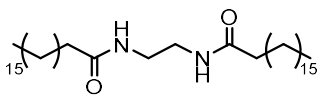


**Figure 2.7.2** – STA graph from the 85% pure stearamide (left) and the same batch after two recrystallizations (right)



**Figure 2.7.3** – *N,N'*-Ethylenebis (stearamide) STA graph after 2 recrystallizations

Table 2.7.2 – Fatty acids and amides STA measurements data

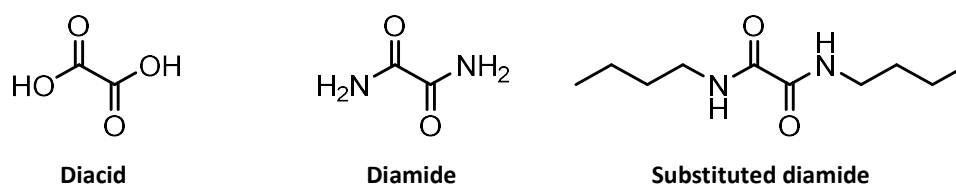
Compound	Structure	MP lit. T (°C)	MP exp. T (°C)	$\Delta H$ Exp (kJ/kg)	Degradation T(TGA)
Methyl fumarate		102	94.1	294.2	102.8
Fumaramide		265	265	Decomposition	183
Stearamide		102	108.2	200.7	-
N,N'-Ethylenebis(stearamide)		144	142.6	181.9	-

## 2.8 Towards carboxylic acids and derivatives

The group of carboxylic acids and derivatives is probably the most promising one together with the well-known group of sugars. At first sight, it might seem that they are not as stable as other groups because of the reactive carboxylic acid group but some dicarboxylic acids do not show decomposition when they melt and an energy capacity close or even bigger than sugar alcohols

As in the sugars, some modifications such as esterification or amidation were carried out in an attempt to overcome the problem of stability that some acids showed. In general terms, esterification has given a material which presents a poor thermal performance because of the loss hydrogen bonding possibility but amidation gave some interesting products with outstanding properties for medium temperature storage.

Regarding this good behaviour for the diamides, some other derivatives were considered such as substituted diamides with different lengths of alkene chains. It might be expected that this can increase the melting energy due to the London interactions of the alkene chain added. Moreover, a symmetrical geometry is maintained



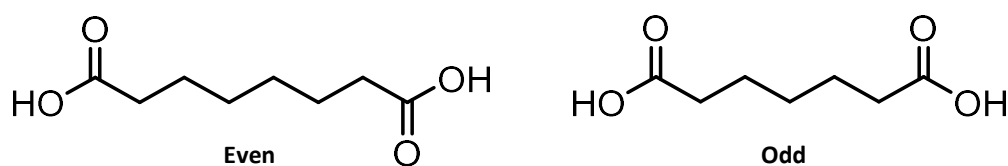
**Scheme 2.8.1** – Dicarboxylic Acid, Diamide and Substituted diamide structures

In the following subchapters our investigations into these directions will be discussed in detail.

### 2.8.1 Dicarboxylic acids

From all the carboxylic acid derivatives, the dicarboxylic acids are both, more stable and able to store more energy than the rest because of their two terminal carboxylic acid moieties and the long alkyl chain in between, which allow a better intramolecular packing, a more efficient hydrogen bonding from the carboxylic acid groups and Van der Waals interactions from the alkyl linker. Considering these facts, the aim was increasing the length of the alkyl chain between the two terminal carboxylic acid groups in order to find a trend that could deliver an outstanding material and to help improving other different compounds in future

Simple dicarboxylic acids show a particular behaviour. Depending on their overall number of carbon atoms they are going to be named “odd” and the functional groups are oriented in the same direction due to the carbon chain length or “even” when they have an even number of carbons and both carboxylic groups are oriented in different directions (Scheme 2.8.2) [71]



Scheme 2.8.2 – Dicarboxylic acid structures

These two different geometries are going to determine the properties of the material. It was observed that because of the functional group orientation, odd or even, the acids offer different values of melting temperatures and enthalpy. Even compounds present a multilayer structure as result of their crystal packing which allow consonance between hydrogen bonding and dispersive interaction. On the other hand, odd compounds offer weak packing because of a strained three-dimensional network [97-99]

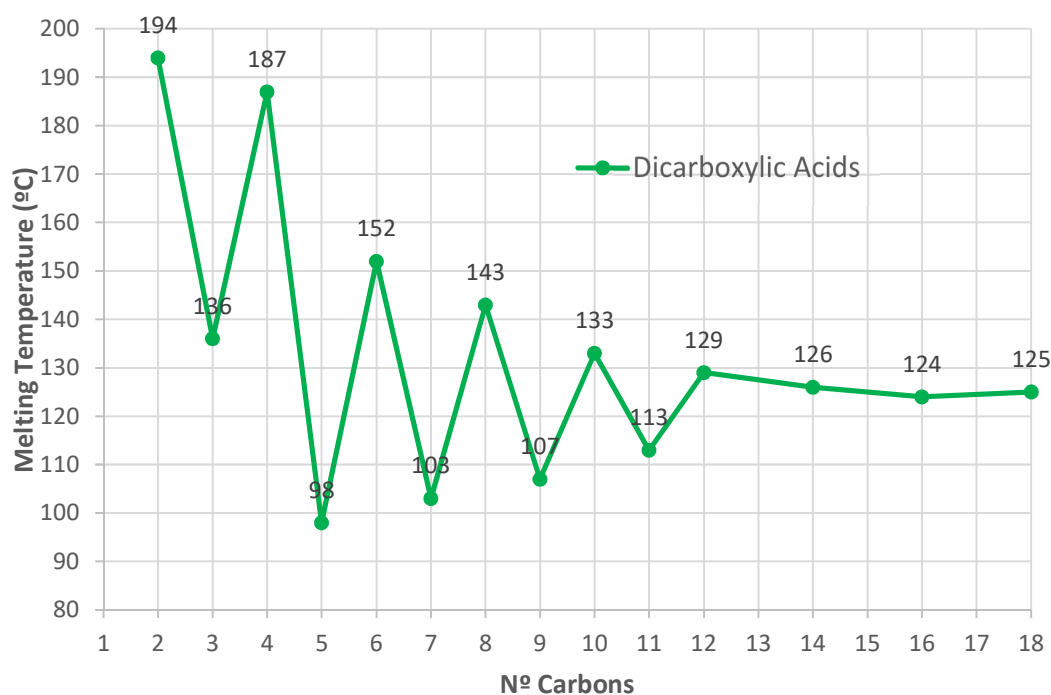


Figure 2.8.1 – Melting points of dicarboxylic acids as a function of number of C-atoms

As a consequence, even dicarboxylic acids show higher melting points and melting enthalpy. A glance at figure 2.8.1 gives a better overview of the differences between odd and even compounds. Even compounds show always higher melting points than odd ones but as the length of the alkyl chain in between the terminal carboxylic acid groups increases, this difference becomes smaller and smaller until it levels out. This levelling is the result of the increase in importance of Van der Waals interactions from

the alkyl chain. As the number of carbons in the alkyl chain increases, the two carboxylic groups have less relevance and the main contribution to the melting energy comes from the aliphatic section. This effect can be observed in the even compounds (acids with 14,16 and 18 carbons) and between odd and even acids.

The odd-even effect is observed in the melting energy as well to some extent (figure 2.8.2). For this reason, it makes no sense in going further on the synthesis of higher dicarboxylic acids than octadecanedioic acid. The whole set of dicarboxylic acids measured (table 2.8.1) fits to the odd-even effect considering the melting points and energies and it only could find some deviations once the melting energy of the C16 and C18 diacid is observed. C16 storage capacity is a bit larger than the one for C18.

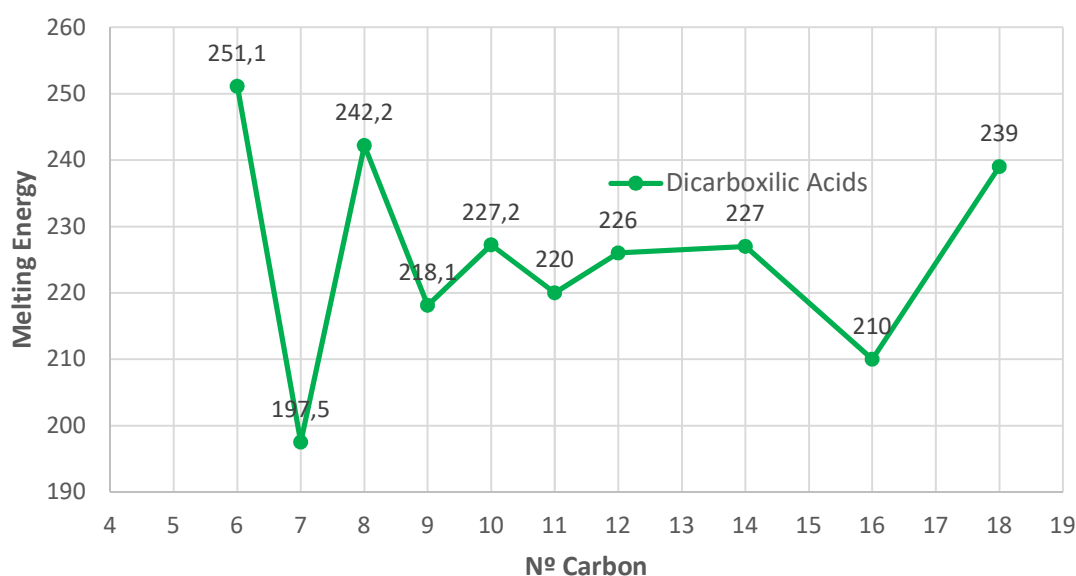


Figure 2.8.2 – Dicarboxylic acid melting energies

However, In the STA machine employed to make these measurements, it was possible to get some valuable information about the stability of the dicarboxylic acids presented on table 2.8.1. As figure 2.8.3 and figure 2.8.4 show, the compound is stable after melting and there is at least 50 °C of difference from the melting point to the degradation point. According to this and the odd-even effect we are going to consider adipic- (C6), suberic- (C8), sebacic- (C10) and dodecanedioic acid (C12) among the most interesting materials. It can be expected that sebacic- and dodecanedioic acid are the more stable ones in long term cycle tests since adipic acid may undergo intramolecular reactions to form a favourable 6-membered ring. In contrast, 10 and 12-membered rings are not so easily formed. Anyhow, most of the dicarboxylic acids seem to fit excellent to our requirements. Only oxalic and succinic acids decompose when they melt.

Finally, some derivatives of dicarboxylic acids as 2,2 – dimethyl succinic acid and diamino pimelic acid were measured but both decompose at melting point too.

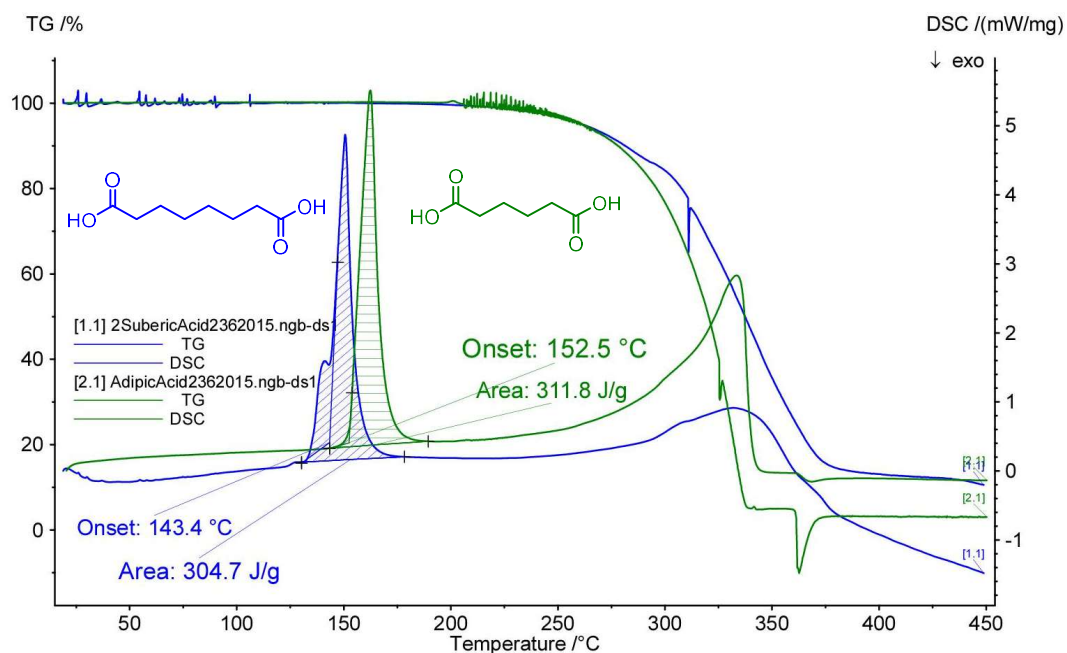


Figure 2.8.3 – Adipic (C6) and suberic (C8) acids STA graphic

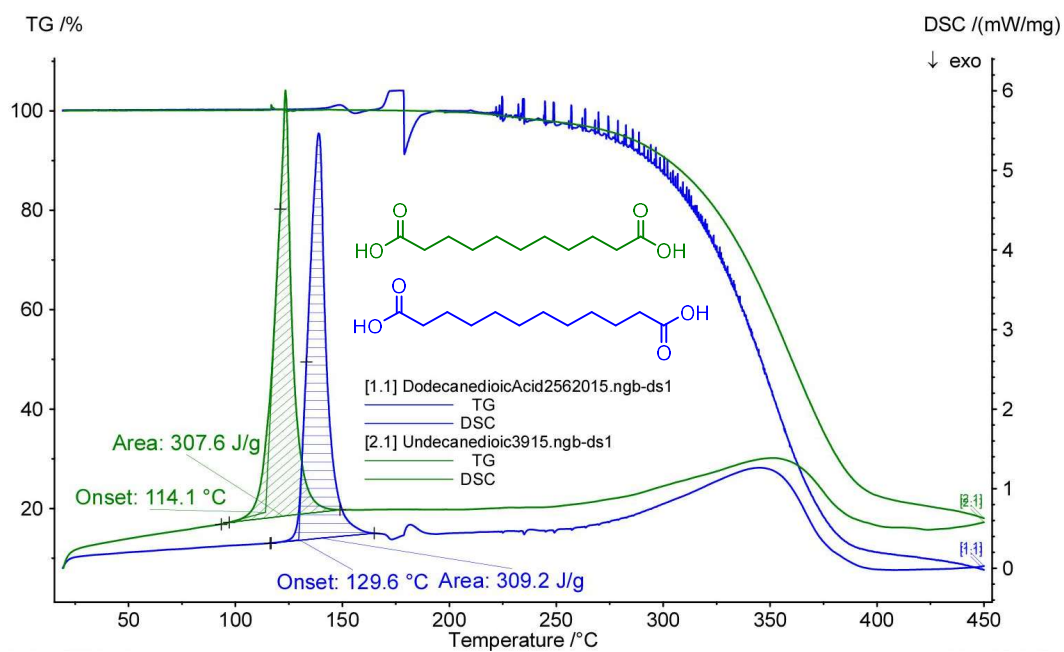
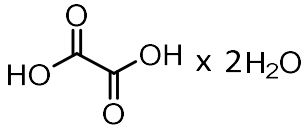
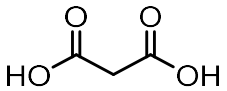
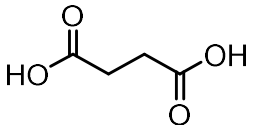
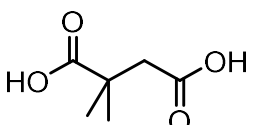
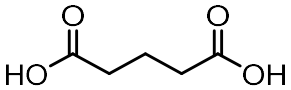
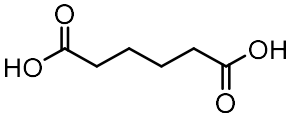
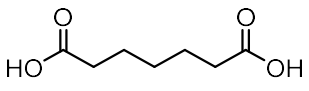
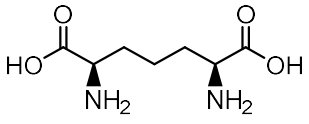
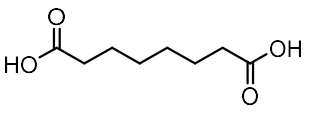
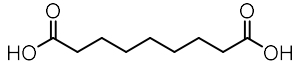
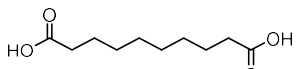
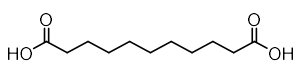
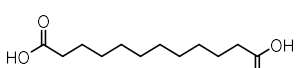
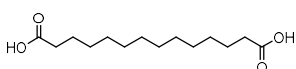
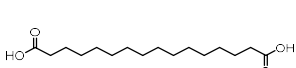
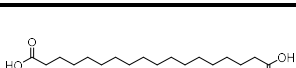


Figure 2.8.4 – Undecanedioic (C11) and dodecanedioic (C12) acids STA graphic

Table 2.8.1 – Dicarboxylic acids STA measurements data

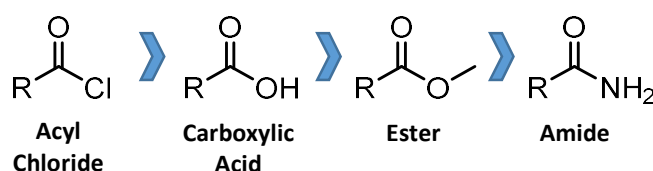
Compound	Structure	MP lit. T (°C)	MP exp. T (°C)	$\Delta H$ Exp (kJ/kg)	Degradation T(TGA)
Oxalic acid dihydrate		101.5	194.3	Decomposition	-
Malonic acid		135	136.3	295	153.8
Succinic acid		187	187.7	Decomposition	197.8
2,2 – dimethyl succinic acid		139	142.9	Decomposition	159.9
Glutaric acid		95	98.7	237.3	190.2
Adipic acid		151	152.4	312.6	208.1
Pimelic acid		105	106.5	322.3	144.2
Diaminopimelic acid		316	267.3	Decomposition	122.1
Suberic acid		143	143.2	239.5	218.5

Compound	Structure	MP lit. T (°C)	MP exp. T (°C)	$\Delta H$ Exp (kJ/kg)	Degradation T(TGA)
Azelaic acid		105	107.1	317	230.3
Sebacic acid		131	133.6	295.4	232.8
Undecanedioic acid		111	113.7	306	220.2
Dodecanedioic acid		127	129.6	308.5	-
Tetradecanedioic acid		123	126.4	240.2	-
Hexadecanedioic acid		124	123.7	213.7	-
Octadecanedioic acid		124	125.5	237.7	-



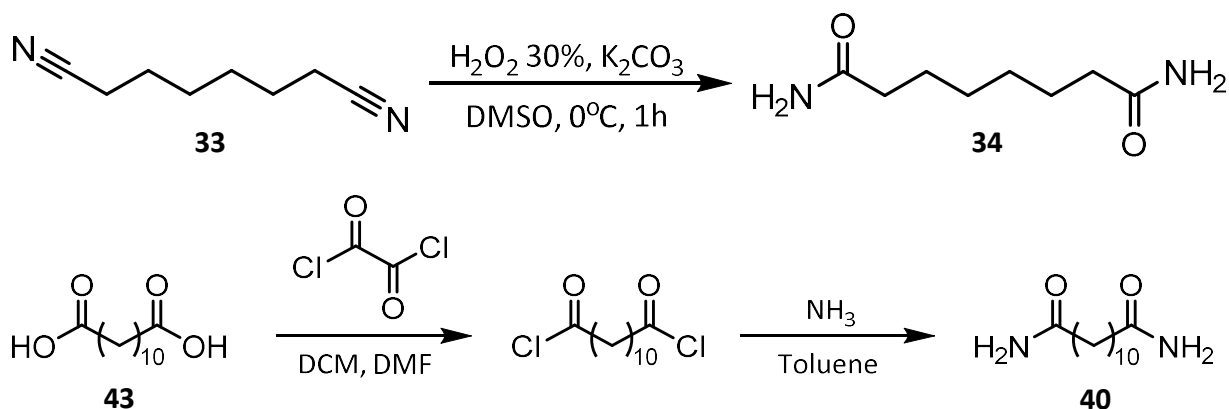
## 2.8.2 Aliphatic- $\alpha,\omega$ -diamides

When modifications of dicarboxylic acids were planned, the first idea that comes to mind were acid derivatives (scheme 2.8.3). Acyl chlorides is easily discarded from the possibilities since they are more reactive than carboxylic acids and additionally corrosive. A key issue is the stability of the material. In this regard, esters and amides are derivatives less reactive than carboxylic acids and therefore more stable. However, Esterification results in a loss of hydrogen bonding. Hence would give compounds with lower melting points and melting energy. Ester derivatives are far from being interesting since they are liquid at room temperature. This is not the case for the Amides since they still preserve hydrogen bonding and hence looked like a very promising group.



**Scheme 2.8.3** – Reactivity of some different acid derivatives

Oxalamide, malonamide, succinamide and adipamide are the commercially available diamides. The rest of the tested  $\alpha,\omega$ -diamides has been synthesized. For the synthesis, two methods were followed and some others were probed. For small scale, hydrolysis of the corresponding dinitrile was carried out using hydrogen peroxide [72]. This method would involve greater costs since dinitriles are expensive as starting materials and security concerns because of a very exothermic reaction with hydrogen peroxide. This one was the first protocol followed to synthesize glutaramide (C5), pimelamide (C7), suberamide (C8), sebacamide (C10), undecanediamide (C11) and dodecanediamide (C12) and because of the aforementioned, a new method was developed for large scale where the starting material was a much more affordable dicarboxylic acid (Scheme 2.8.4) [73]. Considering dodecanediamide, which was synthesized using both methods, it can be concluded that there is no big difference between yields. The yield for the small scale was 86% while for the large scale was 80%. Therefore, this method was employed to obtain azelamide (C9), dodecanediamide (C12), tetradecanediamide (C14), hexadecanediamide (C16) and octadecanediamide (C18). Probably one disadvantage that has to be faced in large scale is the employ of DCM as solvent for the formation of diacyl chlorides due to environmental issues. THF is another solvent possibility which can end up in a pure diamide and might be introduced in industrial processes. In terms of cost efficiency, another protocol from a patent was found and tried [74]. The diamide is obtained using only the respective dicarboxylic acid and Urea. Unfortunately, it did not work



Scheme 2.8.4 – Small-scale protocol (top) and Big scale protocol (bottom)

Regarding physical behaviour of this new class of compounds, higher melting points for the respective diamides were observed (figure 2.8.3). After measurements, aliphatic- $\alpha,\omega$ -diamides presented better thermal properties than the corresponding  $\alpha,\omega$ -dicarboxylic acids. Higher melting points are shown in figure 2.8.3 due to a more favourable hydrogen bonding of the amide functional group in comparison with diacids, however, a levelling of the melting points is present starting in the C12 diamide as well. As for the dicarboxylic acids, the contribution from the alkene chain to the melting point at that moment is more important than the terminal amide moieties. Similarly, for the same reasons the latent energy of the diamides follow exactly the same pattern than their respective dicarboxylic acids shown above but since they could release and absorb a bigger amount of energy (figure 2.8.4). A more accentuated “odd-even” effect was observed.

As it can be seen in the table 2.8.2, the even compounds from the set of aliphatic- $\alpha,\omega$ -diamides are showing outstanding melting energies but unfortunately the first two even compounds, oxalamide and succinamide, decompose once they melt at the high temperatures of 290 and 263 °C respectively. The next two even compounds, adipamide and suberamide, present some of the best latent heats of this project but, as it happened with diacids, in long term cycle tests may undergo intramolecular reactions to form a favourable 6-membered ring. Unlike C6 and C8 diamides, sebacamide and dodecanediamide are better candidates because 10 and 12-membered rings are not so easily formed in intramolecular reactions. Moreover, they show both some of the best thermal behaviour in this study. The rest of even diamides (C14, C16 and C18) offer a stable material but not so extraordinary in terms of storage capacity as dodecanediamide or sebacamide. The same applies to odd diamides, their performance is great with higher melting energies than most of the diacids, undecanediamide shows a latent energy of 281.4 kJ/kg, but they are not the best option in this group. As we increase the number of carbons between the terminal diamides the solubility of the material is worst. Due to that lack of solubility for octadecanediamide in deuterated solvents, it was not possible to record any NMR. Instead a FTIR was measured.

To sum up, in these two graphics can be seen that even diamides as PCM are presented as an optimal material with a higher storage capacity, similar behaviour than dicarboxylic acids and higher ranges of melting temperatures.

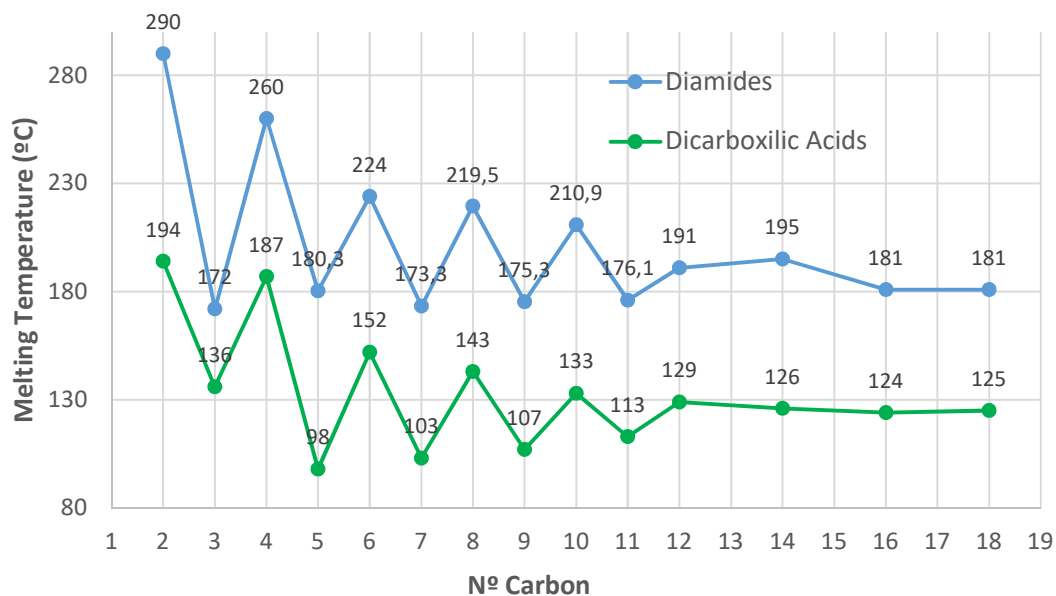


Figure 2.8.3 – Dicarboxylic acid and diamide melting points comparison

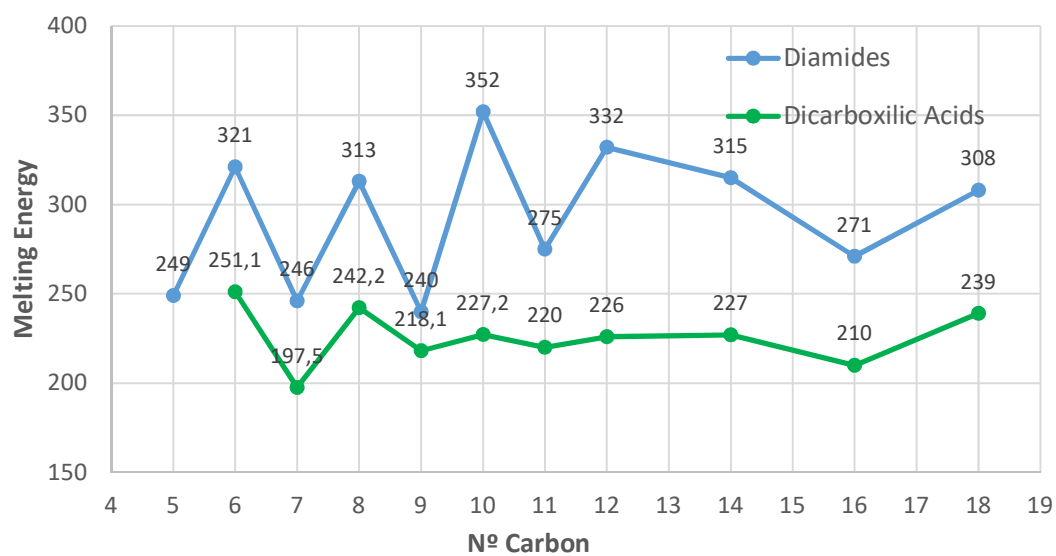


Figure 2.8.4 – Dicarboxylic acid and diamide melting energy comparison

Hence, as it happened with dicarboxylic acids, even diamides are the most interesting materials of this group. In this case, the most favourable in terms of energy and stability were sebacamide and

dodecanediamide. For these two, DSC cycling tests were performed at the Austrian Institute of Technology. Figures 2.8.5 and 2.8.6 to confirm the two diamides as very promising materials. Sebacamide has the highest melting energy obtained in this study, 375 J/g, and the gap between melting and recrystallization is acceptable. Even though dodecanediamide does not have a melting energy as high as sebacamide, it could be considered as a better candidate because of a smaller melting-recrystallization gap and still a high phase energy of 338 J/g.

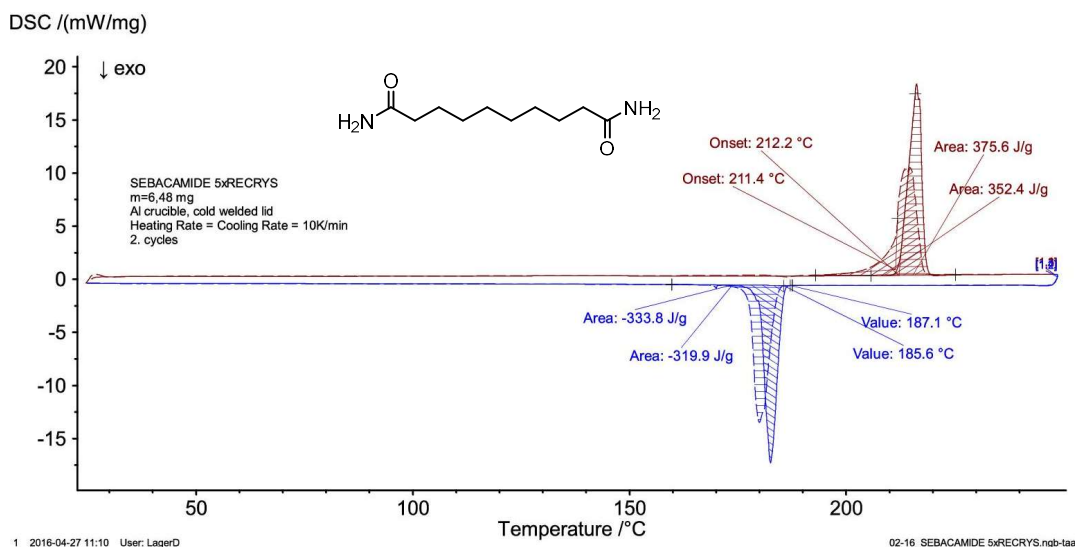


Figure 2.8.5 – Sebacamide DSC cycle test

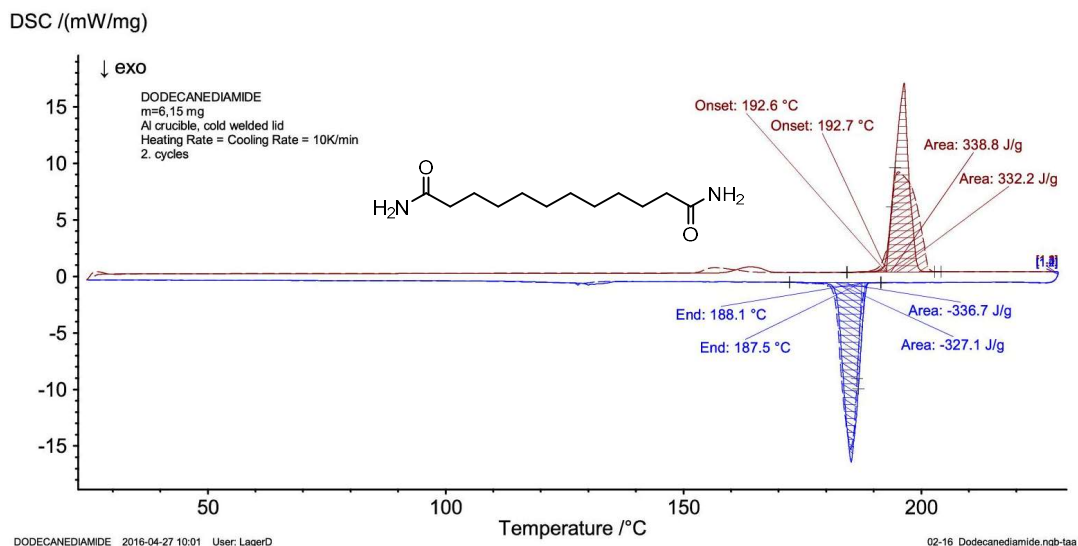
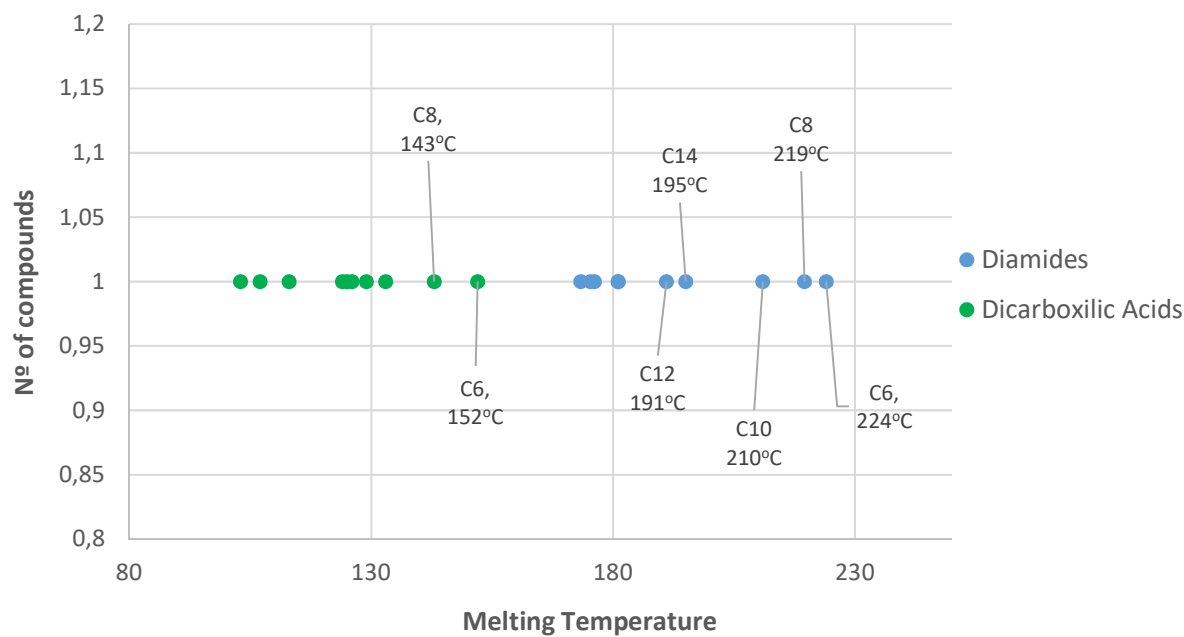


Figure 2.8.6 – Dodecanediamide DSC cycle test

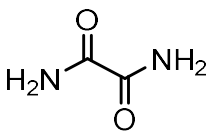
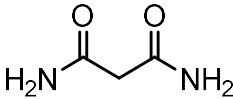
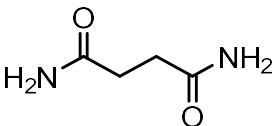
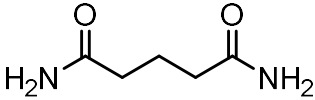
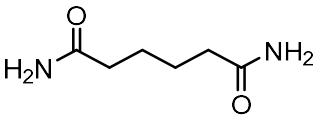
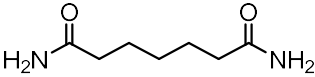
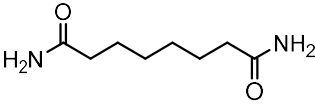
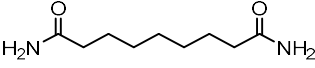
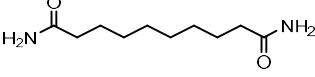
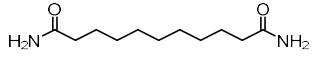
One of the important achievements of the diamides and dicarboxylic acids families is the big range of temperatures covered. Meaning that one or another compound would be more suitable for a particular

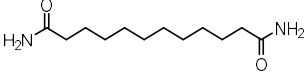
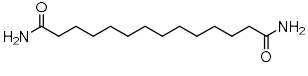
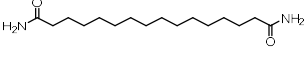
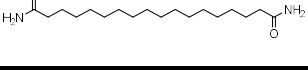
production process and giving more options for industrial applications. Once the data of all the diamides and dicarboxylic acids are compiled, it can be noted from the figure 2.8.7 below that dicarboxylic acids cover a range from 100 to 150 °C and diamides from 175 to 225 °C. According to this information, there are some gaps that ideally should be covered; the one between 80 to 100 °C and the other between 150 to 175 °C, which is addressed in subsequent chapters.



**Figure 2.8.7** – Range of temperature covered within diamides and dicarboxylic acids

Table 2.8.2 – Diamides STA measurements data

Compound	Structure	MP lit. T (°C)	MP exp. T (°C)	$\Delta H$ Exp (kJ/kg)	Degradation T(TGA)
Oxalamide		299	290.2	Decomposition	229.5
Malonamide		171	172.1	304.5	217.1
Succinamide		263	-	Decomposition	-
Glutaramide		181	180.3	260.3	165.7
Adipamide		226	224.7	371.0	268.1
Pimelamide		173	173.3	277.2	238.8
Suberamide		220	219.5	335.1	265.6
Azelamide		177	175.3	247.8	-
Sebacamide		210	210.9	375.6	260.5
Undecane diamide		178	179.1	281.4	244.0

Compound	Structure	MP lit. T (°C)	MP exp. T (°C)	$\Delta H$ Exp (kJ/kg)	Degradation T(TGA)
Dodecane diamide		193	191.0	338.8	246.9
Tetradecane diamide		196	194.6	319.9	-
Hexadecane diamide		179	181.4	282.9	-
Octadecane diamide		179	181.7	264.7	-

### 2.8.3 Diamide derivatives

New compounds were synthesized in order to cover those gaps that dicarboxylic acids and diamides left in the range of certain temperatures (figure 2.8.7). Monosubstituted diamides might be a suitable option. On one hand, the material still presents hydrogen bonding because of the one hydrogen left from the amide nitrogen and, on the other hand, the added alkyl chain is going to contribute with energy from London interactions. Thus, the larger the alkyl chain, the higher the expected stability and also melting energy. Anyhow, different substituted diamides were synthesized to observe the behaviour and to identify a trend.

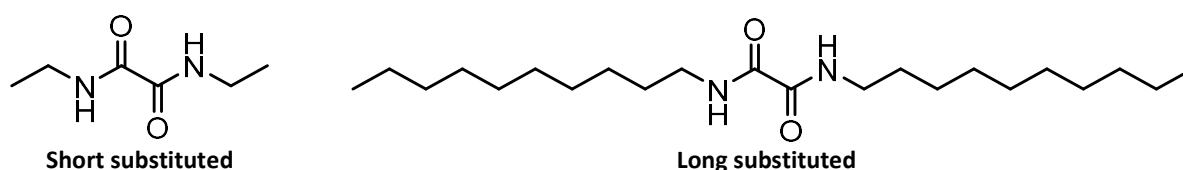
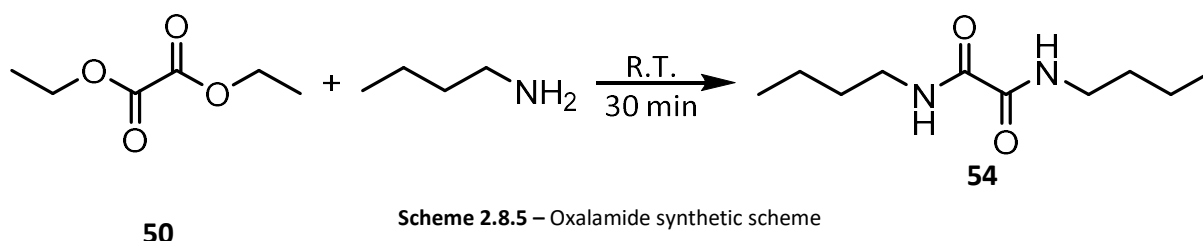


Figure 2.8.8 – short and long substituted diamides

Initially, derivatives of oxalamide were the main target. All of them are reported in the literature and are easily synthesized, starting from diethyl oxalate and the corresponding amine (scheme 2.8.5) [75-77]. Oxalamide tends to decompose at the melting point releasing a high amount of energy but of course being unsuitable for our purposes. The idea is to see if their substituted derivatives are more stable than the parent oxalamide.



To this end the starting material was monosubstituted initially in both functional groups with methyl, ethyl, propyl and butyl. All of these derivatives decompose when they melt. The melting point decreases with the rising length of the alkene chain so longer chains of alkenes were attached. This time, it was carried out with octyl and decyl and no decomposition was observed. However, STA data showed (figure 2.8.9) that these two compounds undergo solid-solid phase transitions which split their storage capacity in two different peaks therefore two different operative points. Initially, that might be a disadvantage for some industrial processes since there is no a single and reliable melting point. Moreover, the energy storage is not as high as other materials and, consequently, N,N'-dioctyl oxalamide and N,N'-didecyl oxalamide were discarded.



In order to finalize the oxalamide derivatives, a last derivative was synthesized. *N,N'*-dioctadecyloxalamide has a linear octadecyl chain at each terminal group and the STA graph present a single peak for melting (figure 2.8.10). In this case an increase in the melting energy is noticeable because of the significant London interactions which are not present to such an extent in shorter derivatives. There are several compounds in the acid/amide group with melting energies over 300J/g so, in this case, an energy of 250J/g is slightly below our range. As we increase the number of carbons of the substituted alkene chain, the solubility of the material is worst. Due to the lack of solubility of *N,N'*-dioctadecyloxalamide in deuterated solvents, it was only possible to record a  $^1\text{H}$  NMR. Moreover, a FTIR was measured.

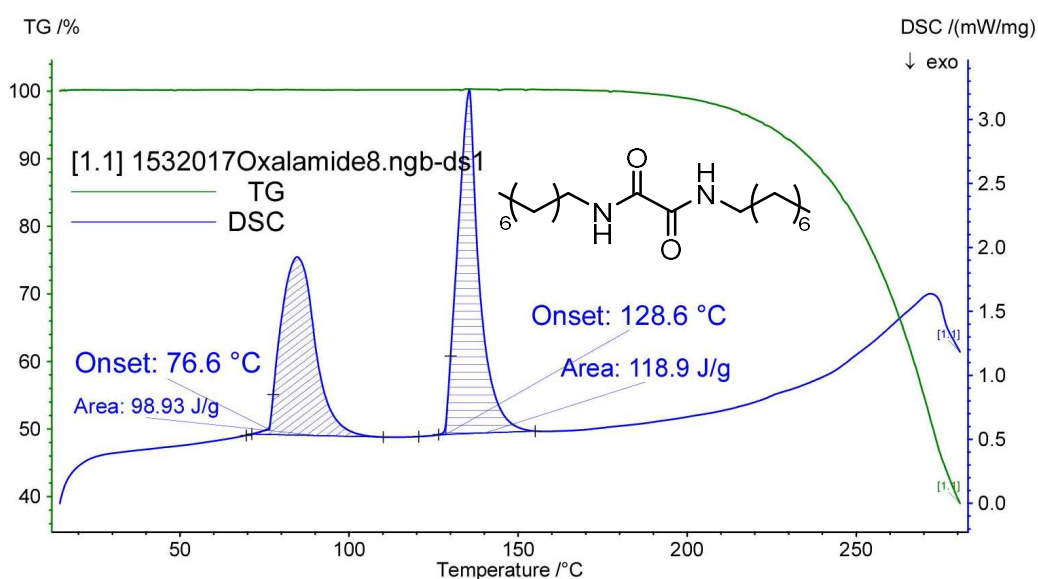


Figure 2.8.9 – Di-octyloxalamide STA measurement

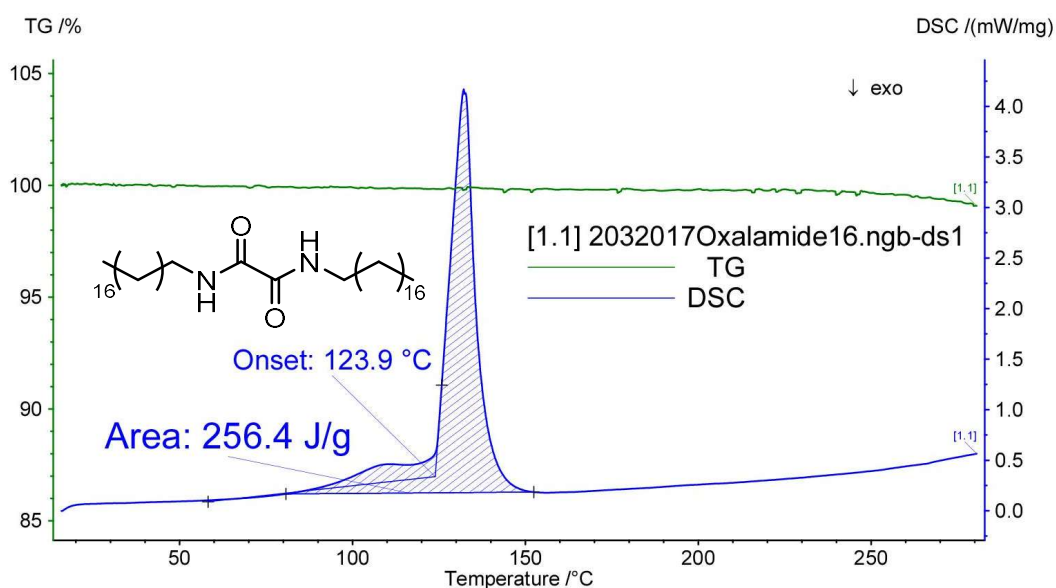
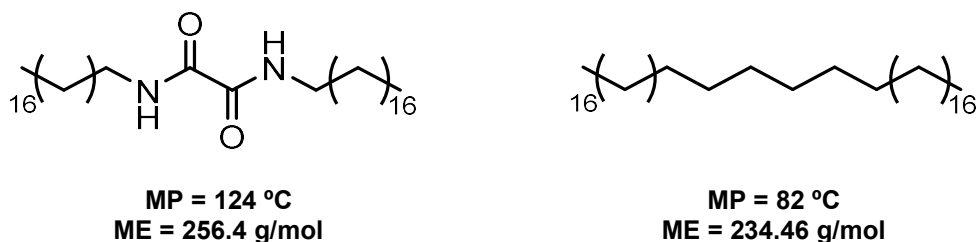


Figure 2.8.10 – Di-octadecyloxalamide STA measurement

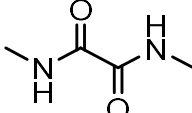
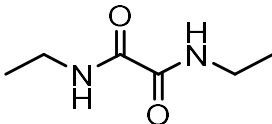
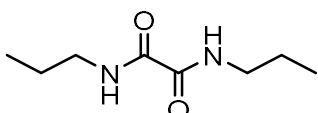
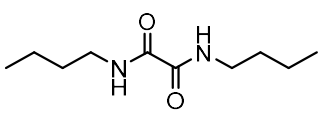
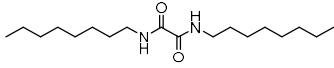
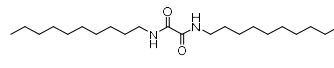
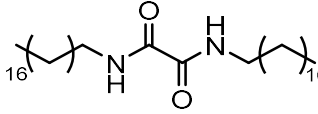
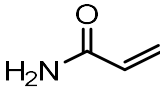
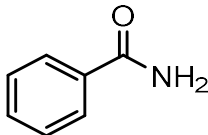
At the end of this chapter, it should be mentioned that the contribution to the phase transition energy for the dioctadecyloxalamide comes basically from the long aliphatic chain and its Van der Waals forces. If the melting energy of the substituted diamide is compared with the respective paraffin (figure 2.8.11), it can be observed that they approximately present the same energy and the amide moiety barely contributes.

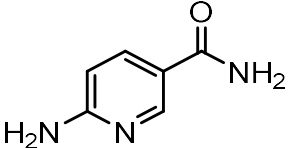


**Figure 2.8.11** – Comparison on the thermal properties of the Dioctadecyloxalamide and its respective paraffin

Finally, three more amide derivatives were evaluated to close this amide chapter. Acrylamide is an easy amide derivative with a conjugated double bond which would be used in next chapters as synthetic starting material. Even though its melting values are fitting to this project, it was discarded because it is an unstable compound which tends to polymerize, therefore, an unreliable material. Moreover, it is a powerful neurotoxic. Benzamide presents a too low melting energy of 238.4 kJ/kg which does not live up to the high performances of other materials that have already been discussed in this thesis. Lastly, 6-amino nicotinamide is a more complex derivative of benzamide which offers a latent energy of 289.1 kJ/kg, however, there is a small gap between melting (246.6 °C) and degradation (274.9 °C) which could generate future stability problems.

Table 2.8.3 – Substituted diamides STA measurements data

Compound	Structure	MP lit. T (°C)	MP exp. T (°C)	$\Delta H$ Exp (kJ/kg)	Degradation T(TGA)
N,N'-dimethyl oxalamide		210	214.9	Decomposition	-
N,N'-diethyl oxalamide		177	180.7	Decomposition	-
N,N'-dipropyl oxalamide		162	166.2	Decomposition	-
N,N'-dibutyl oxalamide		153	155.0	Decomposition	-
N,N'-dioctyl oxalamide		124	128.9	98.93/118.9	-
N,N'-didecyl oxalamide		122	124.7	88.75/135.4	-
N,N'-dioctadecyl oxalamide		120	123.9	256.4	-
Acrylamide		84	83.6	264.1	132
Benzamide		125	126.6	-	-

Compound	Structure	MP lit. T (°C)	MP exp. T (°C)	$\Delta H$ Exp (kJ/kg)	Degradation T(TGA)
6-amino nicotamide	 <chem>NC(=O)c1cc(N)ccn1</chem>	245	246.6	289.1	274.9

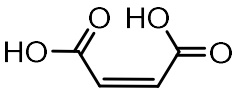
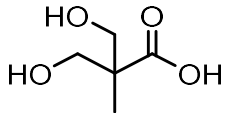
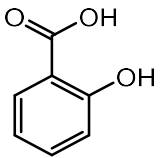
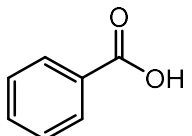
## 2.8.4 Other acids

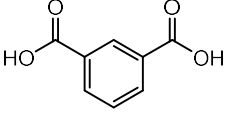
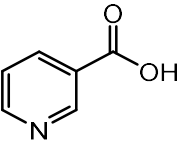
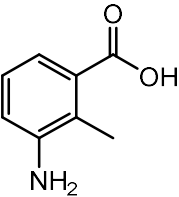
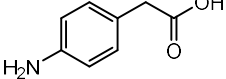
To complete the compound class of acids and derivatives thereof other common acids were studied. Benzoic acid was not measured due to the low melting energy value which was found in the literature [100]. Most of them (maleic acid, nicotinic acid, 4-aminophenyl acetic acid and isophthalic acid) were discarded because of decomposition which was observed during the phase change being impossible to calculate a proper latent energy of both compounds. This observed lack of stability is understandable considering, as it was said before, that carboxylic acid functional groups can undergo decarboxylation reactions upon heating.

Something similar would occur in the 3-amino-2-methyl benzoic acid measurement. In this case, degradation would take place 10 °C after melting (186.5 °C). That allows to calculate a good melting energy of 289.7 kJ/kg but the compound has to be discarded due to degradation issues.

Besides that, salicylic and 2,2-bis(hydroxymethyl)propionic acid have some relevance as materials for PCM application, particularly the second one due to its high energy capacity, 292.3 kJ/kg. Salicylic acid is still a bit under the requirements with a low storage capacity of around 200 kJ/kg. Nevertheless, all these acids did not present thermophysical properties as remarkable as diacids and diamides.

Table 2.8.4 – Other acids STA measurements data

Compound	Structure	MP lit. T (°C)	MP exp. T (°C)	$\Delta H$ Exp (kJ/kg)	Degradation T(TGA)
Maleic acid		135	145	Decomposition	147.5
2,2-Bis(hydroxymethyl)propionic acid		152	153.4	292.3	202.3
Salicylic acid		158	159	201.9	159.8
Benzoic acid		122	-	-	-

Compound	Structure	MP lit. T (°C)	MP exp. T (°C)	$\Delta H$ Exp (kJ/kg)	Degradation T(TGA)
Isophthalic acid		341	-	Decomposition	276.9
Nicotinic Acid		236	236.4	Decomposition	194.4
3-Amino-2-methyl benzoic acid		185	186.5	289.7	196.5
4-Amino phenyl acetic acid		201	209.8	Decomposition	-

## 2.9 Towards 3,6-diazaoctane-1,8-diol and derivatives

After an extended screening of different molecules taking into account their polar functional groups and their symmetry, a more extensive literature research was done. One paper with DSC measurements of a large amount of chemicals was found [78]. Thus, we compile in a single list all the highest solid-liquid phase transition compounds.

**Table 2.9.1** – Highest solid-liquid phase transition compounds with diamides (blue), diacids (green) and sugars (orange)

#	$\Delta H$ Exp (KJ/kg)	MP T (°C)	Name	#	$\Delta H$ Exp (KJ/kg)	MP T (°C)	Name
1	387.28	234.85	Alanylglycine	15	295.05	180.75	Glutaramide
2	367.78	219.85	Glycylglycine	16	283.48	182.95	Succinic acid
3	357.35	187.15	Dulcitol	17	282.47	195.05	4-aminophenylacetic acid
4	348.61	225.95	Adipamide	18	281.67	173.65	Pimelamide
5	343.02	211.15	Sebacamide	19	273.20	236.17	Nicotinic acid
6	339.09	220.05	Suberamide	20	273.07	214.45	Dicyandiamide
7	335.34	100.05	N,N'-bis(2-hydroxyethyl)ethylene diamine	21	265.88	223.75	Myo-inositol
8	332.46	118.20	Meso erythritol	22	260.82	155.15	3-amino-1,2,4-triazol
9	322.77	192.95	Dodecanediamide	23	260.71	137.85	2,2-Dimethylsuccinic acid
10	321.52	170.45	Malonamide	24	256.20	185.65	3-amino-2-methylbenzoic acid
11	300.50	178.05	Undecanediamide	25	255.35	104.55	D-Arabinitol
12	300.43	164.77	Mannitol	26	255.22	174.07	2-aminophenol
13	298.38	181.45	1,1-dimethylurea	27	252.59	187.00	4-aminophenol
14	295.29	177.25	Azelamide	28	252.07	236.85	3,5-dihydroxybenzoic acid

As may be seen, most of the high-energy compounds are mainly located in the diamides family and the sugar alcohols family. The two compounds with the highest melting energy are both amino acid dimers and unfortunately tend to decompose. The next one is dulcitol, a sugar alcohol which is lacking stability as shown during cycle tests [34,35]. The following three are diamides with an even number of carbon atoms; C<sub>6</sub>, C<sub>10</sub>, and C<sub>8</sub> respectively. Finally, a new compound with interesting properties is found in the 7<sup>th</sup> position. N,N'-Bis(2-hydroxyethyl)ethylenediamine (NN-Bis) has a significantly high melting energy with a low melting point. This melting temperature of 100.05°C could allow us to employ a PCM in a range of industrial processes related to steam and its residual heat. The melting point of the best diamides candidates (C<sub>10</sub> and C<sub>12</sub>) is approximately twice as high. Bearing in mind all these features, NN-bis was purchased in order to measure its physical properties in DSC.

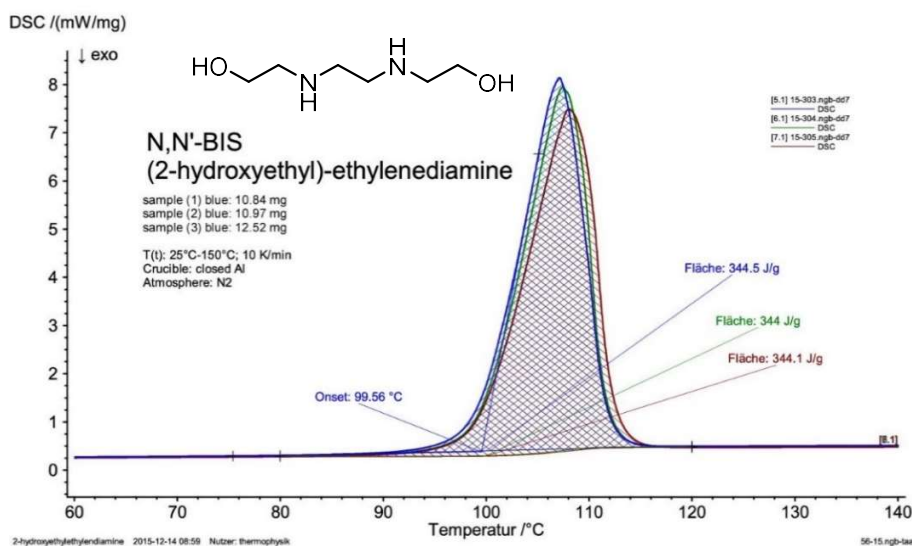


Figure 2.9.1 – NN'-Bis (2-hydroxyethyl)ethylenediamine DSC measurement

Subsequent STA measurements showed no degradation and the expected melting properties. Accordingly, cycle tests were carried out in the DSC machine from the Austrian institute of technology in order to have better accuracy. However, the cycle analysis reveals one possible drawback. The presence of a huge gap between melting and recrystallization meaning that the temperature has to drop from 98.5 °C to 38.85 °C if there is an intention to recover that energy. Such shortcomings are often not an issue at larger scale and additionally, nucleating agents can solve this problem. At small scale in DSCw loss of as observed once we tried to reach again the melting point. Thus, further modifications for reducing this gap had to be undertaken.

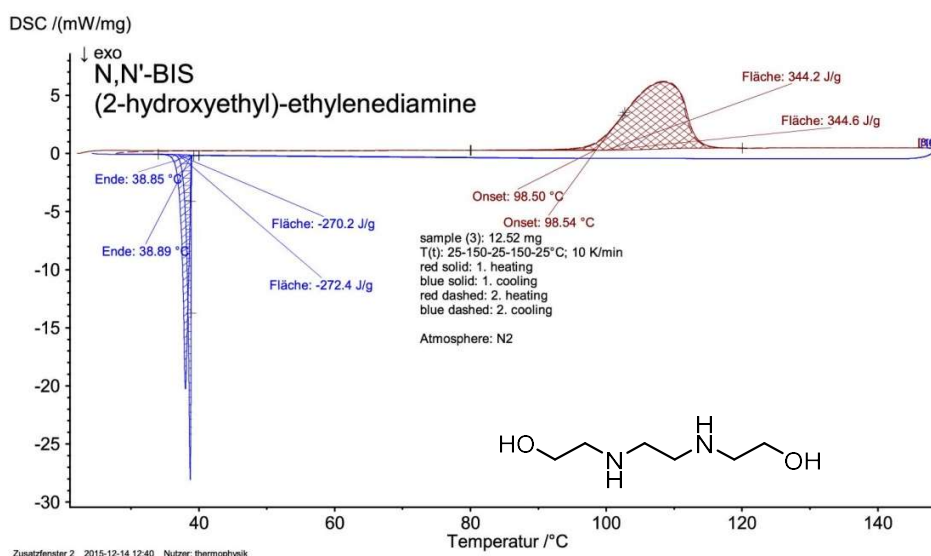
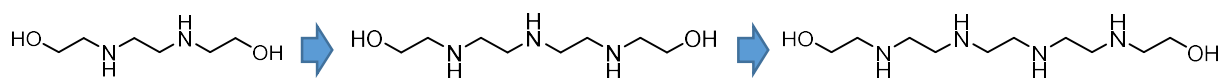


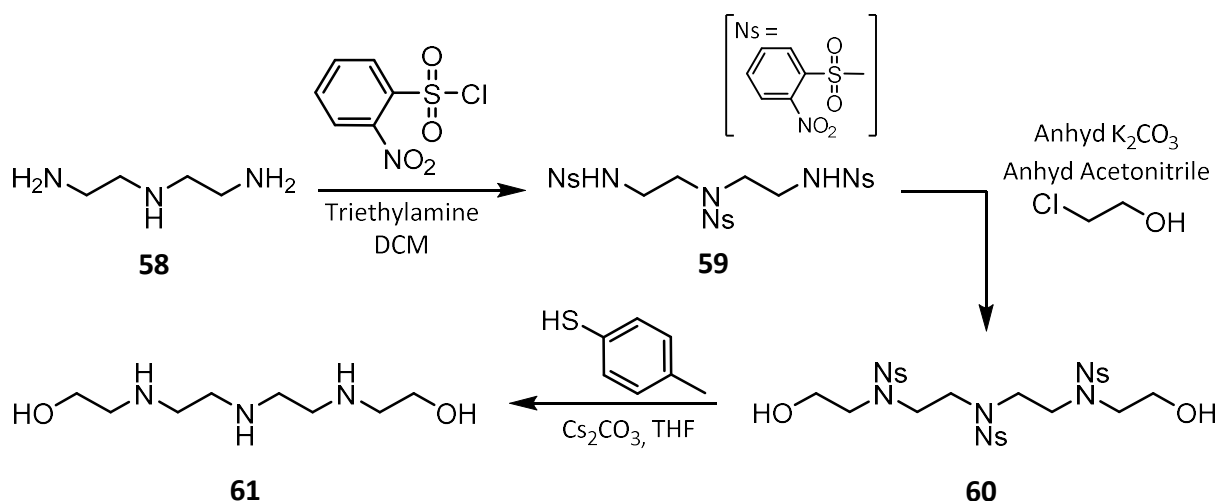
Figure 2.9.2 – NN'-Bis (2-hydroxyethyl)ethylenediamine cycle DSC measurement





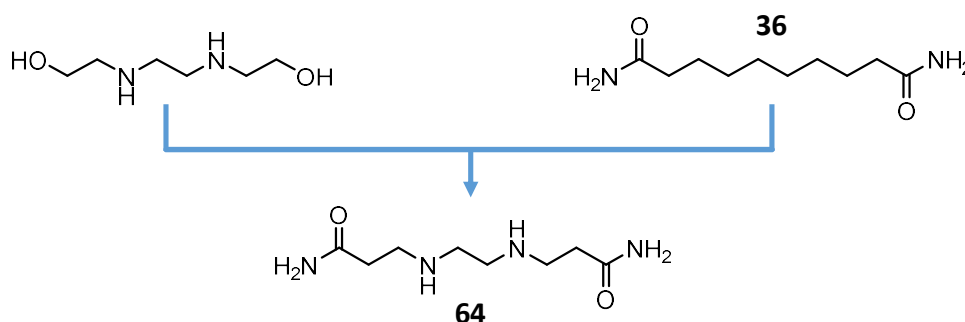
Scheme 2.9.1 – Elongation pattern for NN-bis

First of all, an elongation of the NN-Bis pattern was considered (scheme 2.9.1). Since these derivatives are not known in the literature, different synthetic approaches were tried before ending up with a final protocol. The major problem that has to be faced in this synthesis is the reactivity of secondary amines. These amines are more nucleophilic than primary amines and, therefore, must be protected to avoid secondary amines to react and generate several side products and to achieve the proper elongation reaction on the terminal primary amines. Nevertheless, a double substitution of the primary amines using a modification of a protocol for the NN-bis synthesis with the starting amine was initially tried by using 2 eq. of 2-chloroethanol [79]. As expected, this reaction left several side products, giving rise to the need of using a selective protecting group. For that purpose, two ways of protecting our starting material were found in the literature. One was employing a tosyl group [80] and another a nosyl group [81]. Both are selective protective groups for secondary amines. These groups can only react with one proton of the primary amines due to its voluminous nature and therefore the terminal amines of the starting material (scheme 2.9.2) would leave one proton ready to undergo a nucleophilic substitution with 2-chloroethanol. Finally, once this addition is done, a deprotection reaction would deliver the final product. In this particular case, nosyl protection was chosen because tosyl deprotection needs strongly acidic conditions and nosyl only would need mild conditions which might be favourable to obtain the final product. As can be seen from scheme 2.9.2, an initial protection of the starting polyamine with a nosyl group was done and the product was subjected to a selective substitution using chloroethanol [81]. Finally, the final product was obtained upon cleavage of the protecting group with p-thiocresol [82].



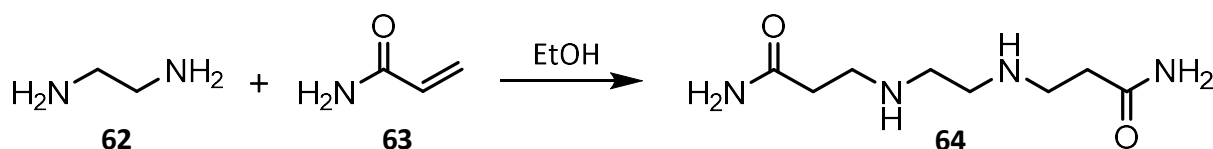
Scheme 2.9.2 – NN'-Bis elongation synthetic route

The first derivative of its kind was synthesized with poor yields. Nevertheless, one of the main goals of this route was to get the final product in sufficient amount for thermophysical measurements. However, in the specific case of this first derivative, we ended up with a liquid as final product. After this result, a further elongation was discarded even though a longer and even derivative would deliver better thermal properties due to the aforementioned odd-even effect. This effect will have a larger impact in terminal groups with a constraint mobility as it can be observed in the amides groups of the  $\alpha,\omega$ -diamides where the carbonyl double bond grants that fixed geometry. Nevertheless, the odd-even effect has also been reported in sugar alcohols where natural-occurring aliphatic sugar alcohols of five carbons showed slightly inferior thermophysical properties than even (4 or 6 carbons) aliphatic sugar alcohols. As it happens in sugar alcohols, the hydroxyl groups on the NN-bis derivatives present more freedom and mobility opportunities in comparison with the aliphatic- $\alpha,\omega$ -diamides and therefore a less accentuated odd-even effect might be observed. For that reason and taking into account that our first odd NN-bis derivative was a liquid, the elongation to synthesize an even derivative was discarded because a big improvement on its thermal properties was not expected



Scheme 2.9.3 – Merging of structures

After experiencing again odd-even effects in the NN-bis elongation and considering the importance of different geometries of terminal moieties, other modification that came to mind was changing the terminal hydroxyl group for a different one. Amide functional groups have been tested with good results in former chapters giving a more effective hydrogen bonding which could increase melting energy. On the other hand, the final compound has to have an even chain length in order to promote a better intermolecular packing which would also favour interactions among molecules and the chain length between terminal groups must be around 10 or 12 atoms. As it was shown, diacids and diamides with 6 or 8 members are not as stable as long-chain diamides since they might undergo intramolecular reaction to form favourable rings. The longer the chain between amide groups is, the less favourable is ring formation. With these as its foundation, the pattern of the newly designed NN-bis derivative (**64**) would correspond to Sebacamide (**36**) in terms of chain length among amide derivatives with a secondary amine in the position 4 and 7 of the chain. This new design might provide improvements in the area of stability and a lower gap between the melting and recrystallization that have already been observed in sebacamide (**36**).



Scheme 2.9.4 – 4,7-diazadecanediamide (Azamide) synthetic scheme

In view of all these facts, a new derivative of NN-bis, 4,7-diazadecanediamide (azamide), was synthesized following the reaction that can be seen in scheme 2.9.4. The compound is known in the literature and it was obtained by Chao et al. [83] in a reaction which was carried out under heating in ethanol, a cheap solvent and with 60% yield in a gram scale experiment. Another advantage of this resulting product is its low cost. Both starting materials are bulk chemicals which can be found at a reasonable price.

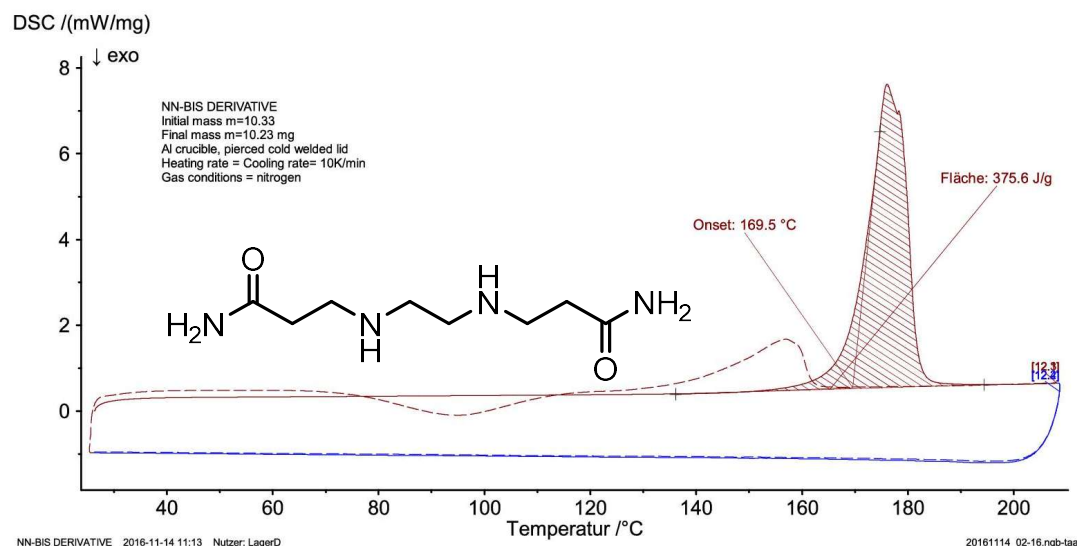


Figure 2.9.3 – 4,7-diazadecanediamide (azamide) **64** cycle DSC measurement

Figure 2.9.3 shows the cycle test for the azamide (**64**). Once the two hydroxy groups from the NN-bis are replaced by amides, an interesting new material is obtained. The melting point is half way between NN-bis and sebacamide, and it still has a phase transition enthalpy as high as sebacamide. On this occasion, however, recrystallization was not observed. Looking at the present situation, another experiment was carried out in order to try the capability of the NN-bis derivative to recrystallize in larger scale. 1.5 g of our product was placed in a closed vial and it was heated to a temperature of 200 °C for 30 min until complete melting. Afterwards the vial was cooled to room temperature and recrystallization was observed. In any case, physical issues such as recrystallization can be always improved by adding different nucleating agents.

	NN-Bis	Azamide	Sebacamide
Structure			
MP T (°C)	99.6	169.5	210.9
$\Delta H$ Exp (kJ/kg)	344.5	375.6	375.6

Table 2.9.2 – Comparison of the thermal properties for NN-bis, sebacamide and its derivative

Nevertheless, recent long-term stability tests found that after some cycles the material is degraded during heating to end up in an orange glass-like shape which is going to lose the ability for storing high amounts of energy

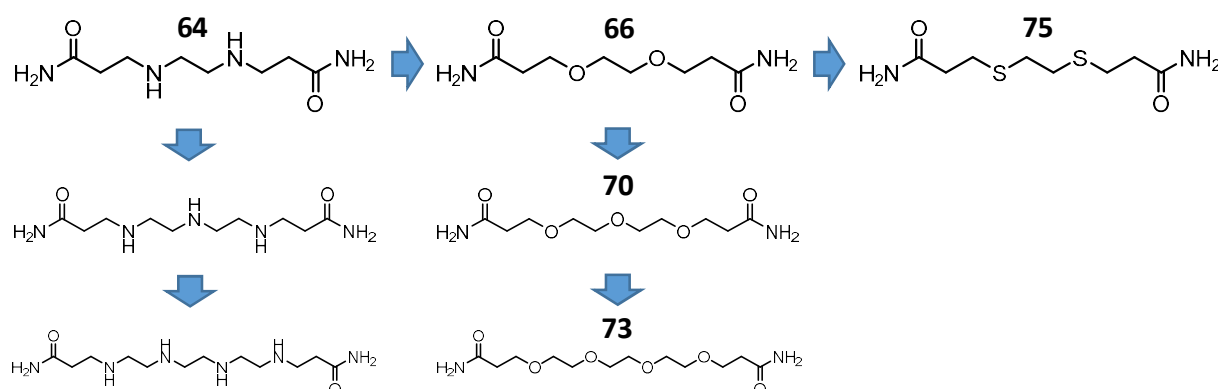


Figure 2.9.4 – Azamide sample after (left) and before (right) after 100 cycles under argon atmosphere

It is at this point when modifications of azamide (**64**) took place to improve the thermal stability. These derivatives were planned in two different ways. On one hand, an elongation of the chain pattern between its two terminal diamides was intended, as we did for the NN-bis. On the other hand, a substitution of the heteroatom located in the main chain was aimed for. Taking into account the good nucleophilicity of other atoms, our targets were oxygen and sulphur instead of nitrogen. For this reason, we tried to synthesize both, 4,7-dioxadecanediamide (oxiamide) (**66**) and 4,7-dithiodecanediamide (sulfuramide) (**75**).

Additionally, for the oxygen derivatives an elongation of the chain was considered. The plan was to obtain the next two compounds in length order, one "odd" and one longer "even" (Scheme 2.9.5), to have a pattern of behaviour of two different even diamides, which usually have a better symmetry for three-dimensional packing and thereby better thermophysical properties. With the help of the odd diamide we could understand how important the disposition of these terminal amide groups would be (odd or even conformation) in this particular family of new materials.

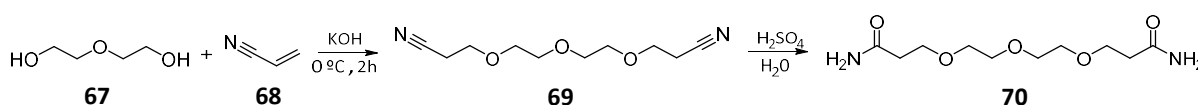
Regarding the sulfuramide, no longer derivatives were initially considered. Mainly as a result of the toxicity related to sulphur compounds but also because of the data linked to the oxygen and nitrogen materials should be checked before further synthetic efforts were undertaken. However, new sulphur derivatives might be included in this study if it were the case that sulfuramide shows promising properties. All these general synthetic considerations are displayed in Scheme 2.9.5.



**Scheme 2.9.5** – 4,7-diazadecanediamide derivatives synthesis map scheme

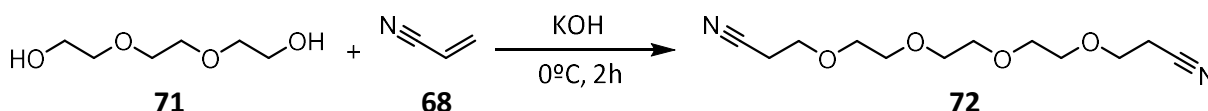
Several methodologies were tried in order to synthesize this group of oxygen derivatives of NN-bis. The first approaches were reported in the literature [84-86]. Similarly to the nitrogen derivative, acrylamide and ethylene glycol were used as starting materials with different alcohols (methanol, ethanol, t-butanol) as solvents. None of them were working properly and oxiamides were not possible to obtain through these procedures. The most suitable of these protocols was the one related to the hydrolysis of terminal nitrile groups (Scheme 2.9.6) [87]. An alternative method for a hydration of the dinitrile with tetrabutylammonium hydroxide [88] was tried with no conversion as a result. For the dinitrile hydrolysis

it was not possible to follow the protocol that was employed to some diamides in small scale because the use of hydrogen peroxide combined with ethers may generate explosive products. In any case, a new hydration method was employed for the dinitrile hydration where the corresponding glycol remains as initial starting material but a mixture of water and  $\text{H}_2\text{SO}_4$  is used instead of hydrogen peroxide [87]. Glycols are converted to dinitriles in excellent yields with a Michael addition [89] and a similar method where 2 equivalents of acrylonitrile are added to the glycol (scheme 2.9.6). Finally, dinitriles are converted to diamides by using an acid as it was mentioned above. In all these diamides poor yields were obtained since optimization was intended to wait until having further DSC data.



Scheme 2.9.6 – 4,7,10-trioxatridecanediamide synthetic scheme

The synthesis of the oxiamide **66** was straightforward since the dinitrile used as starting material was commercially available. It was not the same for the longer derivatives, 4,7,10-trioxatridecanediamide (**70**) and 4,7,10,13-tetraoxahexadecanediamide (**73**). In this case, a previous step is required where the proper dinitrile has to be formed. For such purpose, different ethylene glycols react in a very exothermic way with acrylonitrile (scheme 2.9.7). Once these dinitriles **69** and **72** were in hand, a new reaction was planned to obtain our desired product, oxiamide **70** and **73**, through a hydrolysis of its nitrile groups, as in Scheme 2.9.6.



Scheme 2.9.7 – 4,7,10,13-tetraoxa-1,16-hexadecanedicarbonylamine synthetic scheme

After the task of synthesizing all these derivatives had been completed, we carried out the new corresponding DSC measurements. As can be seen in figure 2.9.4, they offer a good stability after melting and a well-defined peak. Only in the case of the short derivative, oxiamide **66**, we have a solid-solid transition immediately before the melting point. All of them present melting temperatures between 85 and 117 °C but, unfortunately, only one showed a melting energy above 250 J/g (table 2.9.3). Taking all the above into account, it can be found no need to continue further with the elongation and synthesis of new compounds, so it was decided to move on to the next material.

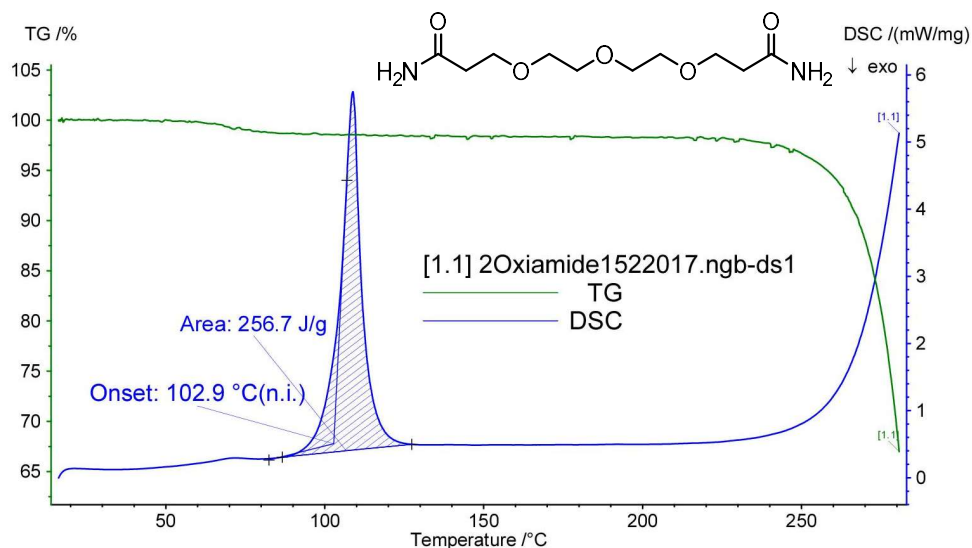


Figure 2.9.4 – 4,7,10-trioxatridecanediamide STA measurement

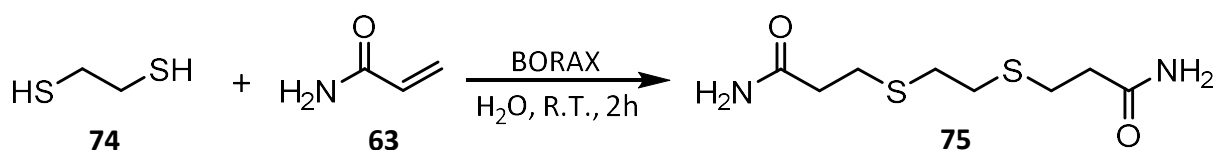
	Oxiamide	4,7,10-trioxatridecanediamide	4,7,10,13-tetraoxahexadecanediamide
Structure			
MP T (°C)	116.9	102.9	189.6
$\Delta H$ Exp (kJ/kg)	206.2	256.7	177.4

Table 2.9.3 – Comparison of the thermal properties for oxygen NN-bis derivatives

Ending the series of modification for the NN-bis, the corresponding sulfuramide was synthesized [90] and measured in the STA machine at the TU Wien. As already indicated, sulphur compounds are better nucleophiles than nitrogen or oxygen ones, meaning that the reaction would take place easily and with

good yields. Due to this reactivity, however, these sulphur compounds are of high toxicity with direct negative consequences for human health and the environment.

Even when the toxicity is usually high, the starting material (1,2-Ethanedithiol **74**) employed in the sulfuramide synthesis presents a low level of toxicity, slightly higher than ethylene glycol. Another feature that is observed is the low expenditure. The rest of reactives involved in the reaction, borax and acrylamide, are cheap and commercially available and everything was carried out using water as solvent. Finally, the yield was 89% in a small scale of 0.2 mmol, which is the best in the class of NN-bis related compounds. The thermal data could be considered good since we have a melting energy around 280 J/g and a melting point of 183.5 °C



Scheme 2.9.8 – Sulfuramide synthetic scheme

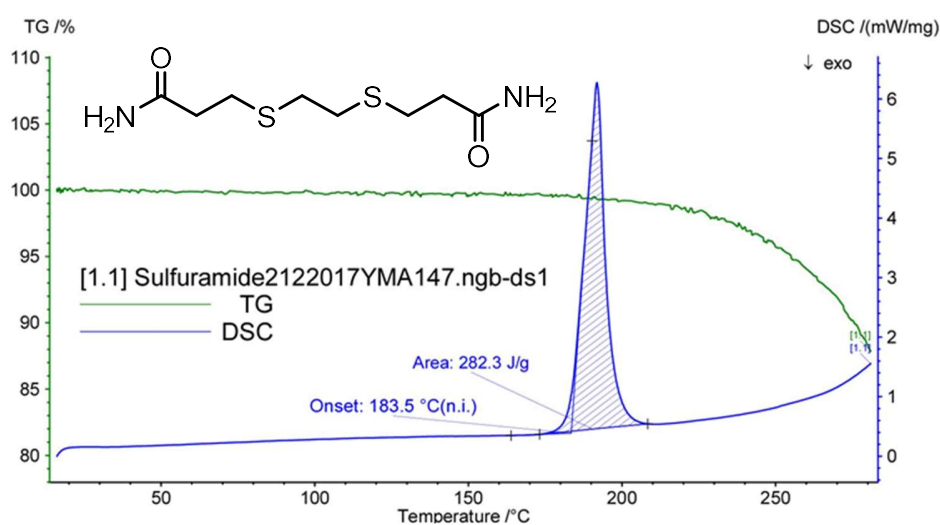
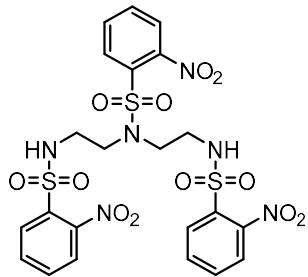
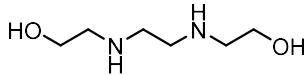
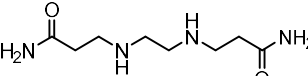
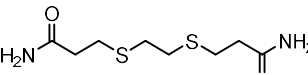
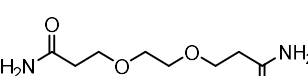
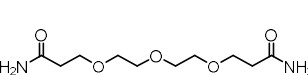
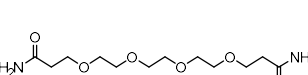


Figure 2.9.5 – Sulfuramide STA measurement

Nevertheless, longer derivatives of sulphur were not considered because of toxicity from the sulphur starting materials involved in the reaction and derivatives of nitrogen present a challenging synthesis with a difficult isolation of the product. Only azamide (**64**) is known in the literature from all the nitrogen derivatives. However, different methodologies were tried to synthesize them but difficulties in the isolation process were experienced even following different protocols from the literature [91-95]. The trend observed in the elongation of the oxamide shows no correlation between even compounds and higher melting energies which is not fitting to the odd-even effect present in diamides and diacids. This is another reason why azamide derivatives were discarded after some attempts.



Table 2.9.4 – NN-bis derivatives DSC/STA measurements data

Compound	Structure	MP lit. T (°C)	MP exp. T (°C)	$\Delta H$ Exp (kJ/kg)	Degradation T(TGA)
1,4,7-Tris(2-nitrobenzenesulfonyl)-1,4,7-triazaheptane		156	132.6	71.07	-
N,N'-Bis(2-hydroxyethyl)-ethylenediamine		100	99.6	344.5	-
4,7-diaza decanediamide		169	169.5	375.6	206.3
4,7-dithio decanediamide (Sulfuramide)		179	183.5	282.3	-
4,7-dioxa Decanediamide (Oxamide)		123	117	206.2	-
4,7,10-trioxa tridecanediamide		103	102	257	-
4,7,10,13-tetraoxa hexadecanediamide		94	99.6	177.4	-

### 3. Conclusions

The main objective from this study was the search and improvement of novel energy-efficient materials which allow storing heat instead of releasing it to the environment unused. Recovering of this thermal energy should be done upon crystallization. Thus, it can be concluded that this goal was achieved considering the set of attractive PCMs which have been developed above. It has been seen progress in three of the several groups investigated: sugar alcohols, carboxylic acids and compounds derived from 3,6-diazaoctane-1,8-diol (NN-bis).

Regarding sugars, sugar alcohols were the most remarkable compounds. Natural-occurring sugar alcohols were widely investigated for PCM applications before, so the scope of this thesis was on modifications of these compound type and the synthesis of longer sugar alcohols hitherto not investigated. Both, modifications and synthesis were planned to avoid drawbacks of these materials such as low thermal stability concomitantly maintaining or even improving their melting energy. With the synthesis of the *D-erythro-D-manno*-octitol it was possible to obtain a melting energy of 352.2 kJ/kg, around 50 kJ/kg higher than one of the best natural-occurring materials, namely Mannitol. The development of a low-cost synthesis is necessary for the upscaling of this new material since the current protocol exceeds the requirement of 5€ per kg required for industrial applications. Moreover, long-term stability tests must be conducted for octitols. Regarding stability, erythritol shows an excellent stability after 100 cycles but there is room for improvement for the rest of the sugars tested. Acetylations were tried as an affordable chemical modification for sugars but they cut half the melting point and melting energy due to the loss of hydrogen bonding, so they were discarded.

Dicarboxylic acids and their diamides are the most outstanding materials from the acids group. They show better thermophysical properties than sugar alcohols and they are able to cover a wide range of temperatures for medium temperature applications, starting from 103 °C and reaching 225 °C. Even though dicarboxylic acids show a great performance as PCMs, diamides tend to present higher storage capacity. From all of these diamides, two are specifically interesting: sebacamide and dodecanediamide. Sebacamide has offered a melting energy of 375.6 kJ/kg, the highest melting energy registered in this study. On the other hand, dodecanediamide has presented 338.8 kJ/kg as melting energy. Nevertheless, dodecanediamide shows a better performance as PCM than sebacamide because the gap between melting and recrystallization is almost non-existent, allowing an ideal adaptation to the system. This is the reason why dodecanediamide was chosen as one of the promising materials to upscale. Once the upscale had been done, it will be necessary to conduct long-term stability test to have an accurate idea about its thermal stability but until now not enough dodecanediamide was provided by the company in charge of supplying the material in large scale. Dicarboxylic acids and diamides have another advantage, a cost-efficient synthesis which can also be improved. In the case of a positive result for the long-term stability tests, one potential new development line might be related to the fact of finding more affordable starting materials or processes, as for example fatty acids or enzymatic methodologies which could contribute to decrease the expense in the production.

Three more interesting organic materials are located in the NN-Bis group. The parent NN-bis itself has an outstanding energy of 344.6 kJ/kg and a very convenient melting point which fits with the boiling point of water. This fact makes it an interesting candidate for industrial applications related to steam. The synthetic route is possibly affordable in bulk amount since it is already a cheap commercially available product. This material only displays a disadvantage regarding recrystallization and the gap between different phase transition temperatures. More research has to be done to improve physical properties. Furthermore, sulfuramide had an easy synthesis with an excellent yield and a phase energy of almost 300 kJ/kg and, finally, azamide is one of the most promising materials which was already upscaled. This material had the highest melting energy together with sebacamide, 375.6 kJ/kg and an easy synthetic route with common chemicals, acrylamide, ethanol and ethylenediamine to finally get the product after a minimal workup. Long-term stability tests unfortunately showed degradation, however azamide should still be kept in mind since there are precedents for the improvement of physical properties once organic compounds are combined with other materials in composites. Research in this direction could take the outstanding materials developed in this study to a new level.

## 4. Experimental

### 4.1 General notes

Unless otherwise noted, **chemicals** were purchased from commercial suppliers and used without further purification. Compounds were synthesised according to (modified) literature procedures with the exception of 3,6,9-triazaundecane-1,11-diol and non natural-occurring sugar alcohols such as perseitol and both octitols.

For **Thin Layer Chromatography** (TLC) aluminium backed silica gel from Merck was used. Spots were visualized under UV light (254 nm)

**NMR-spectra** were recorded on either a Bruker AC 200 ( $^1\text{H}$ : 200MHz,  $^{13}\text{C}$ : 50 MHz) or a Bruker Avance Ultrashield 400 ( $^1\text{H}$ : 400 MHz,  $^{13}\text{C}$ : 101 MHz) and chemical shifts are reported in ppm relative to the nominal solvent signals:  $\text{CDCl}_3$ :  $\delta=7.26$  ppm ( $^1\text{H}$ ),  $\delta=77.16$  ppm ( $^{13}\text{C}$ );  $\text{DMSO-d}_6$ :  $\delta=2.50$  ppm ( $^1\text{H}$ ),  $\delta=39.52$  ppm ( $^{13}\text{C}$ );  $\text{D}_2\text{O}$ :  $\delta=4.79$  ppm ( $^1\text{H}$ );  $\text{MeOD}$ :  $\delta=3.31$  ppm ( $^1\text{H}$ ),  $\delta=49.3$  ppm ( $^{13}\text{C}$ ) and  $\text{CD}_2\text{Cl}_2$ :  $\delta=5.32$  ppm ( $^1\text{H}$ ),  $\delta=53.5$  ppm ( $^{13}\text{C}$ ). The abbreviations used as follows: s, singlet; d, doublet; t, triplet; q, quartet; quin, quintuplet; m, multiplet; dd, doublet of doublets; td, triplet of doublets; ddd, doublet of doublets of doublets; qd, quartet of doublets; quind, quintuplet of doublets.

**DSC and TG measurements** were carried out on a STA 449 F1 JUPITER Netzsch under nitrogen atmosphere.

**Melting points** were determined using a Kofler-type Leica Galen III micro hot stage microscope and are uncorrected.

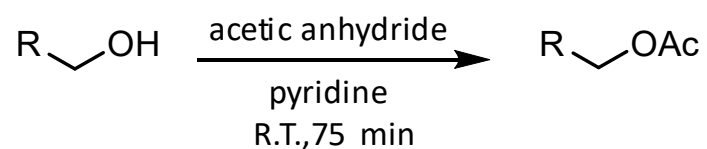
LABconco freezezone 2.5 lyophilizing system was employed as **Lyophilizer** for compound drying.

**Prep HPLC Chromatography** was necessary in the further purification of some materials and was carried out with an Autopurification system of waters using XSELECT CSH C18 5  $\mu\text{m}$  30 x 150 mm column. As solvents HPLC grade methanols and HPLC grade  $\text{H}_2\text{O}$  (containing 0.1% formic acid) were used.

The **Ozone generator** employed was a Sander Ozon Generator model 301 and **Infrared (IR)** were recorded in a PerkinElmer Spotlight 400N FT-NIR Imaging System

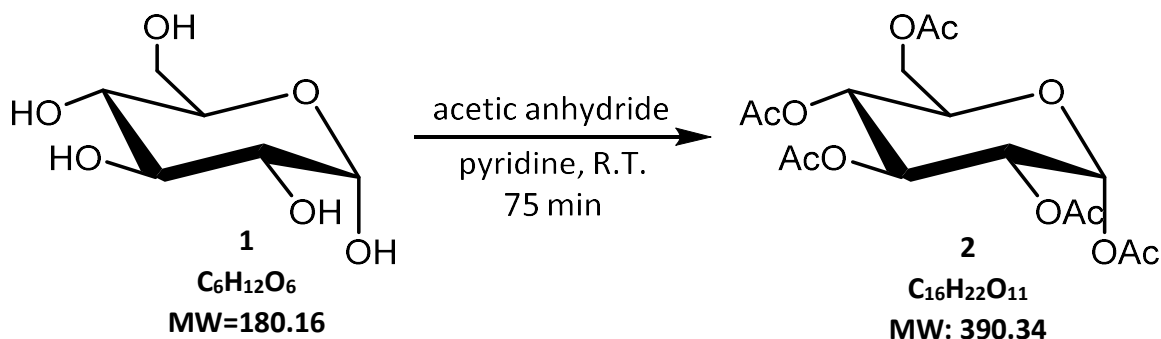
## 4.2 Preparation of acetylated sugar derivatives

### 4.2.1 General procedure A



The respective sugar (1 eq.) and pyridine (5 mL) were placed in an oven-dried 8 mL vial with a magnetic stirring bar. Acetic anhydride (10 eq.) and DMAP (cat.) were added, the vial was closed and the reaction mixture was stirred in a heating block at room temperature for 75 minutes. After this time the reaction was completed according to TLC. Toluene was added in order to co-evaporate pyridine under vacuum which gave the pure product without further purification.

#### 4.2.2 Synthesis of 1,2,3,4,6 - penta - O - acetyl - D - glucopyranose <sup>[101,102,107]</sup>



The product was synthesized according to general procedure A with:

Glucose (500 mg, 2.78 mmol, 1 eq.), acetic anhydride (2.64 mL, 27.8 mmol, 10 eq.), DMAP (catalytic) and pyridine (5 mL)

**Yield:** 99% (1.08 g, 2.76 mmol)

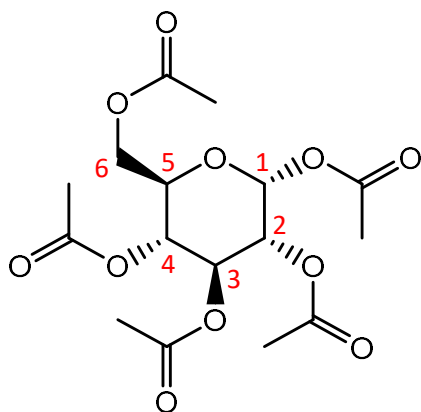
**Melting point:** 107 – 112 °C [Pyridine – toluene] (Lit. MP: 109 °C <sup>108</sup>)

**Melting energy:** 121.2 kJ/kg

**TLC:**  $R_f$  = (PE/EtOAc, 2:1): 0.35

**Appearance:** colourless solid

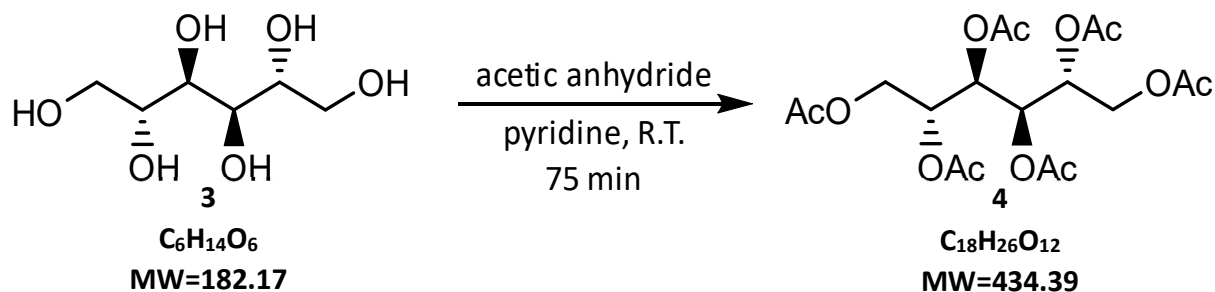
**NMR:**



**<sup>1</sup>H NMR (200 MHz, CDCl<sub>3</sub>):**  $\delta$  = 2.02-2.18 (m, 15H, 5xCH<sub>3</sub>), 4.05-4.14 (m, 2H, H<sub>6</sub>/H<sub>5</sub>), 4.23-4.31 (m, 1H, H<sub>6</sub>), 5.06-5.19 (m, 2H, H<sub>2</sub>/H<sub>3</sub>), 5.47 (t, J=9.84 Hz, 1H, H<sub>4</sub>), 6.33 (d, J=3.57 Hz, 1H, H<sub>1</sub>)

**<sup>13</sup>C NMR (100 MHz, CDCl<sub>3</sub>):**  $\delta$  = 20.4, 20.5, 20.63, 20.66, 20.8 (q, CH<sub>3</sub>), 61.4 (t, C<sub>6</sub>), 67.8 (d, C<sub>2</sub>/C<sub>4</sub>), 69.1 (d, C<sub>3</sub>), 69.8 (d, C<sub>5</sub>), 89.0 (d, C<sub>1</sub>), 168.7, 169.3, 169.6, 170.1, 170.5 (s, 5xC=O)

### 4.2.3 Synthesis of 1,2,3,4,5,6-hexa-O-acetyl-D-mannitol <sup>[101,102]</sup>



The product was synthesized according to general procedure A with:

Mannitol (506 mg, 2.78 mmol, 1 eq.), acetic anhydride (2.64 mL, 27.8 mmol, 10 eq.), DMAP (catalytic) and pyridine (5 mL)

**Yield:** 98% (1.19 g, 2.74 mmol)

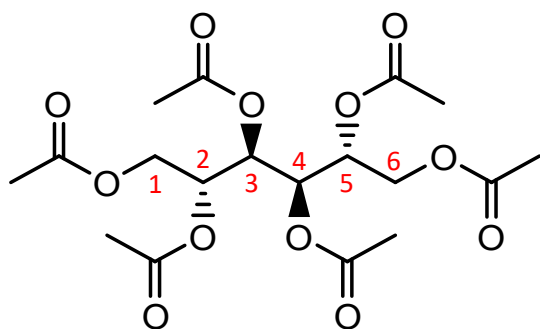
**Melting point:** 123 – 125.5 °C [Pyridine – toluene] (Lit. MP: 120 °C <sup>109</sup>)

**Melting energy:** 164 kJ/kg

**TLC:**  $R_f = (\text{PE}/\text{EtOAc}, 2:1) = 0.4$

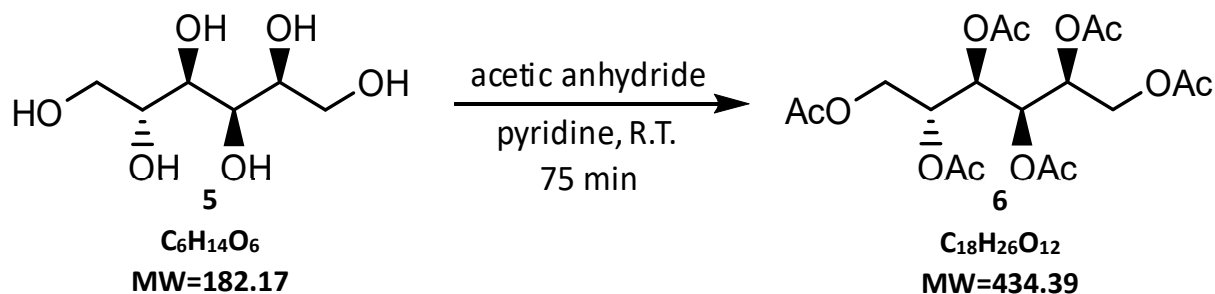
**Appearance:** colourless solid

**NMR:**



<sup>1</sup>H NMR (200 MHz, CDCl<sub>3</sub>):  $\delta = 2.05\text{-}2.09$  (m, 18H, 6xCH<sub>3</sub>), 4.14 (diastereotopic,  $J=12.99, 2.57$  Hz, 4H, H<sub>1</sub>/H<sub>6</sub>), 5.03-5.10 (m, 2H, H<sub>3</sub>/H<sub>4</sub>), 5.45 (d,  $J=8.69$  Hz, 2H, H<sub>2</sub>/H<sub>5</sub>)

#### 4.2.4 Synthesis of 1,2,3,4,5,6-hexa-O-acetyl-D-glucitol <sup>[101,102]</sup>



The product was synthesized according to general procedure A with:

Sorbitol (506 mg, 2.78 mmol, 1 eq.), acetic anhydride (2.64 mL, 27.8 mmol, 10 eq.), DMAP (catalytic) and pyridine (5 mL)

**Yield:** 99% (1.20 g, 2.76 mmol)

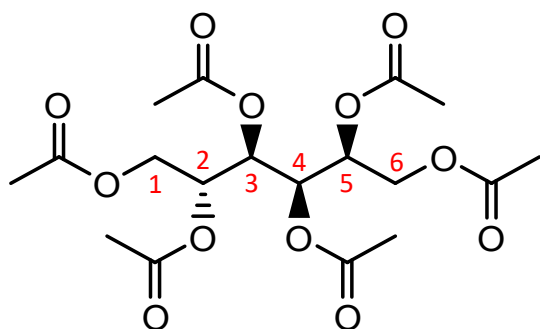
**Melting point:** 98 – 100 °C [Pyridine – toluene] (Lit. MP: 100 °C <sup>110</sup>)

**Melting energy:** 162.4 kJ/kg

**TLC:**  $R_f$  (PE/EtOAc, 2:1) = 0.3

**Appearance:** colourless solid

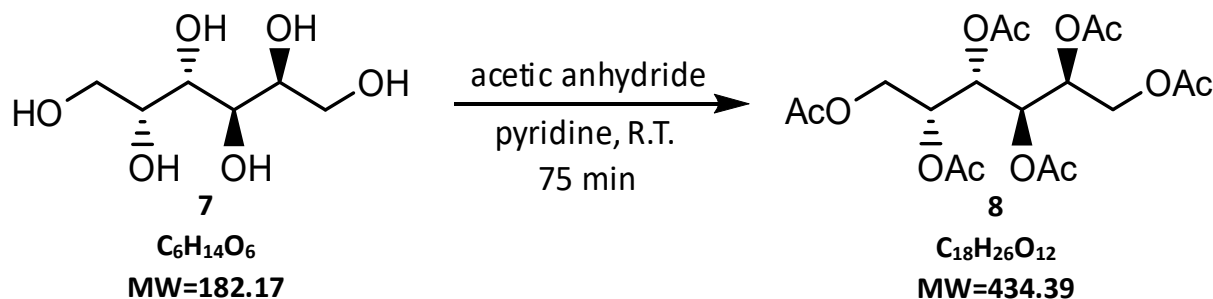
**NMR:**



<sup>1</sup>H NMR (200 MHz, CDCl<sub>3</sub>):  $\delta$  = 2.05-2.13 (m, 18H, 6xCH<sub>3</sub>), 3.97-4.41 (m, 4H, H<sub>1</sub>/H<sub>6</sub>), 5.02-5.28 (m, 2H, H<sub>3</sub>/H<sub>4</sub>), 5.40-5.44 (m, 2H, H<sub>2</sub>/H<sub>5</sub>)



#### 4.2.5 Synthesis of 1,2,3,4,5,6-hexa-O-acetyl-D-galactitol <sup>[101,102]</sup>



The product was synthesized according to general procedure A with:

Dulcitol (506 mg, 2.78 mmol, 1 eq.), acetic anhydride (2.64 mL, 27.8 mmol, 10 eq.), DMAP (catalytic) and pyridine (5 mL)

**Yield:** 99% (1.20 g, 2.76 mmol)

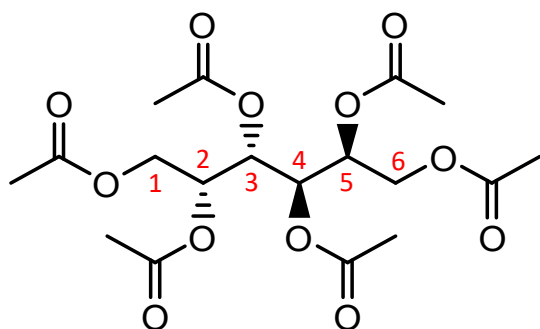
**Melting point:** 171 – 173 °C [Pyridine – toluene] (Lit. MP: 171 °C <sup>111</sup>)

**Melting energy:** 200.7 kJ/kg

**TLC:**  $R_f$  (PE/EtOAc, 2:1) = 0.3

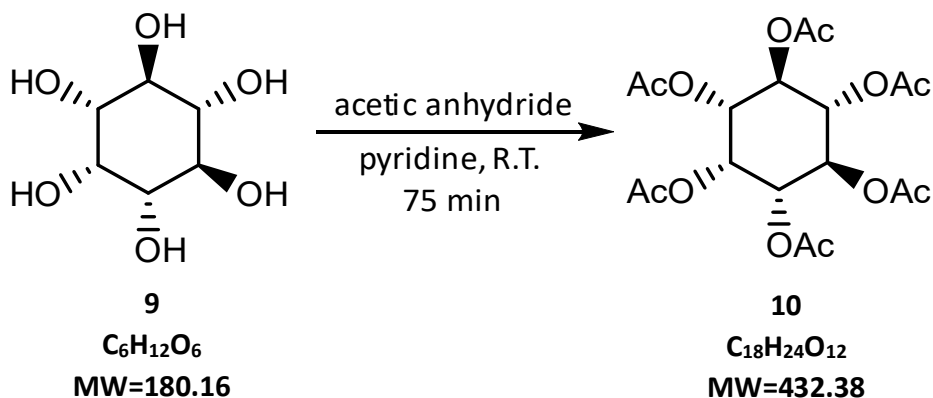
**Appearance:** colourless solid

**NMR:**



<sup>1</sup>H NMR (200 MHz, CDCl<sub>3</sub>):  $\delta$  = 2.02-2.10 (m, 18H, 6xCH<sub>3</sub>), 3.83 (diastereotopic, J=11.50, 7.28 Hz, 2H, CH<sub>2</sub>), 4.28 (diastereotopic, J=12.00, 4.70 Hz, 2H, CH<sub>2</sub>), 5.26-5.35 (m, 4H, 4xCH)

#### 4.2.6 Synthesis of 1,2,3,4,5,6-hexa-O-acetyl-myo-inositol <sup>[101,102,114]</sup>



The product was synthesized according to general procedure A with:

Myo-inositol (500 mg, 2.78 mmol, 1 eq.), acetic anhydride (2.64 mL, 27.8 mmol, 10 eq.), DMAP (catalytic) and pyridine (5 mL)

**Yield:** 62% (0.74 g, 1.71 mmol)

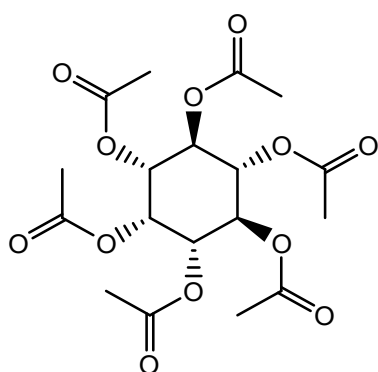
**Melting point:** 216 °C [Pyridine – toluene] (Lit. MP: 214 °C <sup>112</sup>)

**Melting energy:** decomposition

**TLC:**  $R_f$  (PE/EtOAc, 2:1) = 0.28

**Appearance:** colourless solid

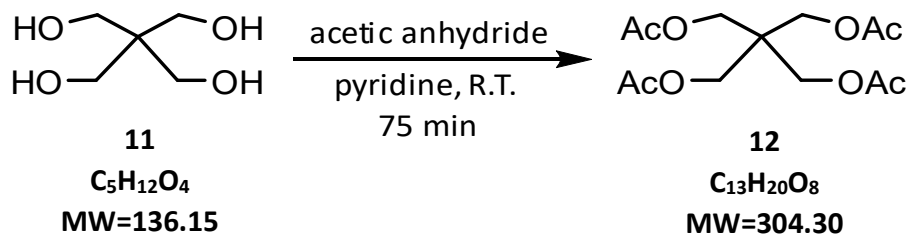
**NMR:**



<sup>1</sup>H NMR (400 MHz, CDCl<sub>3</sub>):  $\delta$  = 1.99-2.20 (m, 18H, 6xCH<sub>3</sub>), 5.06-5.22 (m, 3H, 3xCH), 5.44-5.60 (m, 3H, 3xCH)

<sup>13</sup>C NMR (100 MHz, CDCl<sub>3</sub>):  $\delta$  = 20.46, 20.55, 20.75 (3xq, 6xCH<sub>3</sub>), 68.2 (d, CH), 68.5 (d, 2xCH), 69.4 (d, 2xCH), 71.0 (d, CH) 169.43, 169.67, 169.68, 169.81 (s, 6xC=O)

#### 4.2.7 Synthesis of pentaerythritol tetraacetate <sup>[101,102]</sup>



The product was synthesized according to general procedure A with:

Pentaerythritol (378 mg, 2.78 mmol, 1 eq.), acetic anhydride (2.64 mL, 27.8mmol, 10 eq.), DMAP (catalytic) and pyridine (5 mL)

**Yield:** 100% (845 g, 2.78 mmol)

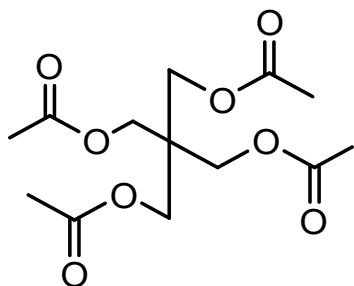
**Melting point:** 76 – 79 °C [Pyridine – toluene] (Lit. MP: 80 °C <sup>113</sup>)

**Melting energy:** 139.9 kJ/kg

**TLC:**  $R_f$  (PE/EtOAc, 2:1) = 0.5

**Appearance:** colourless solid

**NMR:**

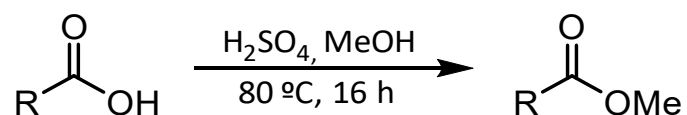


$^1\text{H NMR}$  (400 MHz,  $\text{CDCl}_3$ ):  $\delta$  = 2.07 (s, 12H, 4x $\text{CH}_3$ ), 4.12 (s, 8H, 4x $\text{CH}_2$ )

$^{13}\text{C NMR}$  (100 MHz,  $\text{CDCl}_3$ ):  $\delta$  = 20.7 (t, 4x $\text{CH}_3$ ), 41.6 (s, C), 62.2 (q, 4x $\text{CH}_2$ ), 170.5 (s, 4xCO)

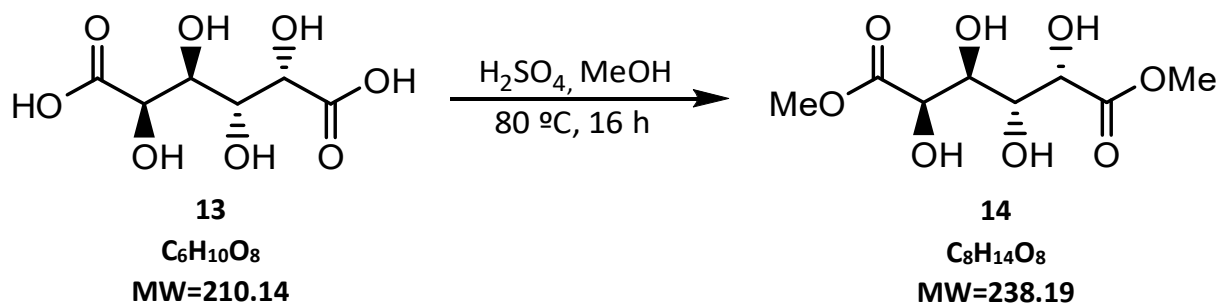
## 4.3 Preparation of mucic acid derivatives

### 4.3.1 General procedure B



Mucic acid (1 eq.) and the desired alcohol (6 mL) were placed in an oven-dried 8 mL vial with a magnetic stirring bar. Sulfuric acid (50  $\mu\text{L}$ ) was added and the vial was closed. Then, the reaction mixture was stirred in a heating block at 80  $^{\circ}\text{C}$  overnight. After this time the reaction became a white suspension and was filtrated and washed several times with the proper alcohol. Finally, the product was dried in high vacuum.

### 4.3.2 Synthesis of dimethyl galactarate <sup>[103]</sup>



The product was synthesized according to general procedure B with:

Mucic Acid (250 mg, 1.19 mmol, 1 eq.), MeOH (6 mL), H<sub>2</sub>SO<sub>4</sub> (50 μL)

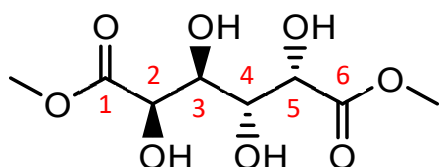
**Yield:** 77% (219 mg, 0.91 mmol)

**Melting point:** 196 °C [MeOH] (Lit. MP: 189 °C <sup>103</sup>)

**Melting energy:** decomposition

**Appearance:** colourless solid

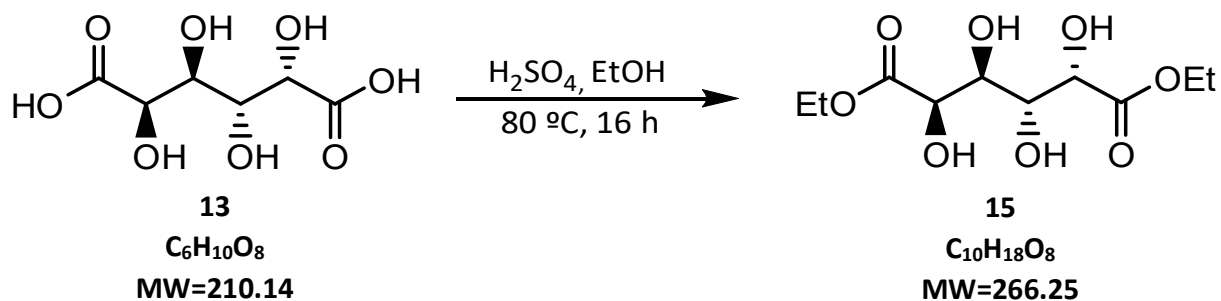
**NMR:**



<sup>1</sup>H NMR (400 MHz, DMSO): δ = 3.64 (s, 6H, 2xCH<sub>3</sub>), 3.78-3.80 (m, 2H, 2xCH), 4.31 (d, J=8.05 Hz, 2H, 2xCH), 4.80-4.83 (m, 2H, OH), 4.92 (d, J=7.93 Hz 2H, OH)

<sup>13</sup>C NMR (100 MHz, DMSO): δ = 51.9 (q, 2xCH<sub>3</sub>), 70.7 (d, C<sub>3</sub>/C<sub>4</sub>), 71.6 (d, C<sub>2</sub>/C<sub>5</sub>), 174.5 (s, C<sub>1</sub>/C<sub>6</sub>)

### 4.3.3 Synthesis of diethyl galactarate <sup>[104]</sup>



The product was synthesized according to general procedure B with:

Mucic Acid (250 mg, 1.19 mmol, 1 eq.), EtOH (3 mL), H<sub>2</sub>SO<sub>4</sub> (25 μL)

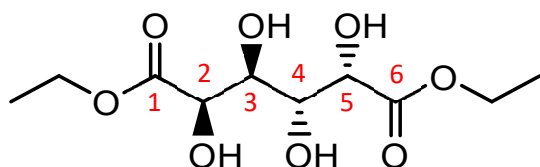
**Yield:** 38% (60 mg, 0.22 mmol)

**Melting point:** 137 – 138 °C [EtOH] (Lit. MP: 158 °C <sup>104</sup>)

**Melting energy:** decomposition

**Appearance:** colourless solid

**NMR:**

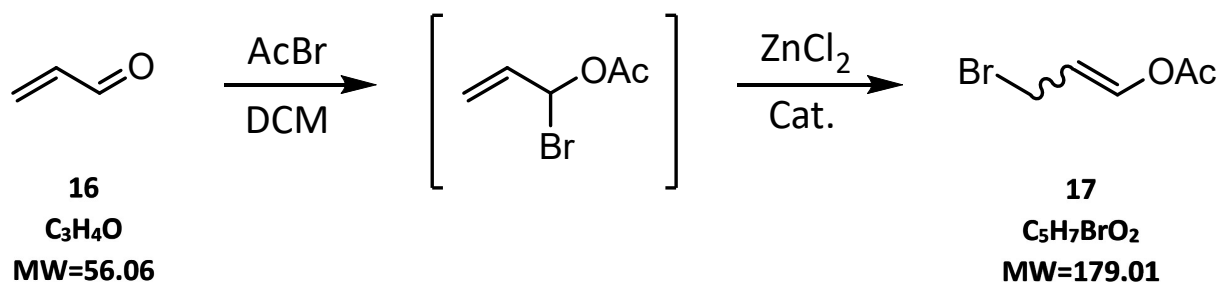


<sup>1</sup>H NMR (400 MHz, DMSO): δ = 1.21 (t, J=7.08 Hz, 6H, 2xCH<sub>3</sub>), 3.78-3.80 (m, 2H, 2xCH), 4.08-4.15 (m, 4H, 2xCH<sub>2</sub>), 4.29 (d, J=7.87 Hz, 2H, 2xCH), 4.78-4.86 (m, 4H, OH)

<sup>13</sup>C NMR (100 MHz, DMSO): δ = 14.6 (q, CH<sub>3</sub>), 60.5 (t, CH<sub>2</sub>), 70.6 (d, 2xCH), 71.7 (d, 2xCH), 174.1 (s, C<sub>1</sub>/C<sub>6</sub>)

## 4.4 Preparation of sugar alcohols

### 4.4.1 Synthesis of (E/Z)-3-bromopropenyl acetate <sup>[66]</sup>



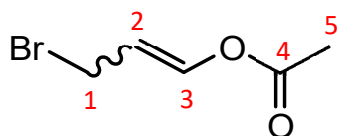
Acrolein (90% purity, containing hydroquinone as stabilizer and < 10% water and cyclic dimer, 10.56 mL, 0.14 mmol, 1 eq.) was dissolved in dry DCM (100 mL) and cooled to -30 °C using acetone and liquid nitrogen. At a temperature about 5 °C, a formation of a white solid was observed. Once the -30 °C temperature is reached, acetyl bromide (9.83 mL, 0.33 mmol, 0.95 eq.) was added first via a syringe within 2 minutes and immediately afterwards dry ZnCl<sub>2</sub> (0.19 g, 1.4 mmol, 0.01 eq.) was added. The reaction mixture was stirred and the cooling bath removed. At the time when the temperature started to increase fast from -20 °C to +10 °C the reaction mixture has to be placed back into the cooling bath and then stirred at -25 °C for another 30 minutes. At this point an NMR was done to check if the reaction was finished

Once complete conversion was observed, the reaction mixture was cooled to -30 °C again and poured into water ice (100 mL). Both phases were separated and the organic phase was washed with cold water. The aqueous phase was checked to be acidic and was extracted again with more and fresh DCM. Afterwards, the combined organic layers were washed with NaHCO<sub>3</sub> twice (100 mL), with brine, dried over Na<sub>2</sub>SO<sub>4</sub> and concentrated to give a crude material as dark liquid. This crude was purified in a vacuum distillation to get 12.85 g of a colourless liquid

**Yield:** 50% (12.85 g, 72.20 mmol)

**Appearance:** Colourless liquid

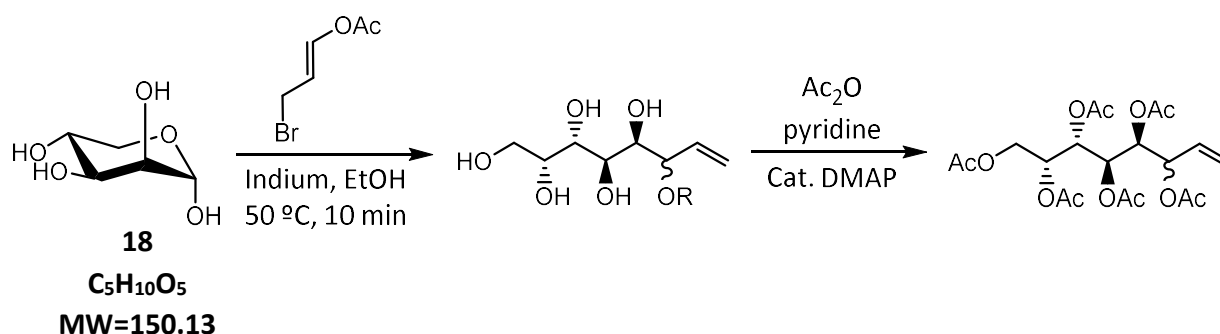
**NMR:** E/Z-mixture



<sup>1</sup>H NMR (200 MHz, CHCl<sub>3</sub>): δ = 2.12, 2.18 (2x s, 3H, H<sub>5</sub>), 3.94-4.08 (m, 2H, H<sub>1</sub>), 5.16-5.75 (m, 1H, H<sub>2</sub>), 7.14-7.43 (m, 1H, H<sub>3</sub>)

The compound was known [67,] and the <sup>1</sup>H NMR was consistent with the literature for that reason no <sup>13</sup>C NMR was recorded.

#### 4.4.2 Synthesis of 1,2-dideoxy-L-glycero-D-manno-oct-1-enitol peracetate (crude) <sup>[66]</sup>



D-Lyxose (1.125 g, 7.5 mmol, 1 eq.) was placed in a round bottom flask with a big magnetic stirring bar and was dissolved with ethanol (45 mL). The reaction mixture was heated at 50°C and stirred at high speed. Then, indium (1.1429 g, 12.45 mmol, 1.66 eq.) was added first and secondly bromopropenylacetate (distilled, 1.125 g, 7.5 mmol, 2.5 eq.) in one go. After 10 minutes the reaction was checked by TLC (C/M/W 7:3:0.5) and complete conversion was observed.

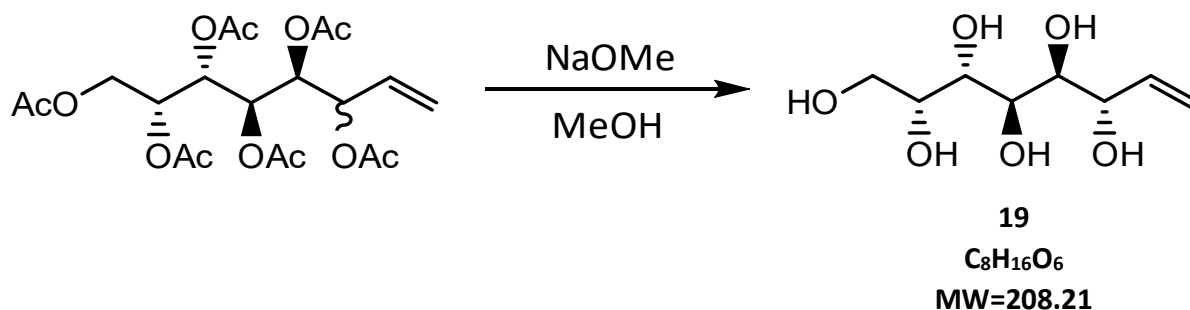
Ten minutes after checking with the TLC, the reaction was cooled and filtered over filter paper to remove indium. Subsequently, it was washed with fresh ethanol and the filtrate was concentrated

Finally, the crude was dissolved in pyridine (20% solution, 26.36 mL) and Ac<sub>2</sub>O (5 eq. per OH group, 70 mL, 0.76 mol, 30 eq.) was poured into the reaction flask. A catalytic amount of DMAP was added and the reaction was left overnight. The next day TLC (1:2 PE/Et<sub>2</sub>O) showed conversion of all starting materials to the targeted compounds. The reaction was then cooled with an ice-bath and iPrOH (5 eq. per OH group, 58 mL, 0.7 mol, 30 eq.) was poured into the reaction flask. Afterwards, the reaction mixture was stirred for 1h and later diluted with DCM. A phase extraction was done using 2N HCl as aqueous phase until this phase remained acidic. The organic phase was separated and washed with water, dried over Na<sub>2</sub>SO<sub>4</sub> and concentrated by co-evaporation with MeOH.

**Yield:** 3.23 g of crude material was obtained.



#### 4.4.3 Synthesis of 1,2-dideoxy-L-glycero-D-manno-oct-1-enitol <sup>[66]</sup>



The crude (3.23 g, 7 mmol, 1 eq.) was dissolved in MeOH and NaOMe was added until a basic pH was reached. The reaction mixture was left for 2 hours under these conditions and after that time TLC (1:2 PE/Et<sub>2</sub>O) showed full conversion to the desired product. Freshly washed (MeOH) DOWEX acidic ion exchange resin was added to neutralize the reaction. Water was poured into the reaction flask to be sure that all the products remained dissolved. Finally, the reaction was filtrated and concentrated by co-evaporation with iPrOH. A recrystallization with water was carried out for a final purification of the product.

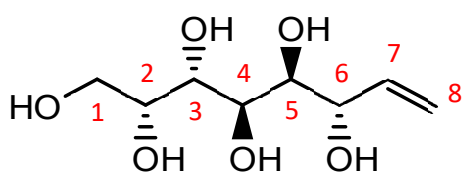
**Yield:** 7% (116 mg, 0.55 mmol)

**Melting point:** 168 – 169 °C [H<sub>2</sub>O] (Lit. MP: 171.9–172.7 °C <sup>66</sup>)

**TLC:** R<sub>f</sub> (CHCl<sub>3</sub>/MeOH/H<sub>2</sub>O, 7:3:0.5) = 0.36

**Appearance:** colourless solid

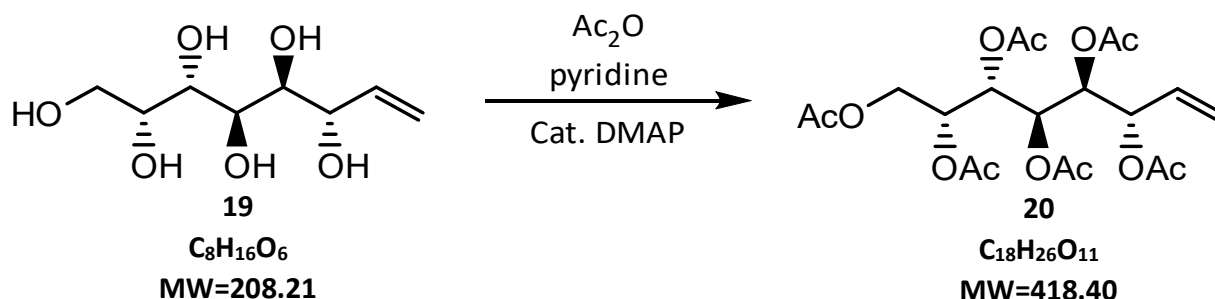
**NMR:**



<sup>1</sup>H NMR (400 MHz, D<sub>2</sub>O): δ = 3.58-3.68 (m, 4H, H<sub>1</sub>/H<sub>3</sub>/H<sub>5</sub>), 3.84-3.92 (m, 2H, H<sub>2</sub>/H<sub>4</sub>), 4.10 (t, J=7.31 Hz, 1H, H<sub>6</sub>), 5.21-5.32 (m, 2H, H<sub>8</sub>), 5.89-5.97 (m, 1H, H<sub>7</sub>)

<sup>13</sup>C NMR (100 MHz, D<sub>2</sub>O): δ = 63.2 (t, C<sub>1</sub>), 68.3 (d, C<sub>4</sub>), 69.3 (d, C<sub>3</sub>), 70.2 (d, C<sub>2</sub>), 71.5 (d, C<sub>5</sub>), 72.4 (d, C<sub>6</sub>), 117.6 (t, C<sub>8</sub>), 137.6 (d, C<sub>7</sub>)

#### 4.4.4 Synthesis of 1,2-dideoxy-L-glycero-D-manno-oct-1-enitol peracetate <sup>[67]</sup>



The pure enitol (0.100 g, 0.47 mmol, 1 eq.) was dissolved in pyridine (20% solution, 0.5 mL) and  $Ac_2O$  (5 eq. per OH group, 1.32 mL, 14.1 mmol, 30 eq.) was poured into the reaction flask. A catalytic amount of DMAP was added and the reaction was left overnight. The next day TLC (1:2 PE/ $Et_2O$ ) showed conversion to the acetylated enitol. The reaction was then cooled with an ice-bath and  $iPrOH$  (5 eq. per OH group, 2 mL, 14.1 mmol, 30 eq.) was poured into the reaction flask. Afterwards, the reaction mixture was stirred for 1h and later diluted with DCM. A phase extraction was done using 2N HCl as aqueous phase until this phase remained acidic. The organic phase was separated and washed with water, dried over  $Na_2SO_4$  and concentrated by co-evaporation with MeOH.

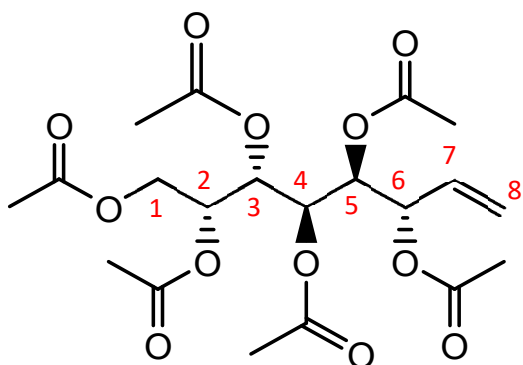
**Yield:** 87% (0.188 g, 0.41 mmol)

**Melting point:** 128 – 129 °C [MeOH]

**TLC:**  $R_f$  (PE/ $Et_2O$ , 1:1) = 0.22

**Appearance:** colourless solid

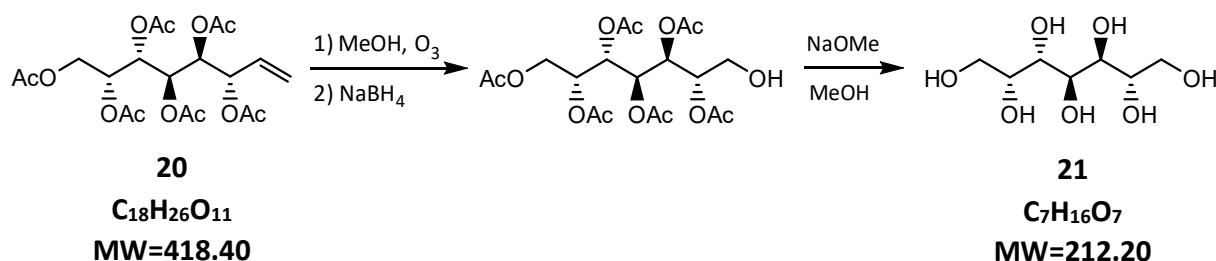
**NMR:**



**$^1\text{H}$  NMR (400 MHz,  $\text{CHCl}_3$ ):**  $\delta$  = 1.94-2.04 (m, 18H, 6x $\text{CH}_3$ ), 3.75 (dd,  $J=11.77, 7.36\text{Hz}$ , 1H,  $\text{CH}_2$ ), 4.21 (dd,  $J=11.82, 4.91\text{ Hz}$ , 1H, CH), 5.04-5.29 (m, 6H,  $\text{CH}_2$ , CH), 5.44 (dd,  $J=9.96, 1.88\text{ Hz}$ , 1H, CH), 5.57-5.62 (m, 1H, CH)

**$^{13}\text{C}$  NMR (100 MHz,  $\text{CHCl}_3$ ):**  $\delta$  = 20.7, 20.9 (q, 6x $\text{CH}_3$ ), 62.3 (t,  $\text{CH}_2$ ), 67.3 (d, CH), 67.7 (d, CH), 67.9 (d, CH), 70.2 (d, CH), 72.4 (d, CH), 120.4 (t,  $\text{CH}_2$ ), 131.3 (d, CH), 169.5, 170.5 (s, 6x $\text{C}=\text{O}$ )

#### 4.4.5 Synthesis of perseitol [67]



The acetylated enitol (200 mg, 0.43 mmol, 1 eq.) was dissolved in MeOH (30 mL) giving a clear solution. The reaction mixture was cooled with acetone and liquid nitrogen until a temperature of  $-78^{\circ}C$  was reached. Ozone was bubbled through the reaction and after around 5 minutes the solution showed an intense blue colour. Ozone was then switched off and oxygen first and nitrogen later were passed through the reaction mixture. The blue colour in the solution disappeared and the complete conversion was confirmed by TLC (1:1 PE/EtOAc). Afterwards, the acetone bath was removed and the temperature of the reaction mixture was allowed to increase from  $-78^{\circ}C$  to  $0^{\circ}C$ . At that temperature an ice bath was installed and  $NaBH_4$  (400 mg, 10.5 mmol, 24.4 eq.) was added in small quantities, controlling that the temperature does not exceed  $10^{\circ}C$ . After full addition, the reaction was running for another 30 min. Finally, DCM was added to the reaction mixture and extracted with  $NH_4Cl$  sat. solution. The organic phase was washed with  $Na_2CO_3$  (5% solution in water), dried with  $Na_2SO_4$  and concentrated to obtain 0.201g of crude material.

This crude material (0.201 g) was dissolved in MeOH and NaOMe was added until a basic pH was reached. The reaction mixture was left 2 hours running and after that time TLC (1:2 PE/ $Et_2O$ ) showed full conversion to the desired product. Freshly washed (MeOH) DOWEX acidic ion exchange resin was added to neutralize the reaction. Water was poured into the reaction mixture to be sure that all the products remained dissolved. Finally, the reaction was filtrated and concentrated by co-evaporation with iPrOH. A recrystallization was carried out for a final purification of the product employing ethanol to get 47 mg of pure Perseitol

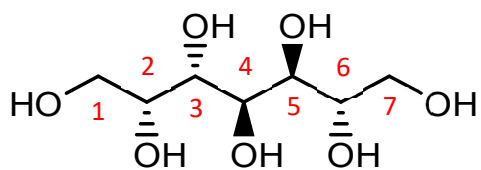
**Yield:** 51% (47mg, 0.22mmol)

**Melting point:** 184 – 185  $^{\circ}C$  [EtOH] (Lit. MP: 188  $^{\circ}C$  <sup>67</sup>)

**Melting energy:** 260.8 kJ/kg

**Appearance:** colourless solid

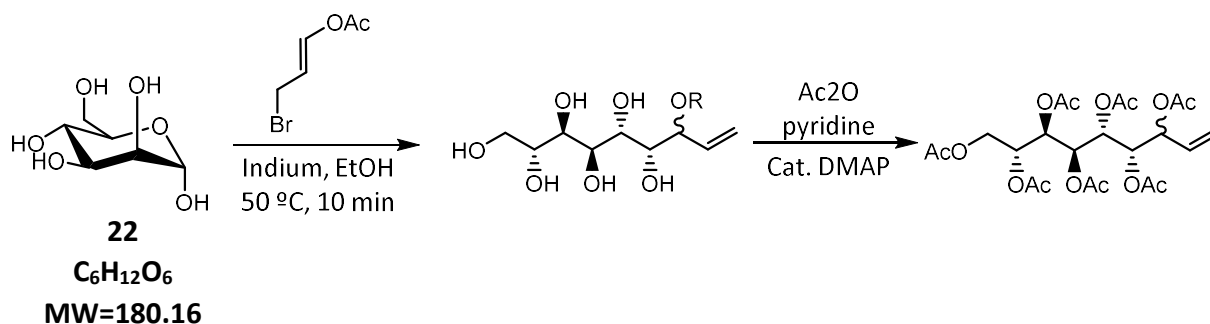
NMR:



$^1\text{H NMR}$  (400 MHz,  $\text{D}_2\text{O}$ ):  $\delta = 3.57\text{-}3.62$  (m, 4H,  $\text{H}_{1\text{-a}}/\text{H}_{1\text{-b}}/\text{H}_{7\text{-a}}/\text{H}_3$ ),  $3.66\text{-}3.71$  (m, 1H,  $\text{H}_6$ ),  $3.72\text{-}3.75$  (m, 1H,  $\text{H}_5$ ),  $3.79$  (dd,  $J=11.81, 2.74$  Hz, 1H,  $\text{H}_{7\text{-b}}$ ),  $3.84$  (d,  $J=9.62$  Hz, 1H,  $\text{H}_4$ ),  $3.91$  (t,  $J=6.38$  Hz, 1H,  $\text{H}_2$ )

$^{13}\text{C NMR}$  (100 MHz,  $\text{D}_2\text{O}$ ):  $\delta = 63.26, 63.28$  (t,  $\text{C}_1/\text{C}_7$ ),  $68.2$  (d,  $\text{C}_4$ ),  $69.1, 69.2$  (d,  $\text{C}_3/\text{C}_5$ ),  $70.2$  (d,  $\text{C}_2$ ),  $70.9$  (d,  $\text{C}_6$ )

#### 4.4.6 Synthesis of 1,2-dideoxy-D-erythro-D-manno-non-1-enitol peracetate <sup>[67]</sup>



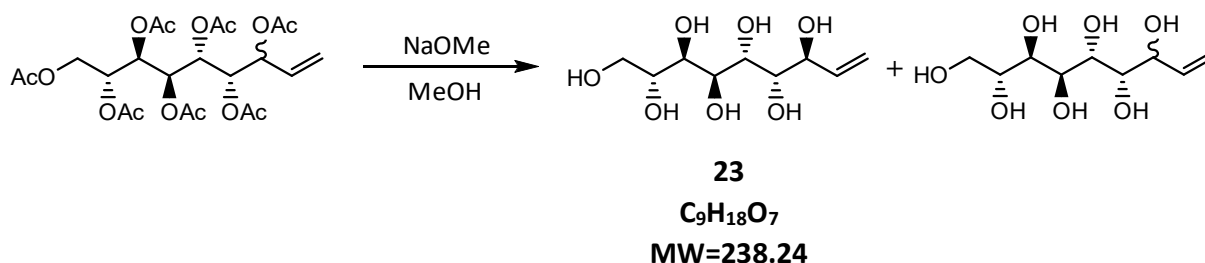
D-Mannose (3 g, 16.7 mmol, 1 eq.) was placed in a round bottom flask with a big magnetic stirring bar and was dissolved with ethanol (120 ml). The reaction mixture was heated at 50°C and stirred at high speed. Then, indium (3.176 g, 27.66 mmol, 1.66 eq.) was added first and secondly bromopropenylacetate (250mg, 1.19mmol, 1 eq.) in one go. After 10 minutes the reaction was checked by TLC (C/M/W 7:3:0.5) and complete conversion was observed.

Ten minutes after checking with the TLC, the reaction was cooled and filtered over filter paper to remove indium. Subsequently, it was washed with fresh ethanol and the filtrate was concentrated

Finally, the crude material was dissolved in pyridine (20% solution) and Ac<sub>2</sub>O (5 eq. per OH group) was poured into the reaction flask. A catalytic amount of DMAP was added and the reaction was left overnight. The next day TLC (1:2 PE/Et<sub>2</sub>O) showed conversion to the mixture of acetylated enitols. The reaction was then cooled with an ice-bath and iPrOH (5 eq. per OH group) was poured into the reaction mixture. Afterwards, the reaction mixture was stirred for 1h and later diluted with DCM. A phase extraction was done using 2N HCl as aqueous phase until this phase remained acidic. The organic phase was separated and washed with water, dried over Na<sub>2</sub>SO<sub>4</sub> and concentrated by coevaporation with MeOH. A yield of 8.56 g as crude material was obtained.

Yield (crude): 8.56

#### 4.4.7 Synthesis of 1,2-dideoxy-D-erythro-D-manno-non-1-enitol <sup>[67,105]</sup>



The crude (8.56 g, 16 mmol, 1 eq.) was dissolved in MeOH (7 mL) and NaOMe was added until a basic pH was reached. After several minutes a white precipitate was formed. Water and MeOH was poured into the reaction flask until the white precipitate was dissolved. The reaction mixture was left 2 hours running and after that time TLC (1:2 PE/Et<sub>2</sub>O) showed full conversion to the desired product. Freshly washed (MeOH) DOWEX acidic ion exchange resin was added to neutralize the reaction. Water was poured into the reaction mixture to be sure that all the products remained dissolved. Finally, the reaction was filtrated and concentrated by coevaporation with iPrOH. A recrystallization was carried out for a final purification of the product employing water (5 mL) and the precipitate was washed with MeOH. 494 mg of pure product **23** and 350 mg of product **23** with a presence of 5% minor isomer were obtained. Moreover, 1.41 g mixture of isomers was obtained too.

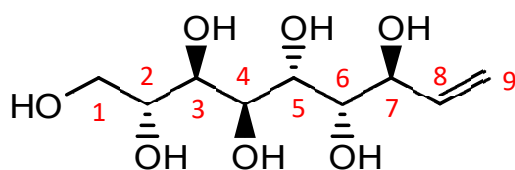
**Yield:** 13% (494 mg, 2 mmol)

**Melting point:** 200 – 202 °C [H<sub>2</sub>O]

**TLC:** R<sub>f</sub> (CHCl<sub>3</sub>/MeOH/H<sub>2</sub>O, 7:3:0.5) = 0.23

**Appearance:** colourless solid

**NMR:**



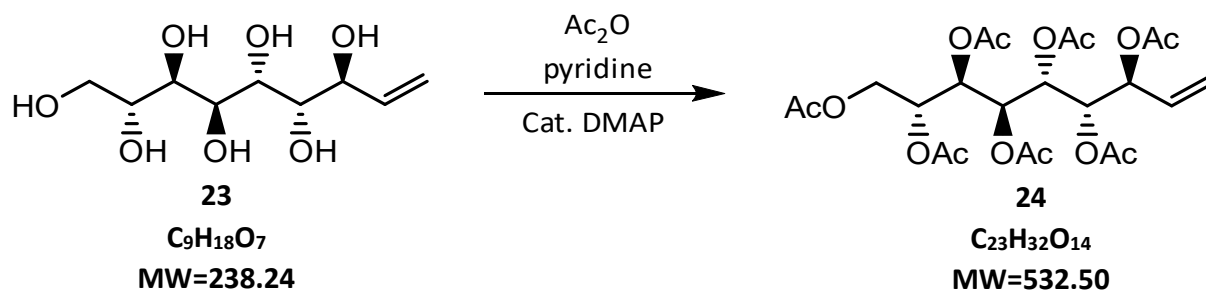
**<sup>1</sup>H NMR (600 MHz, D<sub>2</sub>O):** δ = 3.63 (dd, J=12.11, 6.25 Hz, 1H, H<sub>1</sub>), 3.72-3.74 (m, 2H, H<sub>5</sub>/H<sub>6</sub>)\*, 3.78-3.79 (m, 1H, H<sub>1</sub>), 3.83 (dd, J=11.83, 2.80 Hz, 1H, H<sub>4</sub>), 3.88-3.90 (m, 2H, H<sub>2</sub>/H<sub>3</sub>)\*, 4.15 (t, J=7.43 Hz, 1H, H<sub>7</sub>), 5.27 (dt, J=10.50, 1.21 Hz 1H, H<sub>9</sub>), 5.34 (dt, J=17.21, 1.36 Hz, 1H, H<sub>9</sub>), 5.95-6.00 (m, 1H, H<sub>8</sub>)

**<sup>13</sup>C NMR (150 MHz, D<sub>2</sub>O):** δ = 63.2 (t, C<sub>1</sub>), 68.2 (d, C<sub>2</sub>/C<sub>3</sub>)\*, 69.1 (d, C<sub>4</sub>), 70.9 (d, C<sub>5</sub>)\*, 71.5 (d, C<sub>6</sub>)\*, 72.5 (d, C<sub>7</sub>), 117.6 (t, C<sub>9</sub>), 137.6 (d, C<sub>8</sub>)

\*ambiguous assignment

#### 4.4.8 Synthesis of 1,2-dideoxy-D-erythro-D-manno-non-1-enitol peracetate

[67,105]



The pure enitol (300 mg, 1.26 mmol, 1 eq.) was dissolved in pyridine (20% solution, 1.5 mL) and Ac<sub>2</sub>O (5 eq. per OH group, 4.16 mL, 44.1 mmol, 35 eq.) was poured into the reaction flask. A catalytic amount of DMAP was added and the reaction was left stirring overnight at RT. The next day TLC (1:2 PE/Et<sub>2</sub>O) showed complete conversion. The reaction was then cooled with an ice-bath and iPrOH (5 eq. per OH group, 3.37 mL, 44.1 mol, 35 eq.) was poured into the reaction mixture. Afterwards, the reaction mixture was stirred for 1h and later diluted with DCM. A phase extraction was done using 2N HCl as aqueous phase until this phase remained acidic. The organic phase was separated and washed with water, dried over Na<sub>2</sub>SO<sub>4</sub> and concentrated by co-evaporation with MeOH.

**Yield:** 75% (500 mg, 0.94 mmol)

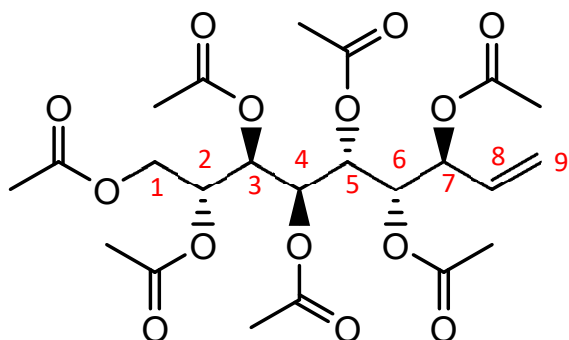
**Melting point:** 129 – 131 °C [MeOH]

**TLC:** R<sub>f</sub> (PE/Et<sub>2</sub>O, 1:1) = 0.11

**Appearance:** colourless solid



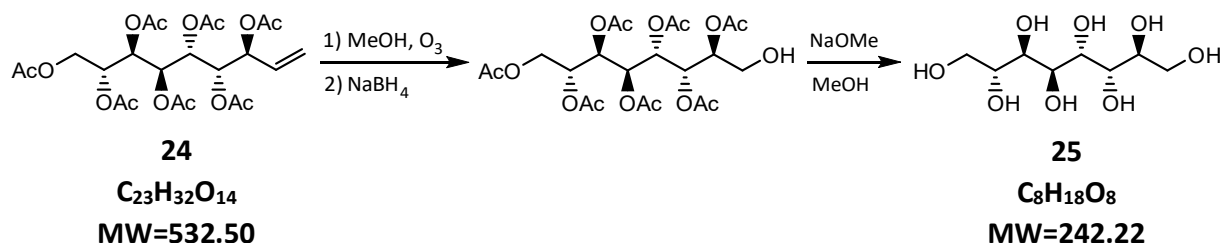
## NMR:



$^1\text{H}$  NMR (400 MHz,  $\text{CHCl}_3$ ):  $\delta$  = 2.02-2.09 (m, 21H, 7x $\text{CH}_3$ ), 3.93 (dd,  $J$ =12.79, 5.66 Hz, 1H,  $\text{H}_1$ ), 4.15 (dd,  $J$ =12.42, 3.07 Hz, 1H,  $\text{H}_1$ ), 4.97-5.01 (m, 1H,  $\text{H}_5$ ), 5.04 (d,  $J$ =3.95 Hz, 2H,  $\text{H}_6/\text{H}_7$ ), 5.23-5.34 (m, 3H,  $\text{H}_4/\text{H}_9$ ), 5.42 (s, 2H,  $\text{H}_2/\text{H}_3$ ), 5.65-5.74 (m, 1H,  $\text{H}_8$ )

$^{13}\text{C}$  NMR (100 MHz,  $\text{CHCl}_3$ ):  $\delta$  = 20.66, 20.69, 20.74, 20.91, 20.93, 21.07 (q, 7x $\text{CH}_3$ ), 61.9 (t,  $\text{C}_1$ ), 66.5 (d,  $\text{C}_2$ ), 66.7 (d), 67.4 (d), 68.3 (d), 69.3 (d), 72.3 (d), 121.0 (t,  $\text{C}_9$ ), 132.2 (d,  $\text{C}_8$ ), 169.58, 169.64, 169.69, 169.92, 169.97, 170.10, 170.54 (s, 7x $\text{C}=\text{O}$ )

#### 4.4.9 Synthesis of D-erythro-D-manno-octitol [67,68,69,105]



The acetylated enitol (400 mg, 0.75 mmol, 1 eq.) was dissolved in MeOH (30 mL) giving a clear solution. The reaction mixture was cooled with acetone and liquid nitrogen until a temperature of  $-78^{\circ}\text{C}$  was reached. Ozone was bubbled through the reaction and after around 5 minutes the solution showed an intense blue colour. Ozone was then switched off and oxygen first and nitrogen later were passed through the reaction mixture. The blue colour in the solution disappeared and complete conversion was confirmed by TLC (1:1 PE/EtOAc). Afterwards, the acetone bath was removed and the temperature of the reaction mixture was allowed to increase from  $-78^{\circ}\text{C}$  to  $0^{\circ}\text{C}$ . At that temperature an ice bath was installed and  $\text{NaBH}_4$  (1.1 g, 29.04 mmol, 38.7 eq.) was added in small quantities, controlling that the temperature does not exceed  $10^{\circ}\text{C}$ . After full addition, the reaction was running for another 30 min. Finally, DCM was added to the reaction mixture and extracted with  $\text{NH}_4\text{Cl}$  sat. solution. The organic phase was washed with  $\text{Na}_2\text{CO}_3$  (5% solution in water), dried with  $\text{Na}_2\text{SO}_4$  and concentrated to obtain 197mg of our intermediate.

This intermediate (197 mg, 0.36 mmol, 1 eq.) was dissolved in MeOH and NaOMe was added until a basic pH was reached. After several minutes a white precipitate was formed. Water and MeOH was poured into the reaction mixture until the white precipitate was dissolved. The reaction mixture was left 2 hours running and after that time TLC (1:2 PE/Et<sub>2</sub>O) showed full conversion to the desired product. Freshly washed (MeOH) DOWEX acidic ion exchange resin was added to neutralize the reaction. Some more water was poured again into the reaction flask and the mixture was refluxed to be sure that all the products remained dissolved. Finally, the reaction was filtrated still hot and concentrated by co-evaporation with iPrOH. Recrystallization from water gave 88.2 mg of the desired octitol.

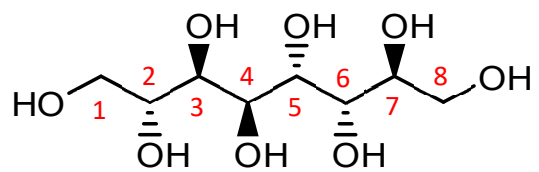
**Yield:** 48 % (88.2 mg, 0.36mmol)

**Melting point:** 263 – 266  $^{\circ}\text{C}$  [ $\text{H}_2\text{O}$ ] (Lit. MP: 262  $^{\circ}\text{C}$  [67,68,69,105])

**Melting energy:** 352.2 kJ/kg

**Appearance:** colourless solid

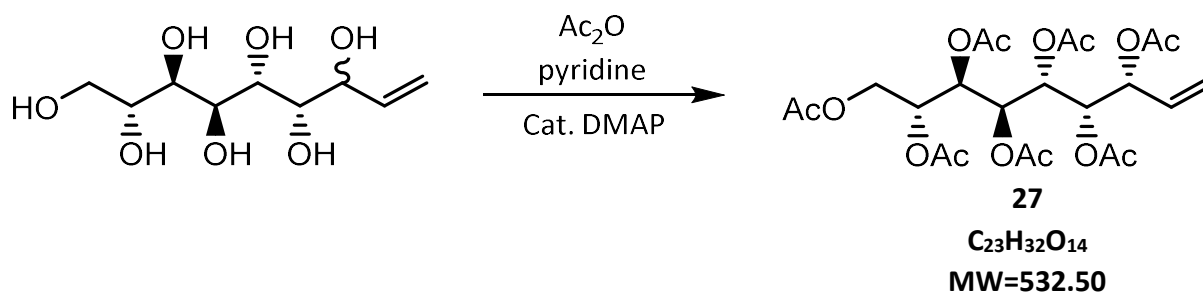
NMR:



<sup>1</sup>H NMR (400 MHz, D<sub>2</sub>O):  $\delta$  = 3.58-3.62 (m, 2H, H<sub>1</sub>/ H<sub>8</sub>), 3.67-3.71 (m, 2H, H<sub>2</sub>/ H<sub>7</sub>), 3.75-3.81 (m, 4H, H<sub>1</sub>/ H<sub>8</sub>/ H<sub>3</sub>/ H<sub>6</sub>), 3.84 (s, 2H, H<sub>4</sub>/ H<sub>5</sub>)

<sup>13</sup>C NMR (100 MHz, D<sub>2</sub>O):  $\delta$  = 63.2 (t, C<sub>1</sub>/C<sub>8</sub>), 68.1 (d, C<sub>4</sub>/C<sub>5</sub>), 69.2 (d, C<sub>3</sub>/C<sub>6</sub>), 70.9 (d, C<sub>2</sub>/C<sub>7</sub>)

#### 4.4.10 Synthesis of 1,2-dideoxy-D-erythro-L-gluco-non-1-enitol peracetate <sup>[67,105]</sup>



The mixture of enitols (1.41 g, 5.88 mmol, 1 eq.) was dissolved in pyridine (20% solution, 18.68 mL) and Ac<sub>2</sub>O (5 eq. per OH group, 19.4 mL, 0.2 mol, 35 eq.) was poured into the reaction flask. A catalytic amount of DMAP was added and the reaction was left overnight at RT. The next day TLC (1:2 PE/Et<sub>2</sub>O) showed conversion from the enitol to the acetylated enitol. The reaction was then cooled with an ice-bath and iPrOH (5 eq. per OH group, 3.37 mL, 0.2 mol, 35 eq.) was poured into the reaction mixture. Afterwards, the reaction mixture was stirred for 1h and later diluted with DCM. A phase extraction was done using 2N HCl as aqueous phase until this phase remained acidic. The organic phase was isolated and washed with water, dried over Na<sub>2</sub>SO<sub>4</sub> and concentrated by coevaporation with MeOH. The crude (2.41g) was separated in a MPLC column (1:1 PE/Et<sub>2</sub>O) and selected fractions were combined and concentrated to end up with 720 mg of the desired product

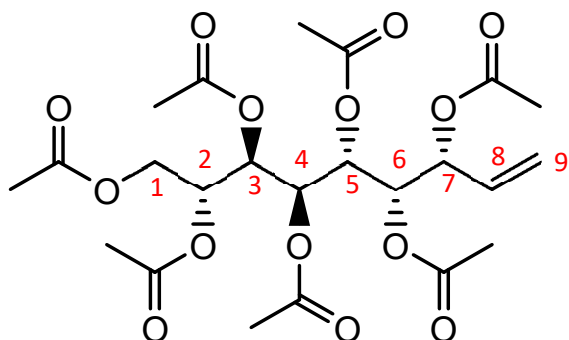
**Yield:** 25% (720 mg, 1.46 mmol)

**Melting point:** 89 – 90 °C [PE]

**TLC:** R<sub>f</sub> (PE/Et<sub>2</sub>O, 1:1) = 0.17

**Appearance:** colourless solid

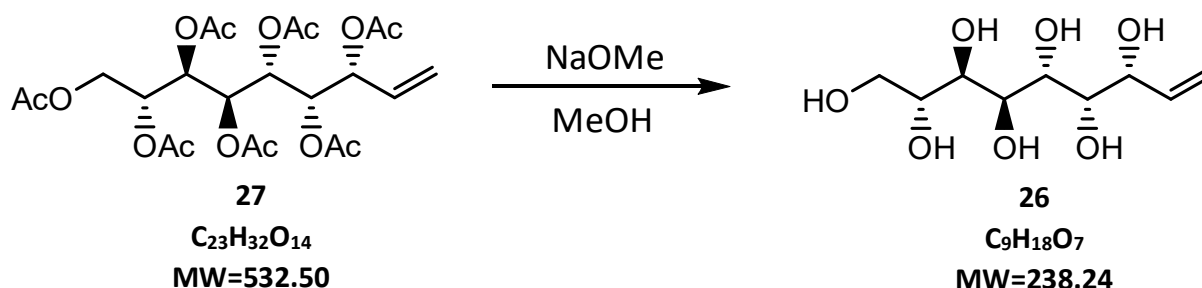
## NMR:



<sup>1</sup>H NMR (400 MHz, D<sub>2</sub>O): δ = 2.03-2.23 (m, 21H, 7xCH<sub>3</sub>), 4.03 (dd, J=12.59, 5.46 Hz, 1H), 4.20 (dd, J=12.58, 3.15 Hz, 1H), 4.99-5.03 (m, 1H, H<sub>2</sub>), 5.11 (dd, J=7.36, 2.59 Hz, 1H), 5.25-5.37 (m, 6H), 5.79-5.87 (m, 1H)

<sup>13</sup>C NMR (100 MHz, D<sub>2</sub>O): δ = 20.63, 20.69, 20.74, 20.84, 20.85, 20.88 (q, 7xCH<sub>3</sub>), 61.8 (t, C<sub>1</sub>), 67.0 (d), 67.3 (d), 67.5 (d), 68.2 (d, C<sub>2</sub>), 70.1 (d), 71.9 (d), 119.8 (t, C<sub>9</sub>), 131.3 (d, C<sub>8</sub>), 169.49, 169.65, 169.84, 169.86, 169.93, 170.54 (s, 7xC=O)

#### 4.4.11 Synthesis of 1,2-dideoxy-D-erythro-L-gluco-non-1-enitol <sup>[67,105]</sup>



The starting material (719 mg, 1.46 mmol, 1 eq.) was dissolved in MeOH and NaOMe was added until a basic pH was reached. After several minutes a white precipitate was formed. Some water and MeOH was poured into the reaction flask and the white precipitate was dissolved. The reaction mixture was left 2 hours running and after that time TLC (1:2 PE/Et<sub>2</sub>O) showed full conversion to the desired product. Freshly washed (MeOH) DOWEX acidic ion exchange resin was added to neutralize the reaction. Water was poured into the reaction mixture to be sure that all the products remained dissolved. Finally, the reaction was filtrated and concentrated by coevaporation with iPrOH. The crude product was triturated with iPrOH and 102 mg of a white solid precipitate were obtained

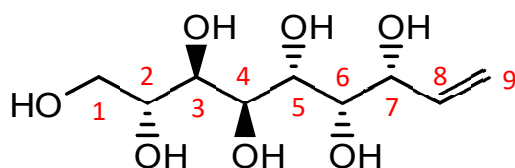
**Yield:** 32% (102 mg, 0.42 mmol)

**Melting point:** 183 – 184 °C [iPrOH]

**TLC:** R<sub>f</sub> (CHCl<sub>3</sub>/MeOH/H<sub>2</sub>O, 7:3:0.5) = 0.3

**Appearance:** colourless solid

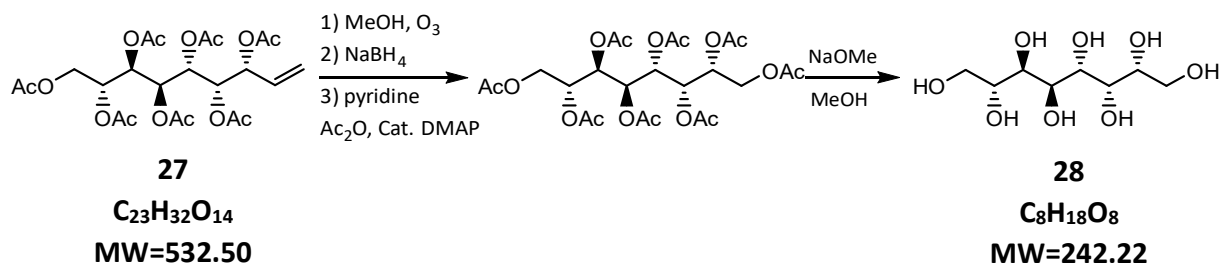
#### NMR



**<sup>1</sup>H NMR (400 MHz, D<sub>2</sub>O):** δ = 3.62-3.65 (m, 1H, H<sub>1</sub>), 3.72-3.74 (m, 2H, 2xCH), 3.78 (dd, J=11.80, 2.54 Hz, 1H, H<sub>1</sub>), 3.84 (d, J=9.52 Hz, 1H, CH), 3.88-3.90 (m, 2H, 2xCH), 4.17 (t, J=7.80 Hz, 1H, CH), 5.23 (d, J=10.54 Hz, 1H, CH), 5.32(d, J=17.51 Hz, 1H, CH), 5.95-5.98 (m, 1H, CH)

**<sup>13</sup>C NMR (100 MHz, D<sub>2</sub>O):** δ = 63.2 (t, C<sub>1</sub>), 68.2 (d), 69.1 (d), 70.9 (d), 71.5 (d), 72.5 (d, C<sub>7</sub>), 117.6 (t, C<sub>9</sub>), 137.6 (d, C<sub>8</sub>)

#### 4.4.12 Synthesis of D-erythro-L-gluco-octitol <sup>[67,68,69,105]</sup>



The acetylated enitol (160 mg, 0.3 mmol, 1 eq.) was dissolved in MeOH (30 mL) giving a clear solution. The reaction mixture was cooled with acetone and liquid nitrogen until a temperature of  $-78^{\circ}C$  was reached. Ozone was bubbled through the reaction and after around 5 minutes the solution showed an intense blue colour. Ozone was then switched off and oxygen first and nitrogen later were passed through the reaction mixture. The blue colour in the solution disappeared and complete conversion was confirmed by TLC (1:1 PE/EtOAc). Afterwards, the cooling bath was removed and the temperature of the reaction mixture was allowed to increase from  $-78^{\circ}C$  to  $0^{\circ}C$ . At that temperature an ice bath was installed and  $NaBH_4$  (440 mg, 11.61 mmol, 38.7 eq.) was added in small quantities, controlling that the temperature does not exceed  $10^{\circ}C$ . After full addition, the reaction was running for another 30 min. A few drops of acetic acid were added until the reaction becomes acidic and afterwards it was concentrated and redissolved twice in MeOH. The crude material was reacylated using pyridine (4 mL) as solvent, an excess of  $Ac_2O$  (3 mL) and a catalytic amount of DMAP. The same work-up protocol as in reaction 3.4.10 was followed and 142 mg of acetylated octitol (yellow oil) were obtained.

The intermediate (142 mg, 0.36 mmol, 1 eq.) was dissolved in MeOH and NaOMe was added until a basic pH was reached. After several minutes a white precipitate was formed. Water and MeOH was poured into the reaction flask until the white precipitate was dissolved. The reaction mixture was left 2 hours running and after that time TLC (1:2 PE/Et<sub>2</sub>O) showed full conversion to the desired product. Freshly washed (MeOH) DOWEX acidic ion exchange resin was added to neutralize the reaction. Some more water was poured again into the reaction and the mixture was refluxed to be sure that all the products remained dissolved. Finally, the reaction was filtrated hot and concentrated by coevaporation with iPrOH. A recrystallization was carried out for a final purification of the product employing water. 11.8 mg of the desired octitol were obtained.

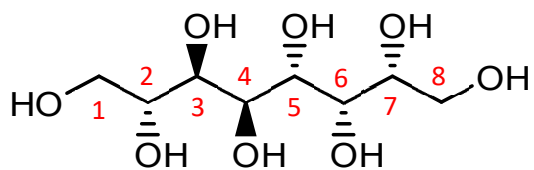
**Yield:** 16% (11.8 mg, 0.048mmol)

**Melting point:** 164 – 166  $^{\circ}C$  [ $H_2O$ ] (Lit. MP: 166  $^{\circ}C$ <sup>67,68,69,105</sup>)

**Melting energy:** 163.8 kJ/kg

**Appearance:** colourless solid

NMR:



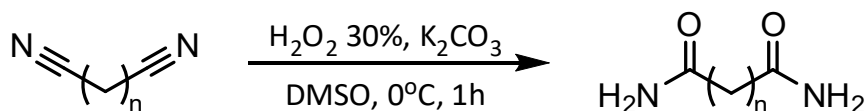
$^1\text{H NMR}$  (400 MHz,  $\text{D}_2\text{O}$ ):  $\delta = 3.62\text{-}3.70$  (m, 2H,  $\text{H}_1/\text{H}_8$ ),  $3.74\text{-}3.83$  (m, 4H,  $\text{H}_1/3\times\text{CH}$ ),  $3.85\text{-}3.91$  (m, 3H,  $\text{H}_8/2\times\text{CH}$ ),  $3.93\text{-}3.96$  (d, 1H, CH).

$^{13}\text{C NMR}$  (100 MHz,  $\text{D}_2\text{O}$ ):  $\delta = 62.3$   $63.2$  (2xt,  $\text{C}_1, \text{C}_8$ ),  $68.3$  (d, C),  $69.0$  (d, C),  $69.6$  (d, C),  $69.8$  (d, C),  $70.8$  (d, C),  $73.2$  (d, C)



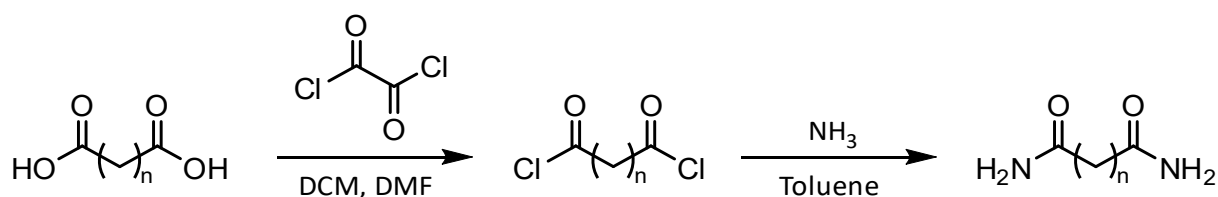
## 4.5 Preparation of aliphatic- $\alpha,\omega$ -diamides

### 4.5.1 General procedure C



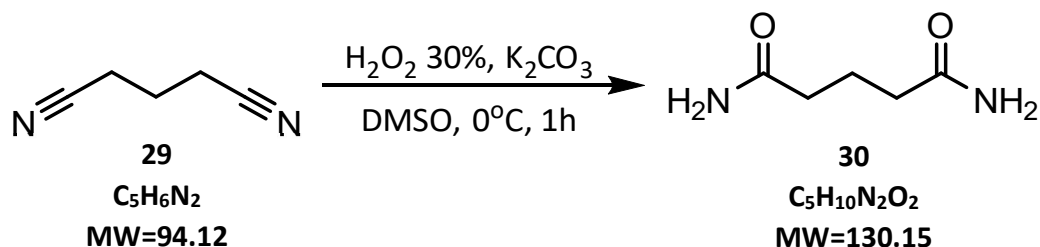
$\text{K}_2\text{CO}_3$  (100 mg) was placed in an oven-dried 50 mL round bottom flask with a magnetic stirring bar and cooled with an ice bath to 0 °C. Afterwards, DMSO (1.5 mL) and the desired dinitrile (1 eq.) were added via syringe. At last,  $\text{H}_2\text{O}_2$  30% solution (0.6 mL) was added dropwise and slowly via syringe at 0 °C under temperature control. The reaction was running for 1 hour at room temperature. The vial was cooled in an ice bath and the resulting suspension was filtrated. A recrystallization was carried out for a final purification of the product employing a suitable solvent.

### 4.5.2 General procedure D



The corresponding dicarboxylic acid (1 eq.) and dichloromethane were placed in a 2 L round bottom flask. The reaction vessel was flushed with argon before oxalyl chloride (2.4 eq.) and a catalytic amount of *N,N*-dimethylformamide (cat.) were added. After 2 hours, the dichloromethane was removed in the rotavapor. To the residue (intermediate diacyl chloride) toluene was added. Ammonia gas was bubbled through the toluene solution during 30 min to finally get the corresponding diamide. The crude product was recrystallized from methanol and dried in vacuo.

### 4.5.3 Synthesis of glutaramide <sup>[72]</sup>



The product was synthesized according to general procedure C with:

1,3-Dicyanopropane (0.47 mL, 5 mmol, 1 eq.), DMSO (1.5 mL), H<sub>2</sub>O<sub>2</sub> 30% solution (0.6 mL), K<sub>2</sub>CO<sub>3</sub> (100 mg).

The solvent employed for the recrystallization was EtOH

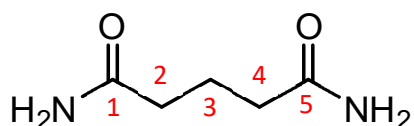
**Yield:** 37% (0.24 g, 1.86 mmol)

**Melting point:** 180 – 181 °C [EtOH] (Lit. MP: 181 °C <sup>72</sup>)

**Melting energy:** 260.3 kJ/kg

**Appearance:** colourless solid

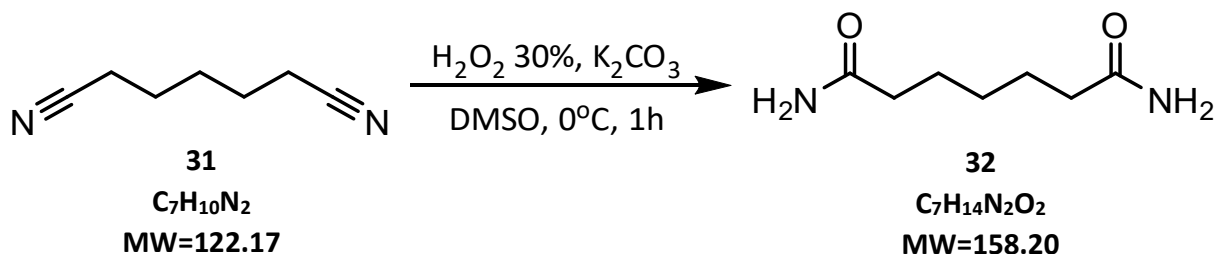
**NMR:**



<sup>1</sup>H NMR (400 MHz, DMSO): δ = 1.65-1.71 (m, 2H, H<sub>3</sub>), 2.02-2.08 (m, 4H, H<sub>2</sub>/H<sub>4</sub>), 6.73 (s, 2H, NH<sub>2</sub>), 7.26 (s, 2H, NH<sub>2</sub>)

<sup>13</sup>C NMR (100 MHz, DMSO): δ = 21.5 (t, C<sub>3</sub>), 34.9 (t, C<sub>2</sub>/C<sub>4</sub>), 174.5 (s, C<sub>1</sub>/C<sub>5</sub>)

#### 4.5.4 Synthesis of pimelamide <sup>[72]</sup>



The product was synthesized according to the general procedure C with:

1,5-Dicyanopentane (0.64 mL, 5 mmol, 1 eq.), DMSO (1.5 mL), H<sub>2</sub>O<sub>2</sub> 30% solution (1.2 mL), K<sub>2</sub>CO<sub>3</sub> (100 mg).

The solvent employed for the recrystallization was EtOH

**Yield:** 88% (0.69 g, 4.4 mmol)

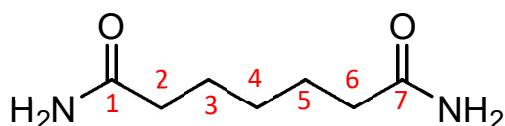
**Melting point:** 172 – 173 °C [EtOH] (Lit. MP: 173 °C <sup>72</sup>)

**Melting energy:** 277.2 kJ/kg

**TLC:** R<sub>f</sub> (PE/EtOAc, 2:1)

**Appearance:** colourless solid

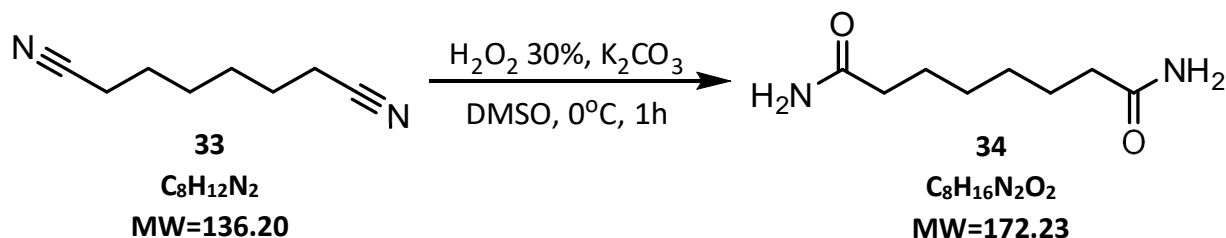
**NMR:**



**<sup>1</sup>H NMR (400 MHz, DMSO):** δ = 1.19-1.23 (m, 2H, H<sub>4</sub>), 1.46 (quin, J=7.42 Hz, 4H, H<sub>3</sub>/H<sub>5</sub>), 2.02 (t, J=7.44 Hz, 4H, H<sub>2</sub>/H<sub>6</sub>), 6.68 (s, 2H, NH<sub>2</sub>), 7.22 (s, 2H, NH<sub>2</sub>)

**<sup>13</sup>C NMR (100 MHz, DMSO):** δ = 25.3 (t, C<sub>4</sub>), 28.8 (t, C<sub>3</sub>/C<sub>5</sub>), 35.4 (t, C<sub>2</sub>/C<sub>6</sub>), 174.7 (s, C<sub>1</sub>/C<sub>7</sub>)

#### 4.5.5 Synthesis of suberamide <sup>[72]</sup>



The product was synthesized according to the general procedure C with:

1,6-Dicyanohexane (0.5 mL, 5 mmol, 1 eq.), DMSO (1.5 mL), H<sub>2</sub>O<sub>2</sub> 30% solution (0.6 mL), K<sub>2</sub>CO<sub>3</sub> (100 mg).

The solvent employed for the recrystallization was EtOH

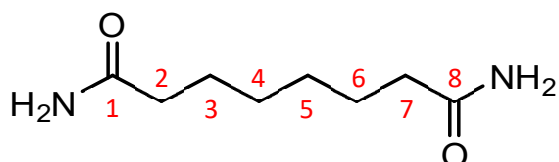
**Yield:** 17% (0.14 g, 0.85 mmol)

**Melting point:** 220 – 222 °C [EtOH] (Lit. MP: 220 °C <sup>72</sup>)

**Melting energy:** 335.1 kJ/kg

**Appearance:** colourless solid

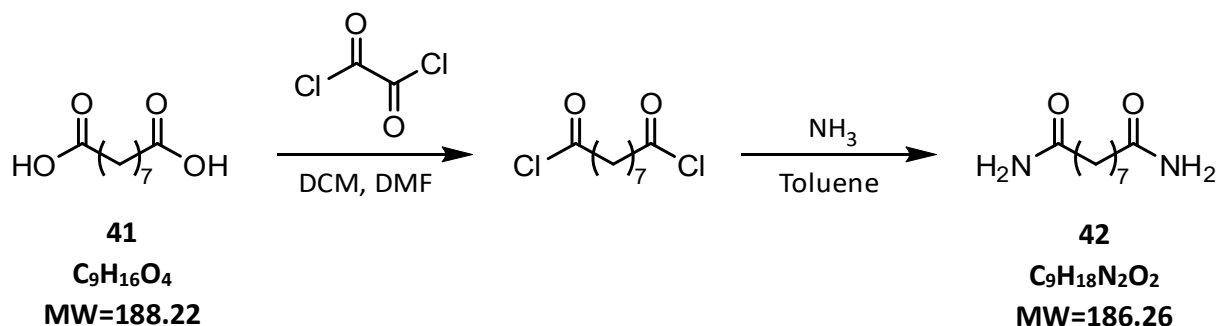
**NMR:**



<sup>1</sup>H NMR (400 MHz, DMSO): δ = 1.20-1.26 (m, 4H, H<sub>4</sub>/H<sub>5</sub>), 1.46 (quin, J=7.22 Hz, 4H, H<sub>3</sub>/H<sub>6</sub>), 2.02 (t, J=7.49 Hz, 4H, H<sub>2</sub>/H<sub>7</sub>), 6.67 (s, 2H, NH<sub>2</sub>), 7.22 (s, 2H, NH<sub>2</sub>)

<sup>13</sup>C NMR (100 MHz, DMSO): δ = 25.4 (t, C<sub>4</sub>/C<sub>5</sub>), 29.0 (t, C<sub>3</sub>/C<sub>6</sub>), 35.5 (t, C<sub>2</sub>/C<sub>7</sub>), 174.7 (s, C<sub>1</sub>/C<sub>8</sub>)

#### 4.5.6 Synthesis of azelamide <sup>[73]</sup>



The product was synthesized according to the general procedure D with:

Azelaic acid (500 mg, 2.66 mmol, 1 eq.), dichloromethane (26 mL) oxalyl chloride (0.55 mL, 6.38 mmol, 2.4 eq.), N,N-dimethylformamide (10 drops, cat.) and 200 mL of toluene.

The solvent employed for the recrystallization was EtOH

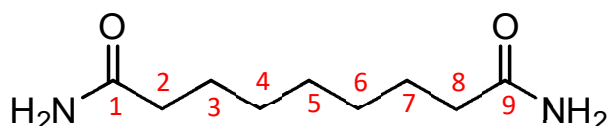
**Yield:** 37% (0.18 g, 0.97 mmol)

**Melting point:** 179 – 180 °C [EtOH] (Lit. MP: 177 °C <sup>73</sup>)

**Melting energy:** 247.8 kJ/kg

**Appearance:** colourless solid

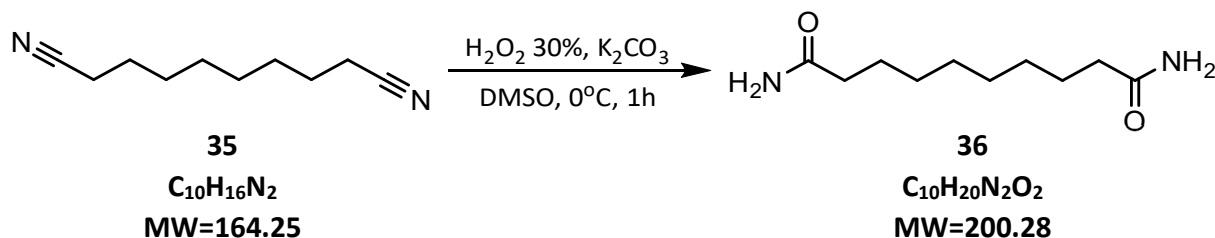
**NMR:**



<sup>1</sup>H NMR (400 MHz, DMSO):  $\delta$  = 1.18-1.29 (m, 6H, H<sub>4</sub>/H<sub>5</sub>/H<sub>6</sub>), 1.46 (quin, J=6.63 Hz, 4H, H<sub>3</sub>/H<sub>7</sub>), 2.02 (t, J=7.38 Hz, 4H, H<sub>2</sub>/H<sub>8</sub>), 6.67 (s, 2H, NH<sub>2</sub>), 7.21 (s, 2H, NH<sub>2</sub>)

<sup>13</sup>C NMR (100 MHz, DMSO):  $\delta$  = 25.5 (t, C<sub>5</sub>), 29.1, 29.0 (t, C<sub>3</sub>/C<sub>4</sub>/C<sub>6</sub>/C<sub>7</sub>), 35.5 (t, C<sub>2</sub>/C<sub>8</sub>), 174.7 (s, C<sub>1</sub>/C<sub>9</sub>)

#### 4.5.7 Synthesis of sebacamide <sup>[72]</sup>



The product was synthesized according to the general procedure C with:

1,8-Dicyanooctane (3.6 mL, 20 mmol, 1 eq.), DMSO (6 mL), H<sub>2</sub>O<sub>2</sub> 30% solution (5 mL), K<sub>2</sub>CO<sub>3</sub> (400 mg).

The solvent employed for the recrystallization was EtOH

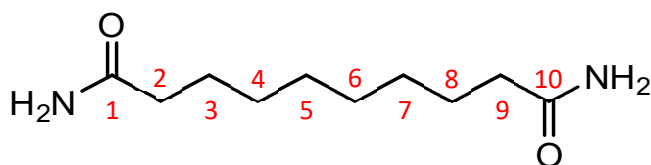
**Yield:** 49% (1.99 g, 9.8 mmol)

**Melting point:** 210 – 212 °C [EtOH] (Lit. MP: 210 °C <sup>72</sup>)

**Melting energy:** 375.6 kJ/kg

**Appearance:** colourless solid

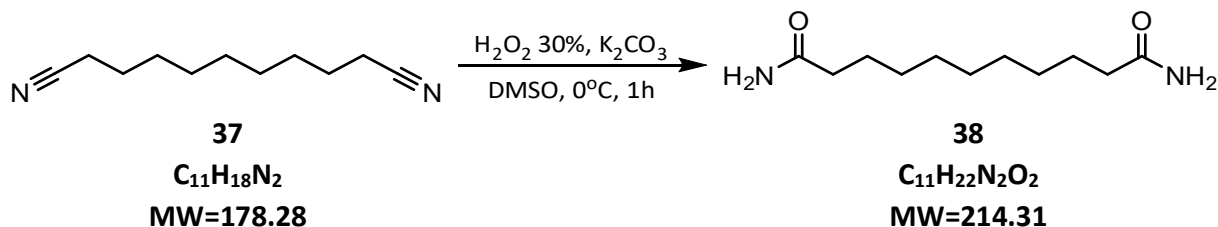
**NMR:**



<sup>1</sup>H NMR (400 MHz, DMSO): δ = 1.18-1.28 (m, 8H, H<sub>4</sub>/H<sub>5</sub>/H<sub>6</sub>/H<sub>7</sub>), 1.46 (quin, J=6.81 Hz, 4H, H<sub>3</sub>/H<sub>8</sub>), 2.02 (t, J=7.35 Hz, 4H, H<sub>2</sub>/H<sub>9</sub>), 6.66 (s, 2H, NH<sub>2</sub>), 7.21 (s, 2H, NH<sub>2</sub>)

<sup>13</sup>C NMR (100 MHz, DMSO): δ = 25.5 (t, C<sub>5</sub>/C<sub>6</sub>), 29.16 (t, C<sub>4</sub>/C<sub>7</sub>), 29.19 (t, C<sub>3</sub>/C<sub>8</sub>), 35.5 (t, C<sub>2</sub>/C<sub>9</sub>), 174.7 (s, C<sub>1</sub>/C<sub>10</sub>)

#### 4.5.8 Synthesis of undecanediamide <sup>[72]</sup>



The product was synthesized according to the general procedure C with:

1,9-Dicyanononene (3.92 mL, 20 mmol, 1 eq.), DMSO (6 mL), H<sub>2</sub>O<sub>2</sub> 30% solution (2.4 mL), K<sub>2</sub>CO<sub>3</sub> (100 mg).

The solvent employed for the recrystallization was water

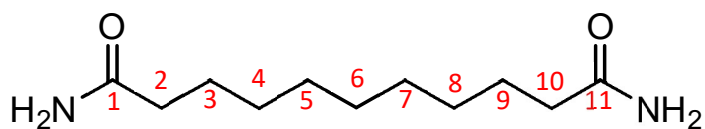
**Yield:** 37% (0.24 g, 1.86 mmol)

**Melting point:** 181 – 182 °C [H<sub>2</sub>O] (Lit. MP: 178 °C <sup>72</sup>)

**Melting energy:** 281.4 kJ/kg

**Appearance:** colourless solid

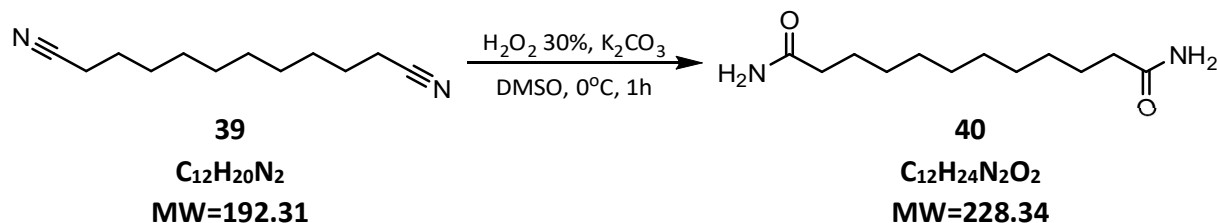
**NMR:**



**<sup>1</sup>H NMR (400 MHz, DMSO):** δ = 1.26-1.32 (m, 10H, H<sub>4</sub>/H<sub>5</sub>/H<sub>6</sub>/H<sub>7</sub>/H<sub>8</sub>), 1.52 (quin, J=7.24 Hz, 4H, H<sub>3</sub>/H<sub>9</sub>), 2.07 (t, J=7.54 Hz, 4H, H<sub>2</sub>/H<sub>10</sub>), 6.73(s, 2H, NH<sub>2</sub>), 7.27(s, 2H, NH<sub>2</sub>)

**<sup>13</sup>C NMR (100 MHz, DMSO):** δ = 25.5 (t, C<sub>6</sub>), 29.1, 29.2, 29.3 (t, C<sub>3</sub>/C<sub>4</sub>/C<sub>5</sub>/ C<sub>7</sub>/ C<sub>8</sub>/C<sub>9</sub>), 35.5 (t, C<sub>2</sub>/C<sub>10</sub>), 174.7 (s, C<sub>1</sub>/C<sub>11</sub>)

#### 4.5.9 Synthesis of dodecanediamide <sup>[72,73]</sup>

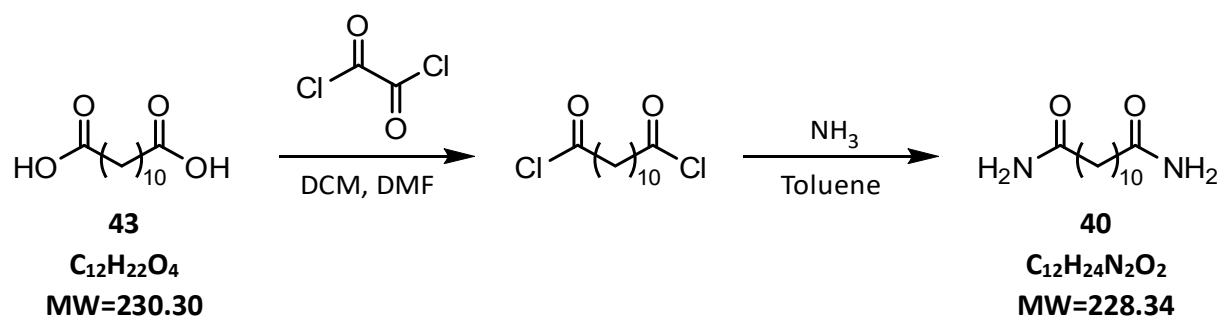


The product was synthesized according to the general procedure C with:

1,10-Dicyanodecane (10.7 mL, 50 mmol, 1 eq.), DMSO (27 mL),  $\text{H}_2\text{O}_2$  30% solution (12 mL),  $\text{K}_2\text{CO}_3$  (1 g).

The solvent employed for the recrystallization was MeOH

**Yield:** 86% (9.82 g, 43 mmol)



In this particular case, the product was also synthesized according to the general procedure D with:

Dodecanedioic acid (20 g, 86.8 mmol, 1 eq.), dichloromethane (800 mL) oxalyl chloride (18.4 mL, 0.208mol, 2.4 eq.), N,N-dimethylformamide (5mL, cat.) and 200 mL of toluene.

**Yield:** 80% (15.86 g, 69.5mmol)

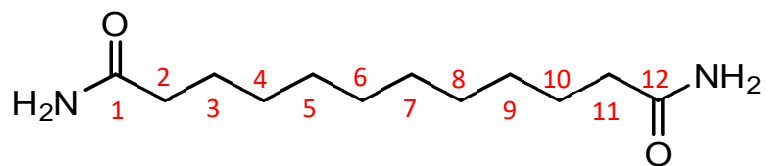
**Melting point:** 191 – 194 °C [MeOH] (Lit. MP: 193 °C <sup>72</sup>)

**Melting energy:** 338.8 kJ/kg

**Appearance:** colourless solid



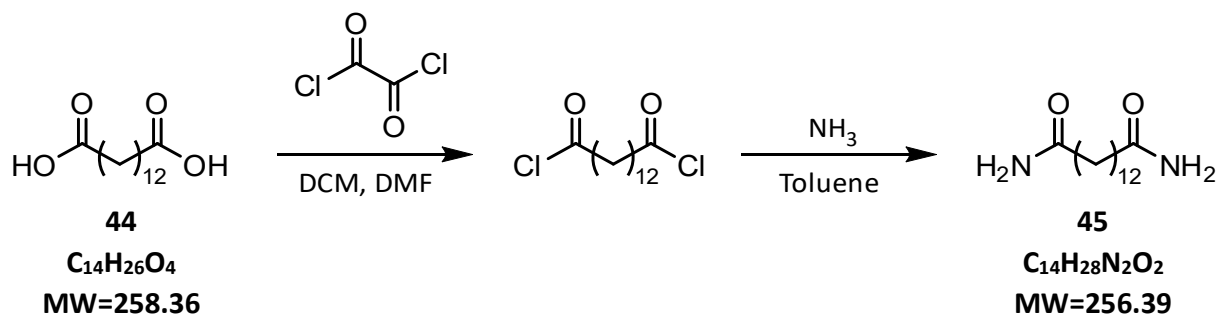
**NMR:**



**<sup>1</sup>H NMR (400 MHz, DMSO):**  $\delta$  = 1.28-1.36 (m, 12H, H<sub>4</sub>/H<sub>5</sub>/H<sub>6</sub>/H<sub>7</sub>/H<sub>8</sub>/H<sub>9</sub>), 1.54 (quin, J=7.04 Hz, 4H, H<sub>3</sub>/H<sub>10</sub>), 2.10 (t, J=7.43 Hz, 4H, H<sub>2</sub>/H<sub>11</sub>), 6.74(s, 2H, NH<sub>2</sub>), 7.29(s, 2H, NH<sub>2</sub>)

**<sup>13</sup>C NMR (100 MHz, DMSO):**  $\delta$  = 25.5 (t, C<sub>6</sub>/C<sub>7</sub>), 29.1 (t, C<sub>5</sub>/C<sub>8</sub>), 29.2 (t, C<sub>4</sub>/C<sub>9</sub>), 29.3 (t, C<sub>3</sub>/C<sub>10</sub>), 35.5 (t, C<sub>2</sub>/C<sub>11</sub>), 174.7 (s, C<sub>1</sub>/C<sub>12</sub>)

#### 4.5.10 Synthesis of tetradecanediamide <sup>[73]</sup>



The product was synthesized according to the general procedure D with:

Tetradecanedioic acid (1.12 g, 4.34 mmol, 1 eq.), dichloromethane (42 mL) oxalyl chloride (0.92 mL, 10.4 mmol, 2.4 eq.), N,N-dimethylformamide (16 drops, cat.) and 200 mL of toluene.

The solvent employed for the recrystallization was MeOH

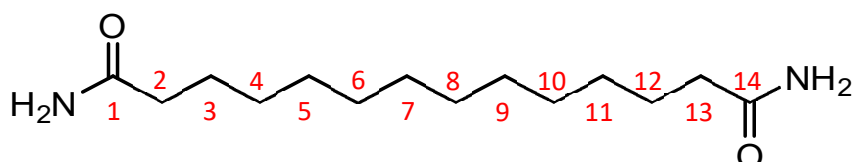
**Yield:** 84% (0.94 g, 3.70 mmol)

**Melting point:** 194 – 196 °C [MeOH] (Lit. MP: 196 °C <sup>73</sup>)

**Melting energy:** 319.9 kJ/kg

**Appearance:** colourless solid

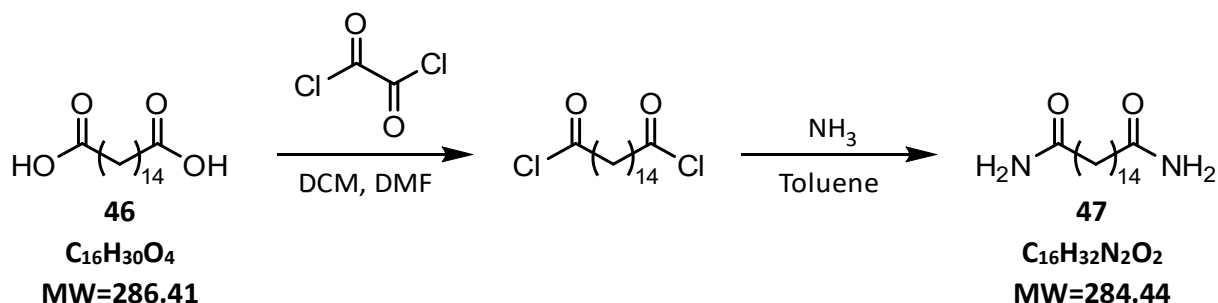
**NMR:**



**<sup>1</sup>H NMR (400 MHz, DMSO):**  $\delta$  = 1.19-1.30 (m, 16H, H<sub>4</sub>/H<sub>5</sub>/H<sub>6</sub>/H<sub>7</sub>/H<sub>8</sub>/H<sub>9</sub>/H<sub>10</sub>/H<sub>11</sub>), 1.46 (quin, J=7.04 Hz, 4H, H<sub>3</sub>/H<sub>12</sub>), 2.01 (t, J=7.60 Hz, 4H, H<sub>2</sub>/H<sub>13</sub>), 6.66 (s, 2H, NH<sub>2</sub>), 7.21 (s, 2H, NH<sub>2</sub>)

**<sup>13</sup>C NMR (100 MHz, DMSO):**  $\delta$  = 25.5 (t, C<sub>7</sub>/C<sub>8</sub>), 29.1 (t, C<sub>6</sub>/C<sub>9</sub>), 29.2 (t, C<sub>5</sub>/C<sub>10</sub>), 29.42 (t, C<sub>4</sub>/C<sub>11</sub>), 29.47 (t, C<sub>3</sub>/C<sub>12</sub>), 35.5 (t, C<sub>2</sub>/C<sub>13</sub>), 174.7 (s, C<sub>1</sub>/C<sub>14</sub>)

#### 4.5.11 Synthesis of hexadecanediamide <sup>[73]</sup>



The product was synthesized according to the general procedure D with:

Hexadecanedioic acid (1.25 g, 4.34 mmol, 1 eq.), dichloromethane (42 mL) oxalyl chloride (0.92 mL, 10.4 mmol, 2.4 eq.), N,N-dimethylformamide (16 drops, cat.) and 200 mL of toluene.

The solvent employed for the recrystallization was MeOH

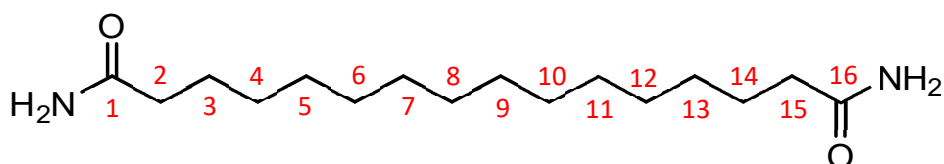
**Yield:** 38% (0.48 g, 1.64 mmol)

**Melting point:** 181 – 184 °C [MeOH] (Lit. MP: 179 °C <sup>73</sup>)

**Melting energy:** 282.9 kJ/kg

**Appearance:** colourless solid

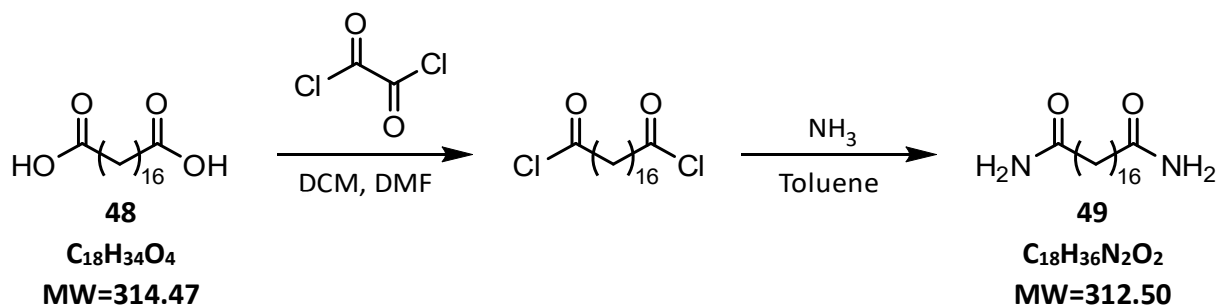
**NMR:**



**<sup>1</sup>H NMR (400 MHz, DMSO):**  $\delta$  = 1.19-1.30 (m, 20H,  $H_4/H_5/H_6/H_7/H_8/H_9/H_{10}/H_{11}/H_{12}/H_{13}$ ), 1.46 (quin,  $J=7.05$  Hz, 4H,  $H_3/H_{14}$ ), 2.01 (t,  $J=7.56$  Hz, 4H,  $H_2/H_{15}$ ), 6.66(s, 2H,  $NH_2$ ), 7.20(s, 2H,  $NH_2$ )

**<sup>13</sup>C NMR (100 MHz, DMSO):**  $\delta$  = 25.5 (t,  $C_7/C_8/C_9/C_{10}$ ), 29.1 (t,  $C_6/C_{11}$ ), 29.2 (t,  $C_5/C_{12}$ ), 29.4 (t,  $C_4/C_{13}$ ), 29.5 (t,  $C_3/C_{14}$ ), 35.5 (t,  $C_2/C_{15}$ ), 174.7 (s,  $C_1/C_{16}$ )

#### 4.5.12 Synthesis of octadecanediamide <sup>[73]</sup>



The product was synthesized according to the general procedure D with:

Octadecanedioic acid (500 mg, 1.59 mmol, 1 eq.), dichloromethane (16 mL) oxalyl chloride (0.34 mL, 3.82 mmol, 2.4 eq.), N,N-dimethylformamide (16 drops, cat.) and 200 mL of toluene.

The solvent employed for the recrystallization was MeOH

**Yield:** 47% (0.23 g, 0.75 mmol)

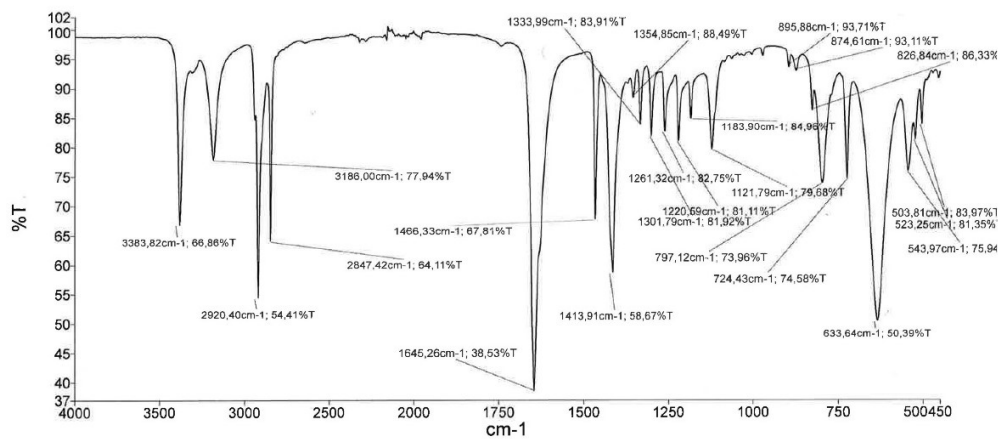
**Melting point:** 181 – 184 °C [MeOH](Lit. MP: 179 °C <sup>73</sup>)

**Melting energy:** 264.7 kJ/kg

**Appearance:** colourless solid

**IR:**

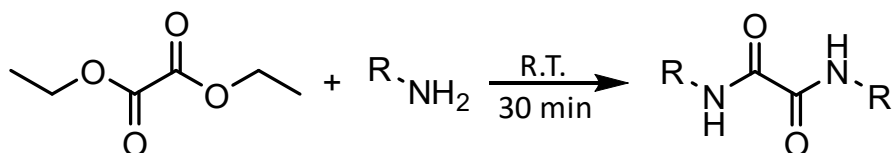
Due to the lack of solubility of octadecanediamide in deuterated solvents, it was not possible to record any NMR. Instead a FTIR was measured.



The resulting spectra shown the characteristic C=O band related to amida groups at  $1645\text{ cm}^{-1}$ . Other bands observed in this FTIR and related to amida groups are the C-N stretch band at  $1466\text{ cm}^{-1}$  and the two N-H stretch bands at  $3383$  and  $3186\text{ cm}^{-1}$ . Therefore, the final product is confirmed.

## 4.6 Preparation of substituted diamides

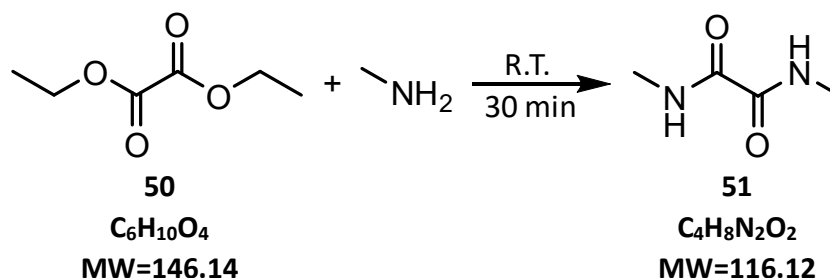
### 4.6.1 General procedure E



Oxalic acid diethyl (1 eq.) ester was placed in an oven-dried 50 mL round bottom flask with a magnetic stirring bar. Afterwards, the desired amine (2.6 eq.) was added via syringe and a white solid precipitate was formed rapidly. The reaction was running for 30 min at room temperature and finally the resulting suspension was filtrated. A recrystallization was carried out for a final purification of the product employing a suitable solvent.

## 4.6.2 Oxalamide derivatives

### 4.6.2.1 N,N'-Dimethyloxalamide <sup>[75-77]</sup>



The product was synthesized according to the general procedure E with:

Oxalic acid diethyl ester (1.46 g, 10 mmol, 1 eq.) and methylamine solution 33 wt. % in absolute ethanol (2.45 mg, 26 mmol, 2.6 eq.). The crude product was recrystallized from water and dried in vacuo to give 77% yield of N,N'-dimethyloxalamide.

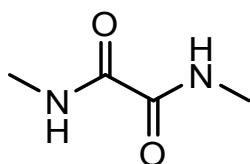
**Yield:** 77% ( 0.89 g, 7.66 mmol)

**Melting point:** 214 – 215 °C [H<sub>2</sub>O] (Lit. MP: 210 °C <sup>75-77</sup>)

**Melting energy:** decomposition

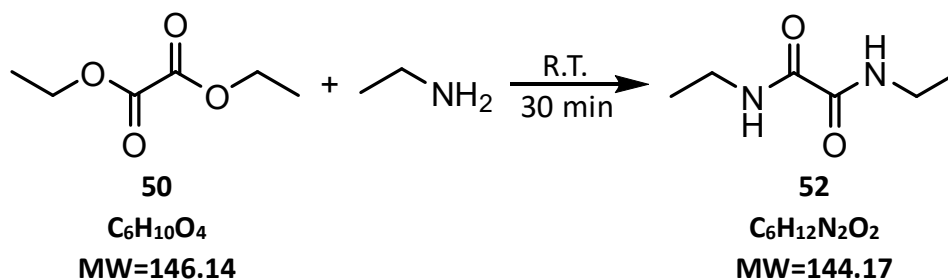
**Appearance:** colourless solid

**NMR:**



<sup>1</sup>H NMR (400 MHz, DMSO): δ = 2.66 (d, J=5.05 Hz, 6H, CH<sub>3</sub>), 8.66 (s, 2H, NH)

<sup>13</sup>C NMR (100 MHz, DMSO): δ = 26.2 (q, CH<sub>3</sub>), 160.9 (s, CO)

4.6.2.2 N,N'-Diethyloxalamide <sup>[75-77]</sup>

The product was synthesized according to the general procedure E with:

Oxalic acid diethyl ester (1.46 g, 10 mmol, 1 eq.) and ethylamine solution 70 % in H<sub>2</sub>O (1.7 mg, 26 mmol, 2.6 eq.). The crude product was recrystallized from ethanol and dried in vacuo to give 22% yield of N,N'-diethyloxalamide.

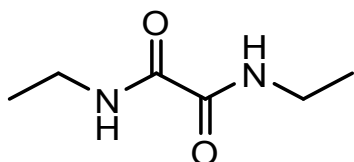
**Yield:** 22% (0.31 g, 2.15 mmol)

**Melting point:** 179 – 182 °C [EtOH] (Lit. MP: 177 °C <sup>75-77</sup>)

**Melting energy:** decomposition

**Appearance:** colourless solid

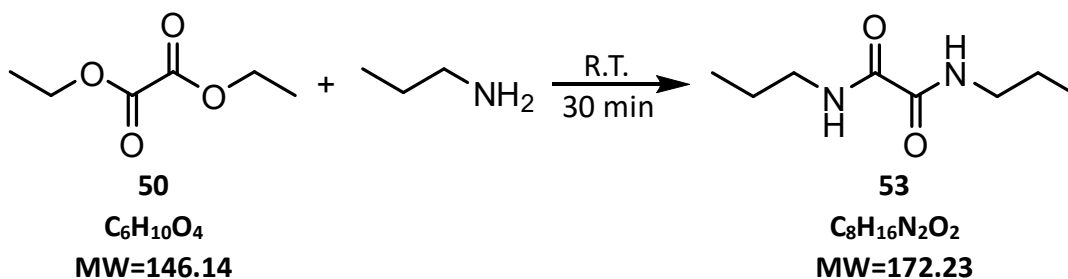
**NMR:**



<sup>1</sup>H NMR (400 MHz, DMSO): δ = 1.04 (t, J=7.01 Hz, 6H, CH<sub>3</sub>), 3.15 (quind, J=7.09, 1.14 Hz, 4H, CH<sub>2</sub>), 8.72 (s, 2H, NH)

<sup>13</sup>C NMR (100 MHz, DMSO): δ = 14.8 (q, CH<sub>3</sub>), 34.1 (t, CH<sub>2</sub>), 160.3 (s, CO)



4.6.2.3 N,N'-Dipropyloxalamide <sup>[75-77]</sup>

The product was synthesized according to the general procedure E with:

Oxalic acid diethyl ester (1.46 g, 10 mmol, 1 eq.) and propylamine (1.44 g, 24 mmol, 2.4 eq.). The crude product was recrystallized from ethanol and dried in vacuo to give 63% yield of N,N'-dipropyloxalamide.

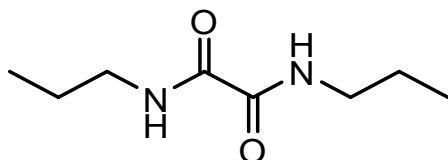
**Yield:** 63% (1.09 g, 6.32 mmol)

**Melting point:** 161 – 169 °C [EtOH] (Lit. MP: 162 °C <sup>75-77</sup>)

**Melting energy:** decomposition

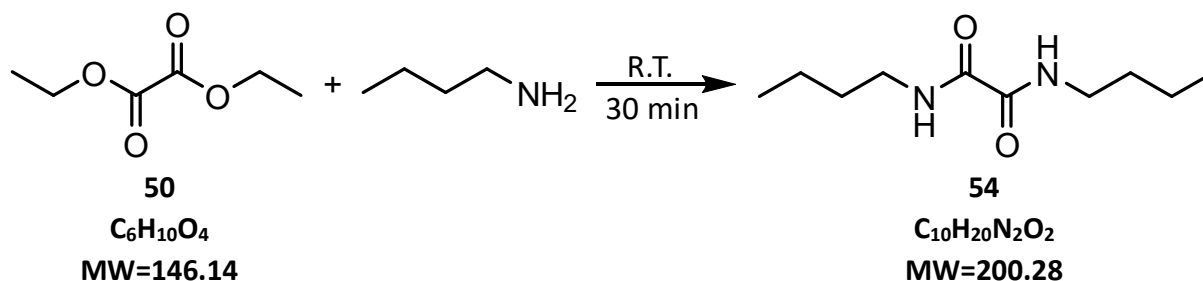
**Appearance:** colourless solid

**NMR:**



<sup>1</sup>H NMR (400 MHz, CDCl<sub>3</sub>): δ = 0.88 (t, J=7.37 Hz, 6H, CH<sub>3</sub>), 1.52 (sextet, J=7.18 Hz, 4H, CH<sub>2</sub>), 3.21 (q, J=7.25 Hz, 4H, CH<sub>2</sub>-N), 7.46 (s, 2H, NH)

<sup>13</sup>C NMR (100 MHz, CDCl<sub>3</sub>): δ = 11.3 (q, CH<sub>3</sub>), 22.5 (t, CH<sub>2</sub>), 41.3 (t, CH<sub>2</sub>-N), 160.3 (s, CO)

4.6.2.4 N,N'-Dibutyloxalamide <sup>[75-77]</sup>

The product was synthesized according to the general procedure E with:

Oxalic acid diethyl ester (1.46 g, 10 mmol, 1 eq.) and butylamine (1.44 g, 24 mmol, 2.4 eq.). The crude product was recrystallized from ethanol and dried in vacuo to give 83% yield of N,N'-dibutyloxalamide.

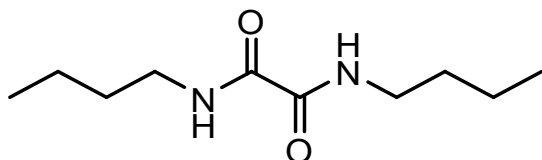
**Yield:** 83% (1.66 g, 8.29 mmol)

**Melting point:** 155 °C [EtOH] (Lit. MP: 153 °C <sup>75-77</sup>)

**Melting energy:** decomposition

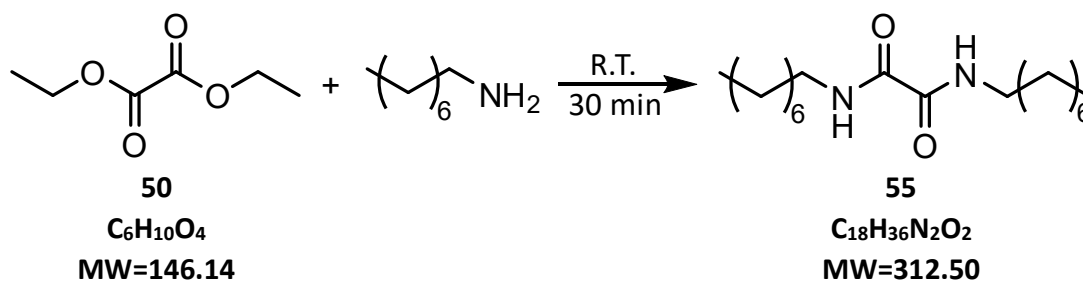
**Appearance:** colourless solid

**NMR:**



<sup>1</sup>H NMR (400 MHz, CDCl<sub>3</sub>): δ = 0.87 (t, J=7.41 Hz, 6H, CH<sub>3</sub>), 1.25 (sextet, J=7.43 Hz, 4H, CH<sub>2</sub>), 1.44 (quin, J=7.00 Hz, 4H, CH<sub>2</sub>), 3.09-3.14 (q, 4H, CH<sub>2</sub>-N), 7.46 (s, 2H, NH)

<sup>13</sup>C NMR (100 MHz, CDCl<sub>3</sub>): δ = 14.0 (q, CH<sub>3</sub>), 19.9 (t, CH<sub>2</sub>), 31.2 (t, CH<sub>2</sub>), 38.9 (t, CH<sub>2</sub>-N), 160.4 (s, CO)

4.6.2.5 N,N'-Dioctyloxalamide <sup>[75-77]</sup>

The product was synthesized according to the general procedure E with:

Oxalic acid diethyl ester (0.73 g, 5 mmol, 1 eq.) and octylamine (1.56 g, 12 mmol, 2.4 eq.). The crude product was recrystallized from ethanol and dried in vacuo to give 98% yield of N,N'-dioctyloxalamide.

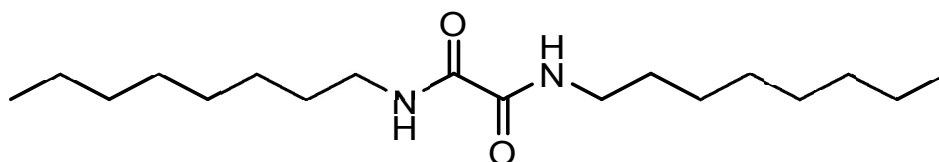
**Yield:** 98% (1.53 g, 4.90 mmol)

**Melting point:** 128 – 129 °C [EtOH] (Lit. MP: 124 °C <sup>75-77</sup>)

**Melting energy:** 118.9 kJ/kg + 98.3 kJ/kg from a solid-solid phase transition

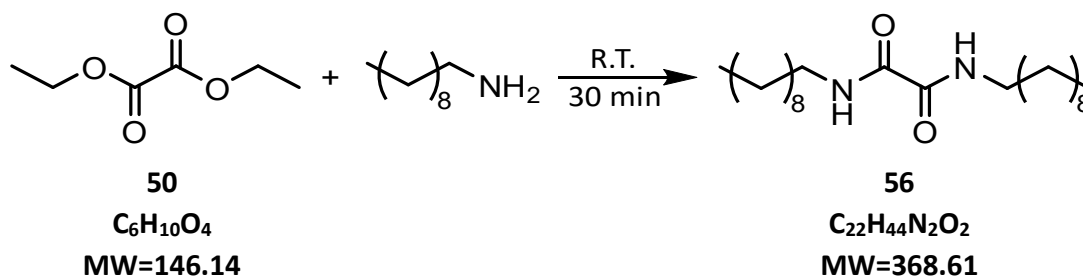
**Appearance:** colourless solid

**NMR:**



**<sup>1</sup>H NMR (400 MHz, CDCl<sub>3</sub>):**  $\delta$  = 0.89 (t, J=6.93 Hz, 6H, H<sub>1</sub>/H<sub>2</sub>), 1.28-1.32 (m, 20H, CH<sub>2</sub>), 1.57 (quin, J=7.12 Hz, 4H, CH<sub>2</sub>), 3.31 (q, J=6.84 Hz, 4H, CH<sub>2</sub>-N), 7.49 (s, 2H, NH)

**<sup>13</sup>C NMR (100 MHz, CDCl<sub>3</sub>):**  $\delta$  = 14.0 (q, CH<sub>3</sub>), 22.6, 26.8, 29.14, 29.17, 29.2, 31.7 (t, CH<sub>2</sub>), 39.7 (t, CH<sub>2</sub>-N), 159.8 (s, CO)

4.6.2.6 N,N'-Didecyloxalamide <sup>[75-77]</sup>

The product was synthesized according to the general procedure E with:

Oxalic acid diethyl ester (0.657 g, 4.5 mmol, 1 eq.) and decylamine (1.48 g, 9.5 mmol, 2.12 eq.). The crude product was recrystallized from ethanol and dried in vacuo to give 99% yield of N,N'-didecyloxalamide.

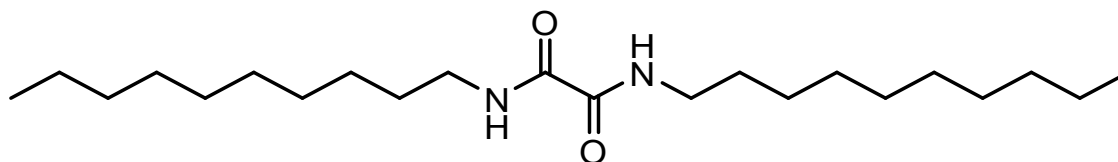
**Yield:** 99% (1.51 g, 4.46 mmol)

**Melting point:** 126 – 127 °C [EtOH] (Lit. MP: 122 °C <sup>75-77</sup>)

**Melting energy:** 135.4 kJ/kg + 88.7 kJ/kg from a solid-solid phase transition

**Appearance:** colourless solid

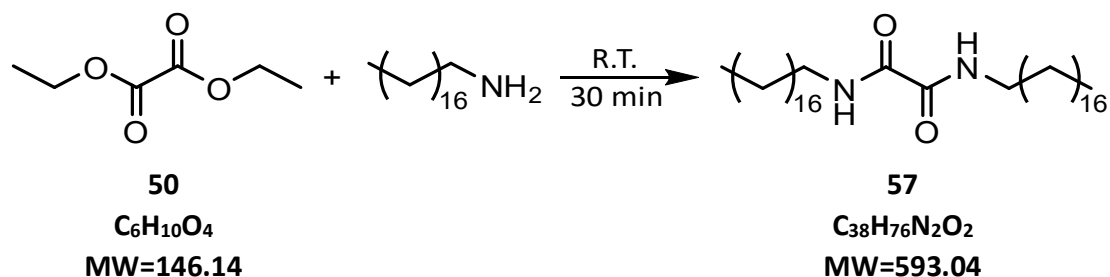
**NMR:**



**<sup>1</sup>H NMR (400 MHz, CDCl<sub>3</sub>):**  $\delta$  = 0.90 (t, J=7.02 Hz, 6H, CH<sub>3</sub>), 1.27-1.32 (m, 28H, CH<sub>2</sub>), 1.57 (quin, J=7.15 Hz, 4H, CH<sub>2</sub>), 3.31 (q, J=6.79 Hz, 4H, CH<sub>2</sub>-N), 7.48 (s, 2H, NH)

**<sup>13</sup>C NMR (100 MHz, CDCl<sub>3</sub>):**  $\delta$  = 14.0 (q, CH<sub>3</sub>), 22.6, 26.8, 29.22, 29.28, 29.4, 29.5, 31.8 (t, CH<sub>2</sub>), 39.7 (t, CH<sub>2</sub>-N), 159.8 (s, CO)

## 4.6.2.7 N,N'-Dioctadecyloxalamide [75-77]



The product was synthesized according to the general procedure E with:

Oxalic acid diethyl ester (0.292 g, 2 mmol, 1 eq.) and octadecylamine (1.08 g, 4.5 mmol, 2.25 eq.). The crude product was recrystallized from ethanol and dried in vacuo to give 75% yield of N,N'-dideoxyloxalamide.

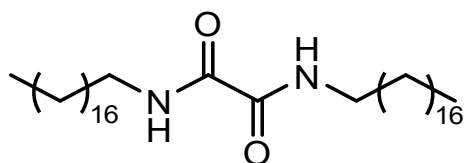
**Yield:** 75% (0.89 g, 1.51 mmol)

**Melting point:** 123 – 124 °C [EtOH] (Lit. MP: 120 °C <sup>75-77</sup>)

**Melting energy:** 256.4 kJ/kg

**Appearance:** colourless solid

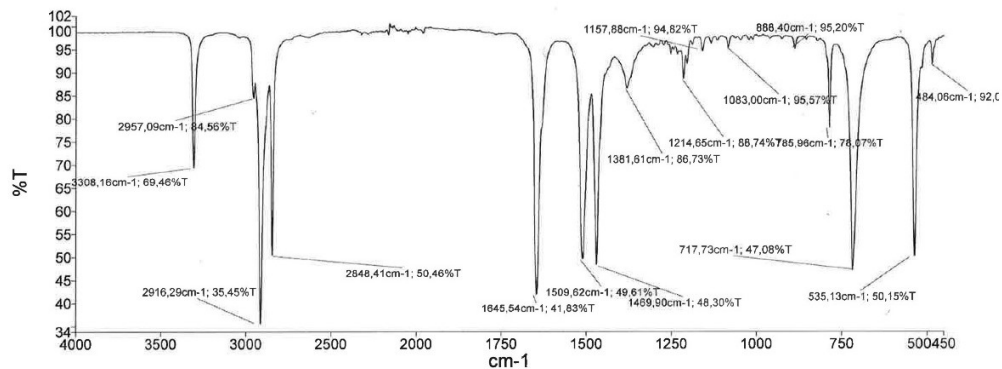
**NMR:**



<sup>1</sup>H NMR (400 MHz, CDCl<sub>3</sub>): δ = 0.87 (t, 6H, CH<sub>3</sub>), 1.25 (2, 64H, CH<sub>2</sub>), 3.30 (q, 4H, CH<sub>2</sub>-N), 7.43 (s, 2H, NH)

**IR:**

Due to the lack of solubility of N,N'-dioctadecyloxalamide in deuterated solvents, it was only possible to record a  $^1\text{H}$  NMR. Moreover, a FTIR was measured.

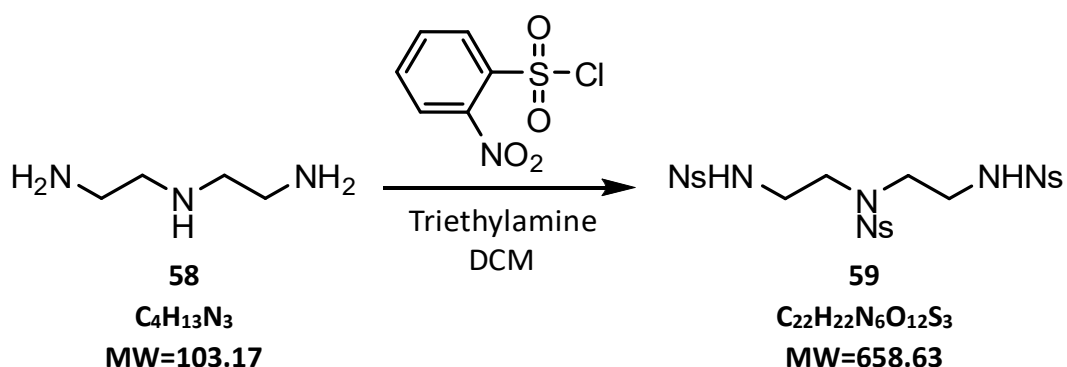


The resulting spectra shown the characteristic C=O band related to amida groups at  $1645\text{ cm}^{-1}$ . Other bands observed in this FTIR and related to amida groups are the C-N stretch band at  $1509\text{ cm}^{-1}$  and the N-H stretch band at  $3308\text{ cm}^{-1}$ . Therefore, the final product is confirmed.

## 4.7 Preparation of 3,6-diazaoctane-1,8-diol derivatives

### 4.7.1 Synthesis of 3,6,9-triazaundecane-1,11-diol

#### 4.7.1.1 Synthesis of 1,4,7-Tris(2-nitrobenzenesulfonyl)-1,4,7-triazaheptane <sup>[81]</sup>



A heterogeneous mixture of 2-nitrobenzenesulfonyl chloride (3.33 g, 15 mmol, 15 mmol) in anhydrous dichloromethane (1.6 mL) was placed in a 8-ml vial and stirred under argon atmosphere at 0°C. Simultaneously, a solution of 1,5-diamino-3-azapentane (0.26 mL, 0.25 g, 2.4 mmol) and trimethylamine (2.4 mL, 17.22 mmol) in anhydrous dichloromethane (1.2 mL) was placed in another 8 mL vial and stirred under argon atmosphere at 0 °C for 10 min. Afterwards, the diethylenetriamine solution was added dropwise in 30 min into the heterogeneous mixture of 2-nitrobenzenesulfonyl chloride and was kept stirring at room temperature for the next 3 hours. After this time the reaction was completed according to TLC (PE/EtOAc 1:4).

For the work-up, 3 extractions with aqueous HCl 2M (50 mL) and another 2 extractions with a saturated NaHCO<sub>3</sub> solution (50 mL) were done. The organic layer was dried over sodium sulfate, filtered and evaporated. The resulting crude material was purified by column chromatography (MPLC) by gradient elution (PE/EtOAc 50:50 - 10/90). Evaporation of the solvent gave 1.2 g of the desired product.

**Yield:** 76% (1.2 g, 1.82 mmol)

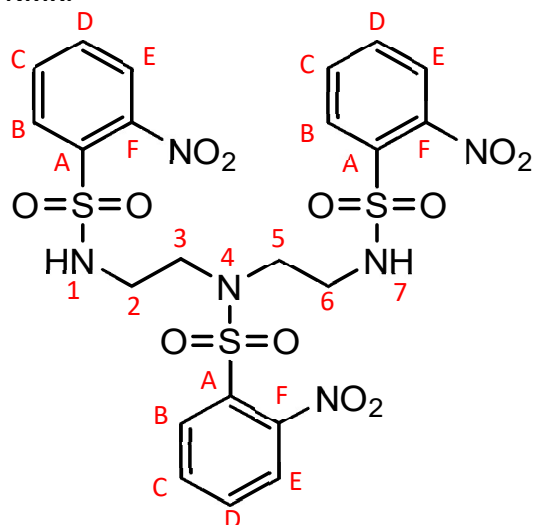
**Melting point:** 132 – 133°C [EtOAc] (Lit. MP: 156 °C <sup>81</sup>)

**Melting energy:** 71.1 kJ/kg

**TLC:** R<sub>f</sub>(PE/EtOAc, 1:4) = 0.65

**Appearance:** colourless solid

**NMR:**

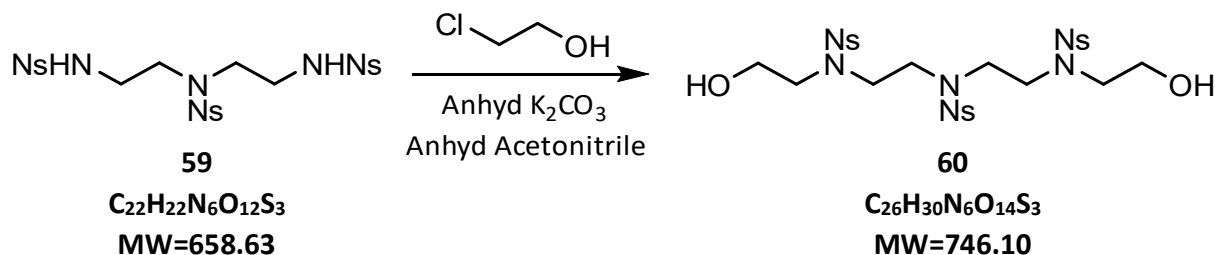


**<sup>1</sup>H NMR (400 MHz, DMSO):**  $\delta$  = 3.06 (t, J=7.07 Hz, 4H, H<sub>2</sub>/H<sub>6</sub>), 3.38 (t, J=6.89 Hz, 4H, H<sub>3</sub>/H<sub>5</sub>), 7.82-8.00 (m, 12H, H<sub>B</sub>/H<sub>C</sub>/H<sub>D</sub>/H<sub>E</sub>), 8.19 (s, 2H, H<sub>1</sub>/H<sub>7</sub>)

**<sup>13</sup>C NMR (100 MHz, DMSO):**  $\delta$  = 41.3 (t, C<sub>1</sub>/C<sub>4</sub>), 48.0 (t, C<sub>2</sub>/C<sub>3</sub>), 124.5 (d, C<sub>E</sub>), 129.4 (d, C<sub>B</sub>), 132.4 (d, C<sub>D</sub>), 132.7 (s, C<sub>A</sub>), 134.1 (d, C<sub>C</sub>), 147.5 (s, C<sub>F</sub>)



#### 4.7.1.2 Synthesis of 1,4,7-Tris(2-nitrobenzenesulfonyl)-3,6,9-triazaundecane-1,11-diol <sup>[81]</sup>



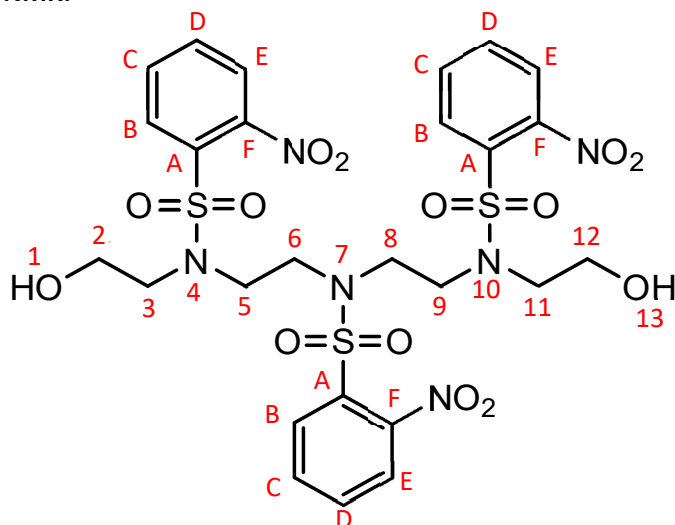
2-Chloroethanol (0.120 g, 1.49 mmol, 4 eq.) was added to a solution of 1,4,7-Tris(2-nitrobenzenesulfonyl)-1,4,7-triazaheptane (0.246 g, 0.373 mmol, 1 eq.) dissolved in anhydrous acetonitrile (0.74 ml). Afterwards a catalytic amount of anhydrous potassium carbonate (0.206 g, 1.49 mmol, 4 eq) was placed in the same vial; the reaction was refluxed (120 °C) under stirring for 4 hours. After cooling the mixture was dissolved in water (50 mL) and extracted 4 times with dichloromethane (25 mL). The combined organic layer was dried over sodium sulfate, filtered and evaporated. Crude yield at this point was 97,6%. The resulting crude material was purified by a column chromatography (MPLC). To this end, 10 minutes of PE/EtOAc 1:1 and then a gradient PE/EtOAc 50:50 - 10/90 was programmed.

**Yield:** 48% (0.135 mg, 0.18 mmol)

**TLC:**  $R_f$  (PE/EtOAc, 1:4) = 0.18

**Appearance:** yellow oil

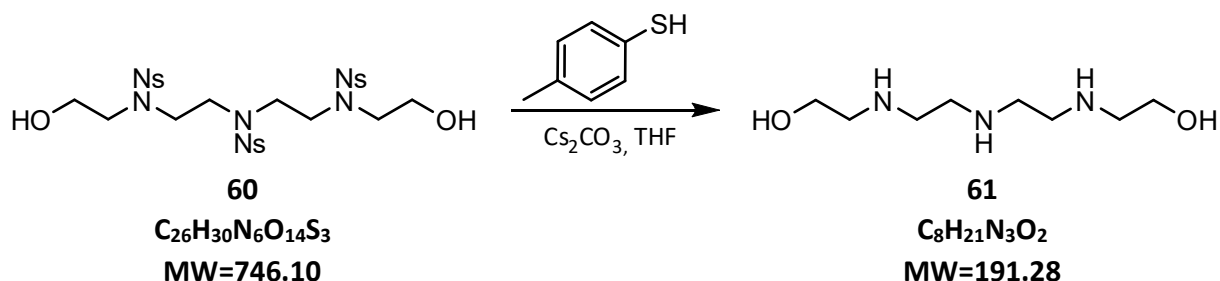
NMR:



$^1\text{H NMR}$  (400 MHz,  $\text{CD}_2\text{Cl}_2$ ):  $\delta$  = 2.19 (s, 2H, OH), 3.39 (t,  $J=5.07$  Hz, 4H,  $\text{H}_6/\text{H}_8$ ), 3.46-3.48 (m, 4H,  $\text{H}_5/\text{H}_9$ ), 3.54-3.56 (m, 4H,  $\text{H}_3/\text{H}_{11}$ ), 3.68 (t,  $J=5.03$  Hz, 4H,  $\text{H}_2/\text{H}_{12}$ ), 7.57-7.92 (m, 12H,  $\text{H}_B/\text{H}_C/\text{H}_D/\text{H}_E$ )

$^{13}\text{C NMR}$  (100 MHz,  $\text{CD}_2\text{Cl}_2$ ):  $\delta$  = 48.1 (t,  $\text{C}_5/\text{C}_9$ ), 48.2 (t,  $\text{C}_6/\text{C}_8$ ), 51.6 (t,  $\text{C}_3/\text{C}_{11}$ ), 61.2 (t,  $\text{C}_2/\text{C}_{12}$ ), 124.2 (d,  $\text{C}_E$ ), 130.5 (d,  $\text{C}_B$ ), 130.8 (d,  $\text{C}_D$ ), 132.2 (s,  $\text{C}_A$ ), 134.1 (d,  $\text{C}_C$ ), 148.1 (s,  $\text{C}_F$ )

## 4.7.1.3 Synthesis of 3,6,9-triazaundecane-1,11-diol [82]

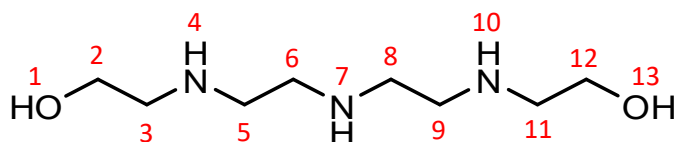


The starting material (0.5 g, 0.67 mmol, 1 eq.) was dissolved in dry THF (1.35 mL).  $\text{Cs}_2\text{CO}_3$  (2.18 g, 6.7 mmol, 10 eq.) and p-thiocresol (0.83 g, 6.7 mmol, 10 eq.) were added to this solution. The reaction was stirred overnight and after this time the starting material was consumed according to TLC (PE/EtOAc 1:4). For the work-up, a filter funnel (5cm diameter) with 10g of silica was prepared and the reaction mixture was poured in there. Several solvents were flushed through this funnel starting with PE (200 mL), then EtOAc (200 mL), ethanol (200 mL) and finally methanol (200 mL). The methanol fraction was concentrated and a crude yield of 174% was obtained due to silica impurities. Further purification was done by HPLC.

**Yield:** 15% (19 mg, 0.09 mmol)

**Appearance:** colourless liquid

**NMR:**



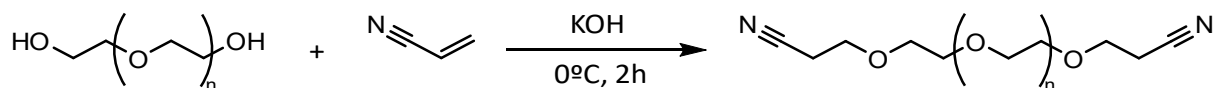
$^1\text{H NMR}$  (400 MHz, MeOD):  $\delta$  = 2.96 (t,  $J=5.26$  Hz, 4H,  $\text{H}_3/\text{H}_{11}$ ), 3.16 (q,  $J=5.25$  Hz, 8H,  $\text{H}_5/\text{H}_6/\text{H}_8/\text{H}_9$ ), 3.84 (t,  $J=5.32$  Hz, 4H,  $\text{H}_2/\text{H}_{12}$ )

$^{13}\text{C NMR}$  (100 MHz, MeOD):  $\delta$  = 44.2 (t,  $\text{C}_6/\text{C}_8$ ), 46.4 (t,  $\text{C}_5/\text{C}_9$ ), 48.9 (t,  $\text{C}_3/\text{C}_{11}$ ), 56.3 (t,  $\text{C}_2/\text{C}_{12}$ )



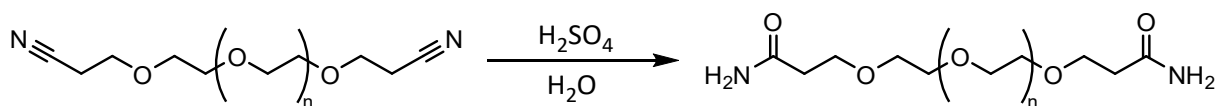
## 4.9 Preparation of oxamides

### 4.9.1 General procedure F - Dinitrile formation



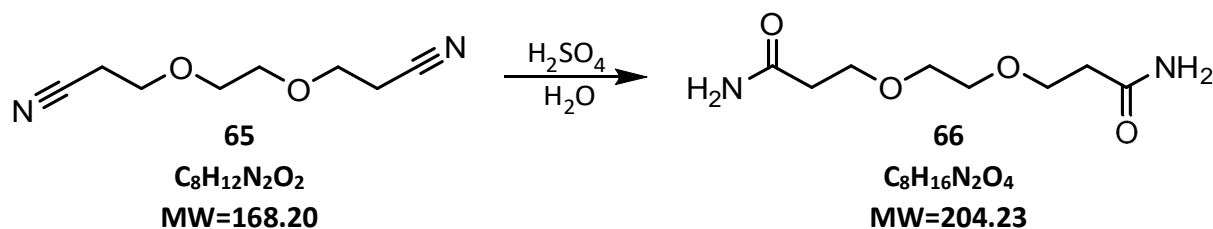
The corresponding ethylene glycol (1 eq.) is placed in a round bottom flask with acrylonitrile (14 eq.). It was stirred at 0 °C for 30 min and afterwards potassium carbonate was added to the reaction mixture. The reaction mixture was stirred again for another 2 hours at 0 °C. Some drops of HCl (2M) were added to quench the reaction and the solvent was evaporated. This crude material was redissolved in dichloromethane and filtered through celite. This filtrate was concentrated to finally get the desired dinitrile derivative.

### 4.9.2 General procedure G - Dinitrile hydrolysis



The corresponding dinitrile (1 eq.) was placed in a round bottom flask and stirred at 70 °C. A solution of sulfuric acid and water (2 eq. H<sub>2</sub>SO<sub>4</sub> + 2 eq. H<sub>2</sub>O) was added dropwise to our corresponding dinitrile during 15min. After 3 hours the reaction was finished and neutralized with NaOH (25% solution). The solution was cooled to 10 °C and filtered to remove sodium sulphate. The filtrate was concentrated and an oil was obtained. After recrystallization with dioxane, a white solid appeared.

### 4.9.3 Synthesis of 4,7-dioxa-1,10-octanedicarboxamide <sup>[87]</sup>



The product was synthesized according to general G procedure with:

1,2-Bis-(2-cyanoethoxy)ethane (1.9 mL, 12 mmol, 1 eq.),  $\text{H}_2\text{SO}_4$  (1.25 mL, 24mmol, 1 eq.), and  $\text{H}_2\text{O}$  (0.432 mL, 24mmol, 1 eq.)

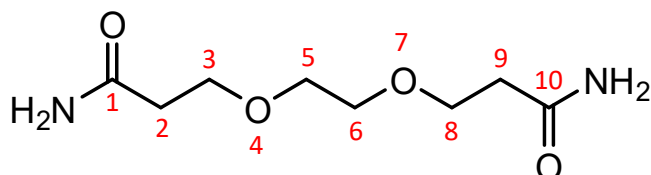
**Yield:** 15% (0.361 g, 1.76 mmol)

**Melting point:** 116 – 118 °C [Dioxane] (Lit. MP: 123 °C <sup>87</sup>)

**Melting energy:** 206 kJ/kg

**Appearance:** colourless solid

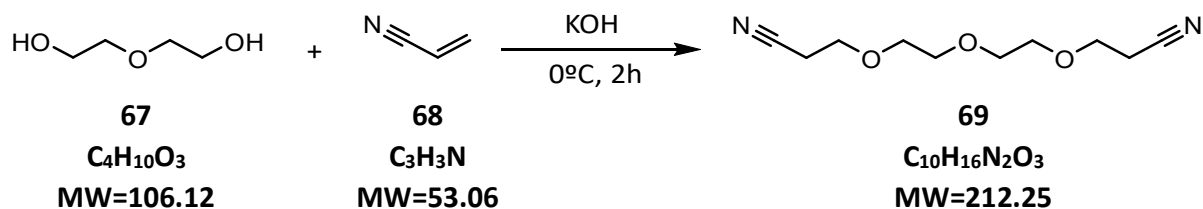
**NMR:**



**<sup>1</sup>H NMR (400 MHz, DMSO):**  $\delta$  = 2.27 (t, J=6.41 Hz, 4H, H<sub>5</sub>/H<sub>6</sub>), 3.46 (s, 4H, H<sub>3</sub>/H<sub>8</sub>), 3.57 (t, J=6.40 Hz, 4H, H<sub>2</sub>/H<sub>9</sub>), 6.78 (s, 2H, NH<sub>2</sub>), 7.28 (s, 2H, NH<sub>2</sub>)

**<sup>13</sup>C NMR (100 MHz, DMSO):**  $\delta$  = 36.3 (t, C<sub>2</sub>/C<sub>9</sub>), 67.2 (t, C<sub>3</sub>/C<sub>8</sub>), 69.8 (t, C<sub>5</sub>/C<sub>6</sub>), 172.6 (s, C<sub>1</sub>/C<sub>10</sub>)

#### 4.9.4 Synthesis of 4,7,10-trioxa-tridecanedinitrile <sup>[89]</sup>



The product was synthesized according to general procedure F with:

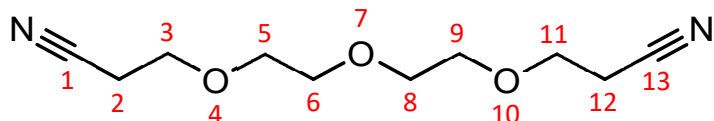
Diethylene glycol (0.91 mL, 10.3 mmol, 1 eq.), acrylonitrile (9.56 mL, 0.145 moles, 14 eq.), and KOH (60 mg)

**Yield:** 99% (2.16 g, 10.19 mmol)

**TLC:**  $R_f$  (PE/EtOAc, 1:1) = 0.11

**Appearance:** yellow oil

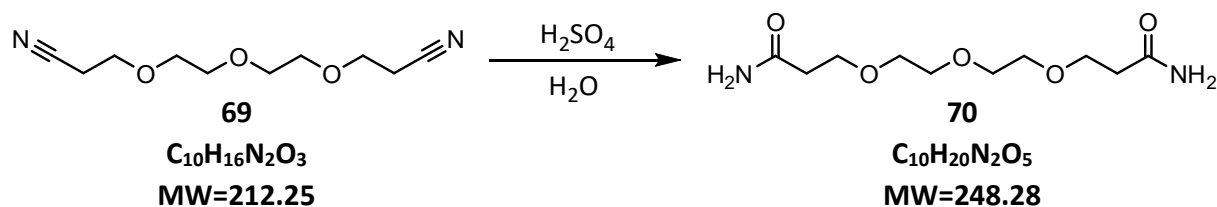
**NMR:**



$^1H$  NMR (400 MHz,  $CDCl_3$ ):  $\delta$  = 2.62 (t,  $J=6.38$  Hz, 4H,  $H_2/H_{12}$ ), 3.67 (s, 8H,  $H_5/H_6/H_8/H_9$ ), 3.72 (t,  $J=6.38$  Hz, 4H,  $H_3/H_{11}$ )

$^{13}C$  NMR (100 MHz,  $CDCl_3$ ):  $\delta$  = 18.9 (t,  $C_2/C_{12}$ ), 65.9 (t,  $C_3/C_{11}$ ), 70.6 (t,  $C_5/C_9$ ), 70.7 (t,  $C_6/C_8$ ), 117.9 (s,  $C_1/C_{13}$ )

#### 4.9.5 Synthesis of 4,7,10-trioxa-1,13-undecanedicarboxamide <sup>[87]</sup>



The product was synthesized according to general procedure G with:

Bis(2-(2-cyanoethoxy)ethyl)ether (2.31 mL, 12 mmol, 1 eq.), H<sub>2</sub>SO<sub>4</sub> (1.25 mL, 24mmol, 1 eq.), and H<sub>2</sub>O (0.432 mL, 24mmol, 1 eq.)

**Yield:** 10% (315 mg, 1.26 mmol)

**Melting point:** 102-103 °C [Dioxane] (Lit. MP: 103 °C <sup>87</sup>)

**Melting energy:** 257 kJ/kg

**Appearance:** colourless solid

**NMR:**

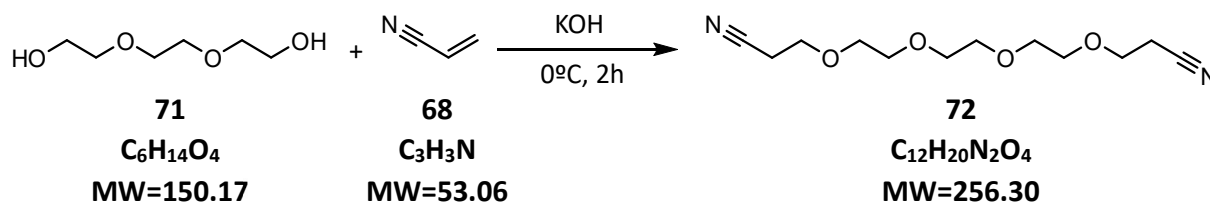


**<sup>1</sup>H NMR (400 MHz, CDCl<sub>3</sub>):** δ = 2.44 (t, J=5.70 Hz, 4H, H<sub>2</sub>/H<sub>12</sub>), 3.53-3.58 (m, 8H, H<sub>5</sub>/H<sub>6</sub>/H<sub>8</sub>/H<sub>9</sub>), 3.67 (t, J=5.66 Hz, 4H, H<sub>3</sub>/H<sub>11</sub>), 5.94 (s, 2H, NH<sub>2</sub>), 6.71 (s, 2H, NH<sub>2</sub>)

**<sup>13</sup>C NMR (100 MHz, CDCl<sub>3</sub>):** δ = 36.2 (t, C<sub>2</sub>/C<sub>12</sub>), 66.9 (t, C<sub>3</sub>/C<sub>11</sub>), 70.1 (t, C<sub>5</sub>/C<sub>6</sub>/C<sub>8</sub>/C<sub>9</sub>), 174.3 (s, C<sub>1</sub>/C<sub>13</sub>)



#### 4.9.6 Synthesis of 4,7,10,13-tetraoxahexadecanedinitrile <sup>[89]</sup>



The product was synthesized according to general procedure F with:

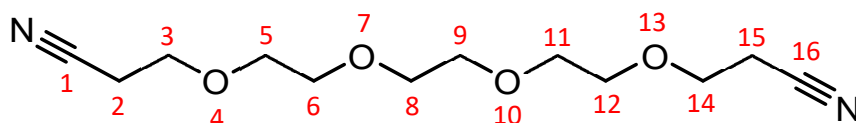
Triethylene glycol (0.70 mL, 5.15mmol, 1eq.), acrylonitrile (4.78mL, 72mmoles, 14eq.), KOH (30 mg)

**Yield:** 99% (1.36g, 5.09mmol)

**TLC:**  $R_f$  (PE/EtOAc, 1:1) = 0.14

**Appearance:** yellow liquid

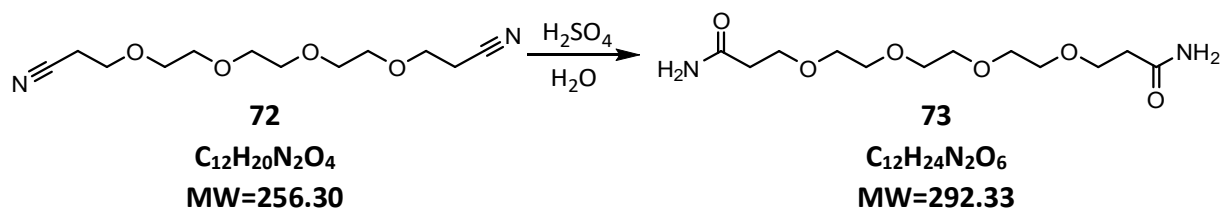
**NMR:**



$^1\text{H NMR}$  (400 MHz,  $\text{CDCl}_3$ ):  $\delta$  = 2.62 (t,  $J=6.44$  Hz, 4H,  $\text{H}_2/\text{H}_{15}$ ), 3.67 (s, 12H,  $\text{H}_5/\text{H}_6/\text{H}_8/\text{H}_9/\text{H}_{11}/\text{H}_{12}$ ), 3.72 (t,  $J=6.61$  Hz, 4H,  $\text{H}_3/\text{H}_{14}$ )

$^{13}\text{C NMR}$  (100 MHz,  $\text{CDCl}_3$ ):  $\delta$  = 18.8 (t,  $\text{C}_2/\text{C}_{15}$ ), 65.9 (t,  $\text{C}_3/\text{C}_{14}$ ), 70.5 (t,  $\text{C}_5/\text{C}_{12}$ ), 70.6 (t,  $\text{C}_6/\text{C}_{11}$ ), 70.7 (t,  $\text{C}_8/\text{C}_9$ ), 117.9 (s,  $\text{C}_1/\text{C}_{16}$ )

#### 4.9.7 Synthesis of 4,7,10,13-tetraoxa-1,16-hexadecanedicarboxamide <sup>[87]</sup>



The product was synthesized according to general procedure G with:

$\alpha,\omega$ -Di(cyanoethylene)triethylene tetraoxide (1.648 g, 6.43 mmol, 1 eq.),  $H_2SO_4$  (1.25 mL), and  $H_2O$  (0.432 mL)

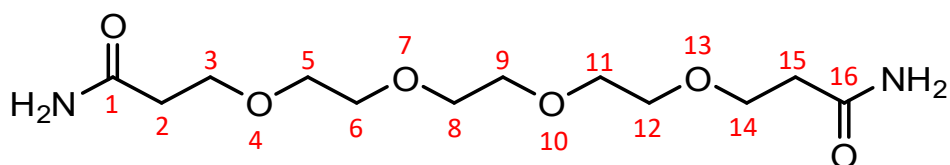
**Yield:** 7% (146 mg, 0.49 mmol)

**Melting point:** 89 – 91 °C [Dioxane] (Lit. MP: 94 °C <sup>87</sup>)

**Melting energy:** 177.4 kJ/kg

**Appearance:** colourless solid

**NMR:**



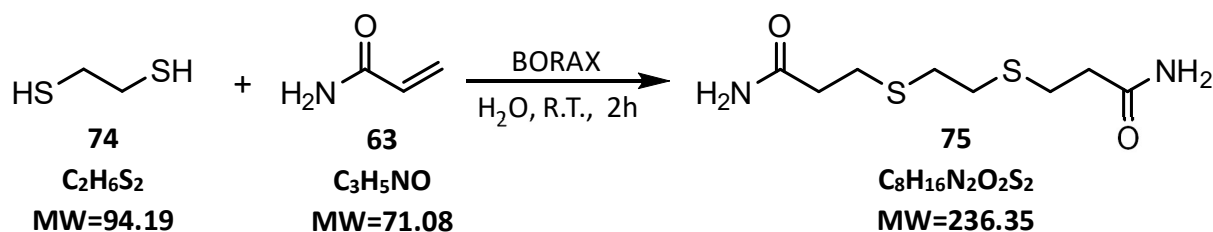
<sup>1</sup>H NMR (400 MHz,  $CDCl_3$ ):  $\delta$  = 2.55 (t,  $J=5.50$  Hz, 4H,  $H_2/H_{15}$ ), 3.62 (m, 8H,  $CH_2$ ), 3.66-3.68 (m, 4H,  $CH_2$ ), 3.77 (t,  $J=5.41$  Hz, 4H,  $H_3/H_{14}$ ), 6.08 (s, 2H,  $NH_2$ ), 7.78 (s, 2H,  $NH_2$ )

<sup>13</sup>C NMR (100 MHz,  $CDCl_3$ ):  $\delta$  = 36.2 (t,  $C_2/C_{15}$ ), 67.0 (t,  $C_3/C_{14}$ ), 69.8 (t,  $C_5/C_{12}$ ), 69.9 (t,  $C_6/C_{11}$ ), 70.4 (t,  $C_8/C_9$ ), 175.1 (s,  $C_1/C_{16}$ )

## 4.10 Preparation of sulfaramides

### 4.10.1 Synthesis of 3-[2-(2-carbamoylethylsulfanyl)ethylsulfanyl]propionamide

[90]



Borax decahydrate (152 mg, 0.2 mmol) was placed in an 8 mL vial and was dissolved in water (2 mL). Afterwards acrylamide (157 mg, 2.2 mmol, 2.2 eq.) was added via syringe followed by the dithiol (95 mg, 1mmol, 1eq.). In one hour, some white precipitate was formed but the reaction was left overnight. For the work-up, the reaction was filtered under vacuum and the filtrate was recrystallize with MeOH

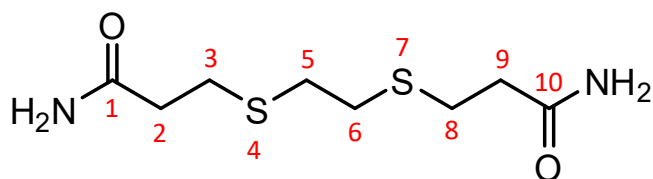
**Yield:** 89% (212 mg, 0.89 mmol)

**Melting point:** 179 – 181 °C [MeOH] (Lit. MP: 179 °C<sup>90</sup>)

**Melting energy:** 282.3 kJ/kg

**Appearance:** colourless solid

**NMR:**



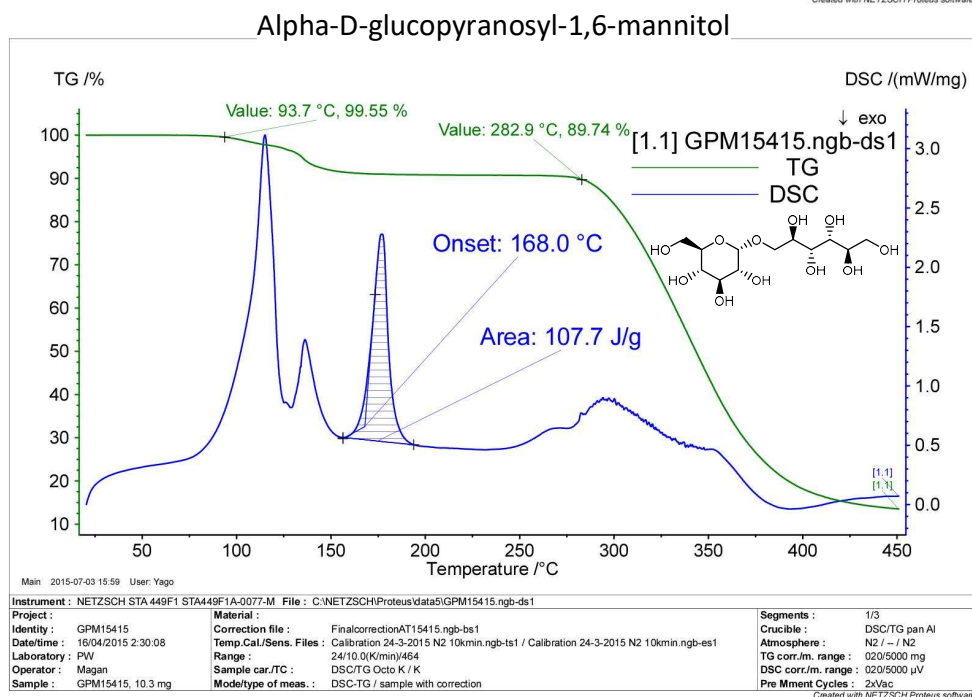
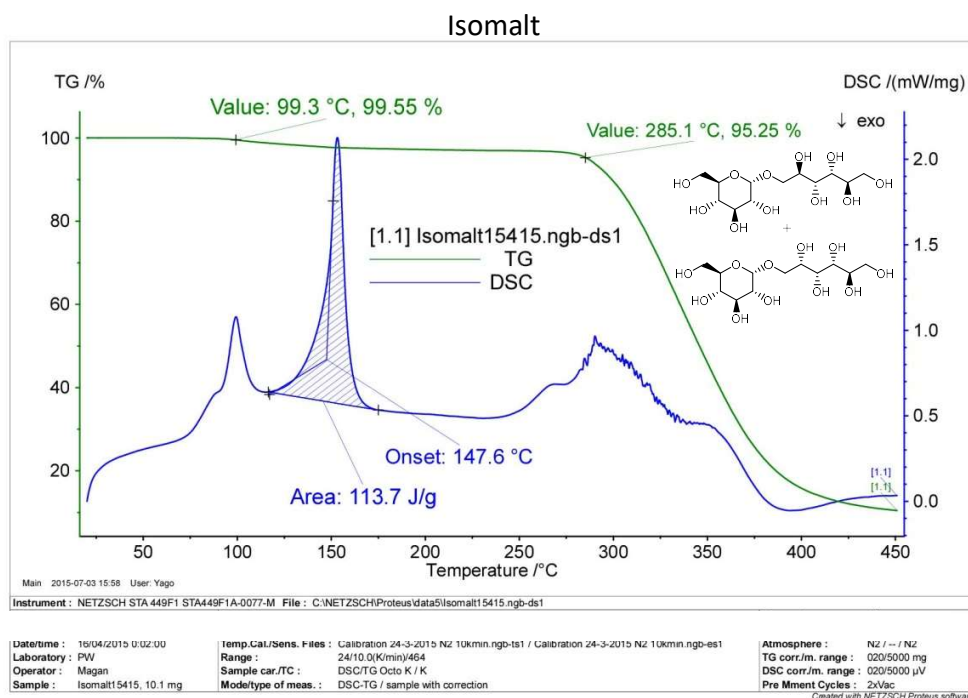
**<sup>1</sup>H NMR (400 MHz, DMSO):**  $\delta$  = 2.33 (t, J=7.33 Hz, 4H, H<sub>5</sub>/H<sub>6</sub>), 2.65-2.73 (m, 8H, H<sub>2</sub>/H<sub>3</sub>/H<sub>8</sub>/H<sub>9</sub>), 6.84 (s, 2H, NH<sub>2</sub>), 7.33 (s, 2H, NH<sub>2</sub>)

**<sup>13</sup>C NMR (100 MHz, DMSO):**  $\delta$  = 27.3 (t, C<sub>5</sub>/C<sub>6</sub>), 31.7 (t, C<sub>3</sub>/C<sub>8</sub>), 36.1 (t, C<sub>2</sub>/C<sub>9</sub>), 172.9 (s, C<sub>1</sub>/C<sub>10</sub>)

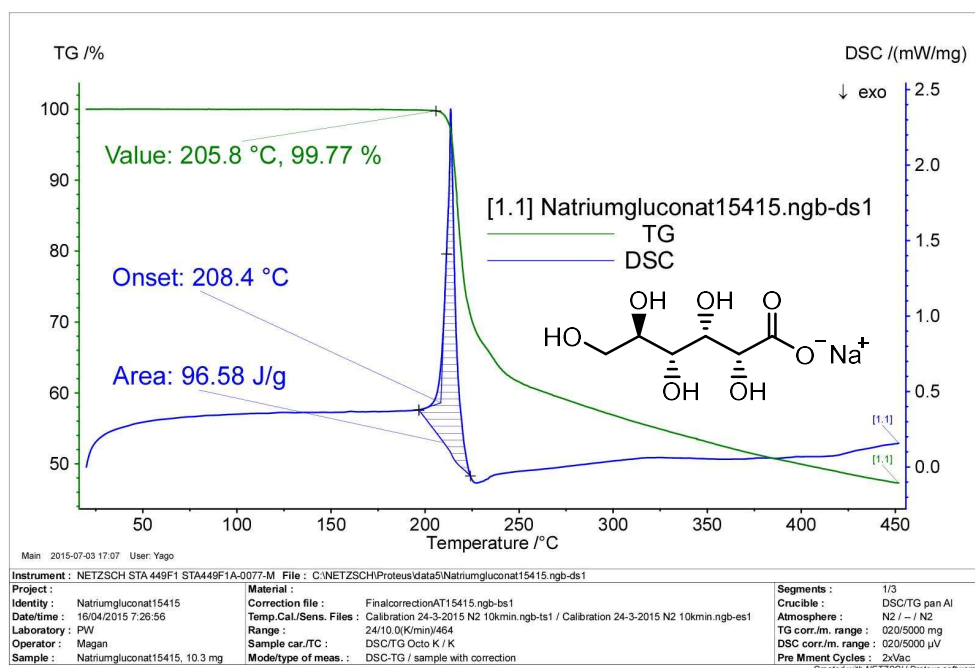
## 5. Appendix

### 5.1 TU STA graphics

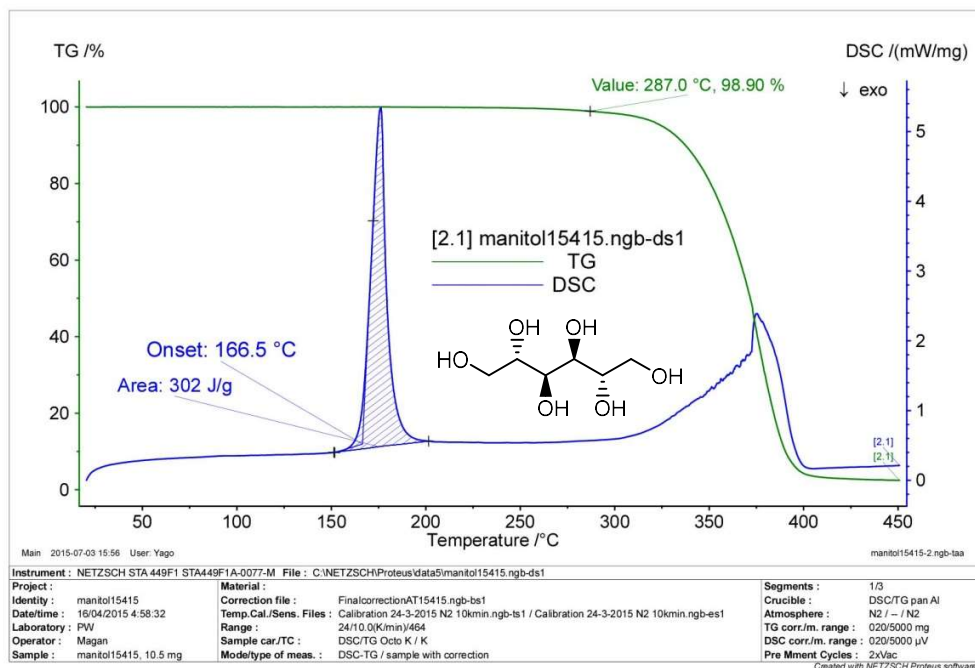
#### 5.1.1 Sugars and derivatives



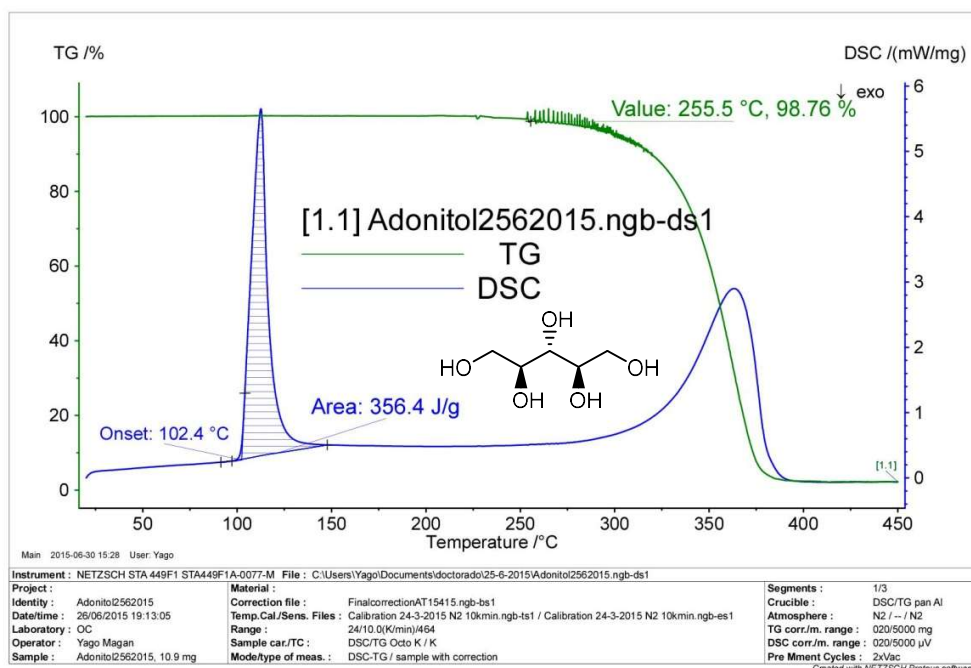
## Sodium gluconate



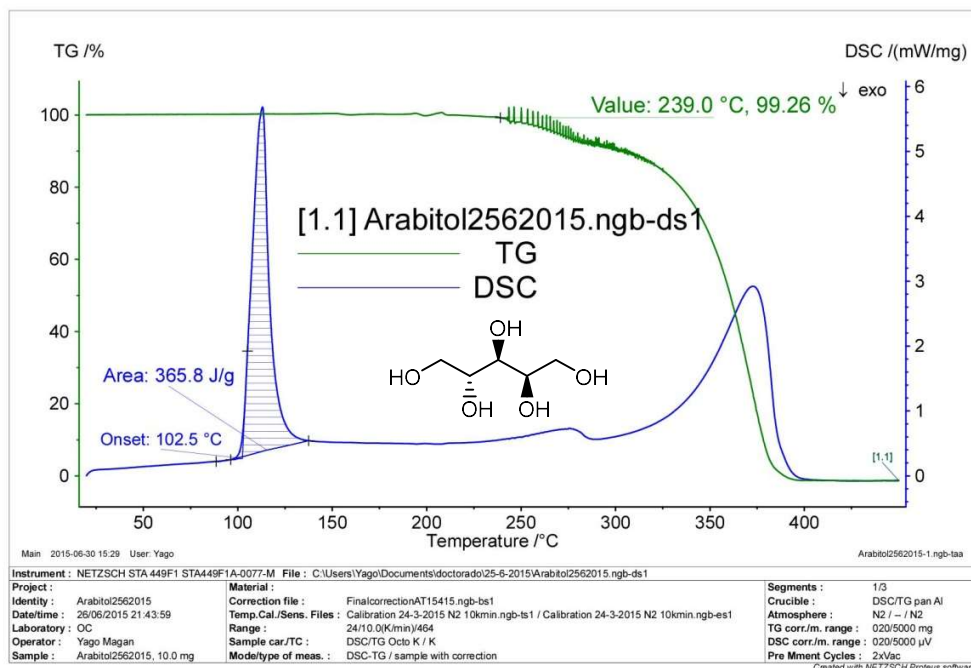
## Mannitol



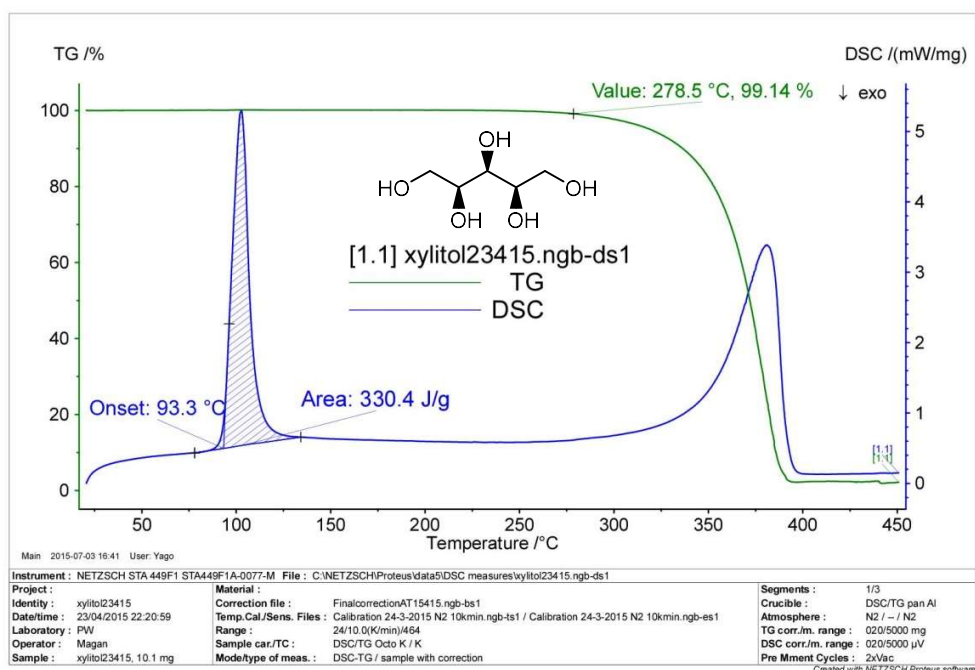
## Ribitol/Adonitol



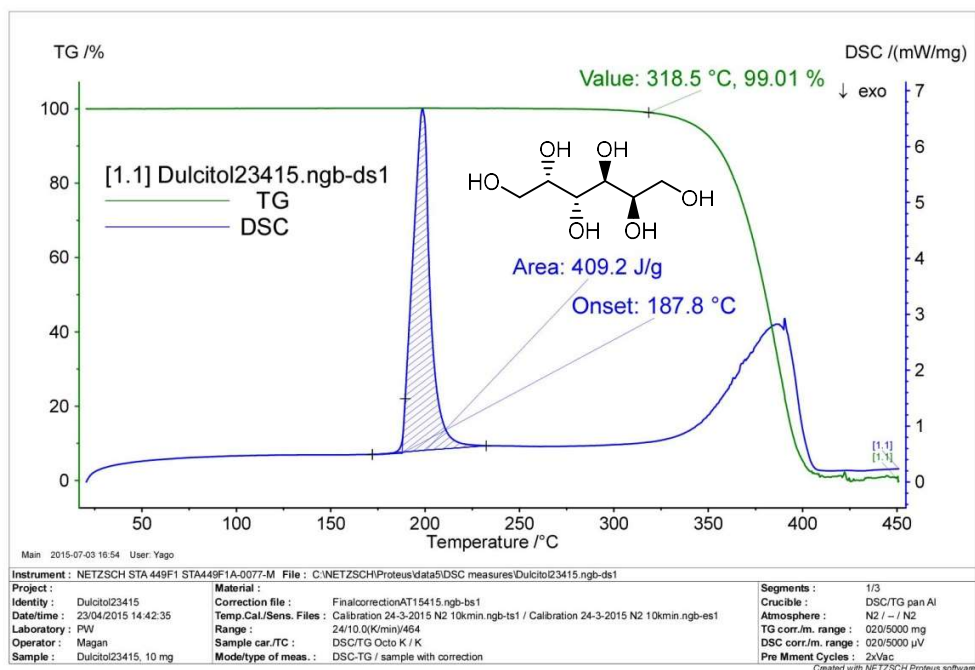
## Arabitol



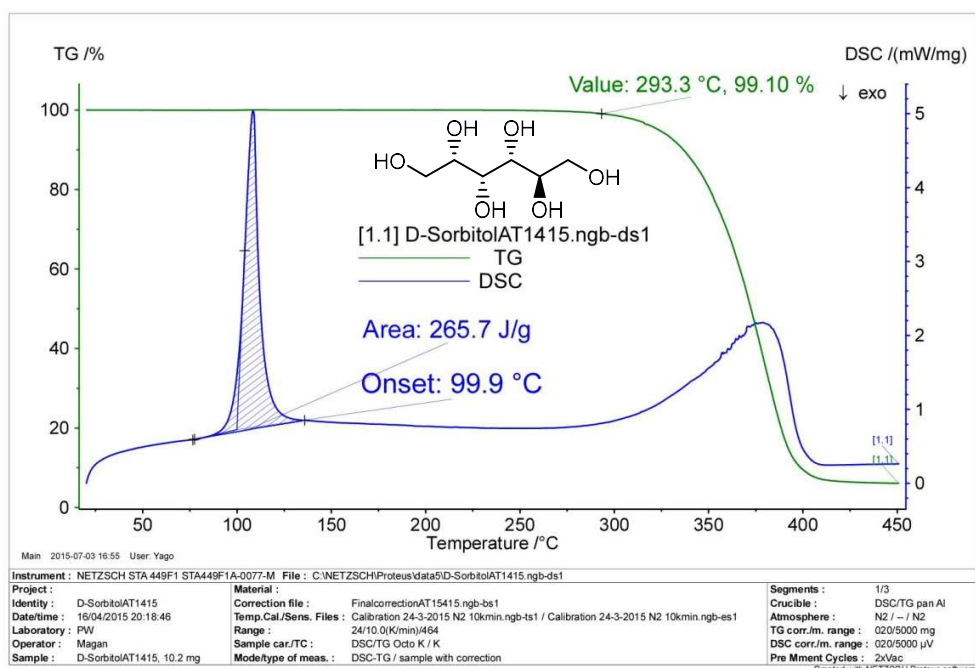
## Xylitol



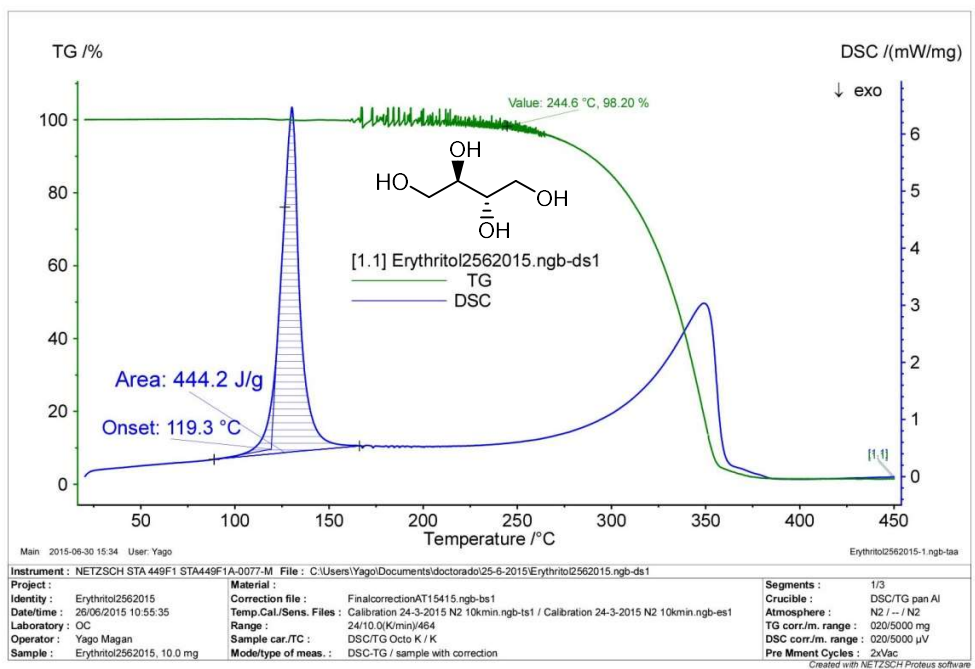
## Dulcitol/galactitol



## Sorbitol/glucitol

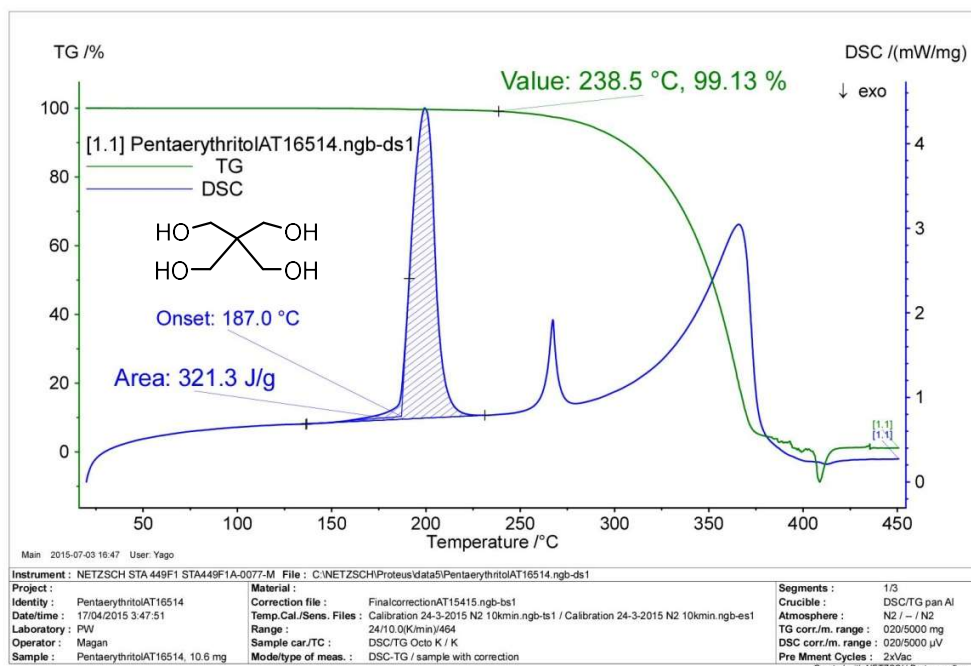


## Erythritol

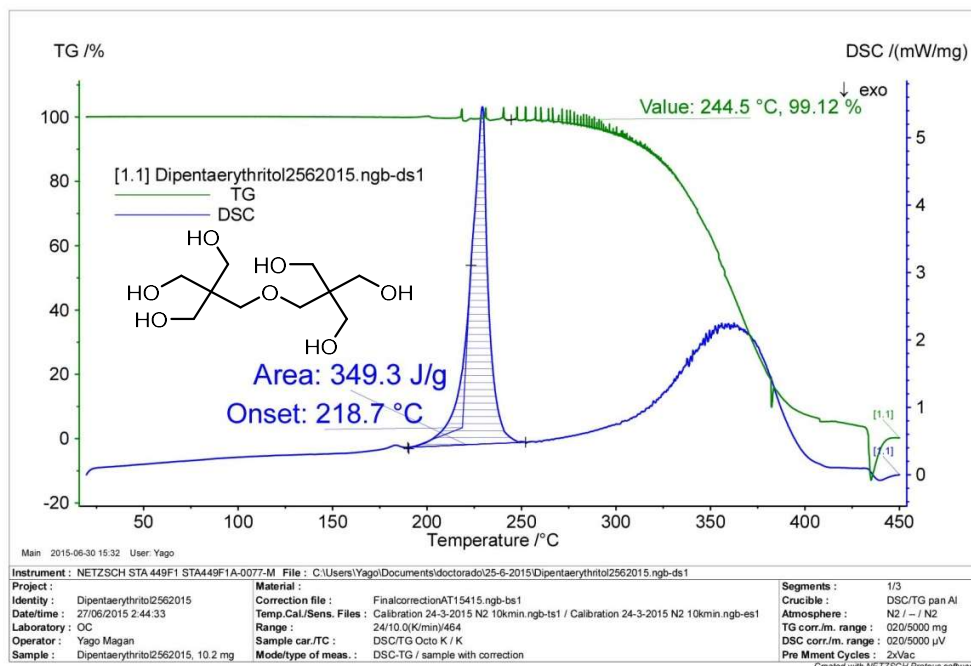




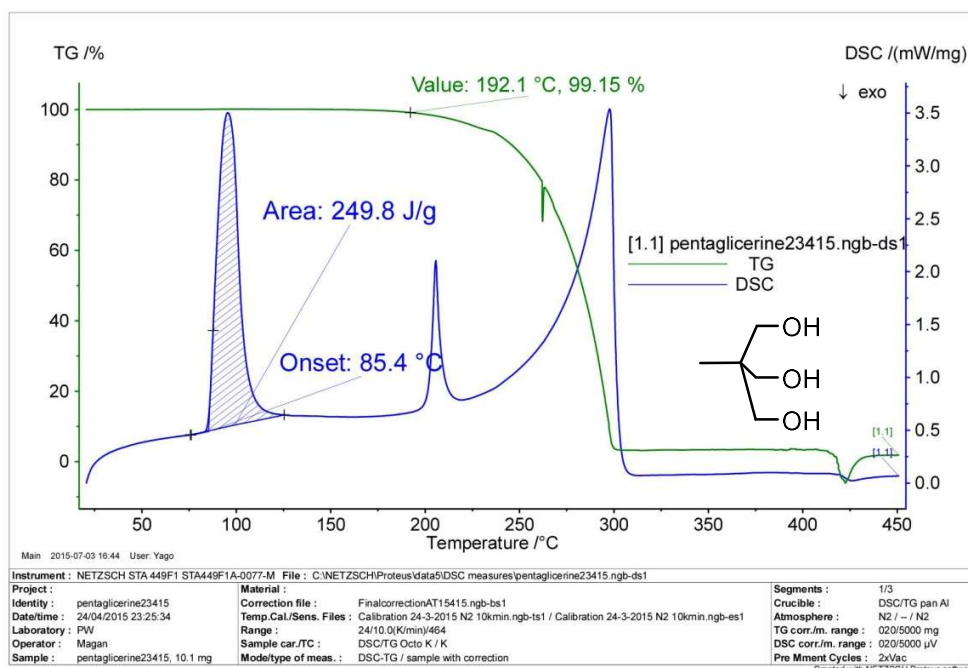
## Pentaerythritol



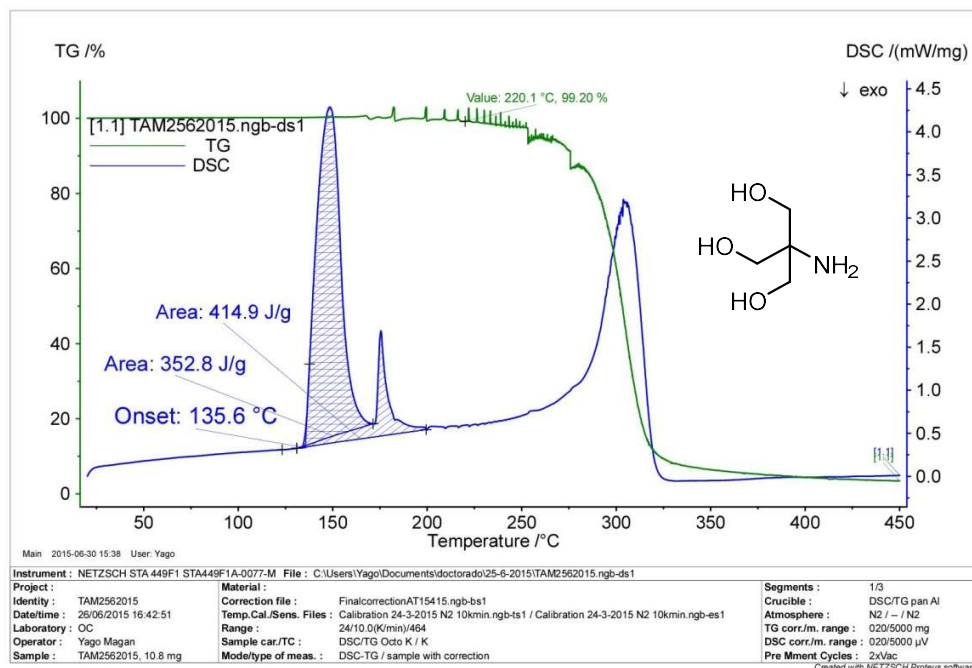
## Dipentaerythritol



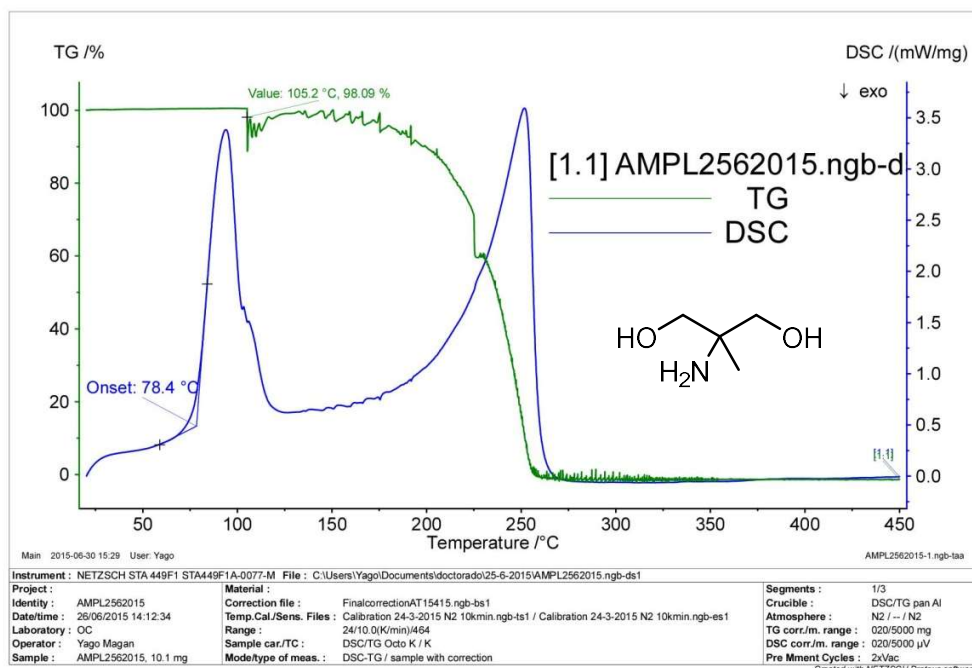
## Pentaglycerine



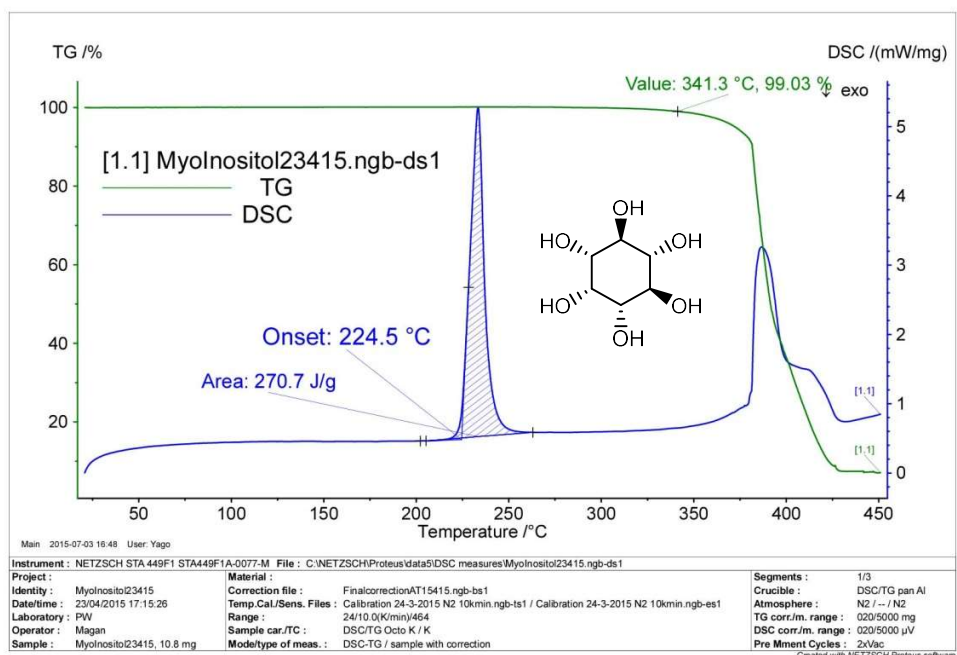
## Tris(hydroxymethyl)aminomethane (TAM)



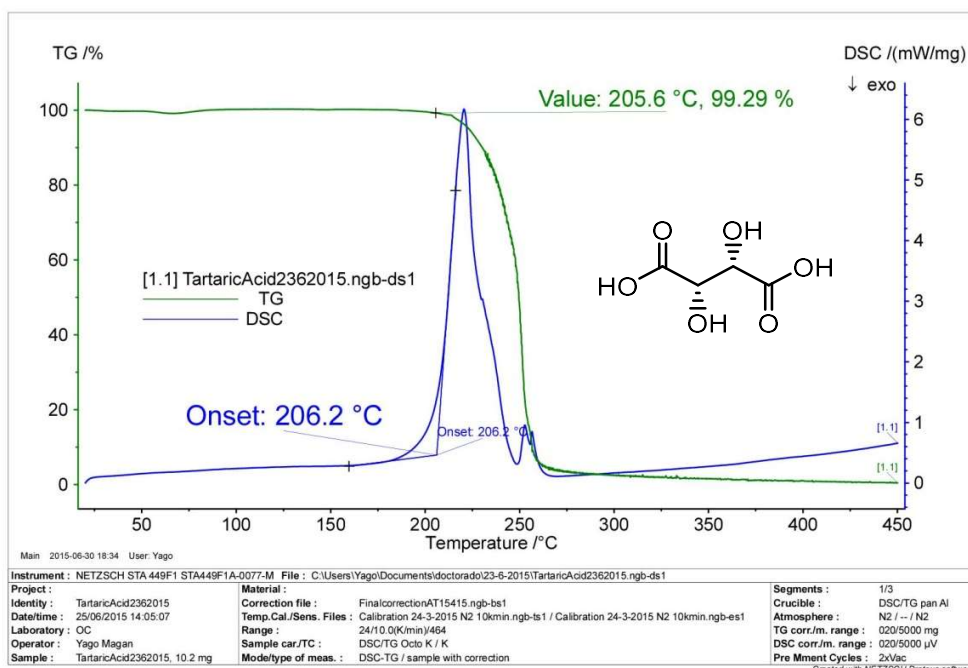
## Aminoglycol (AMPL)



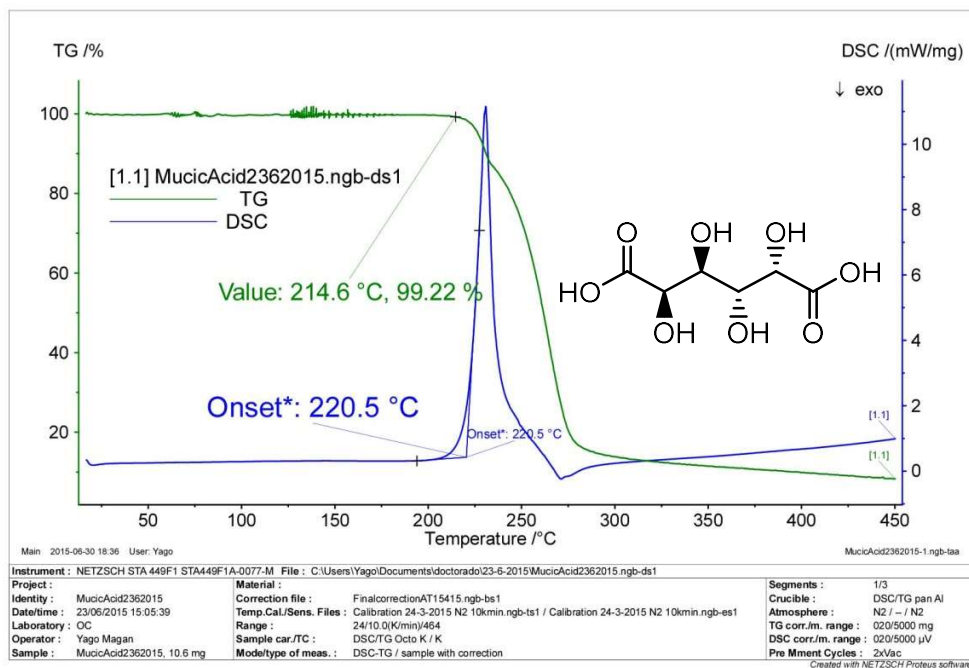
## Myo-inositol



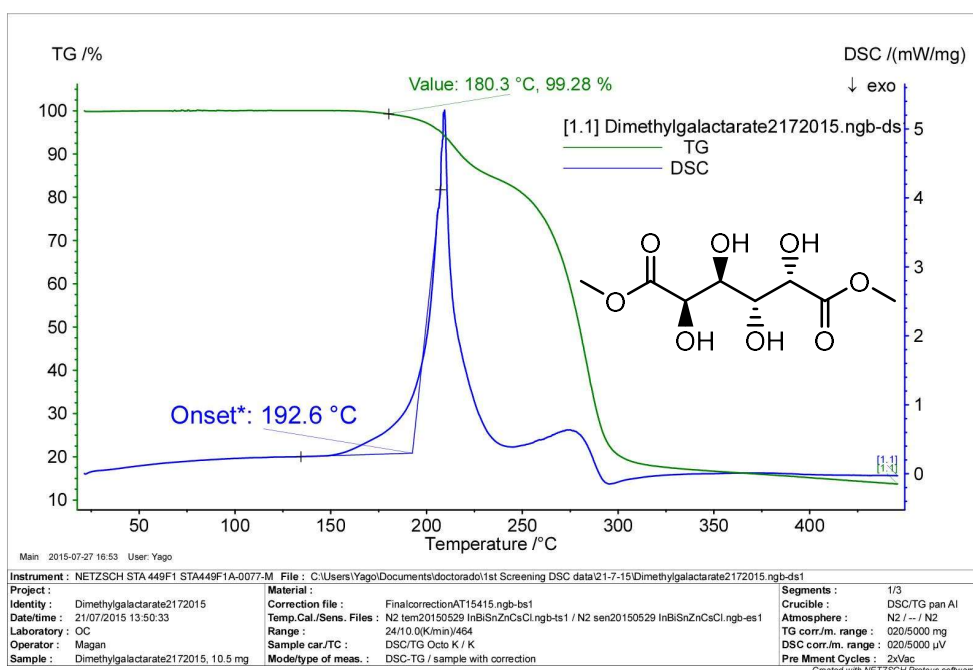
## Tartaric acid



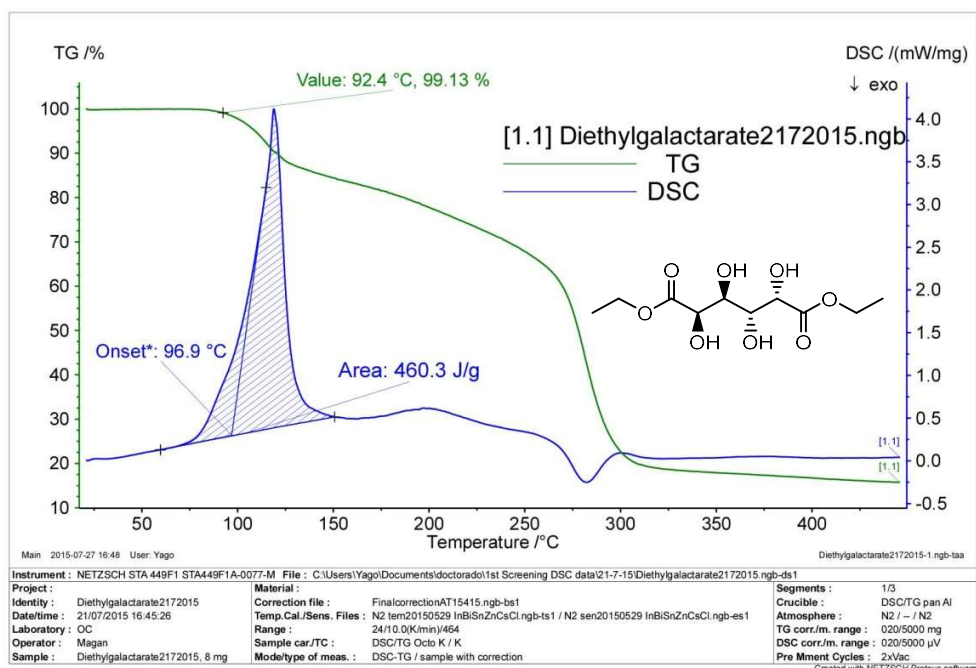
## Mucic acid



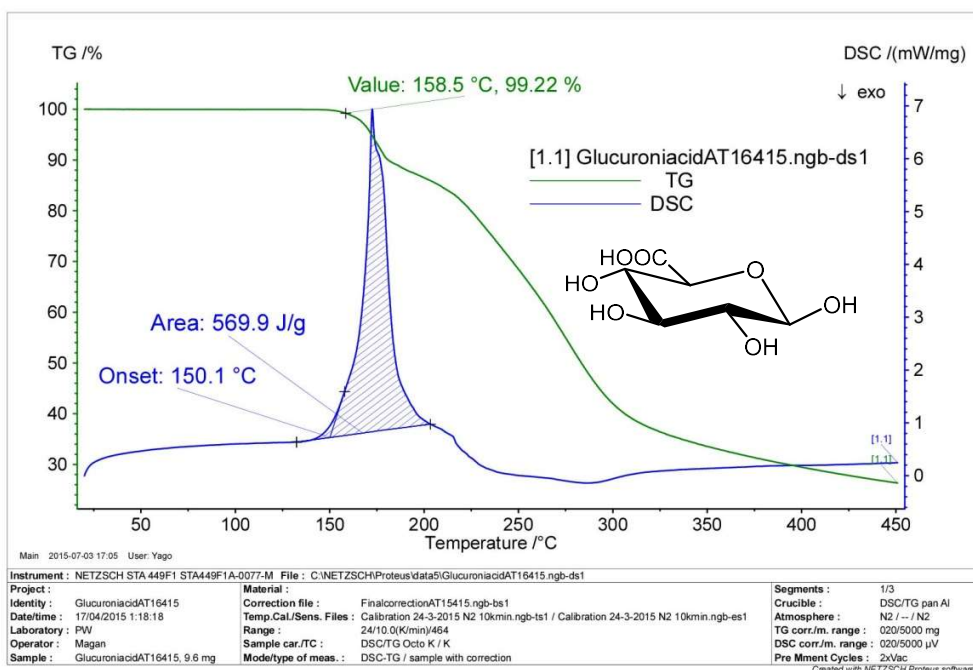
## Dimethyl galactarate



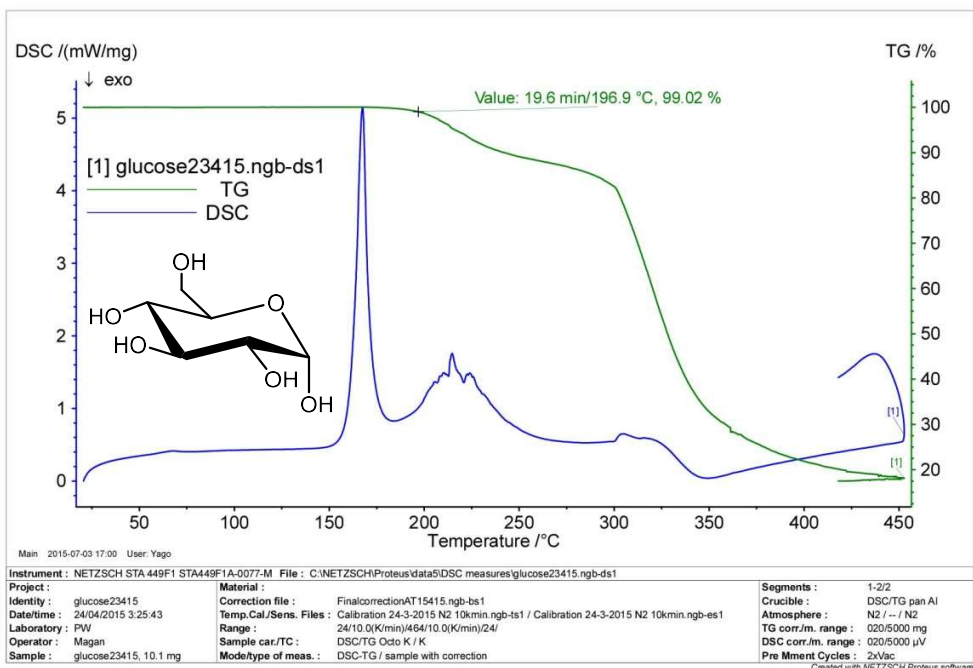
## Diethyl Galactarate



## Glucuronic acid

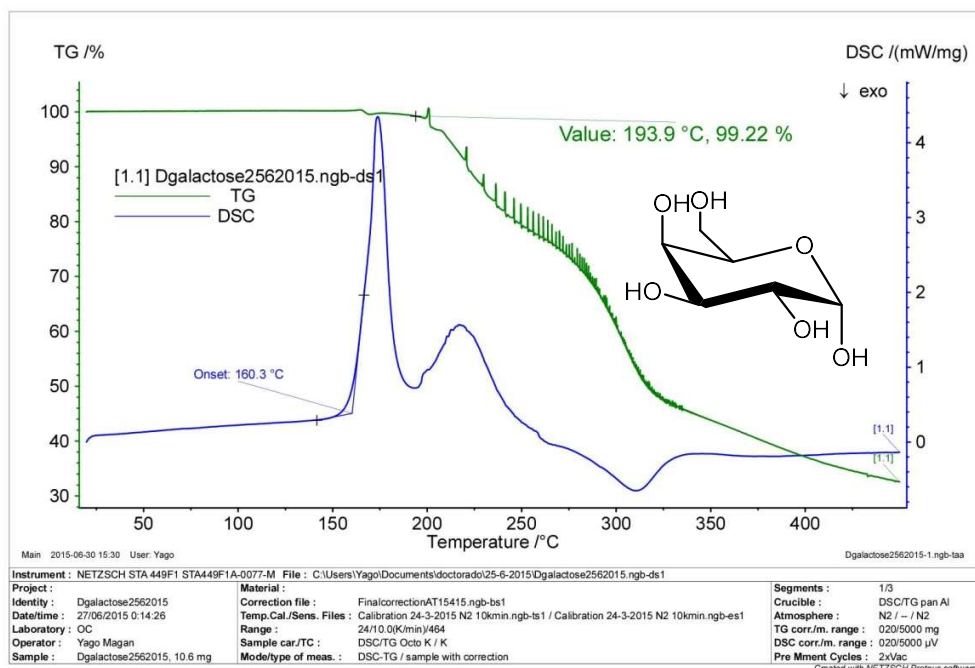


## Glucose-D

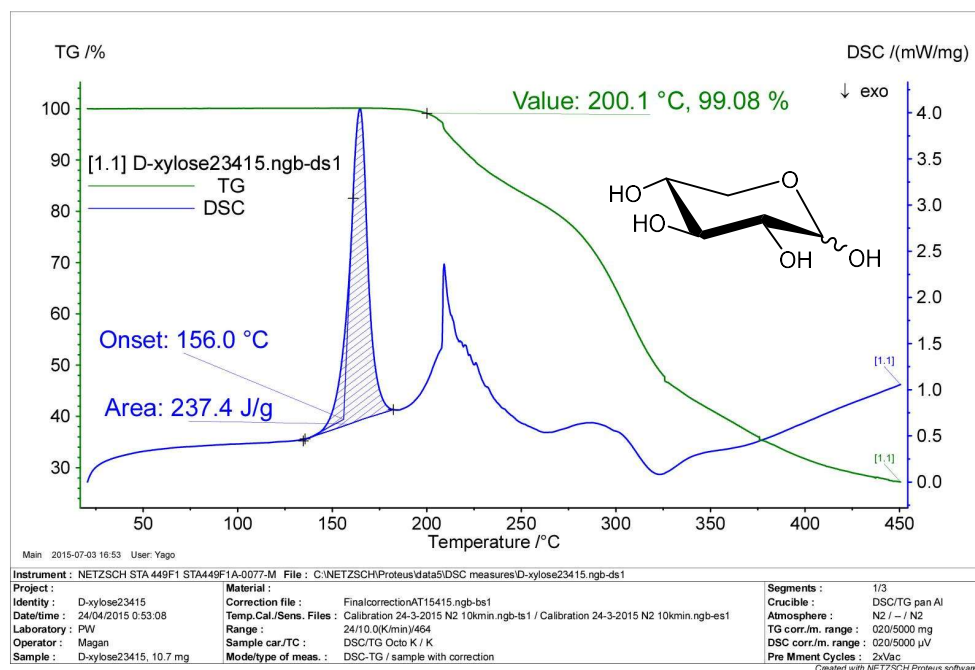




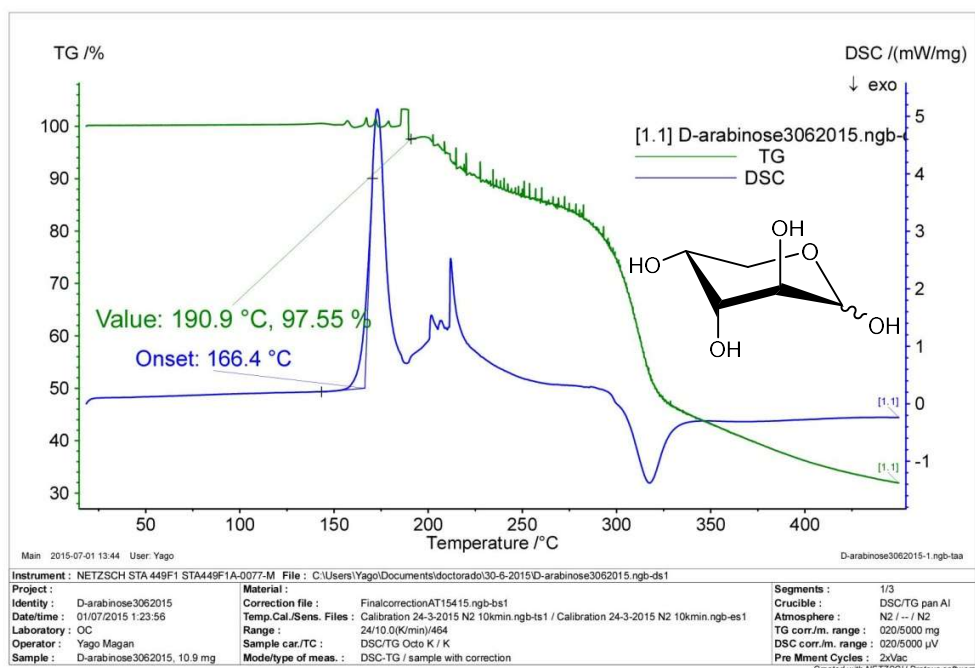
## Galactose



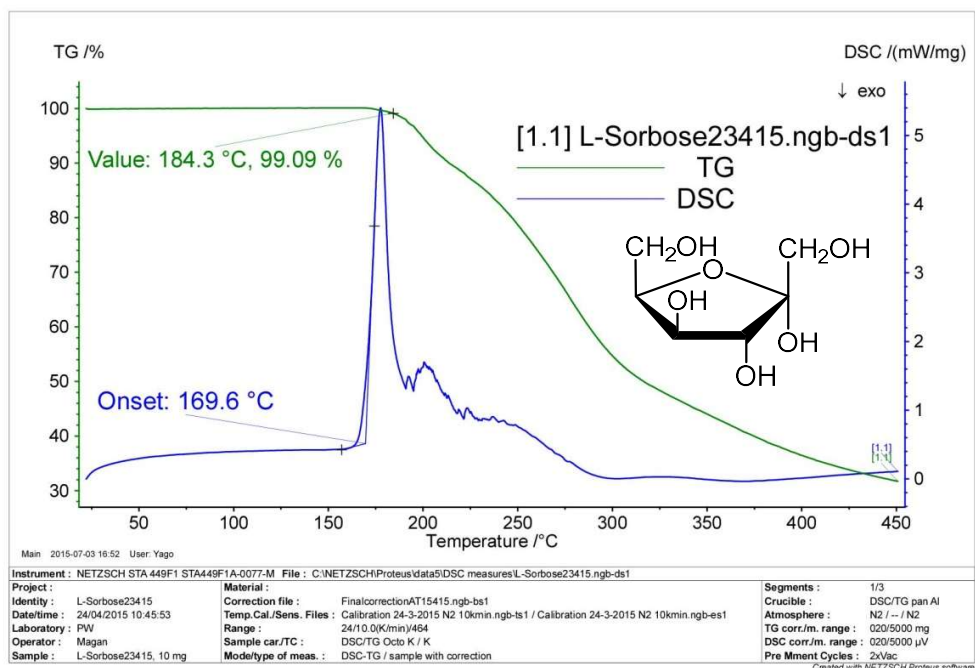
## Xylose



## Arabinose

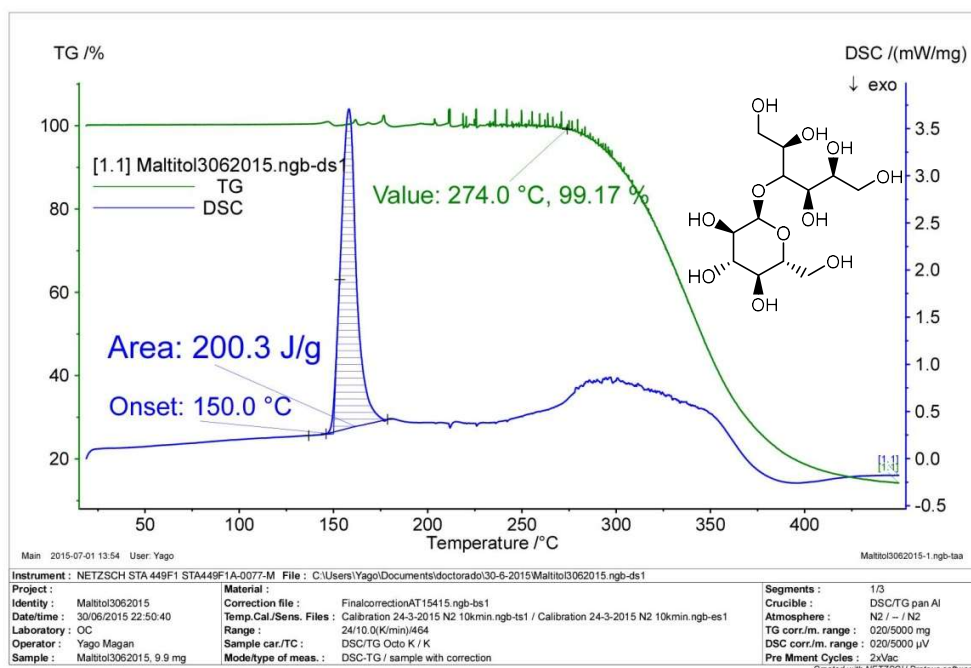


## Sorbitose

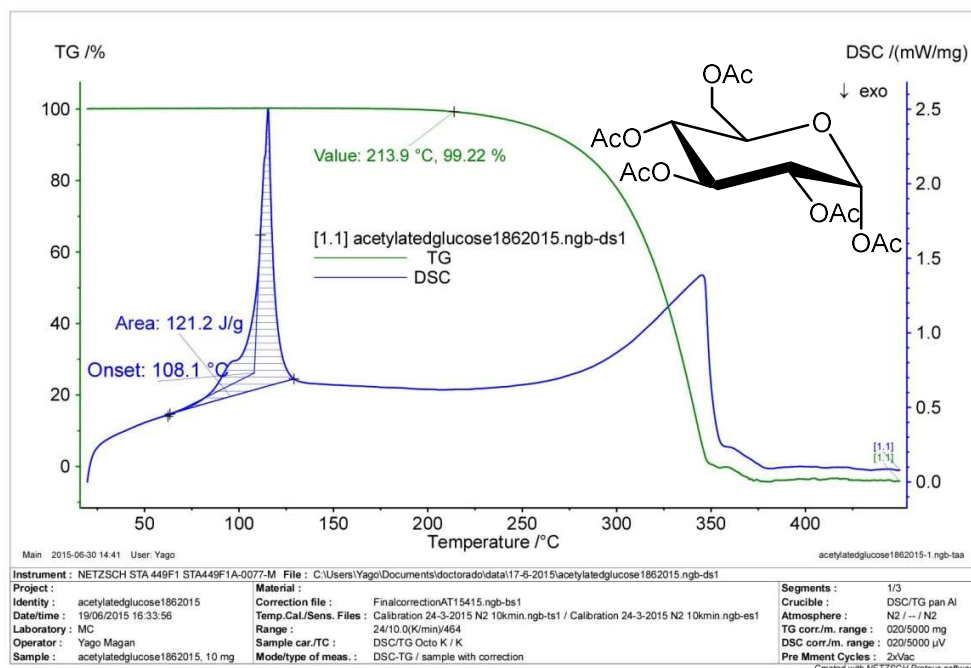




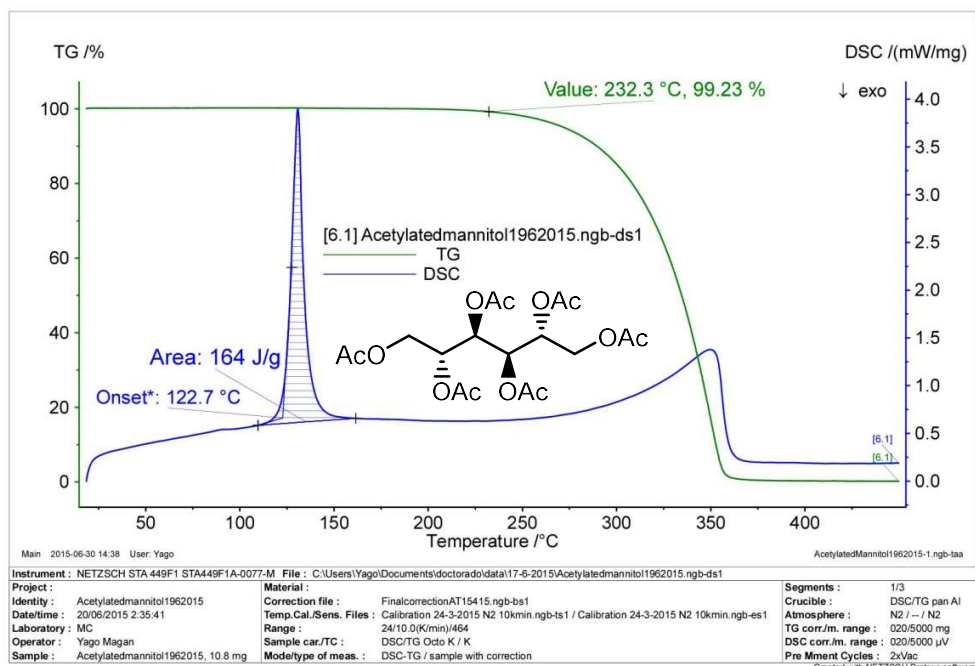
## Maltitol



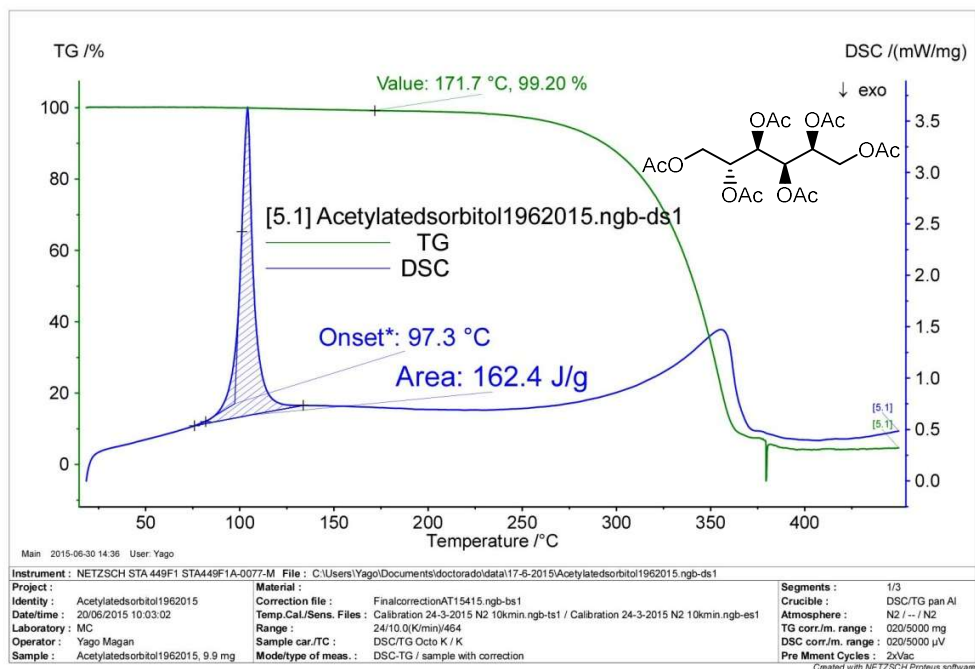
## Acetylated Glucose



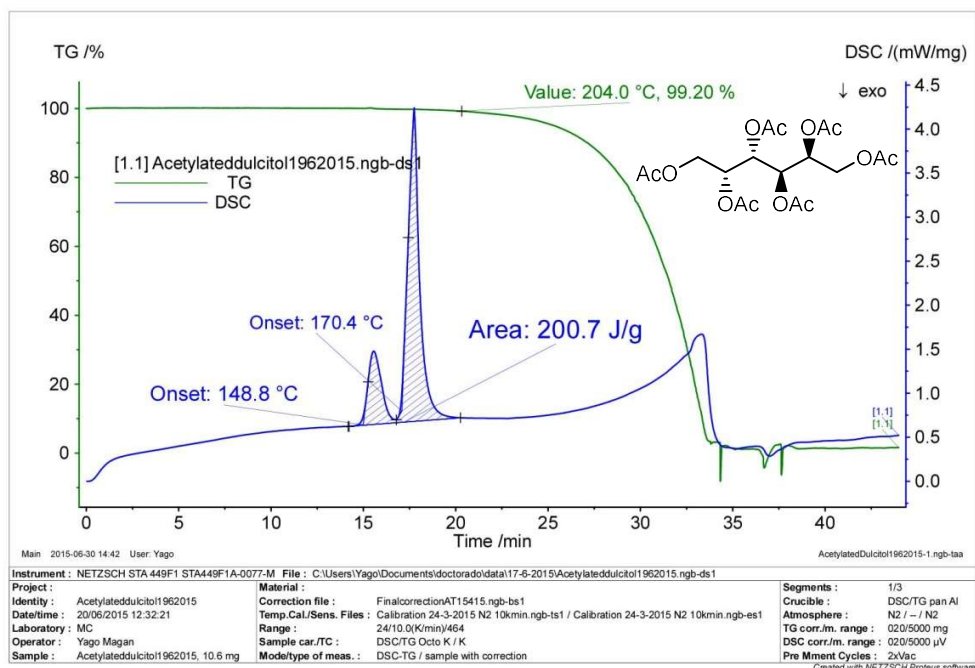
## Acetylated mannitol



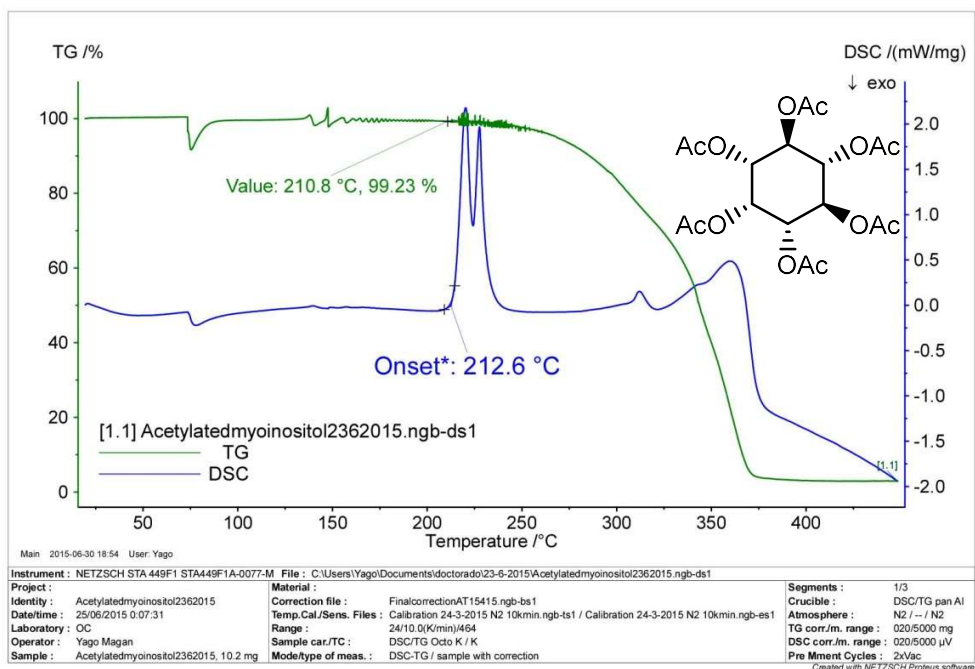
## Acetylated sorbitol



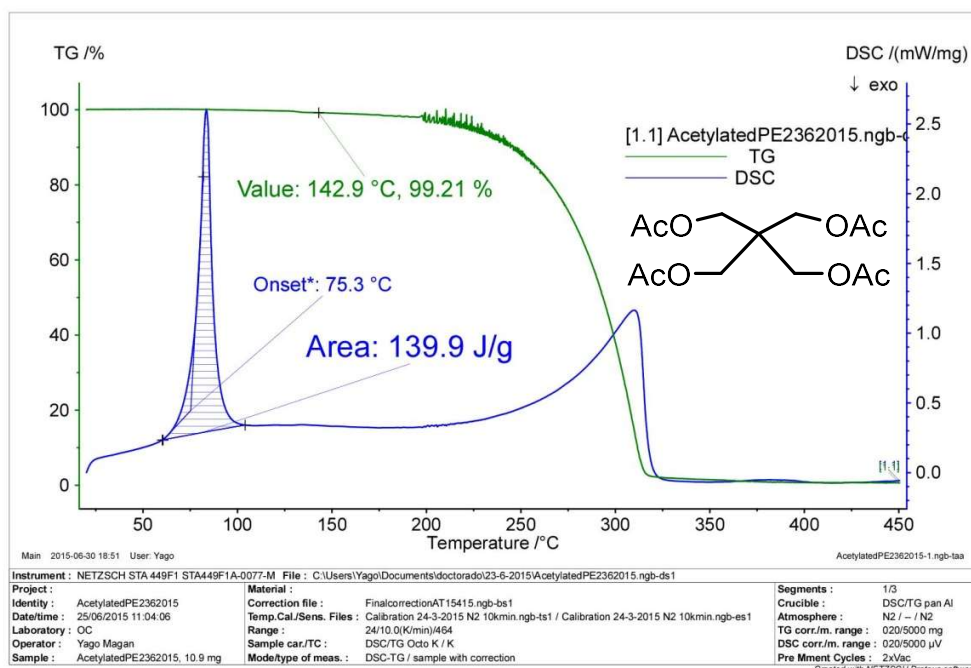
## Acetylated dulcitol



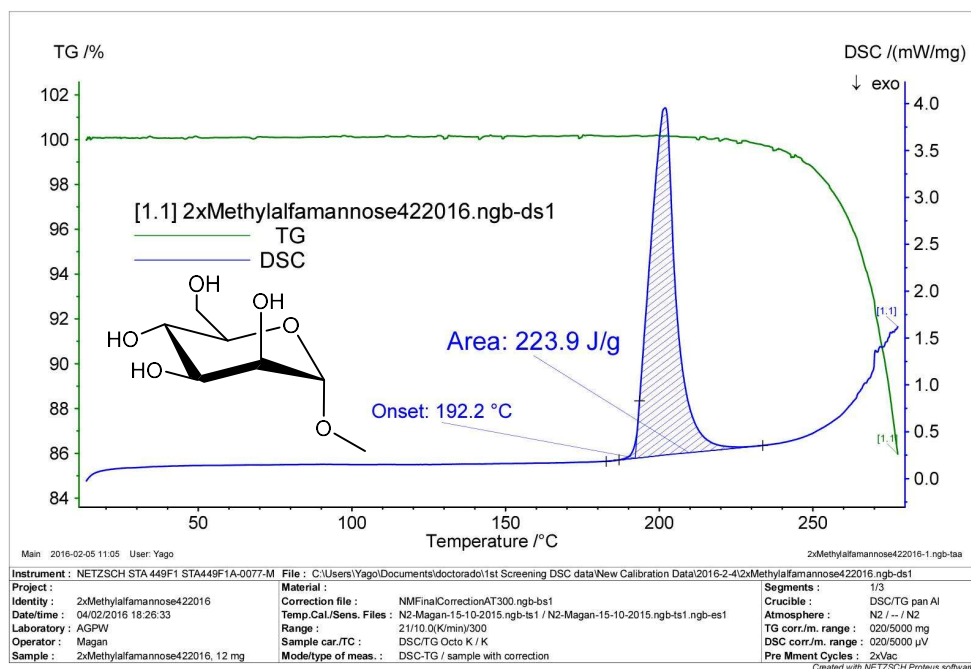
## Acetylated myo-inositol



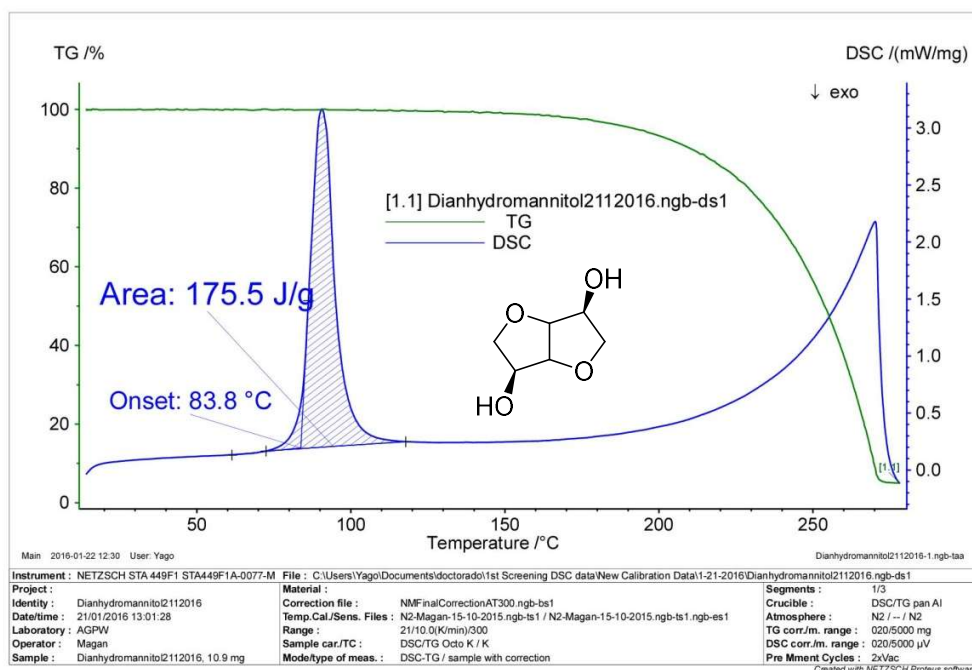
## Acetylated Pentaerythritol



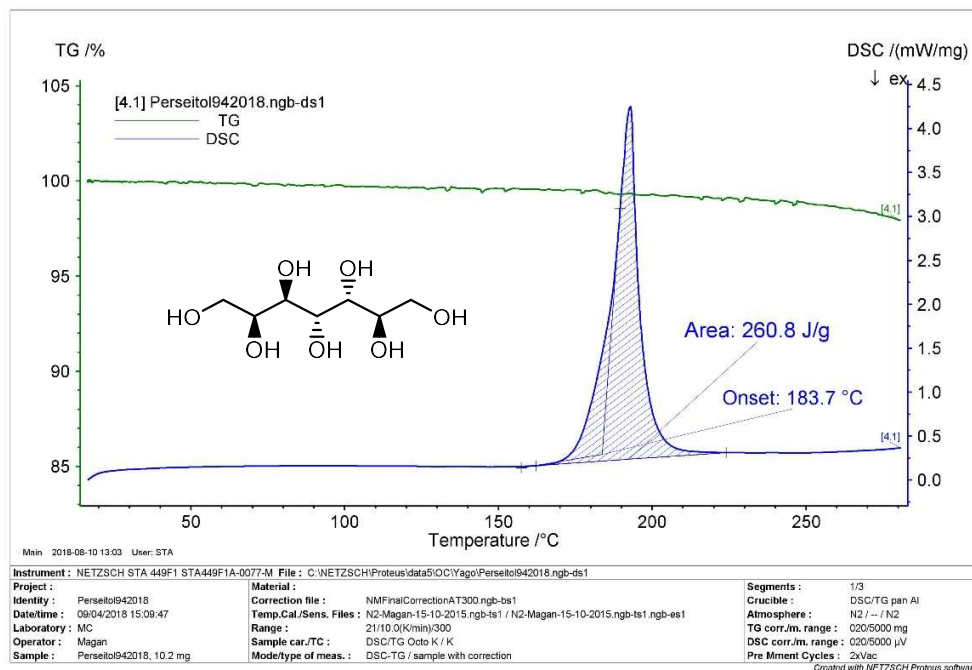
## Methyl α-D-mannopyranoside



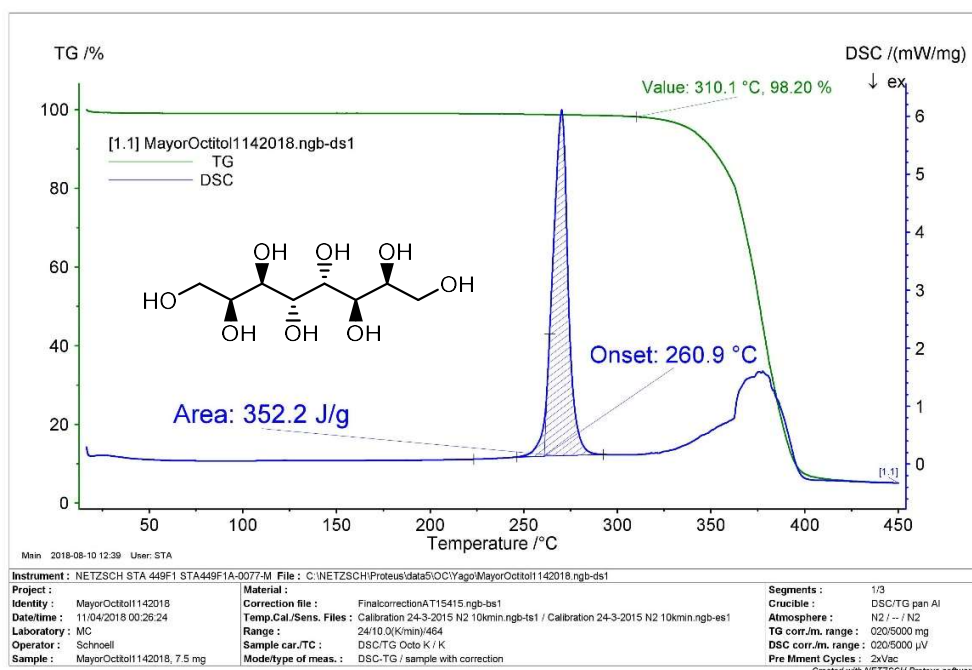
## Dianhydromannitol



## Perseitol

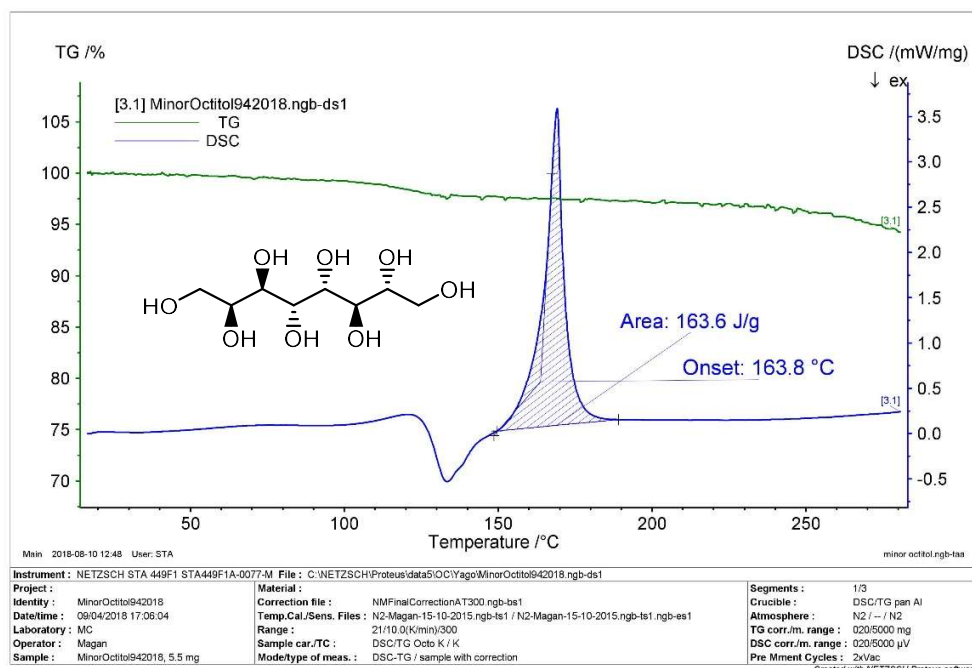


## D-erythro-D-manno-octitol



Create PDF files without this message by purchasing novaPDF printer (<http://www.novapdf.com>)

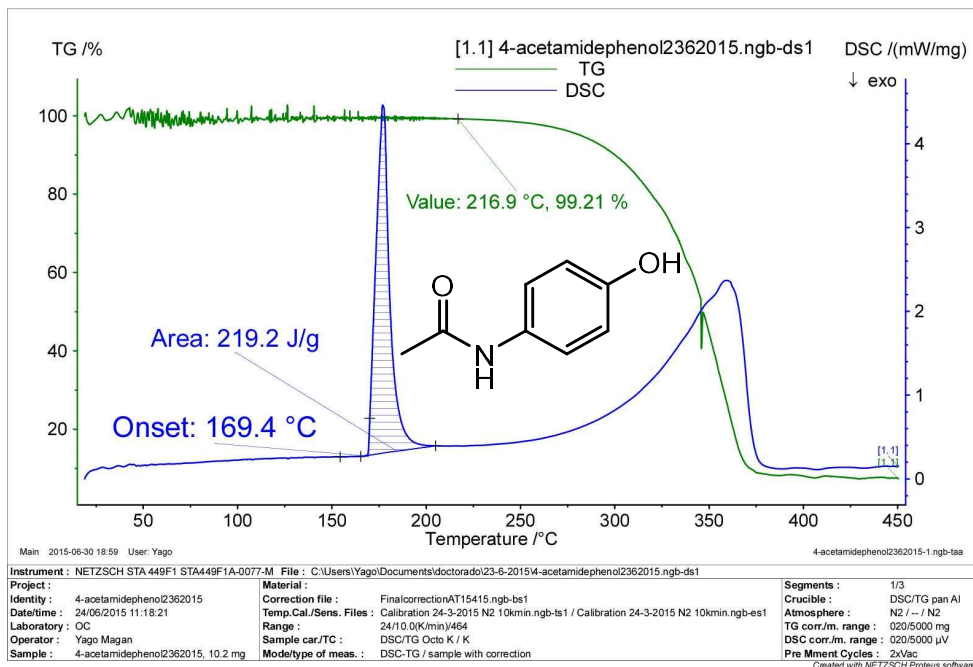
## D-erythro-L-gluco-octitol



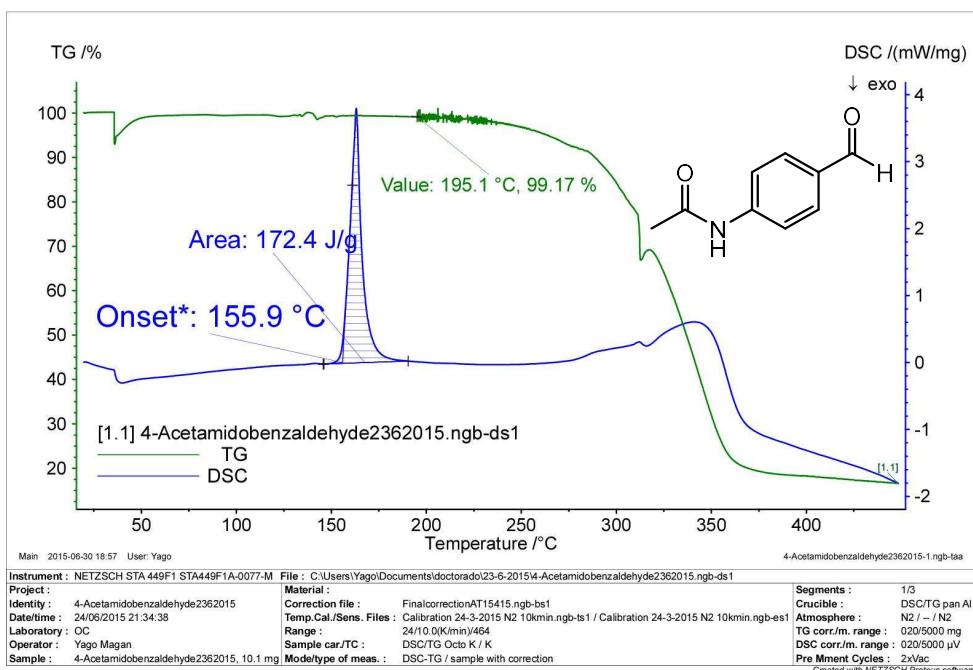


## 5.1.2 Arene

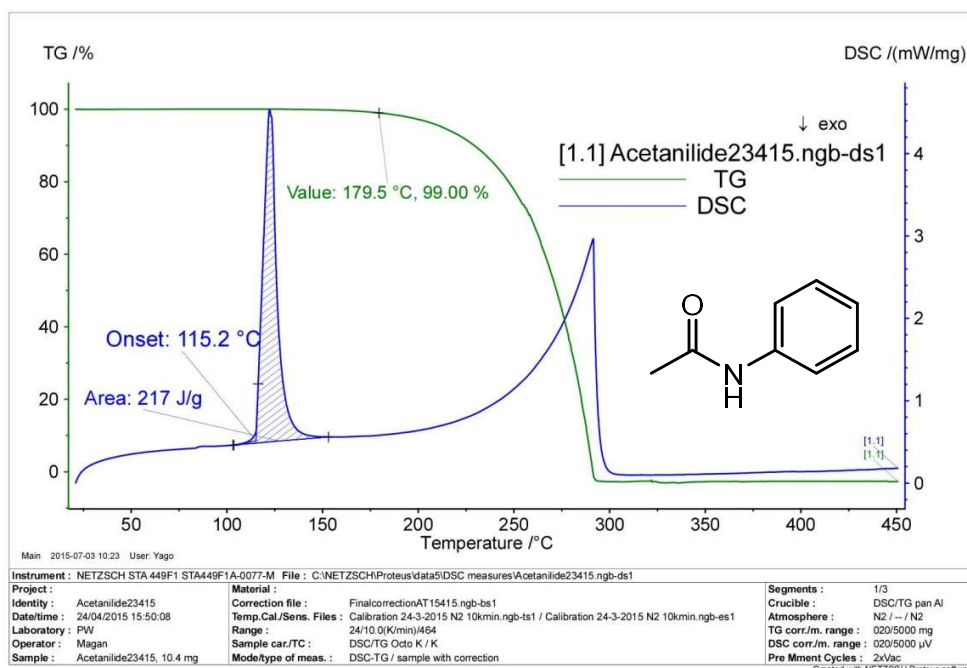
## 4-Acetamidophenol



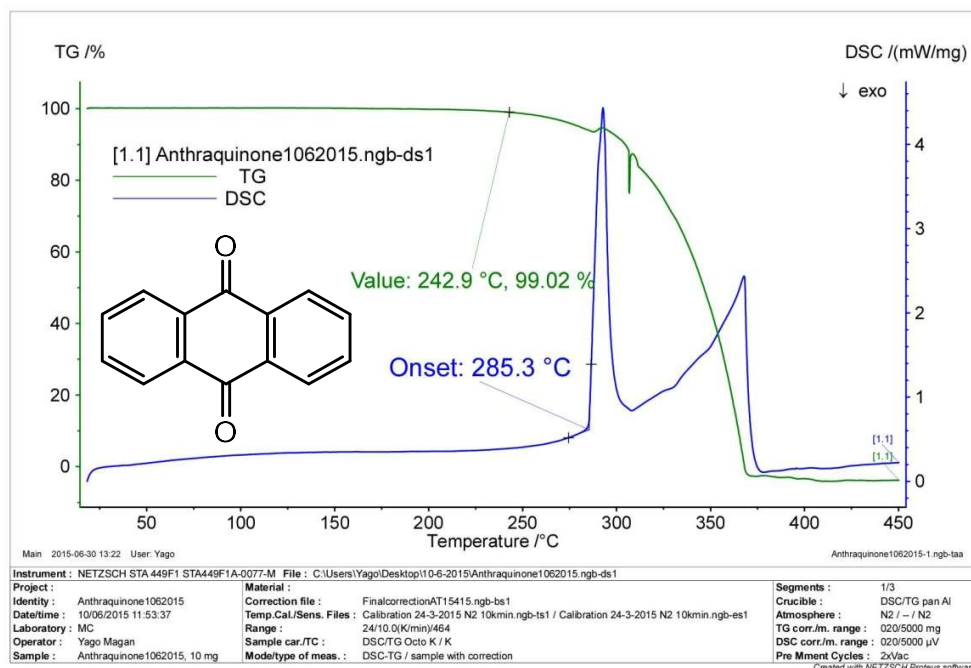
## 4-Acetamidobenzaldehyde



## Acetanilide

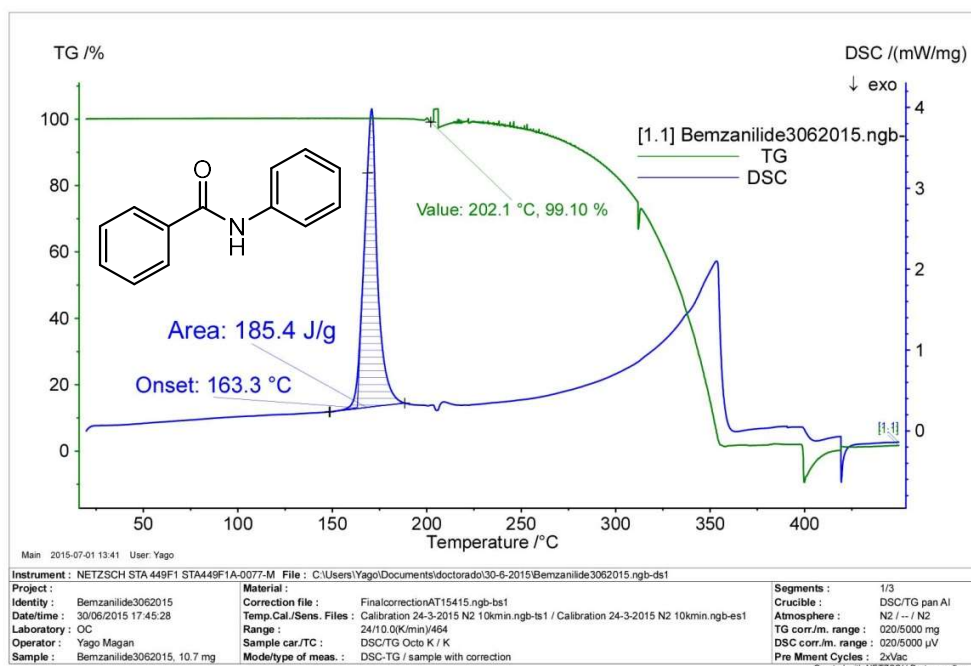


## Anthraquinone

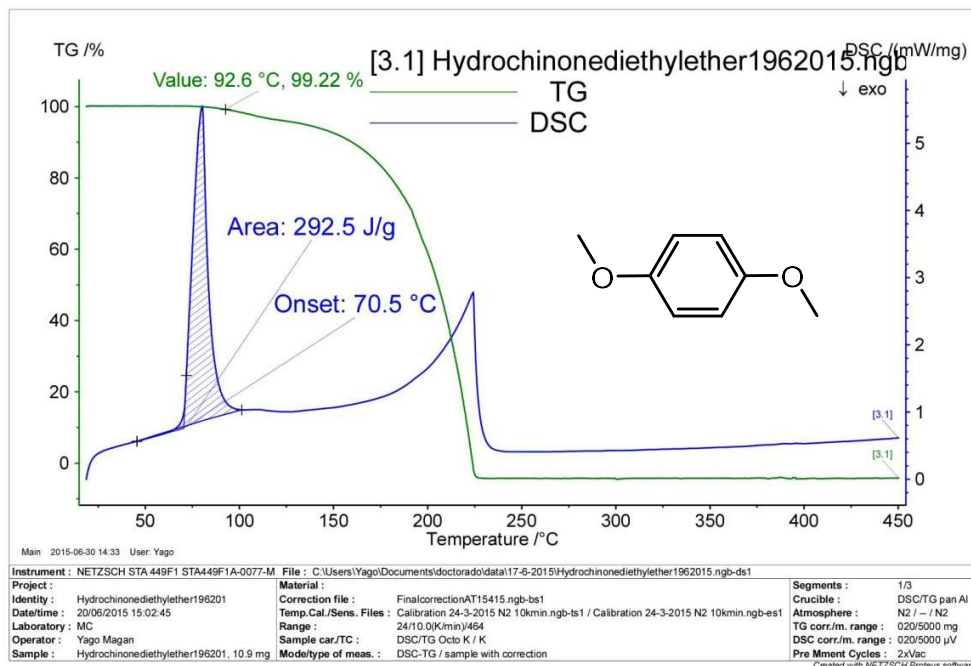




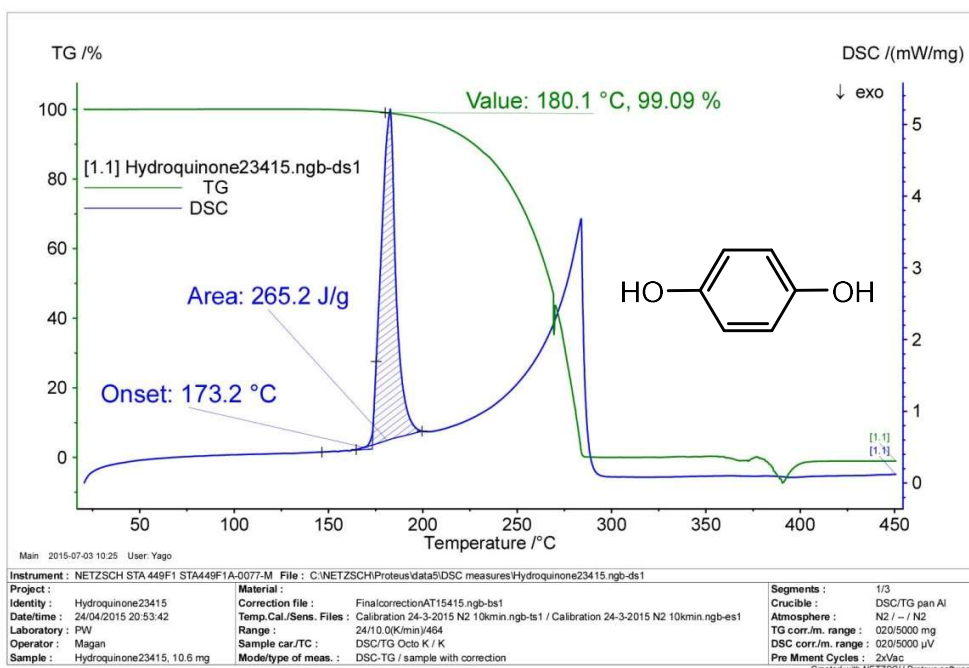
## Benzanilide



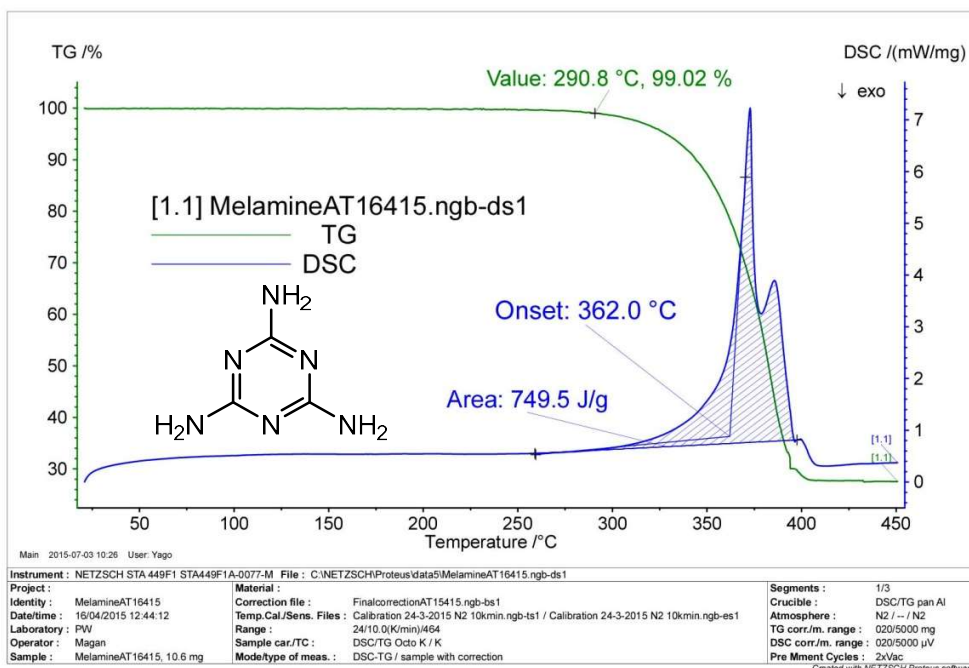
## Hydrochinon Diethylether



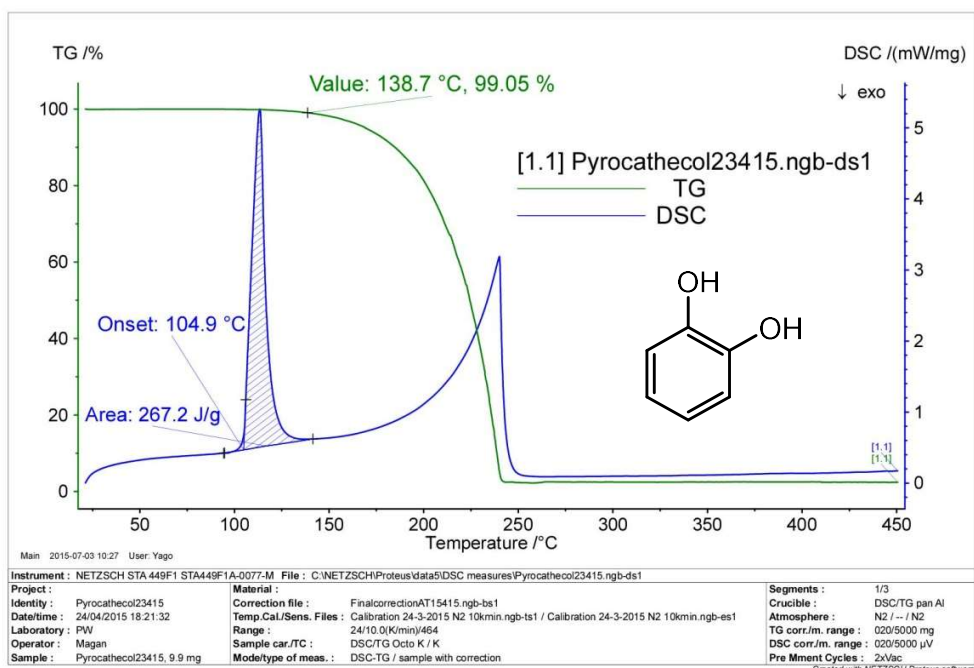
## Hydroquinone



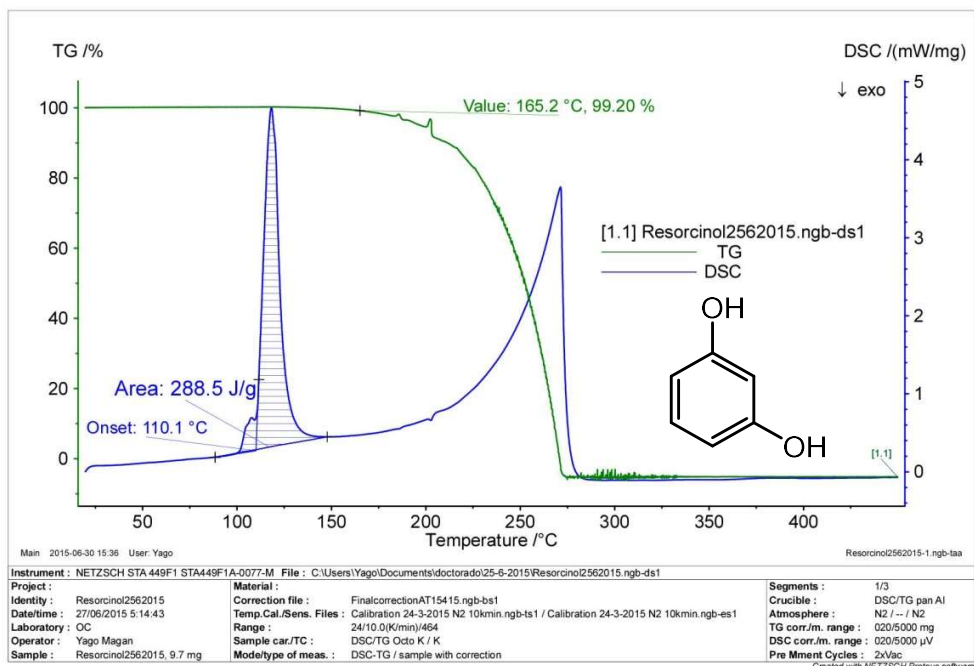
## Melamine



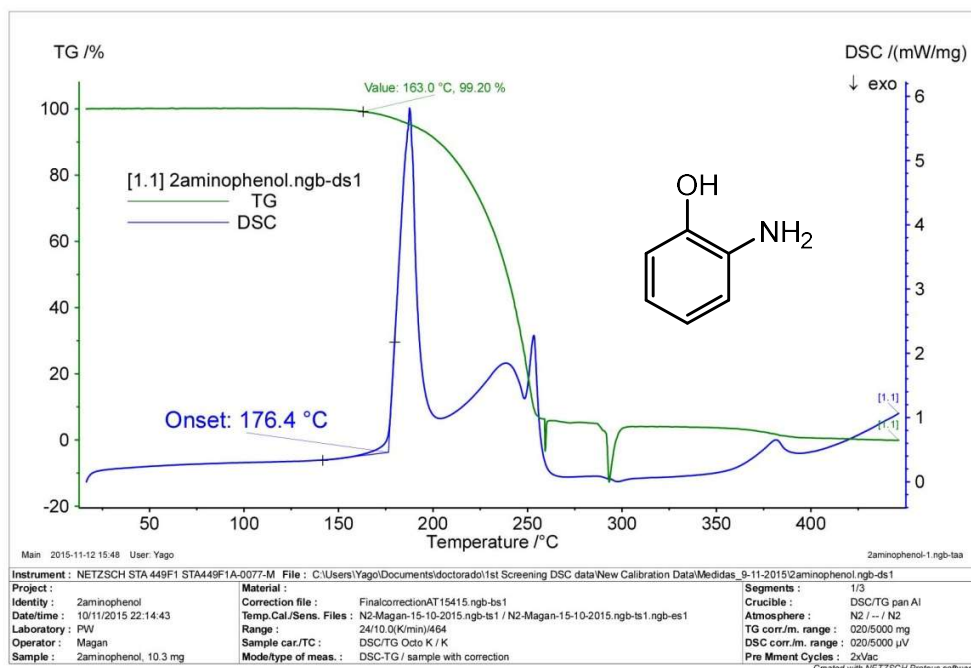
## Pyrocatechol



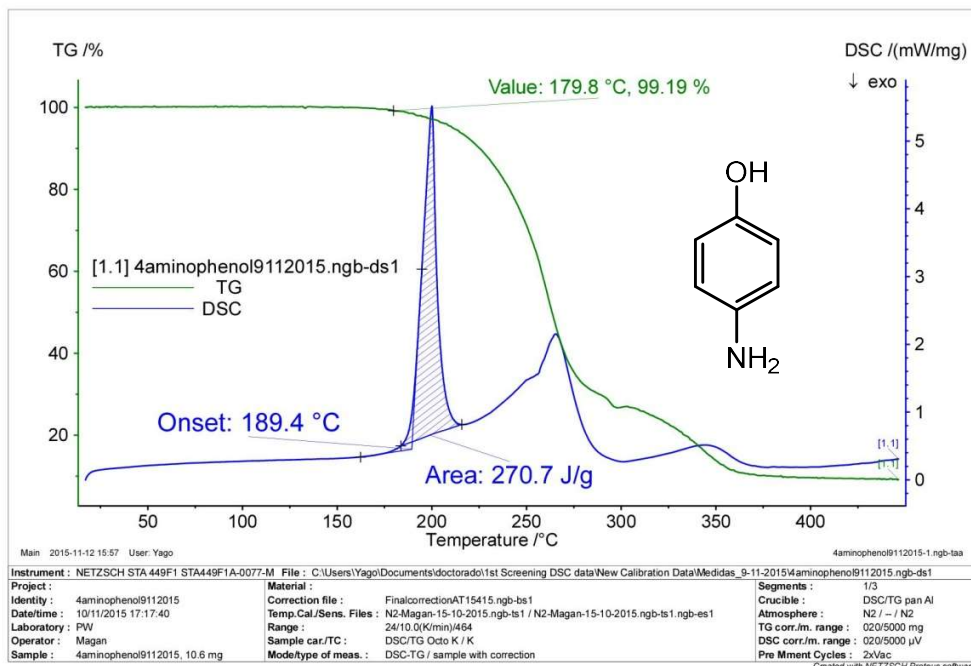
## Resorcinol



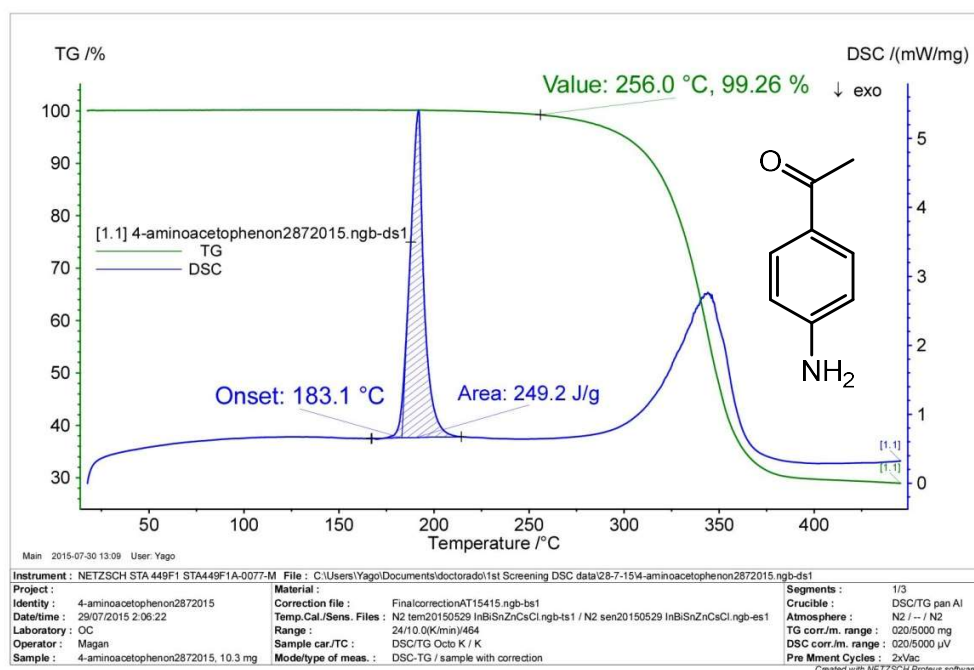
## 2-Aminophenol



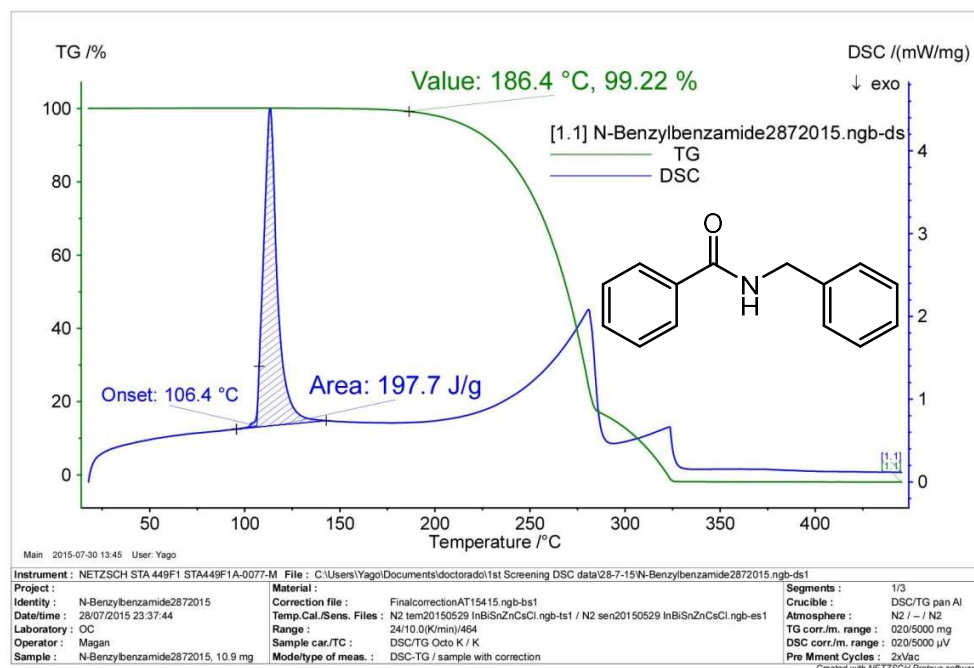
## 4-Aminophenol



## 4-Aminoacetophenone



## N-Benzylbenzamide

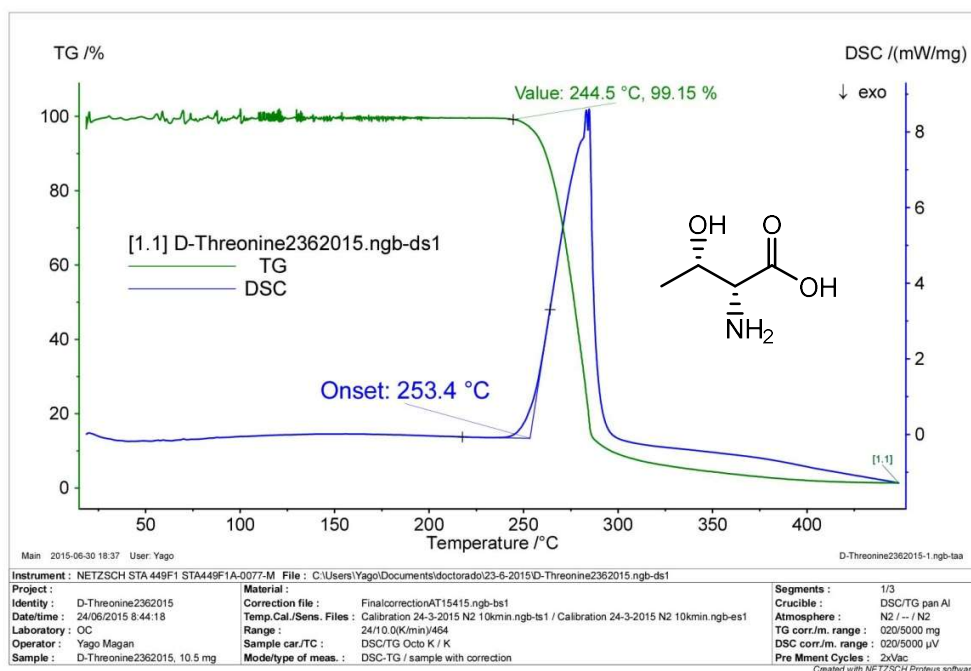




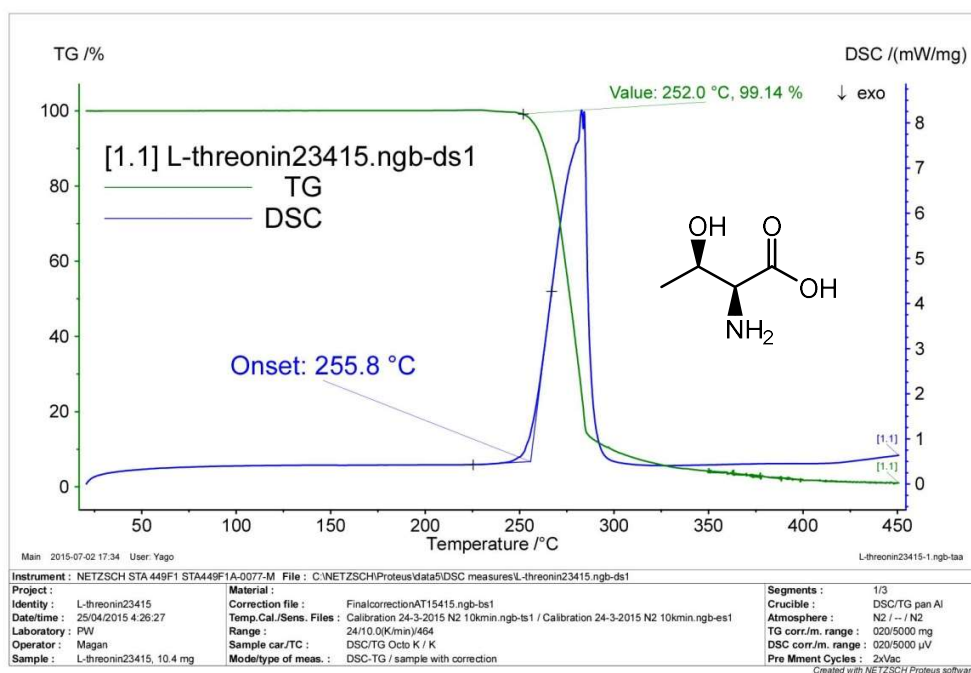


## 5.1.3 Amino acids

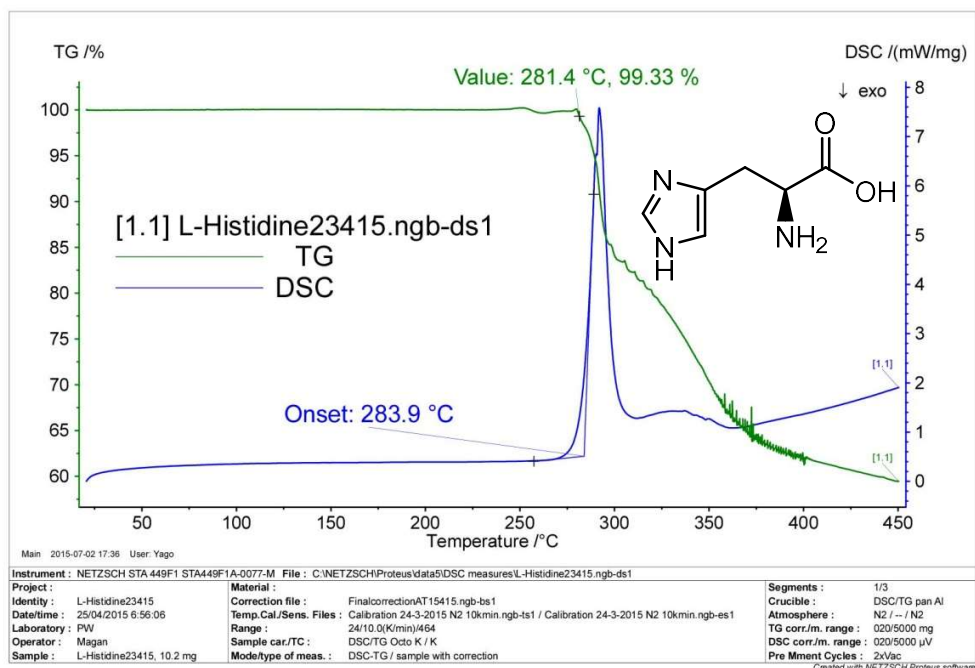
## D-Threonine



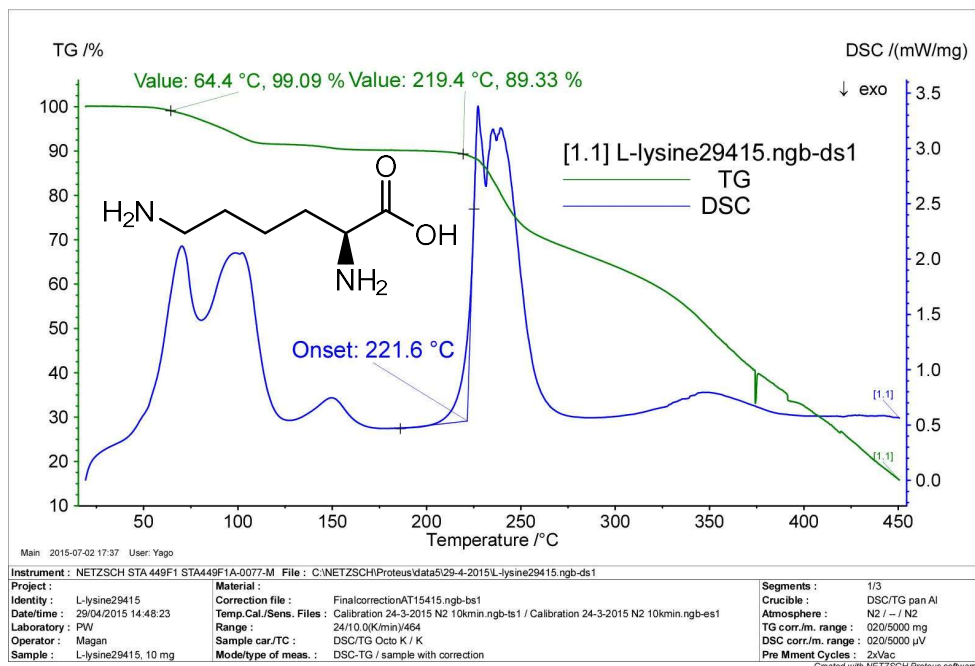
## L-Threonine



## L-Histidine

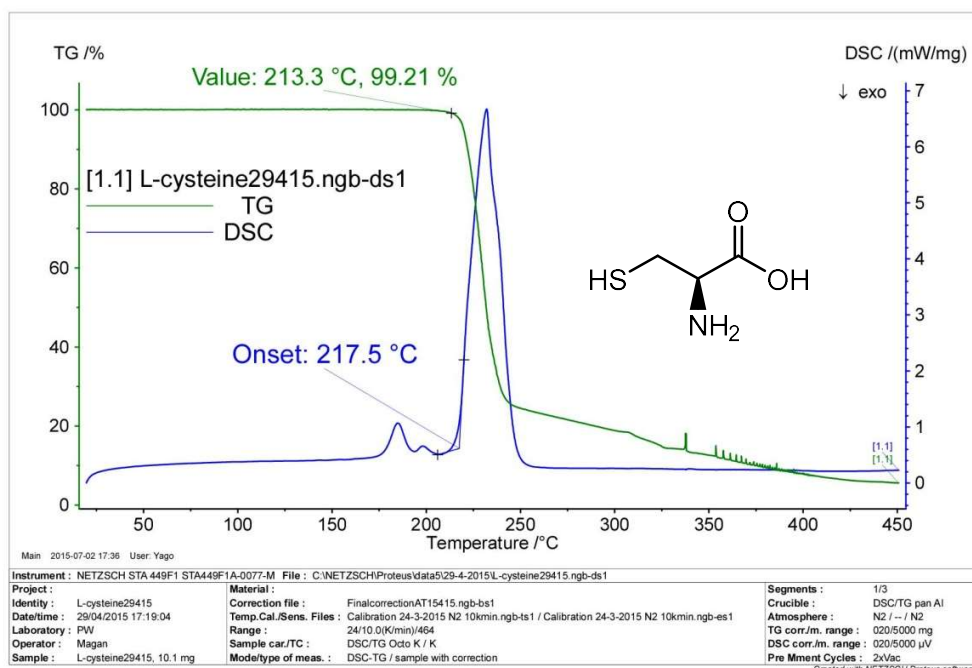


## L-Lysine

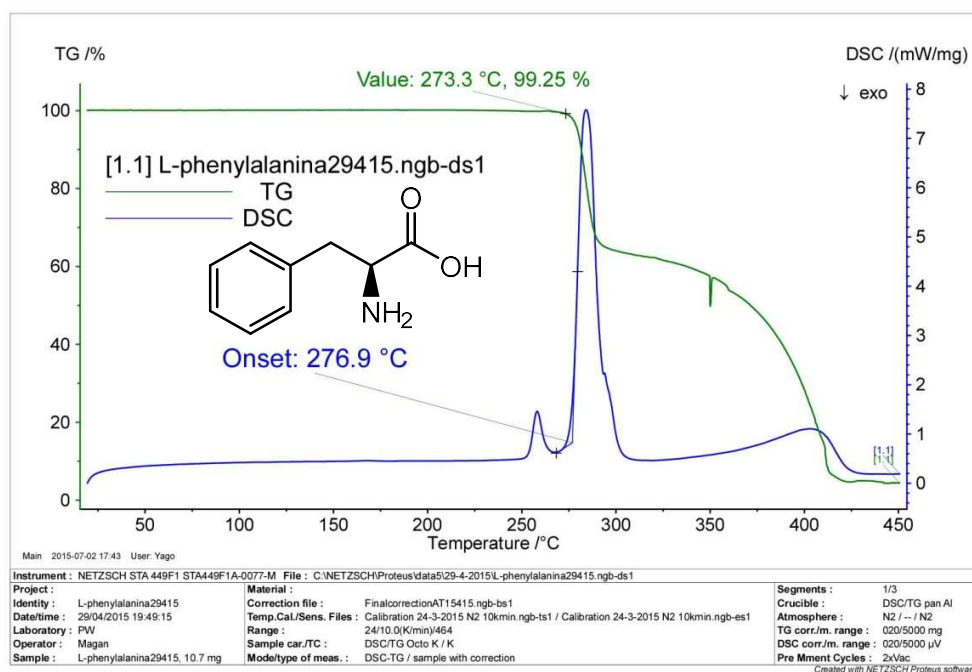




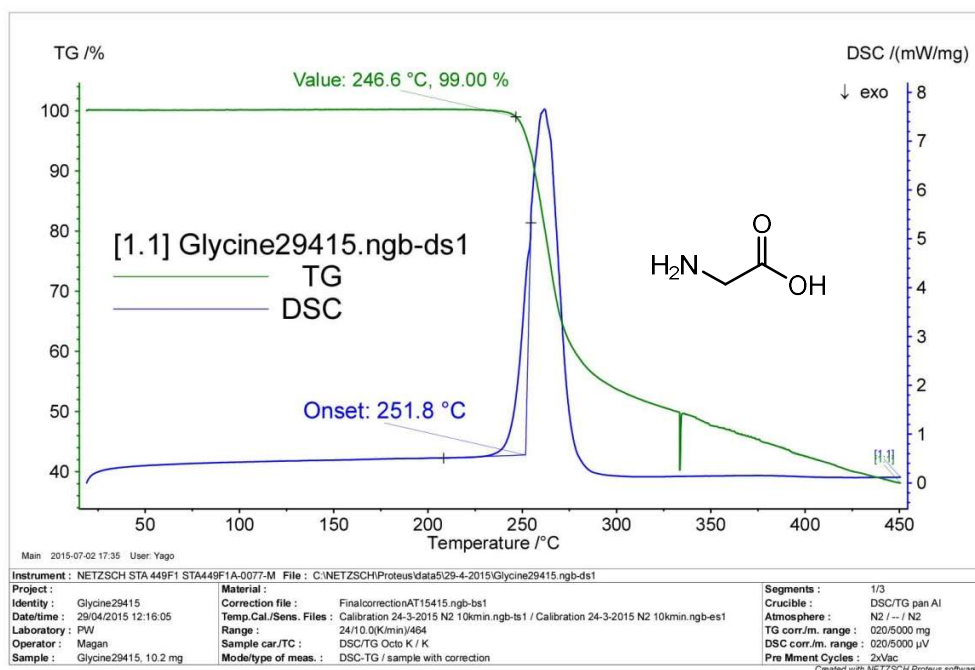
## L-Cysteine



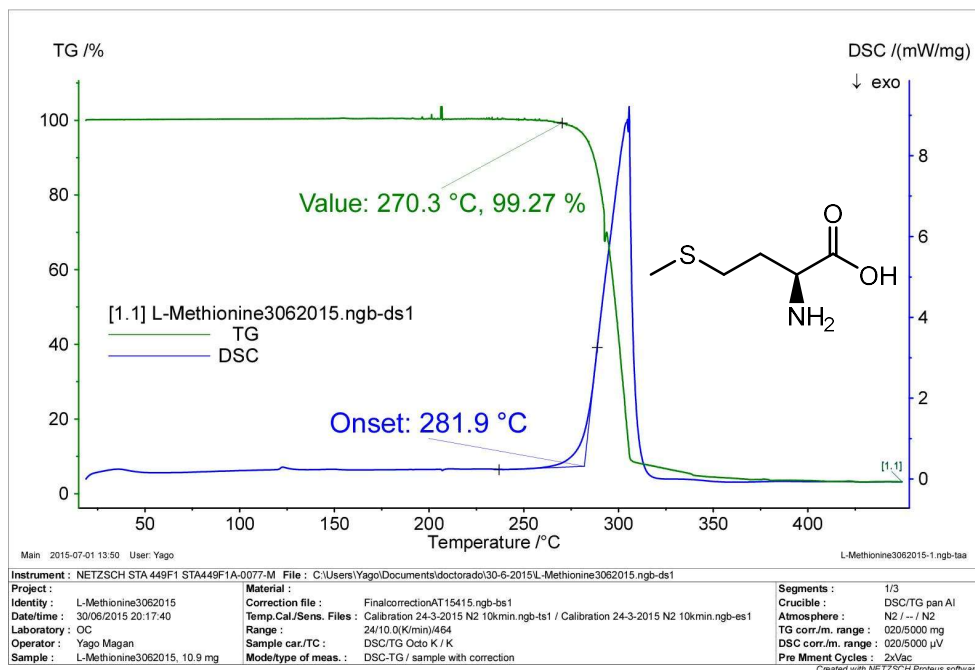
## L-Phenylalanine



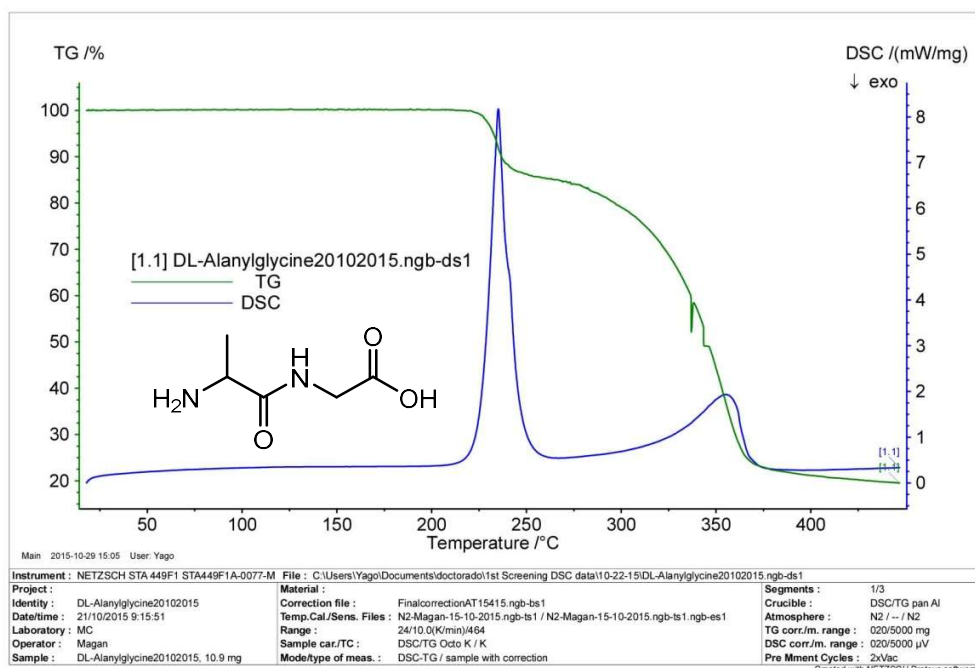
## Glycine



## L-Methionine

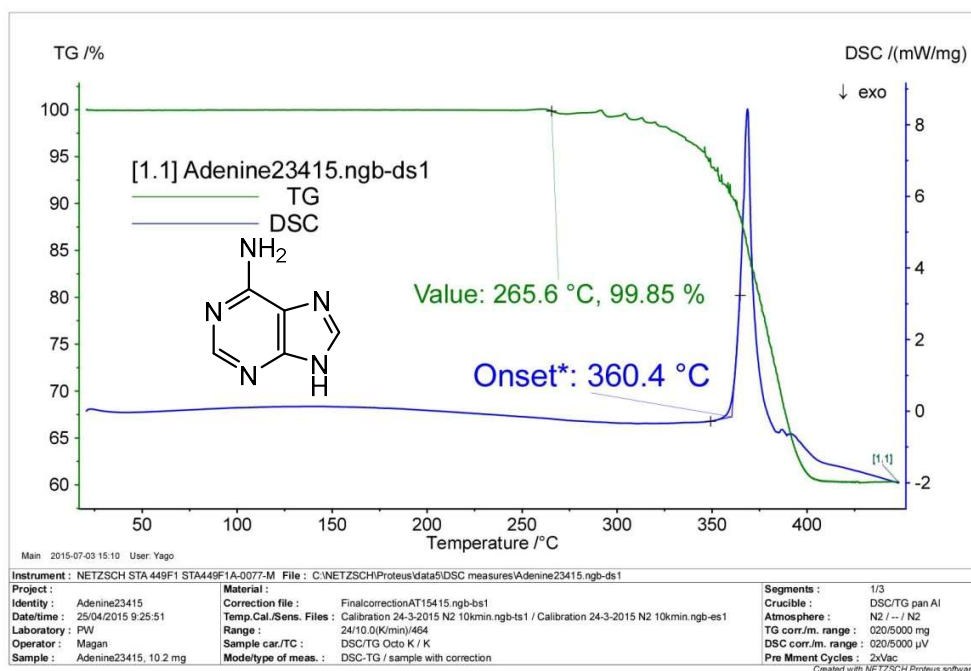


## DL-Alanylglycine

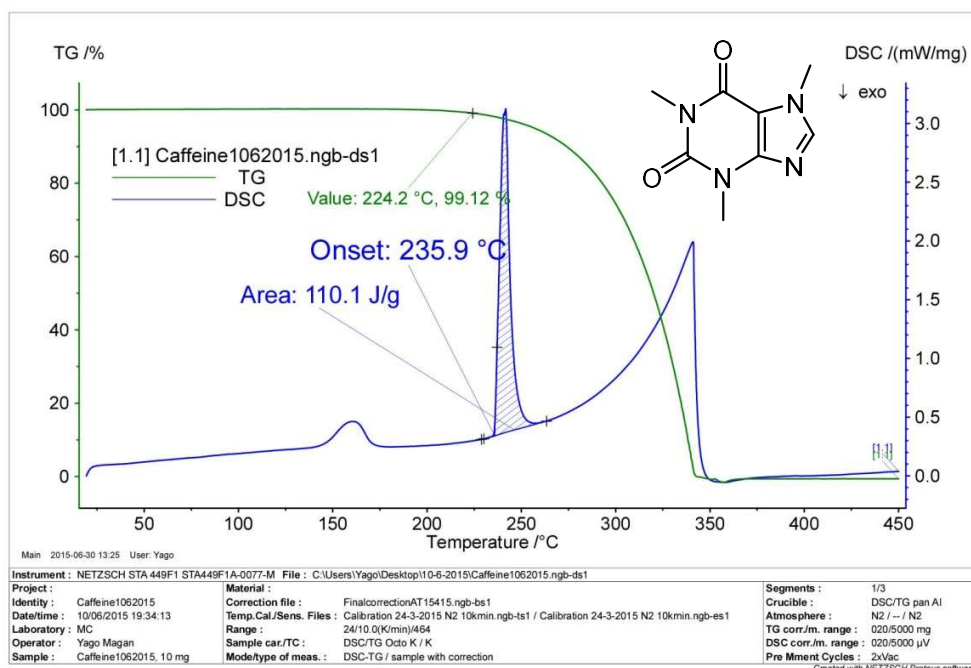


## 5.1.4 Purines and pyrimidines

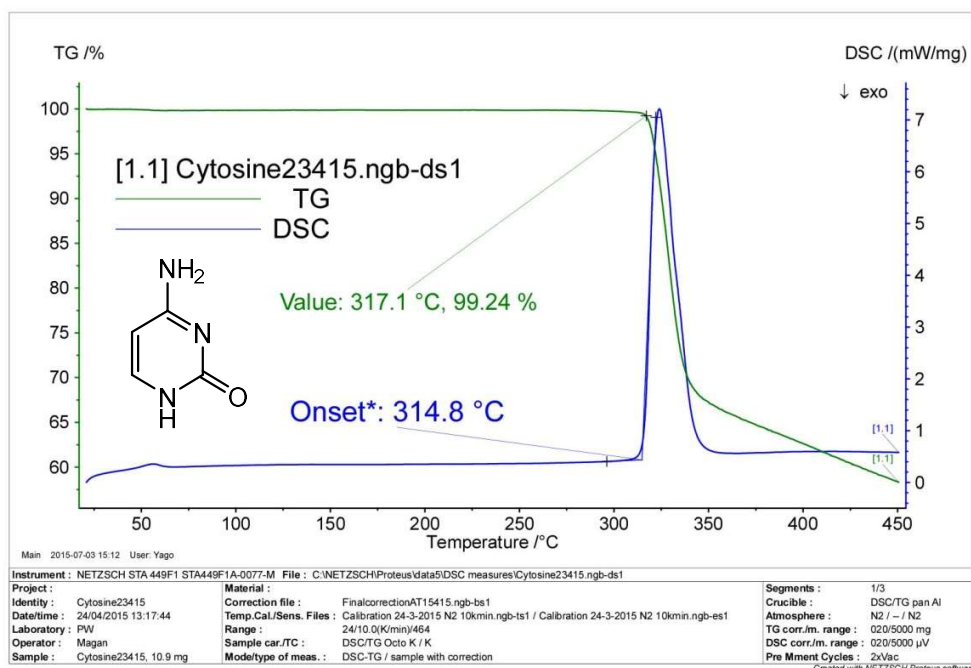
## Adenine



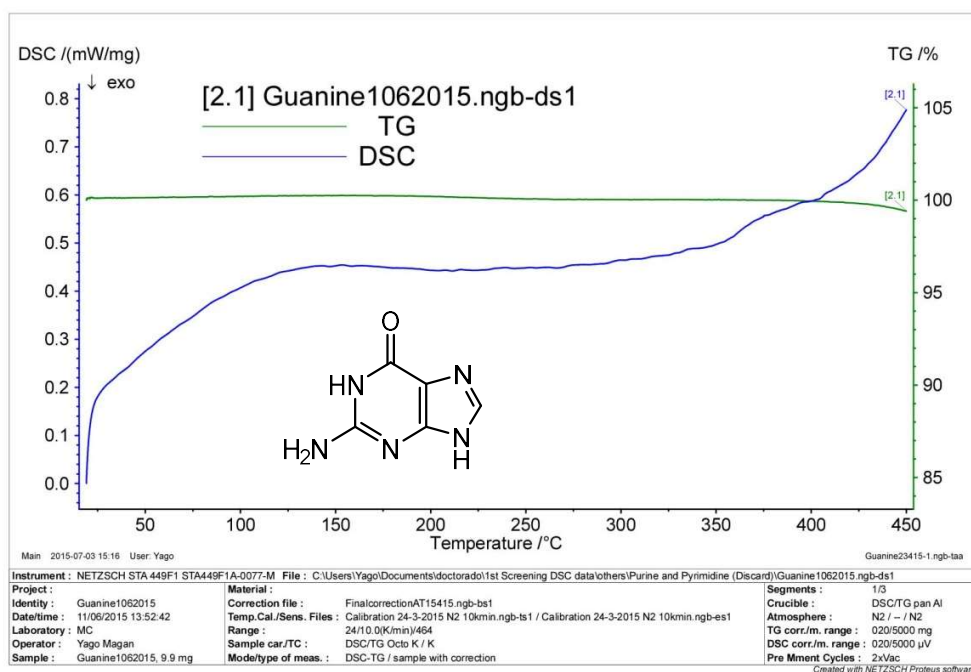
## Caffeine



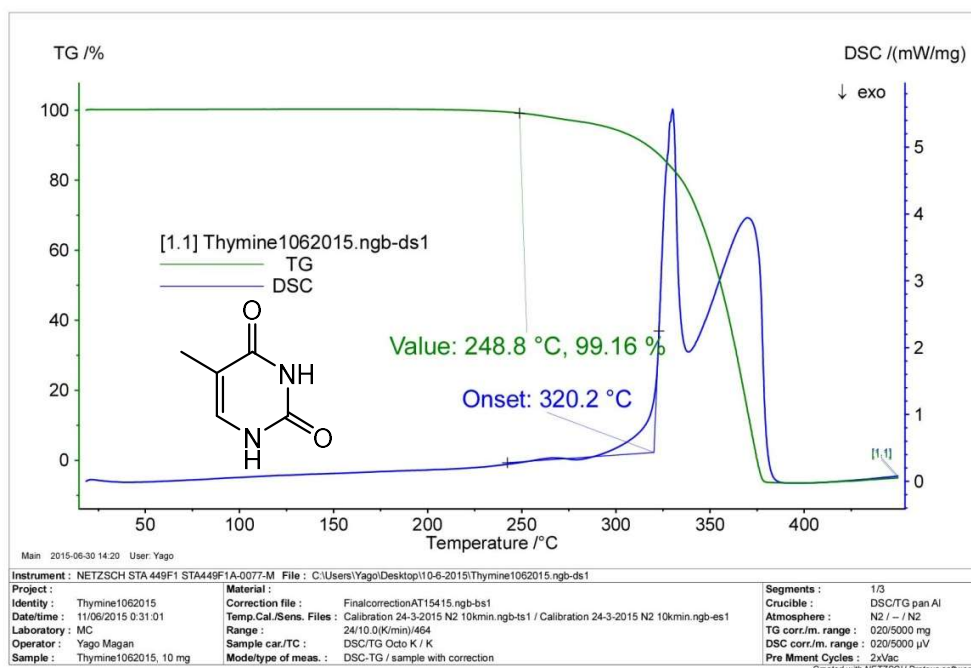
## Cytosine



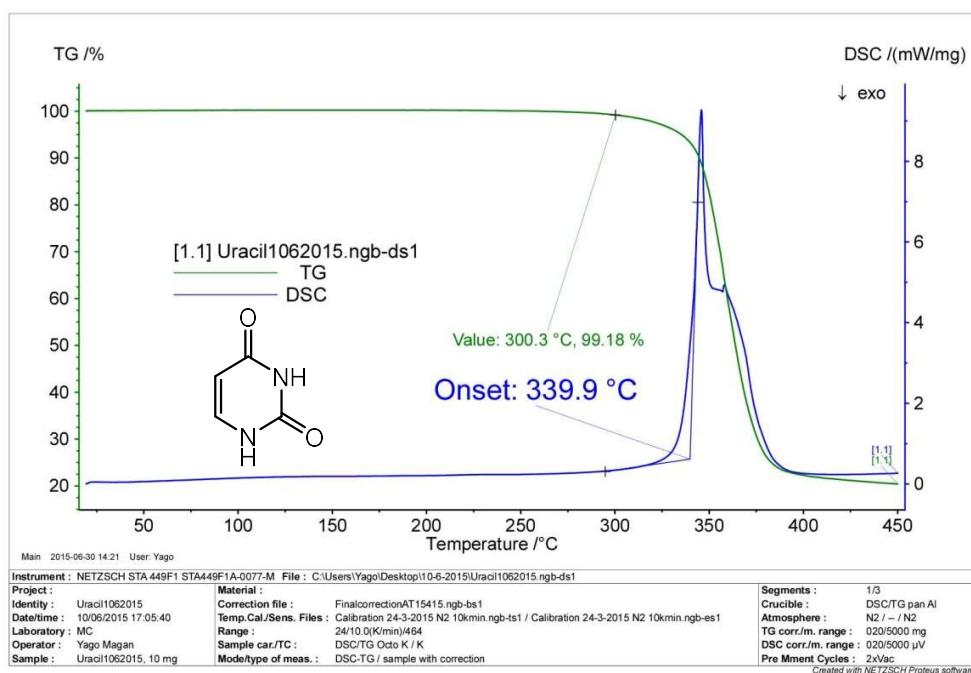
## Guanine



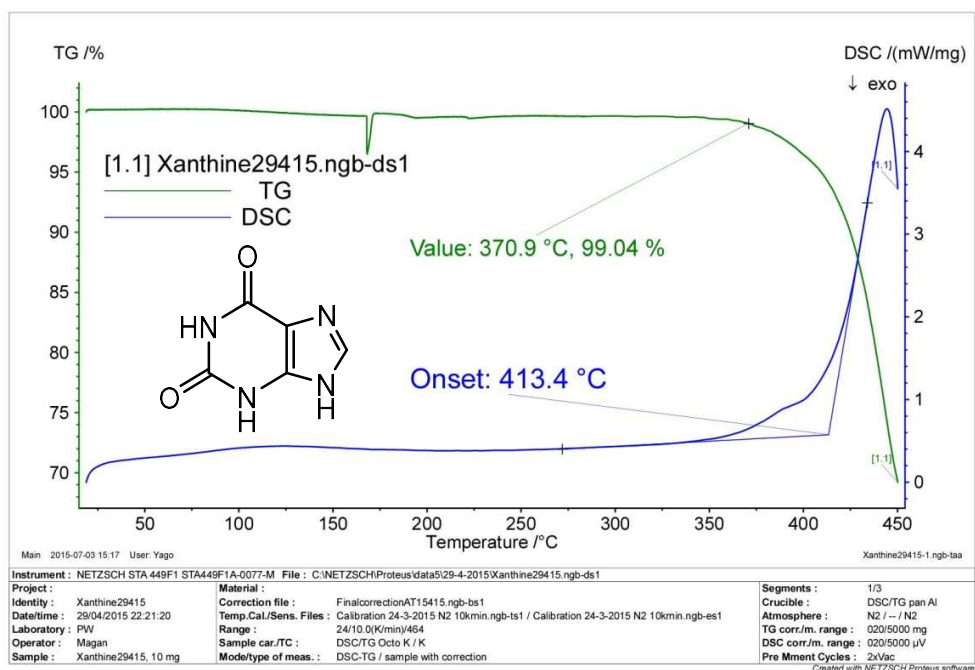
## Thymine



## Uracil



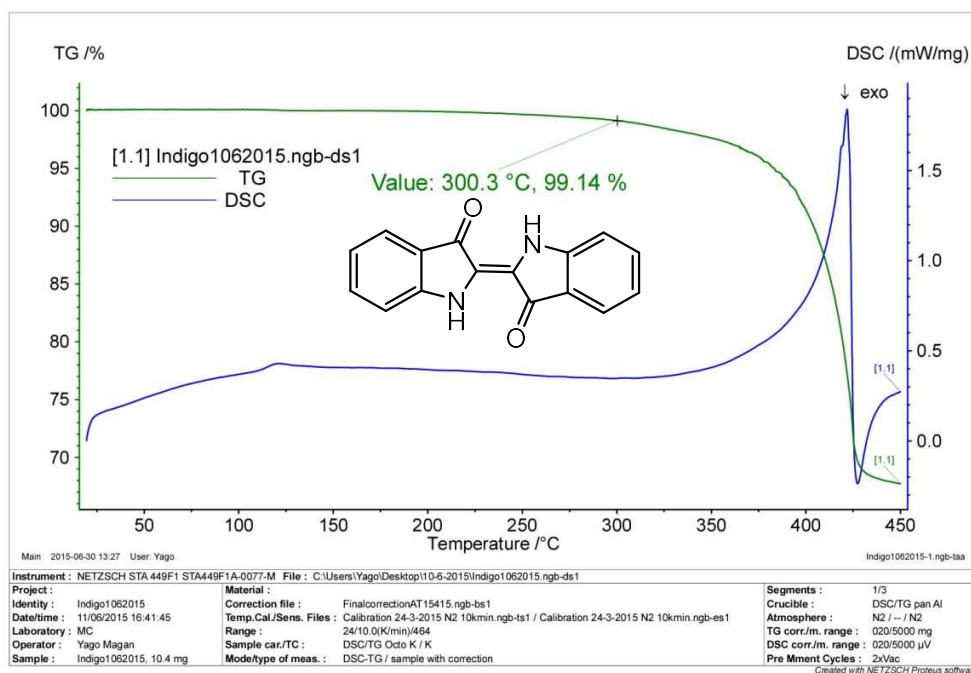
## Xanthine



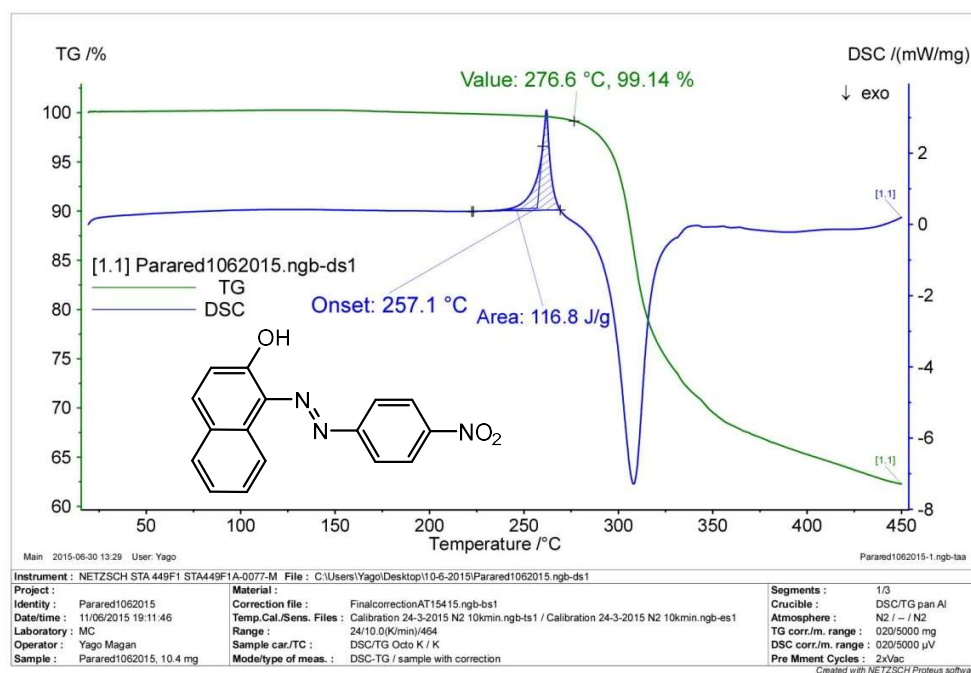


## 5.1.5 Dyes

## Indigo

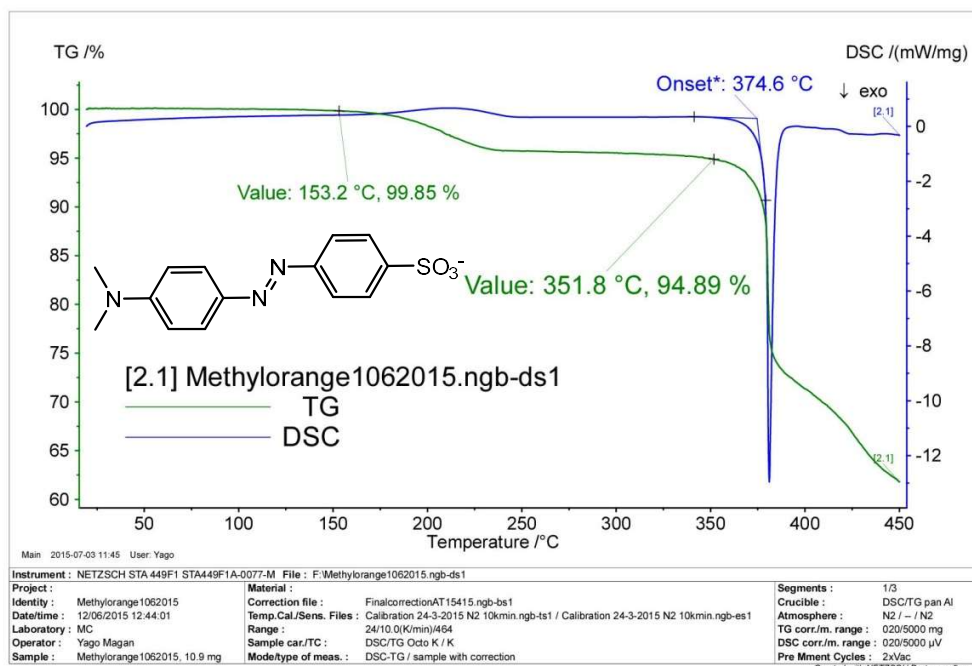


## Para Red

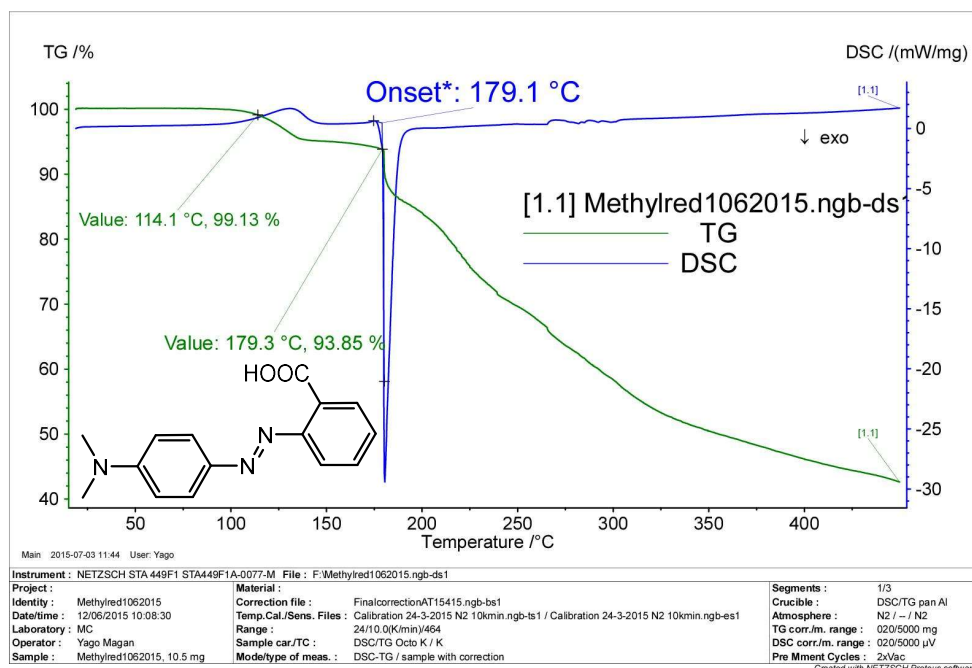




## Methyl orange

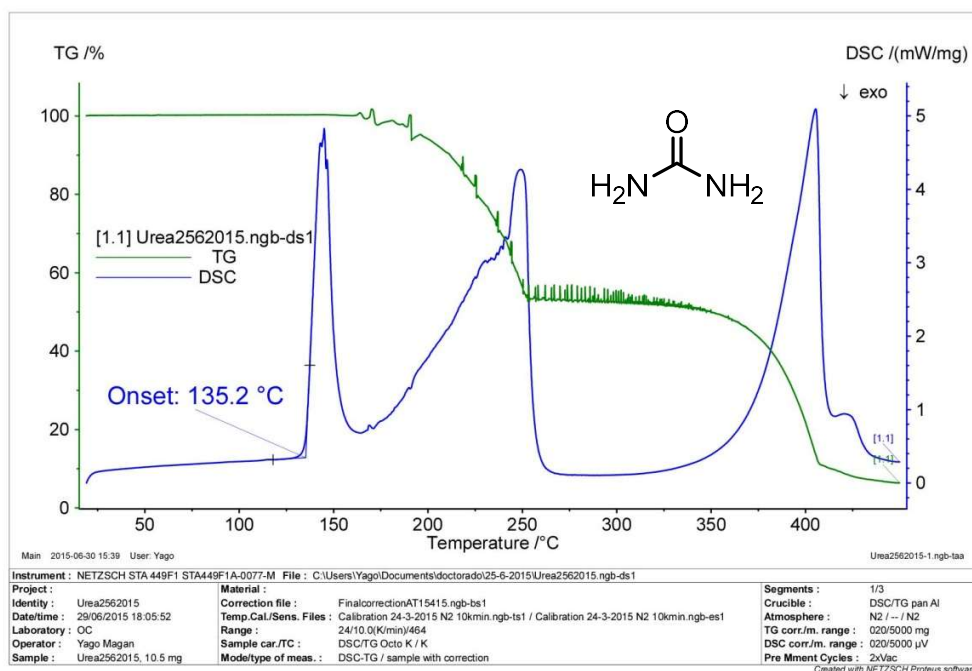


## Methyl red

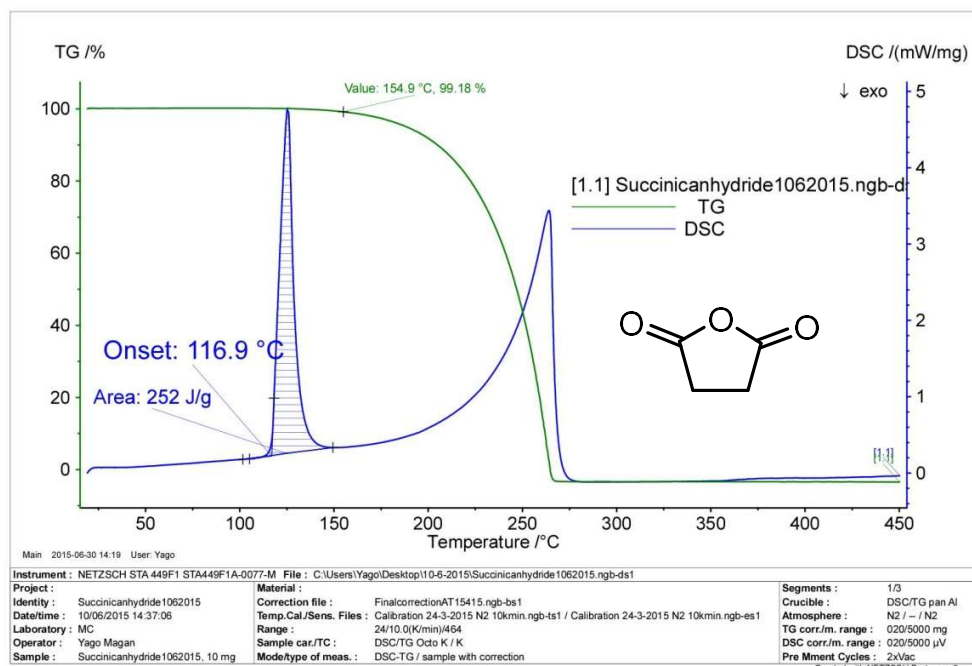


## 5.1.6 Other organic compounds

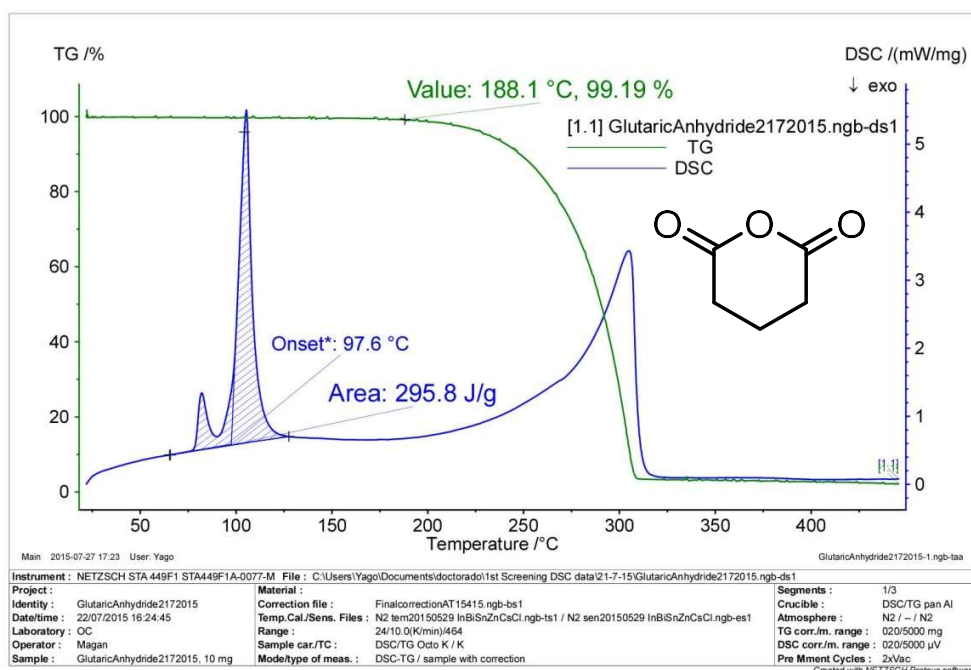
## Urea



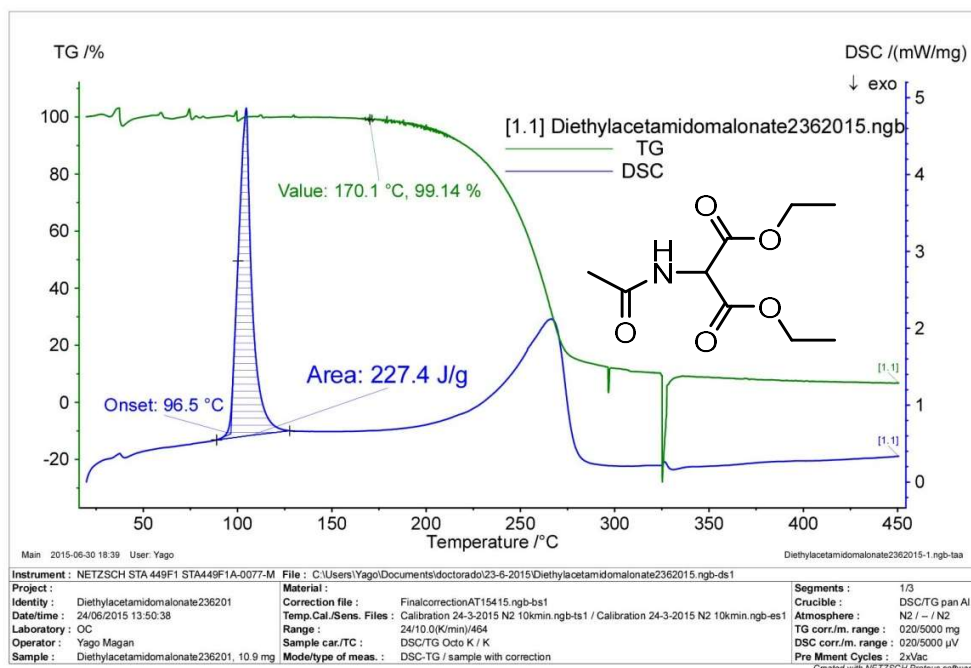
## Succinic anhydride



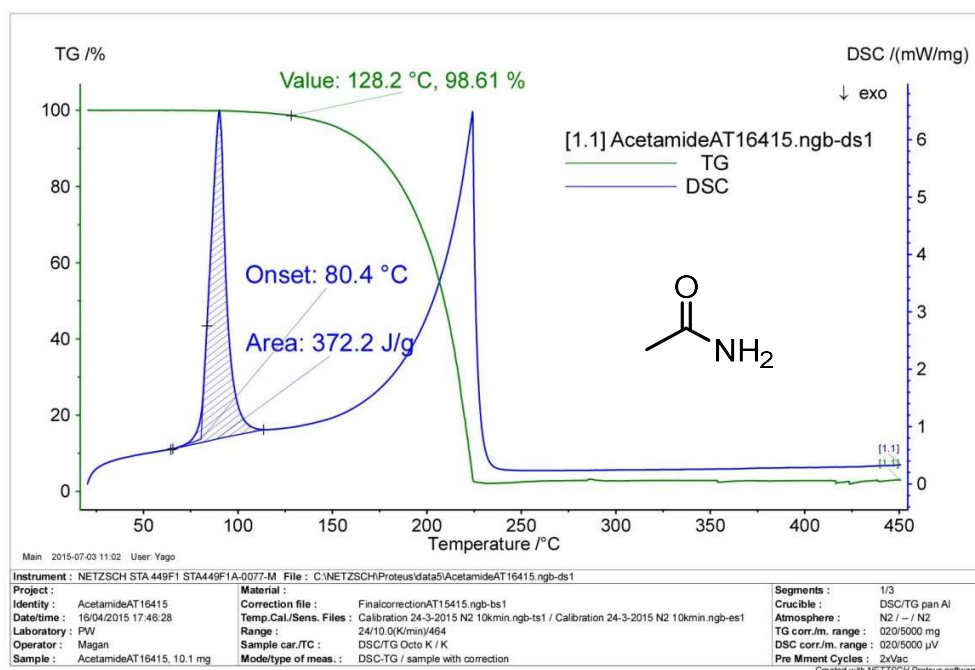
## Glutaric anhydride



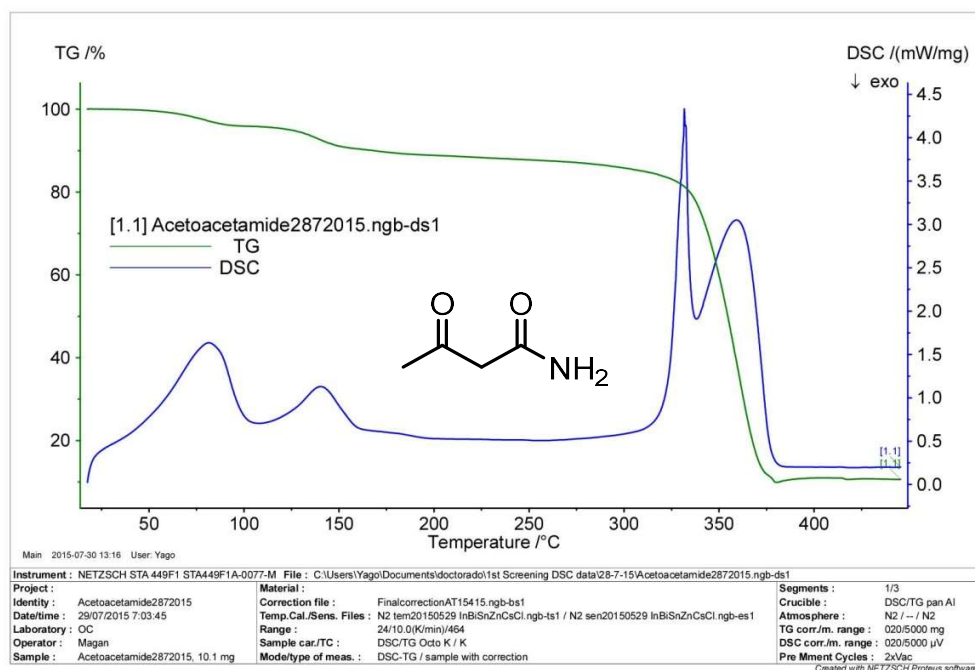
## Diethylacetamidomalonate



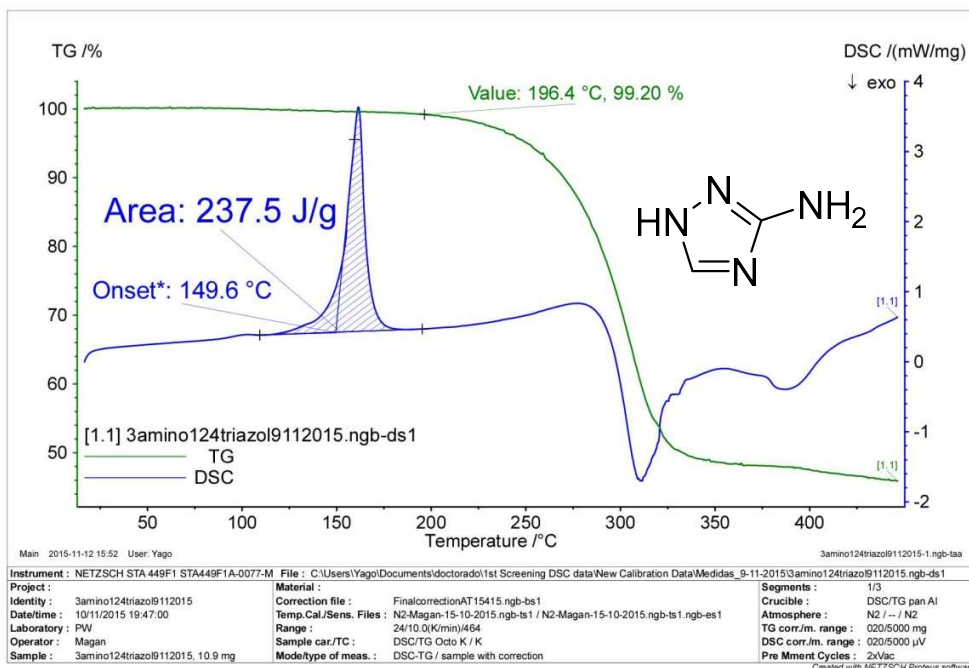
## Acetamide



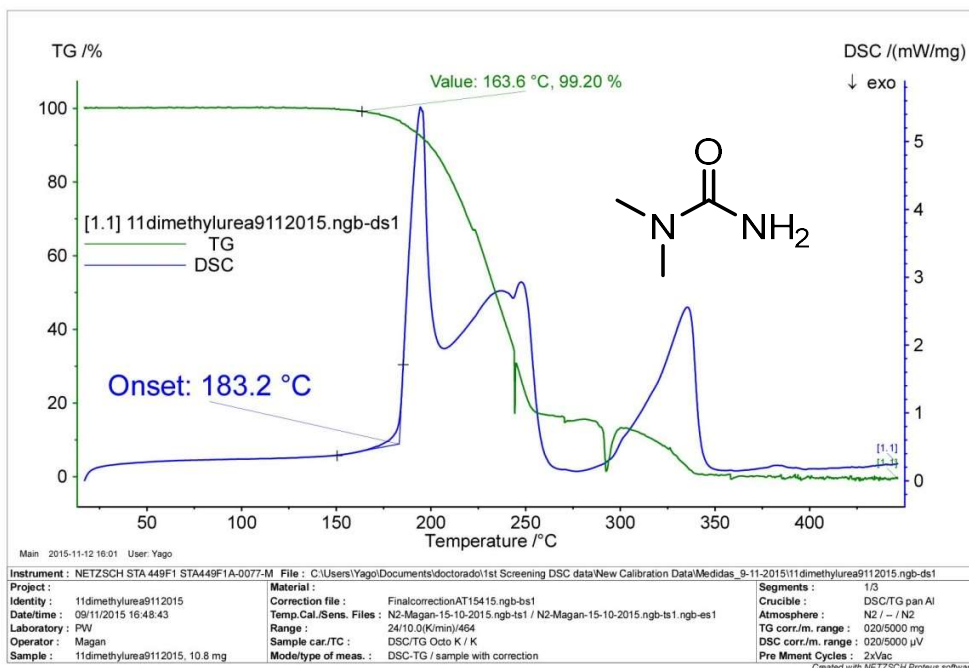
## Acetoacetamide



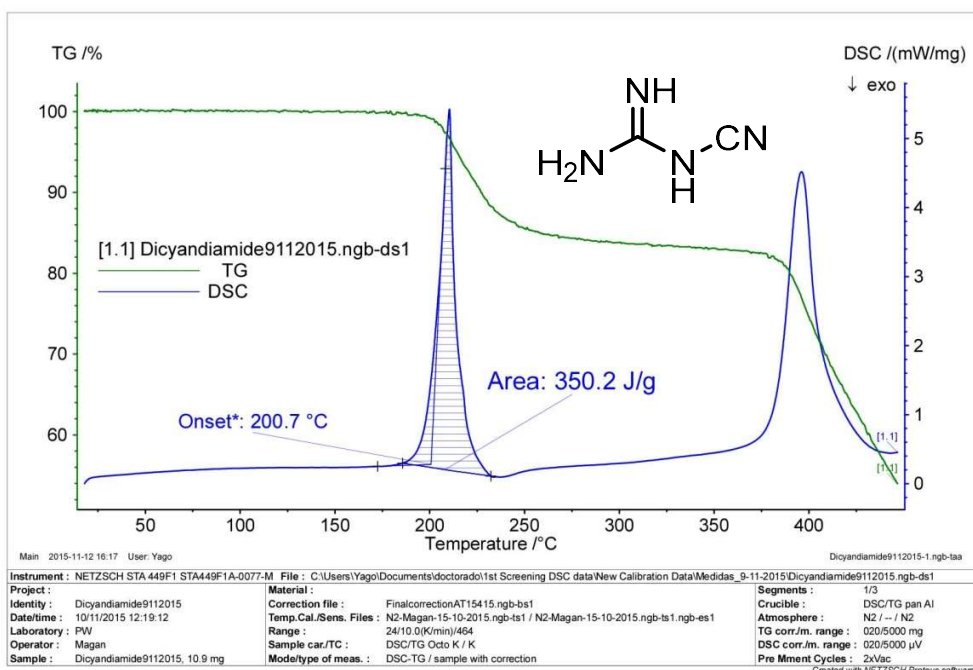
## 3-amino-1,2,4-triazol



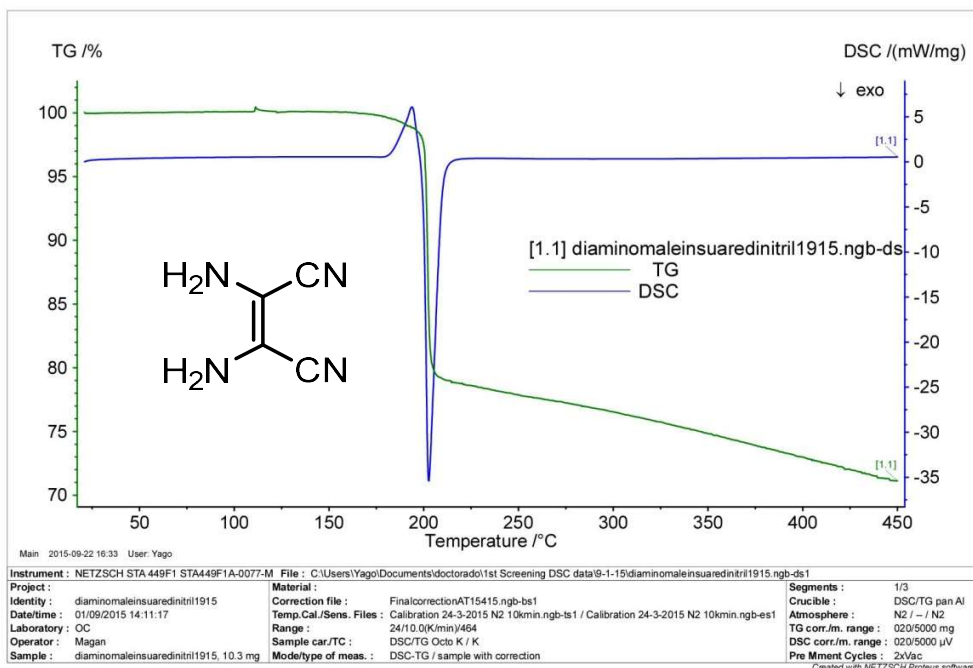
## 1,1-dimethylurea



## Dicyandiamide

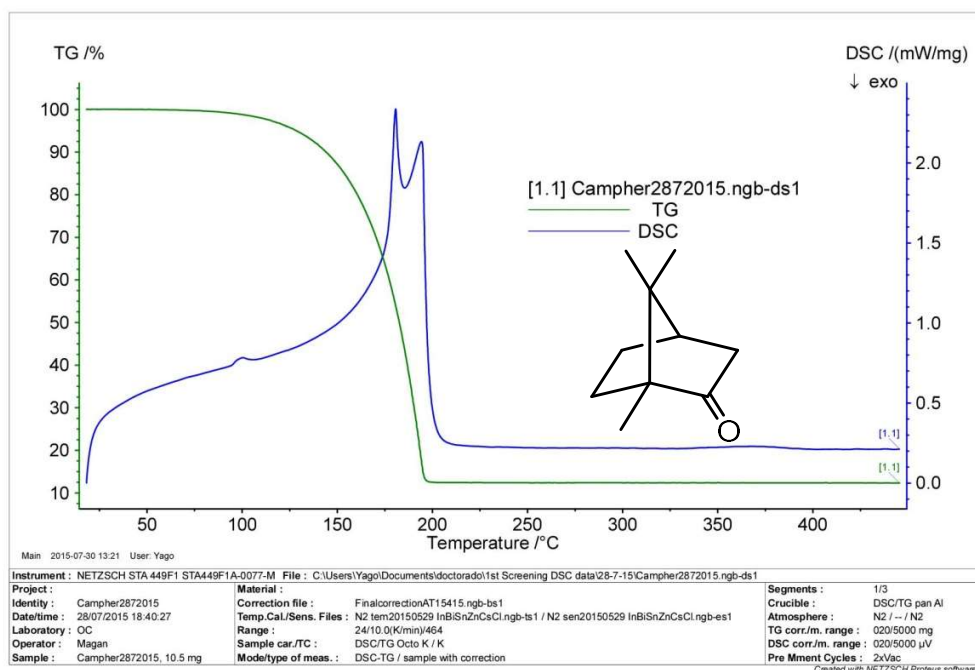


## Diaminomaleonitrile

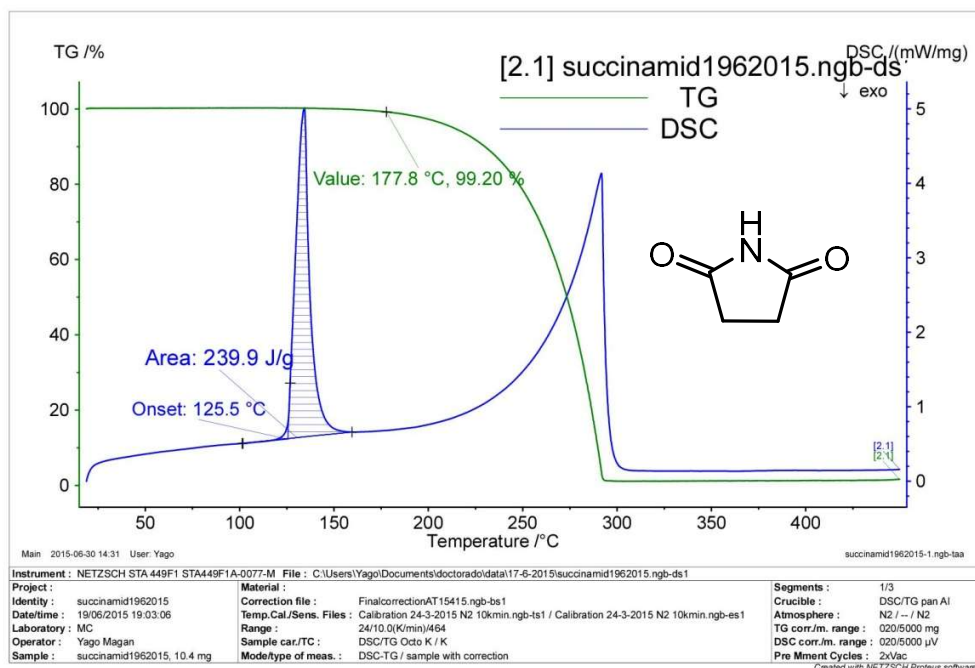




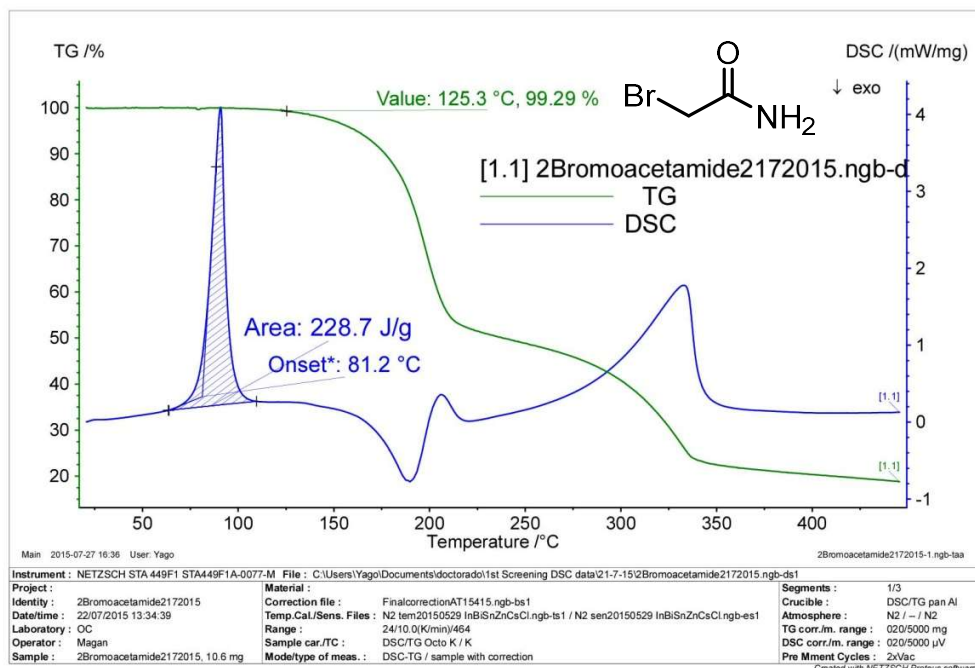
## Campher



## Succinimide



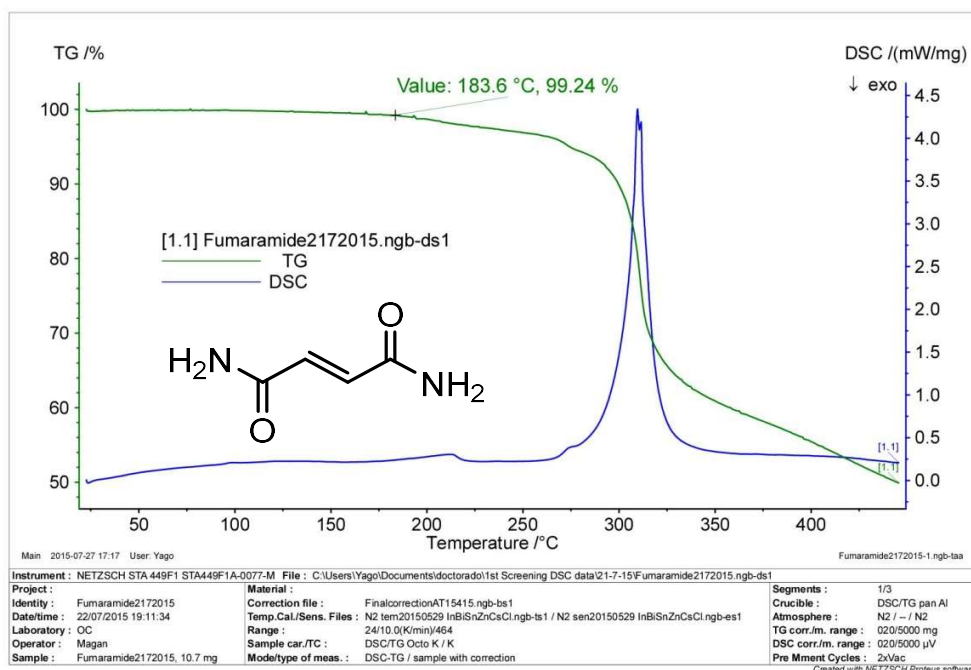
## 2-Bromoacetamide



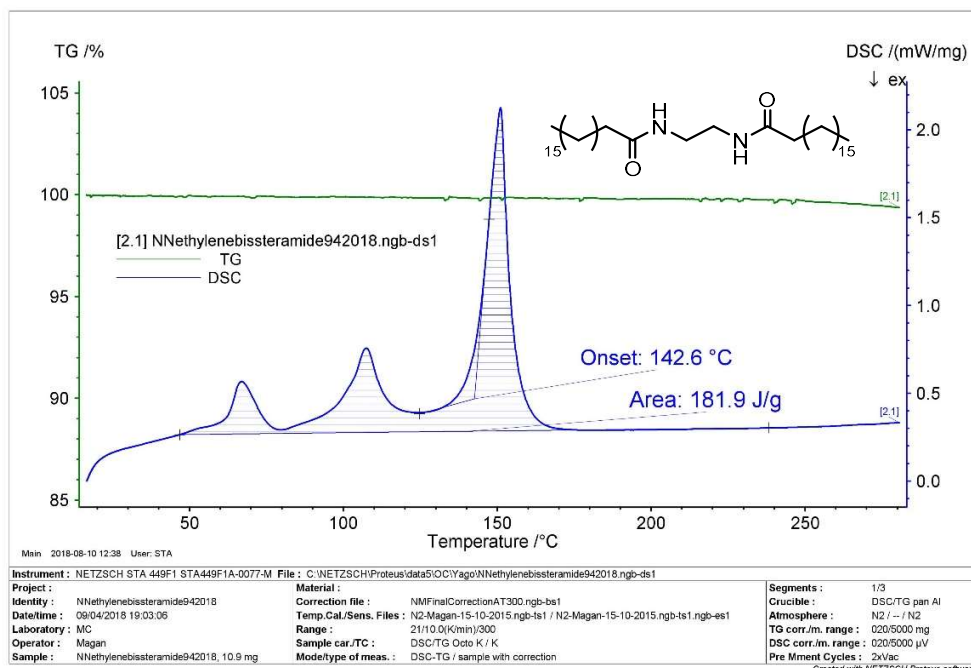




## Fumaramide

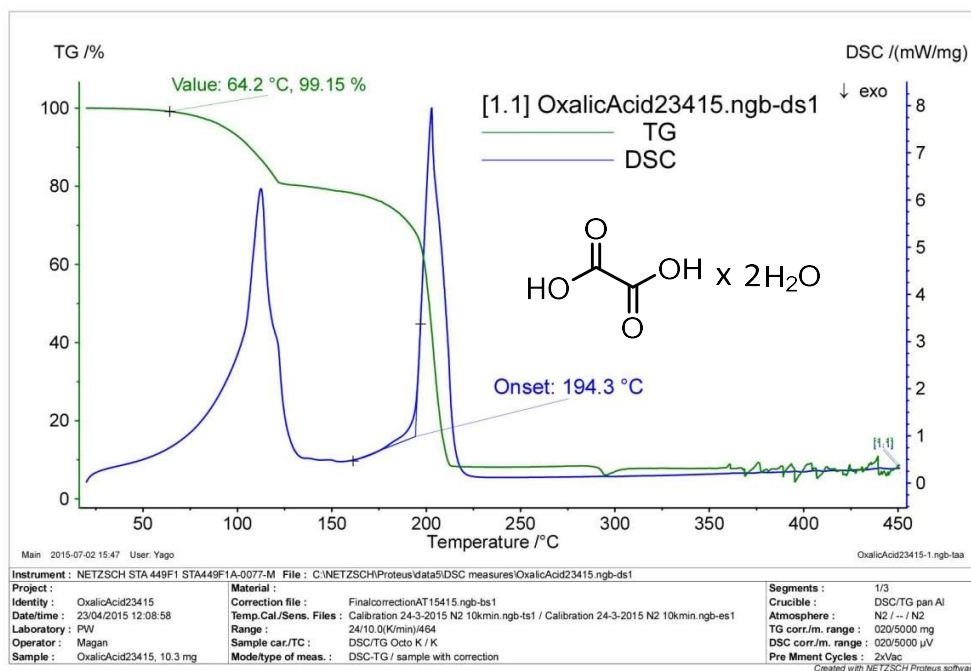


## N,N'-Ethylenebis (stearamide)

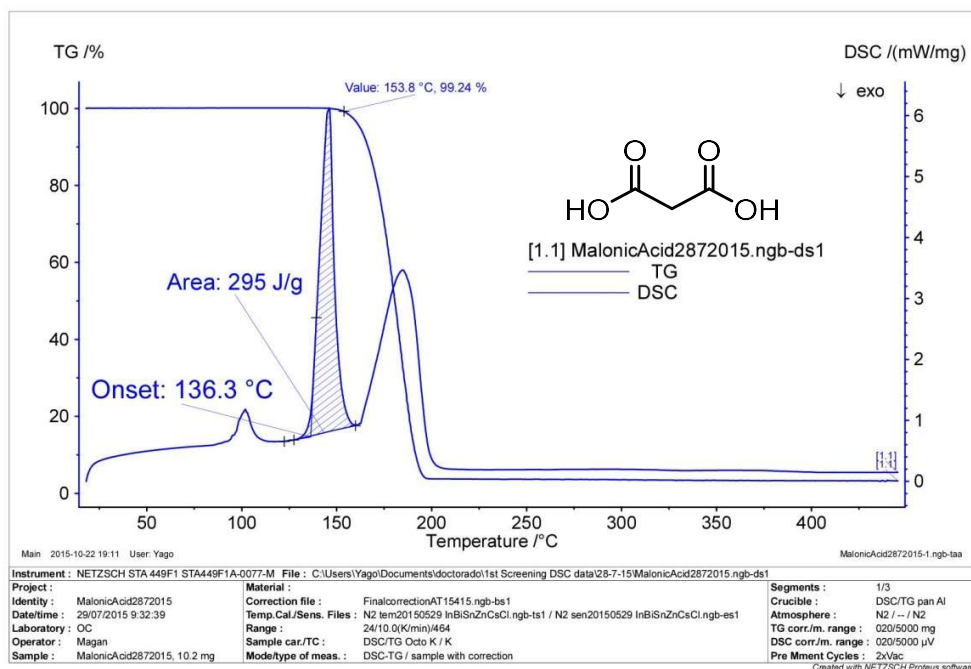


## 5.1.8 Acids and derivatives

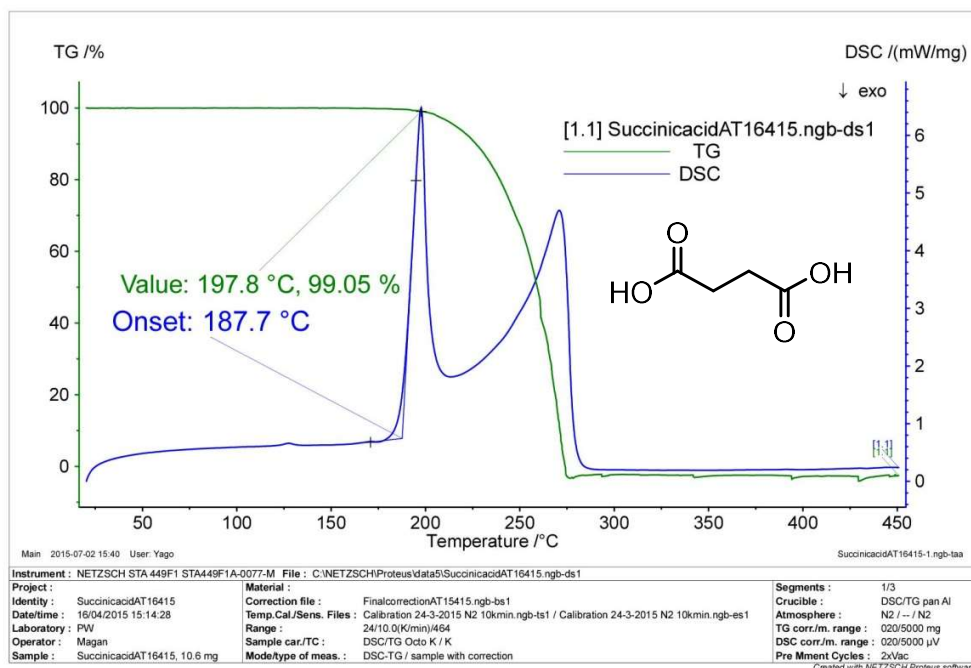
## Oxalic acid dihydrate



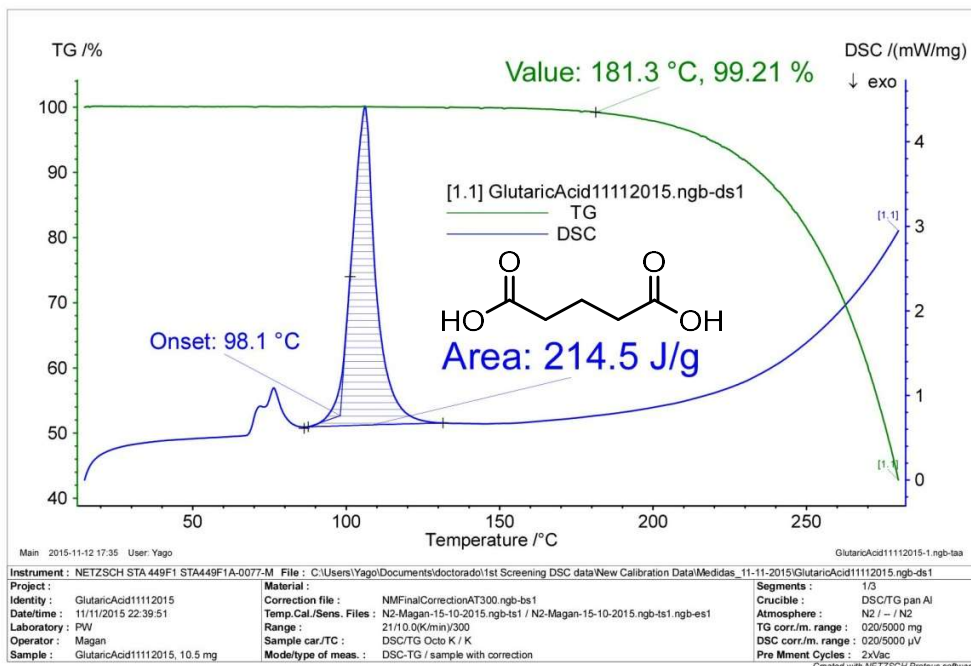
## Malonic acid



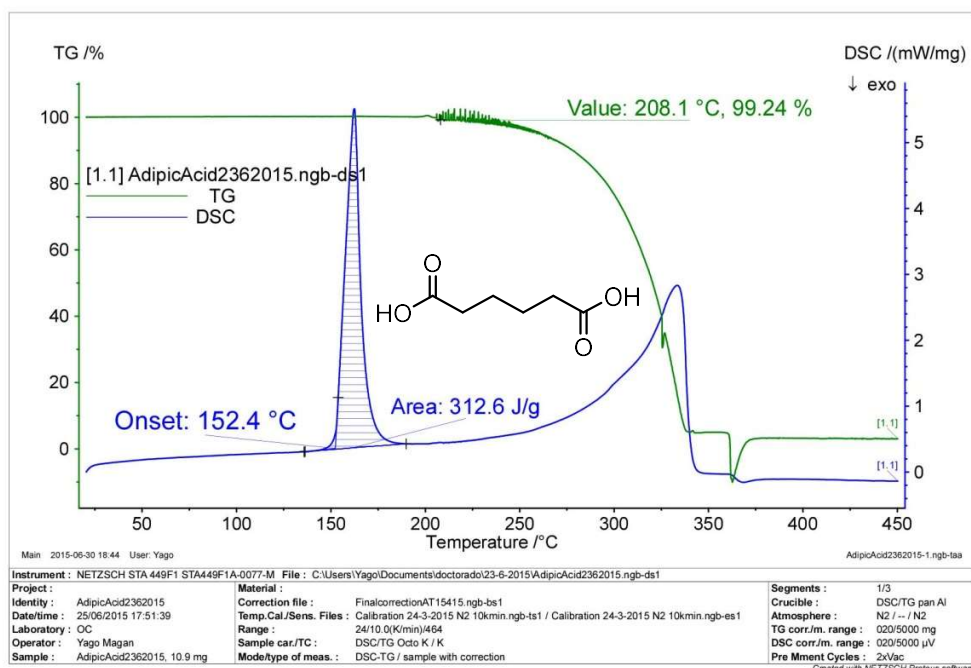
## Succinic acid



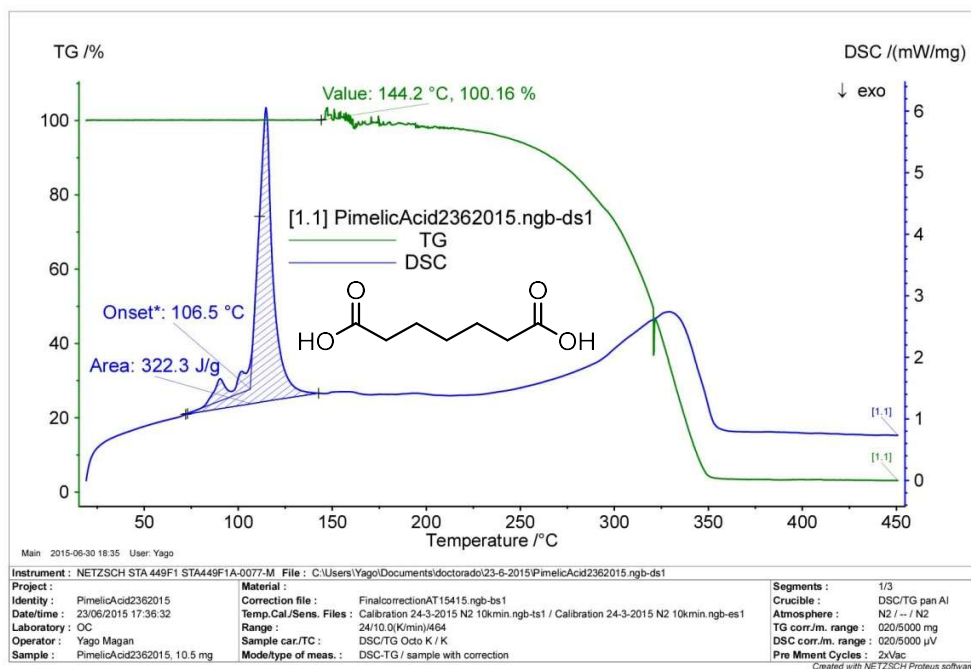
## Glutaric acid



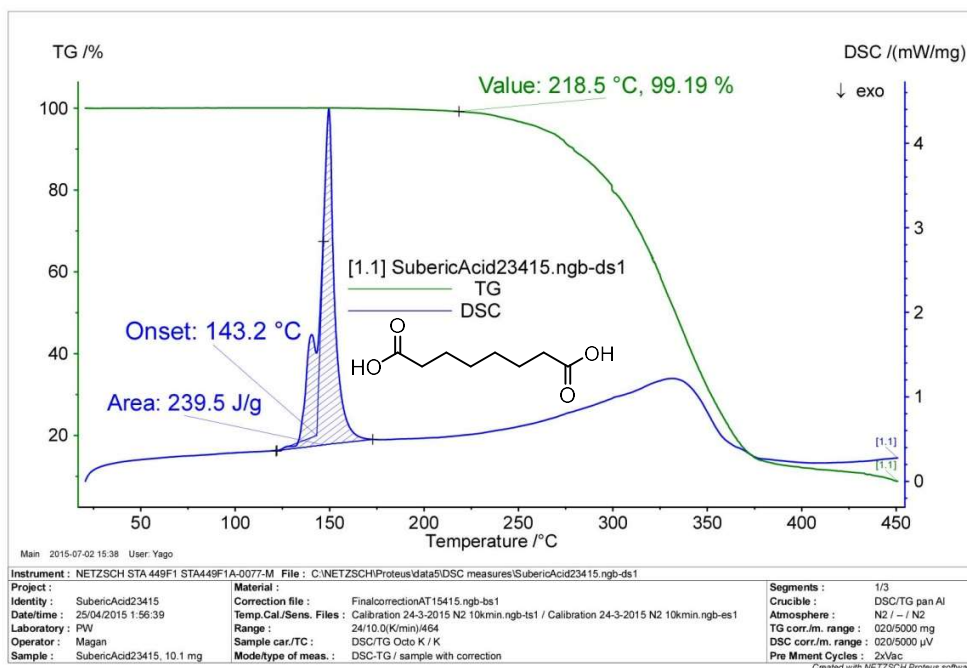
## Adipic Acid



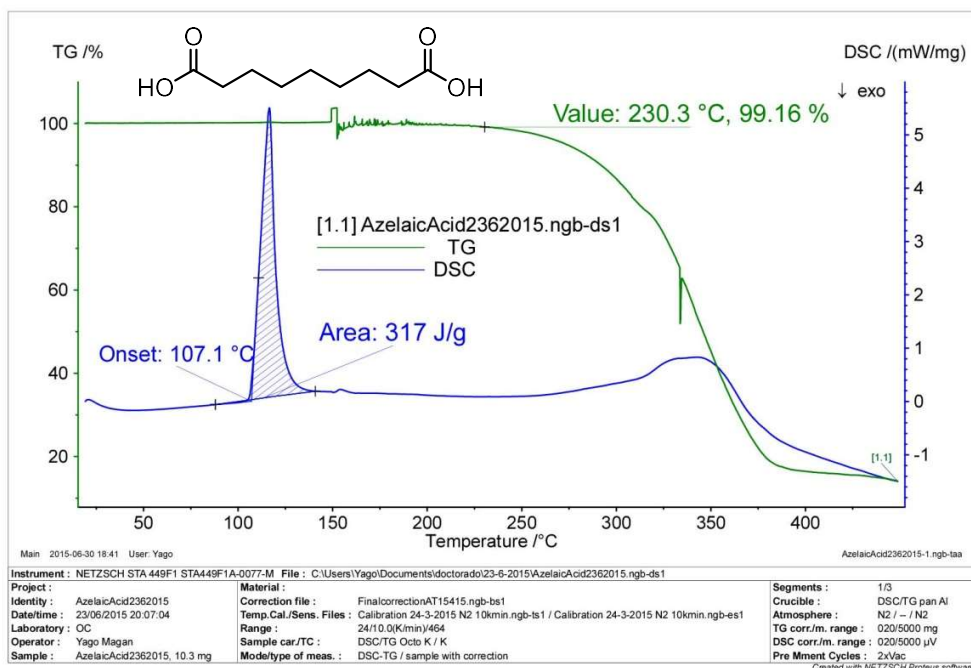
## Pimelic acid



## Suberic acid

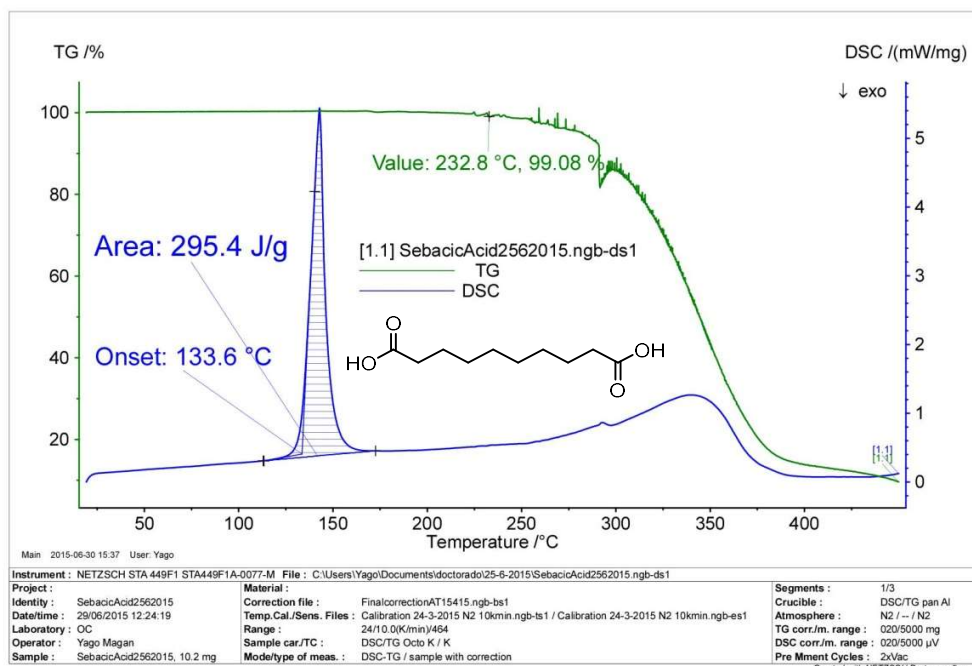


## Azelaic acid

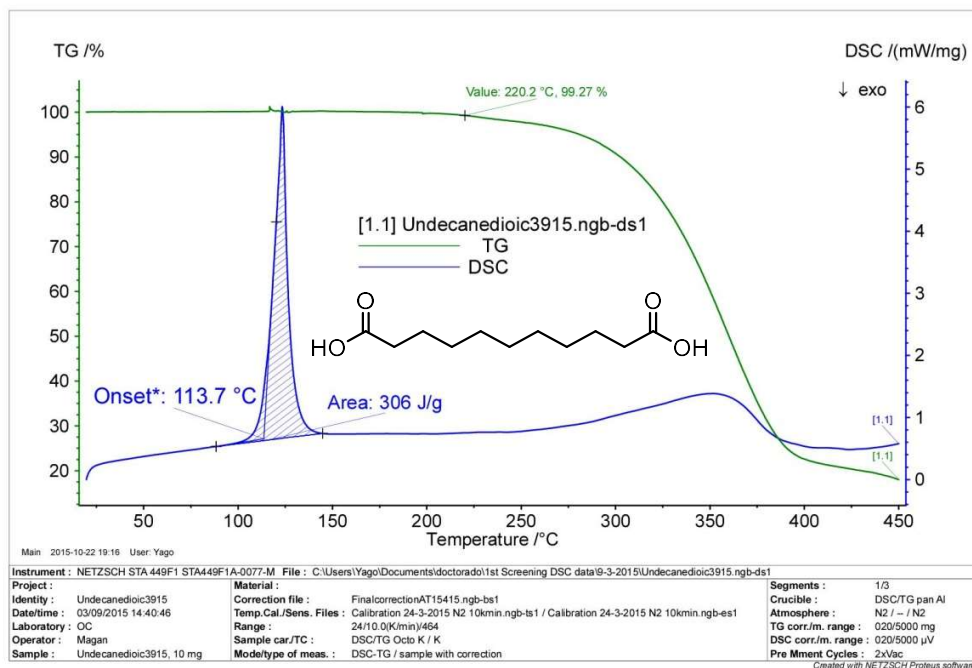




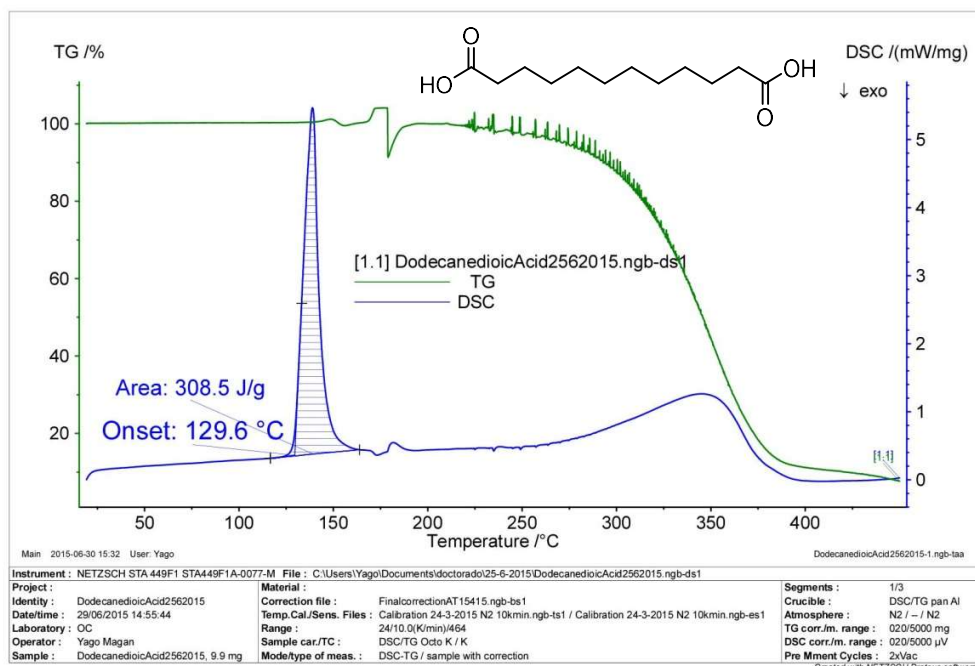
## Sebacic acid



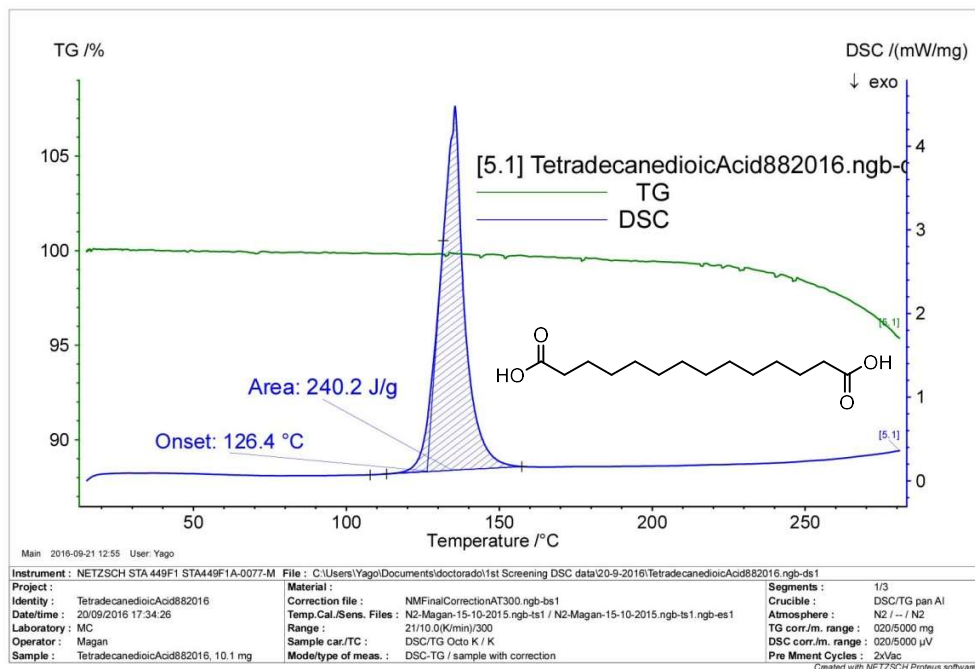
## Undecanedioic acid



## Dodecanedioic acid

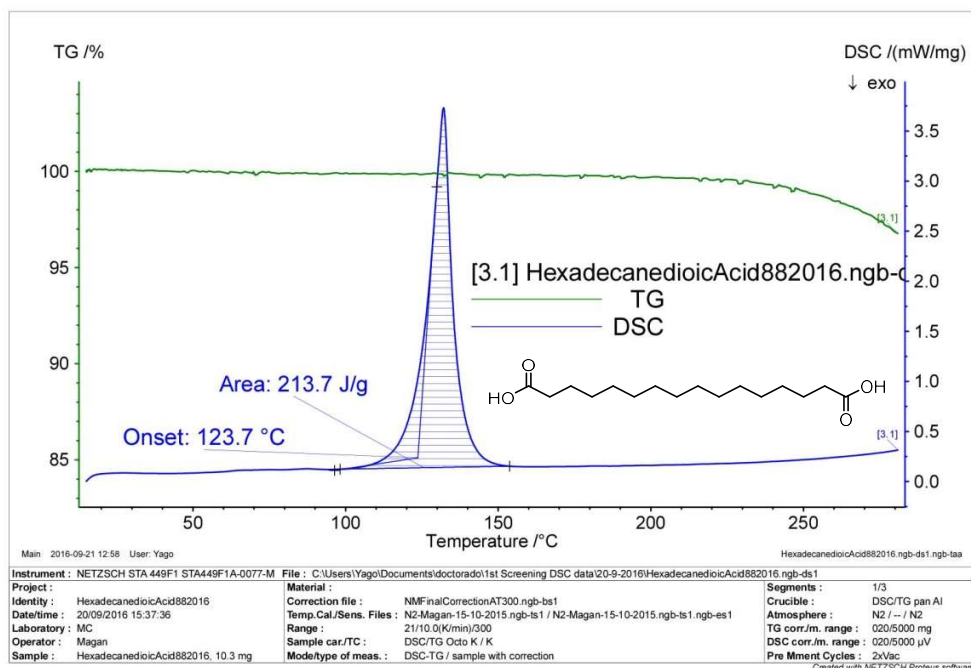


## Tetradecanedioic acid

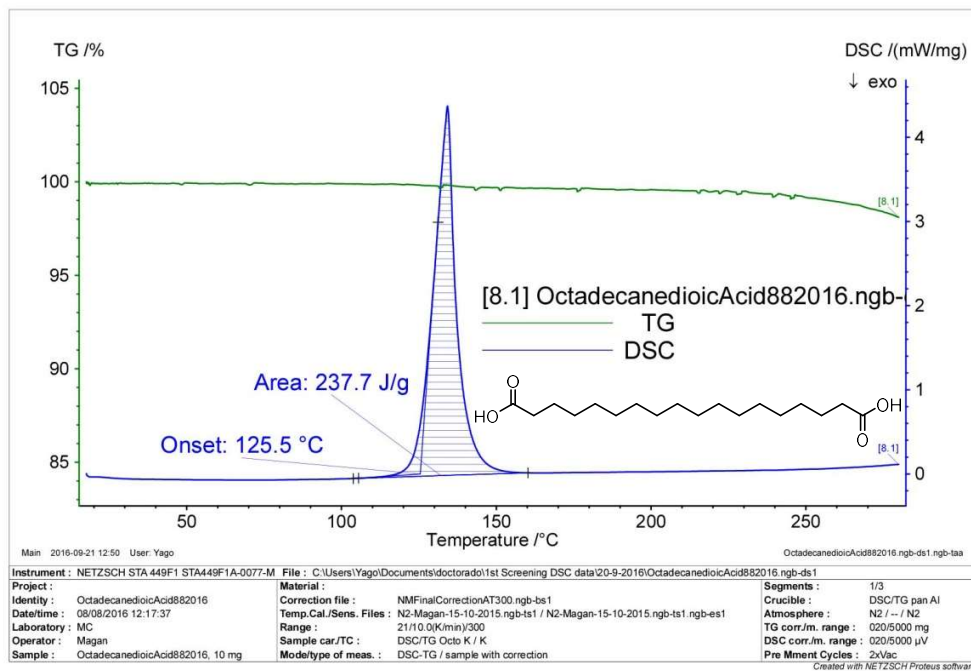




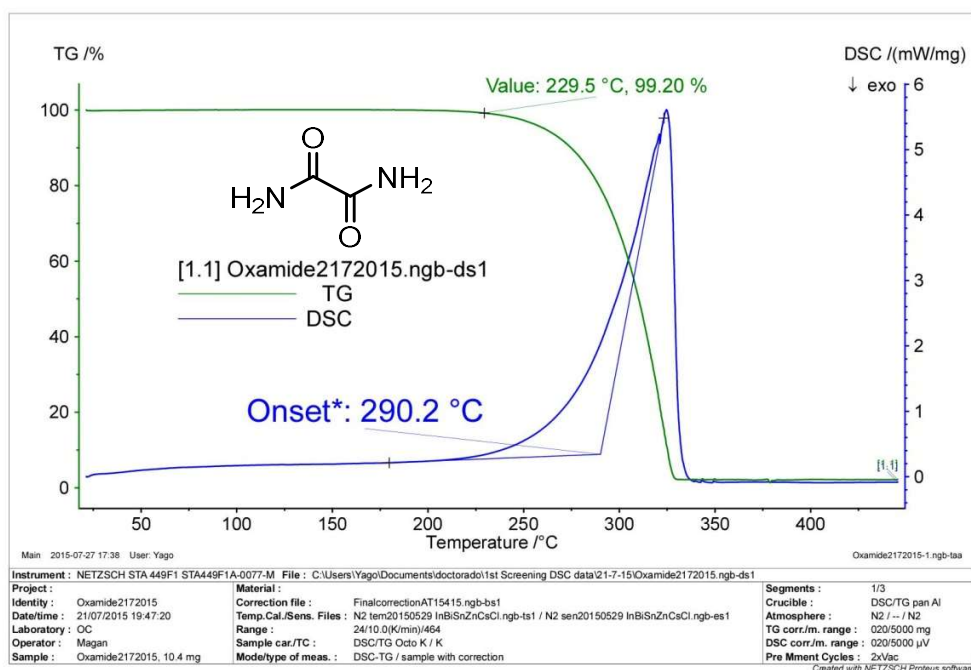
## Hexadecanedioic acid



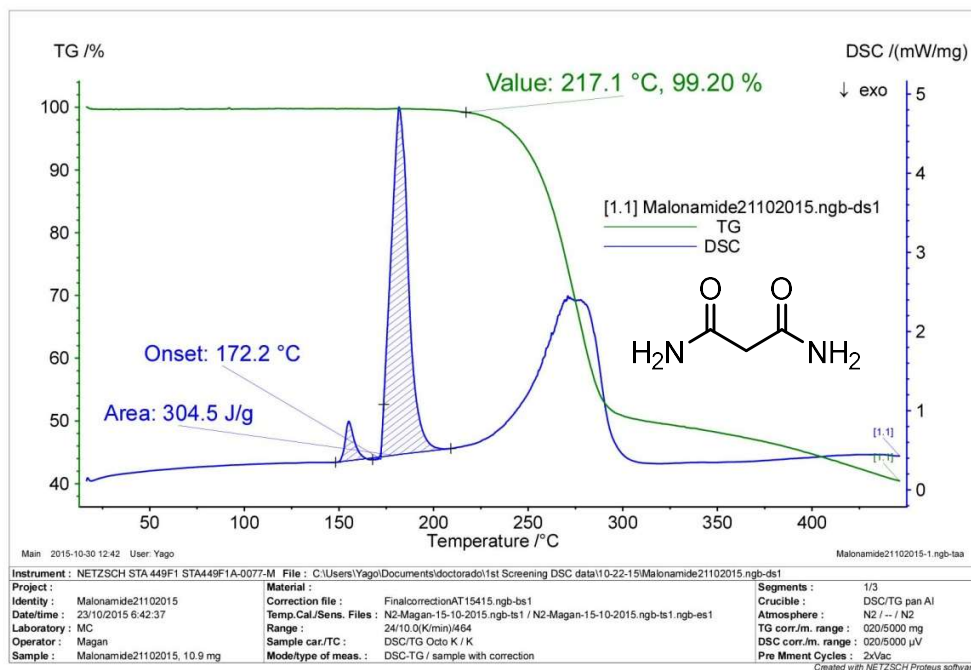
## Octadecanedioic acid



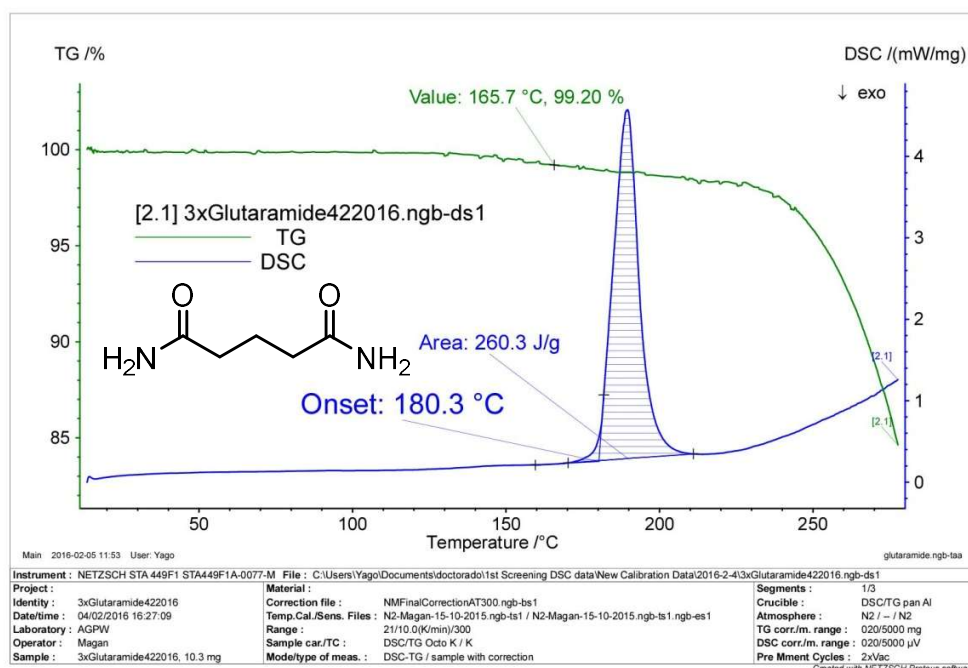
## Oxalamide



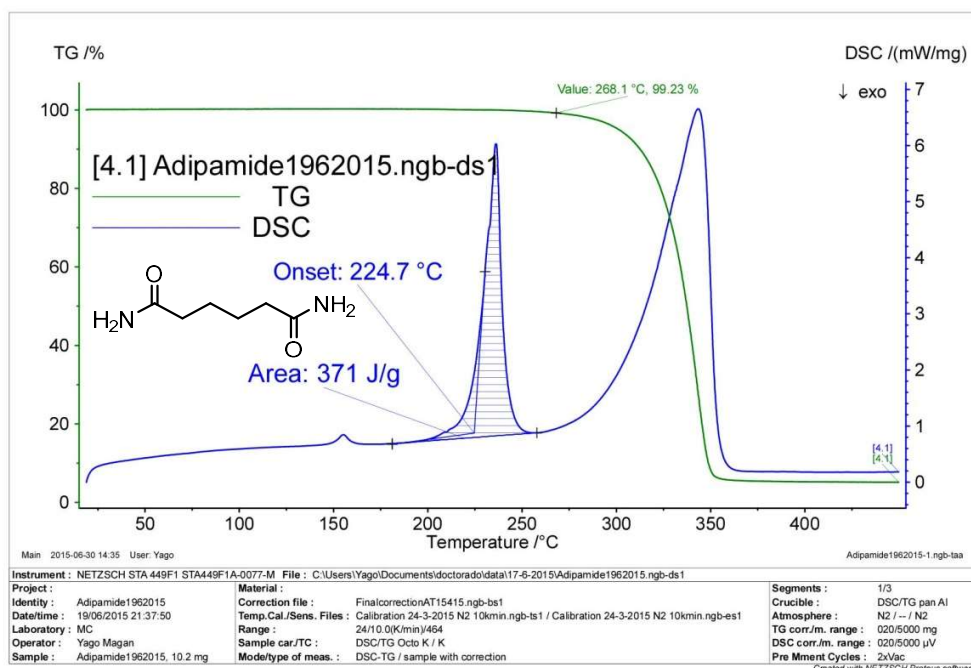
## Malonamide



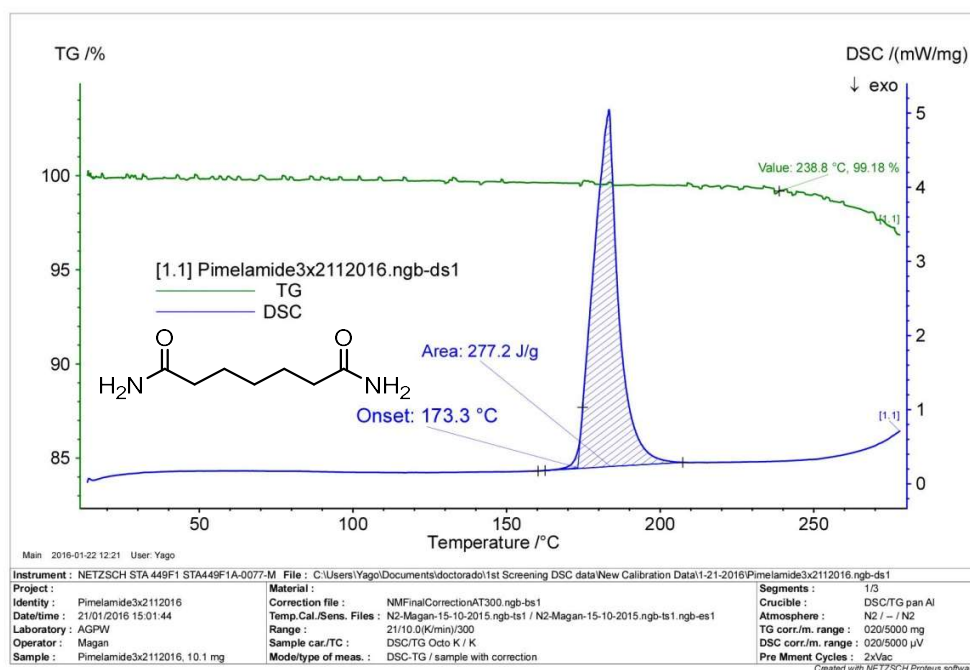
## Glutaramide



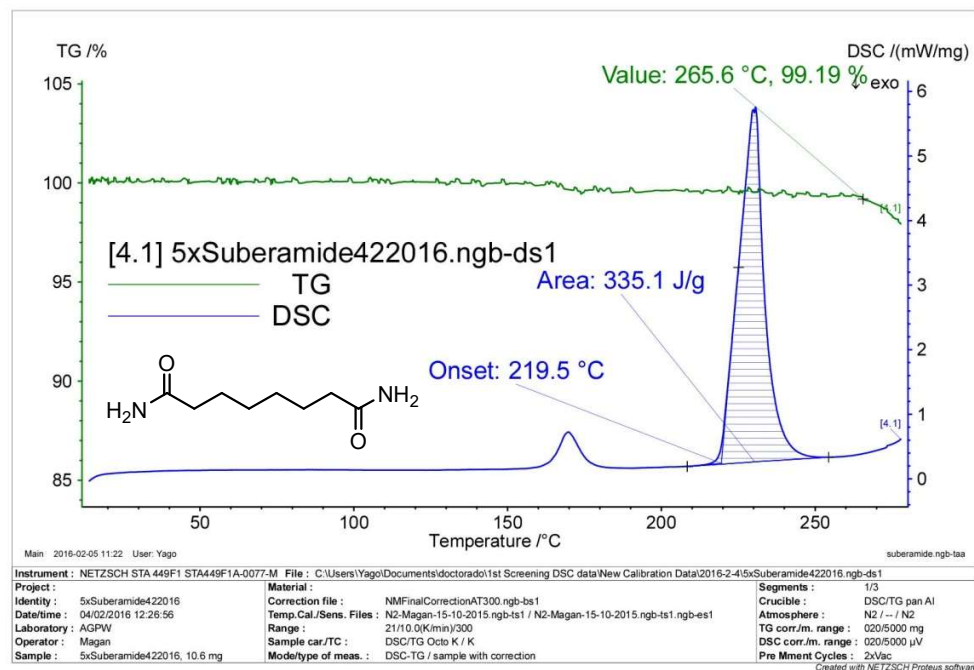
## Adipamide



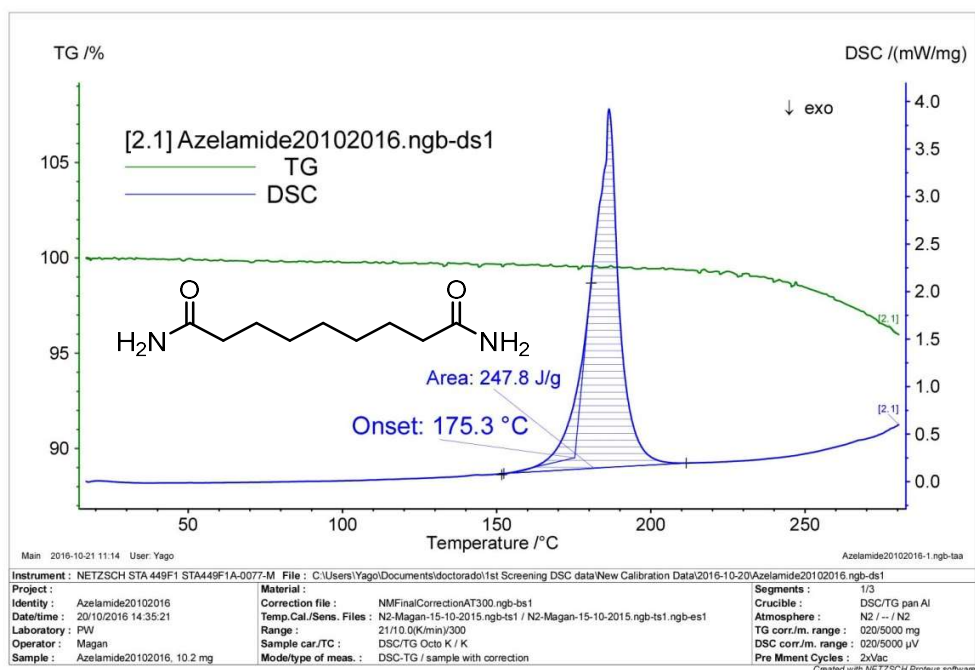
## Pimelamide



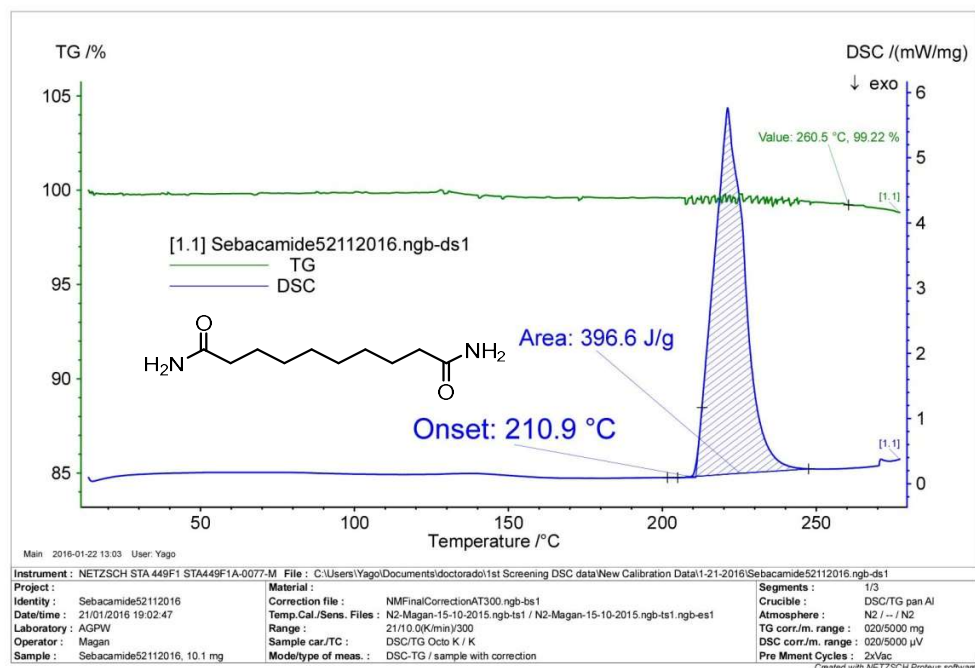
## Suberamide



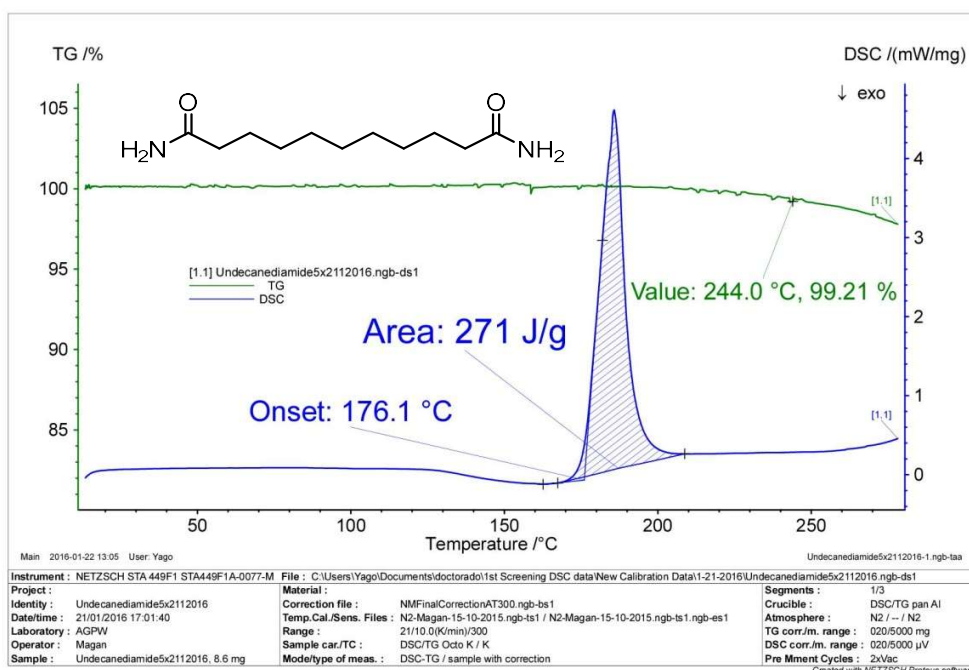
## Azelamide



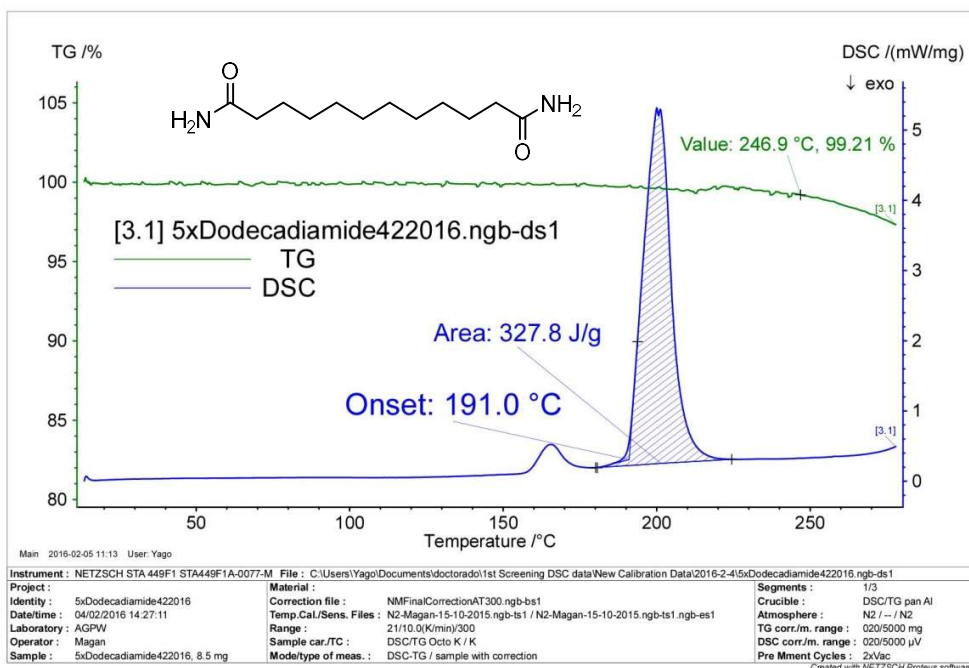
## Sebacamide



## Undecanediamide

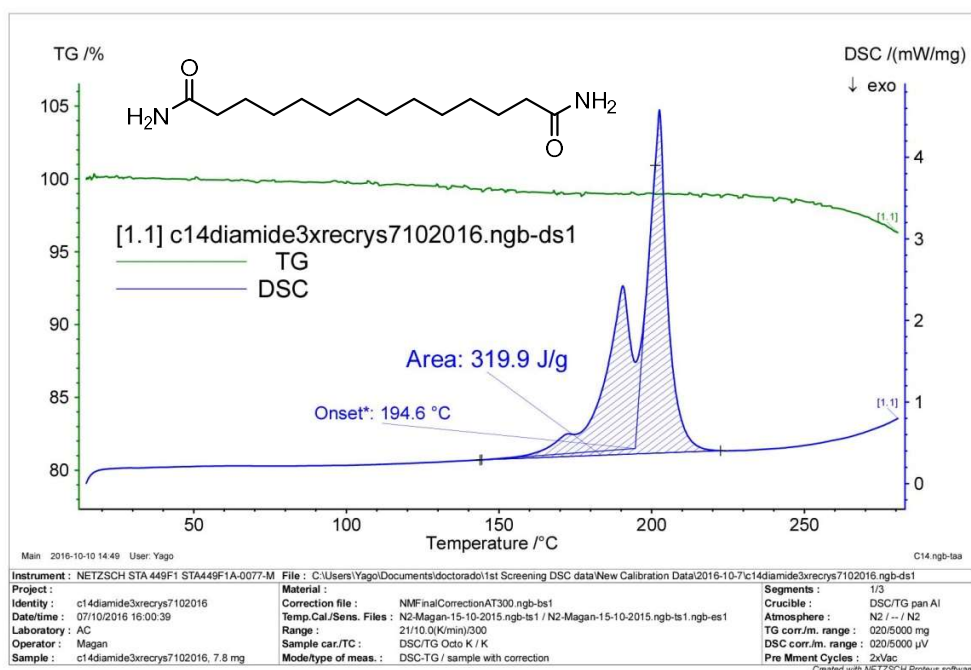


## Dodecanediamide

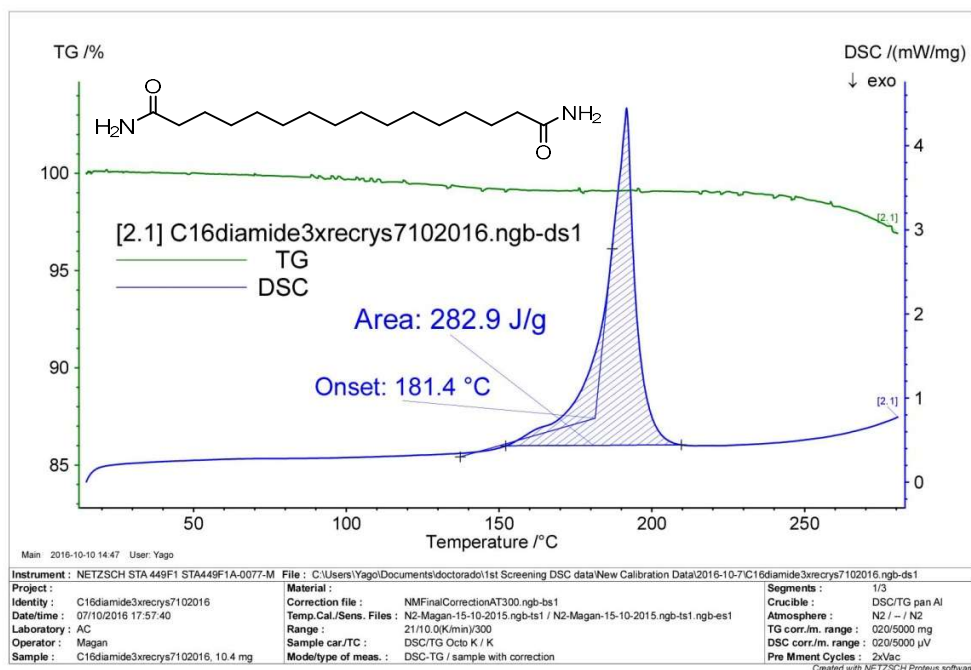




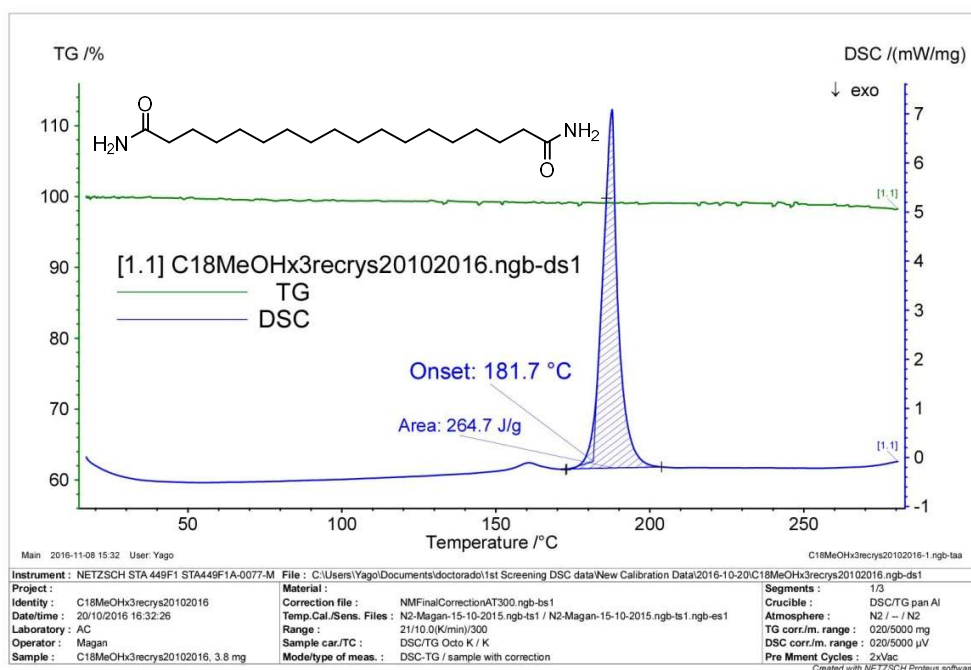
## Tetradecanediamide



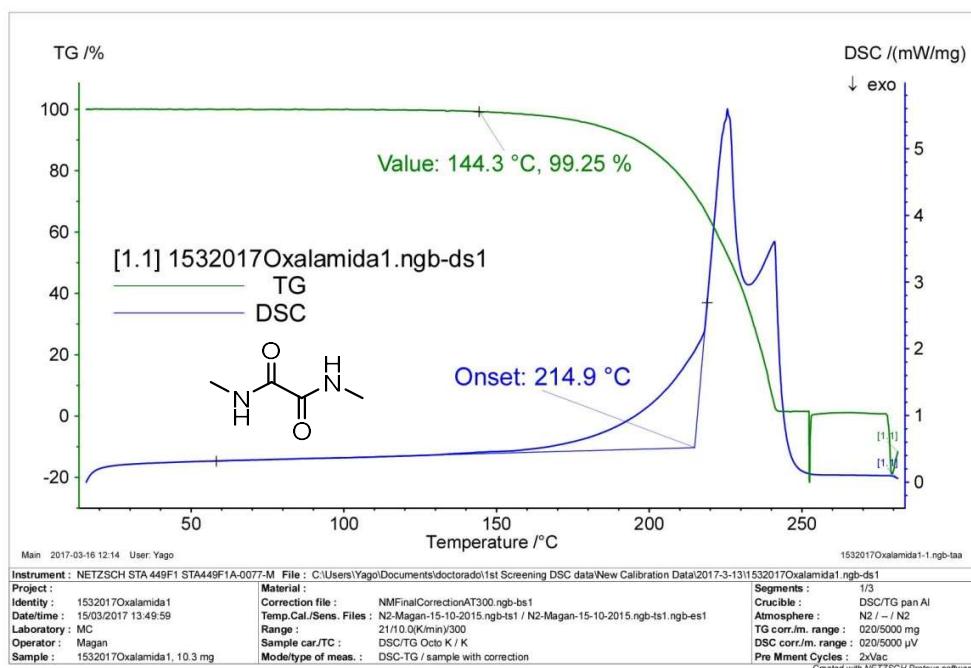
## Hexadecanediamide



## Octadecanediamide

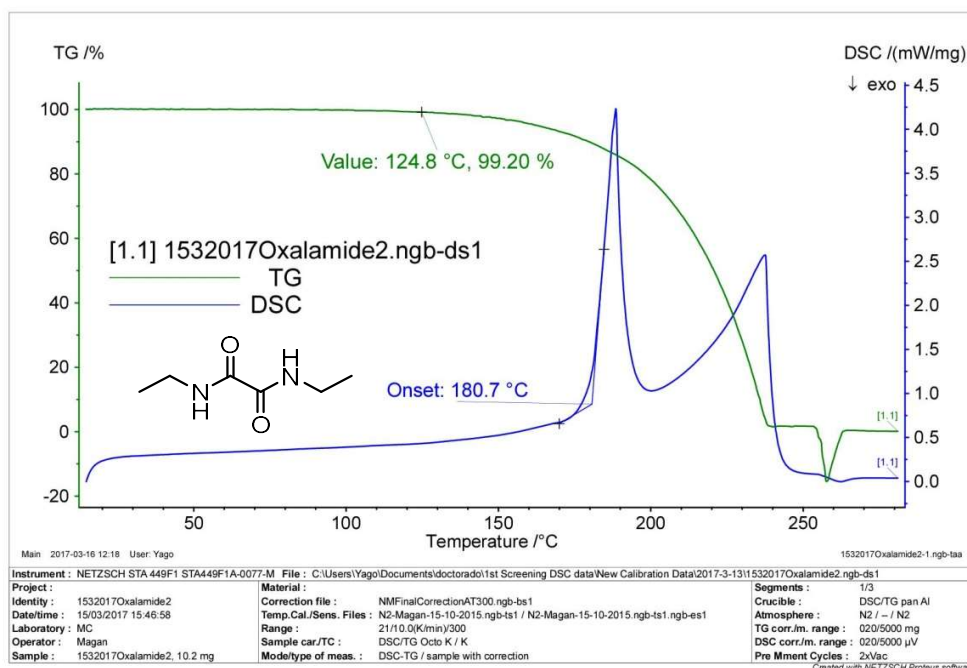


## N,N'-dimethyloxalamide

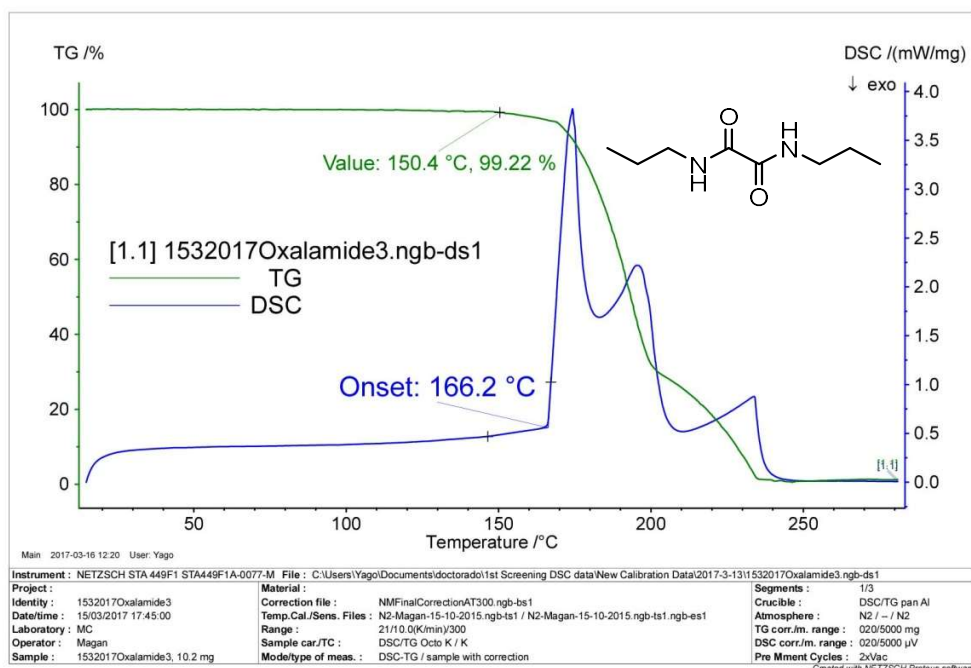




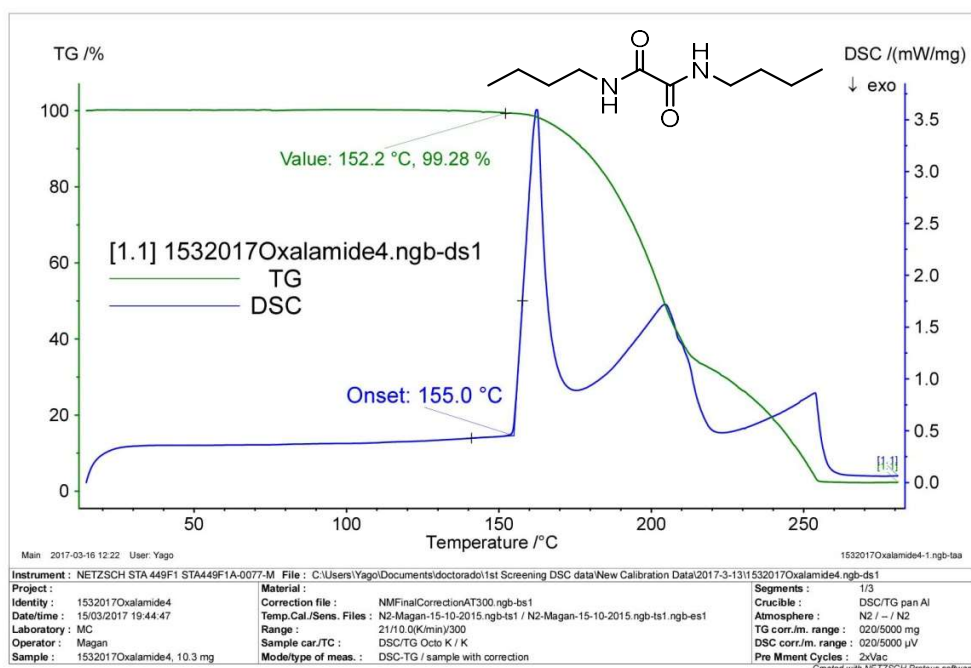
## N,N'-diethyloxalamide



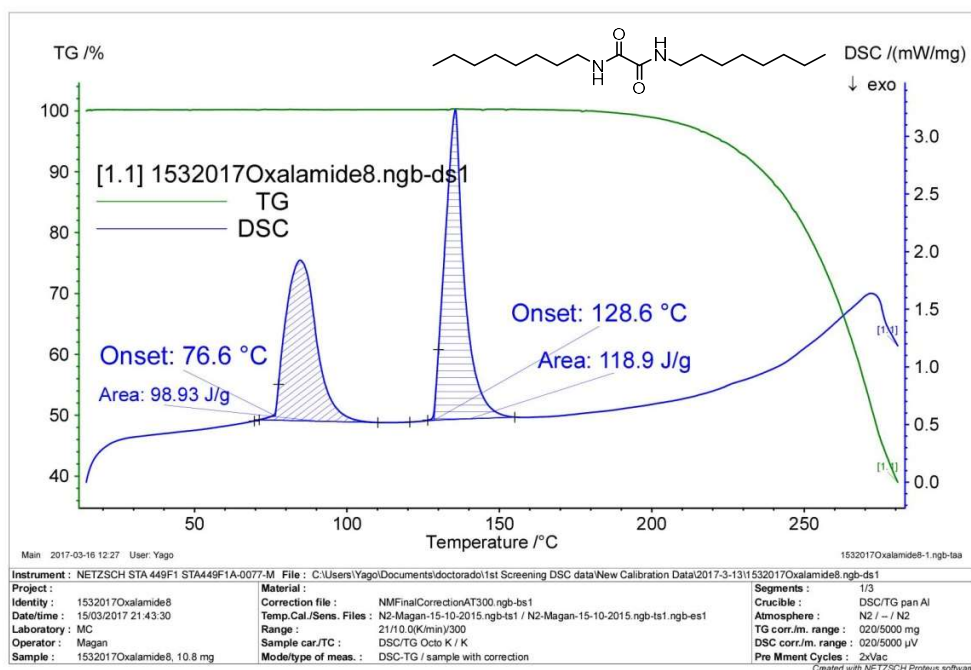
## N,N'-dipropyloxalamide



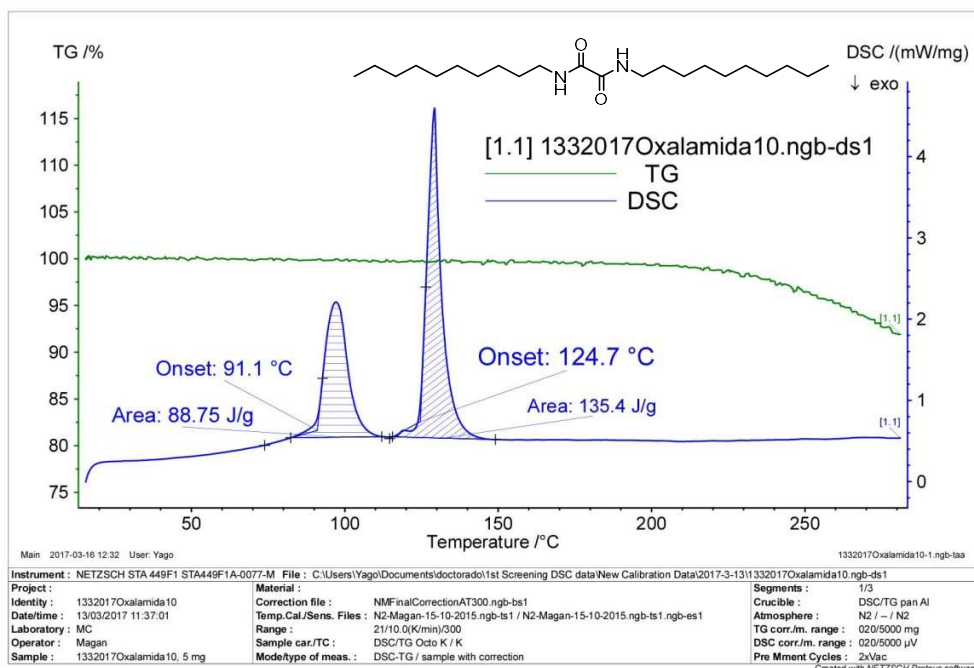
## N,N'-dibutyloxalamide



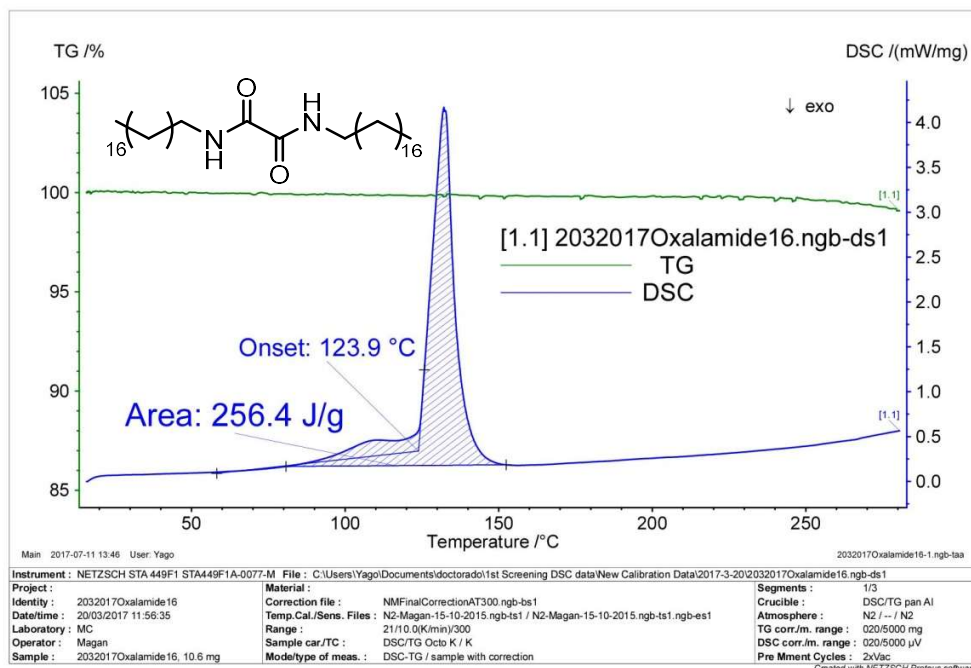
## N,N'-dioctyloxalamide



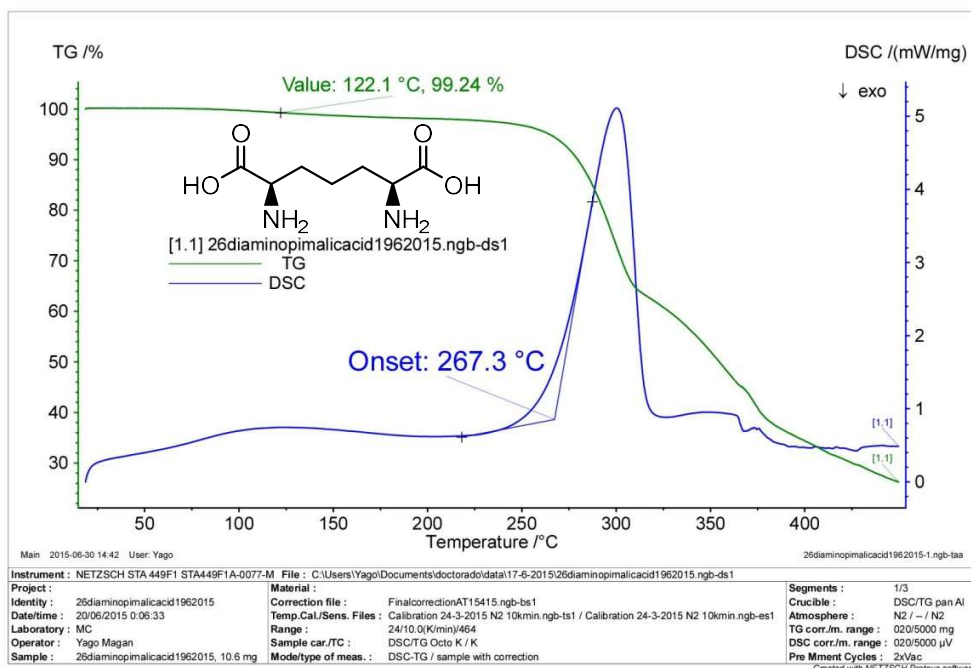
## N,N'-didecyloxalamide



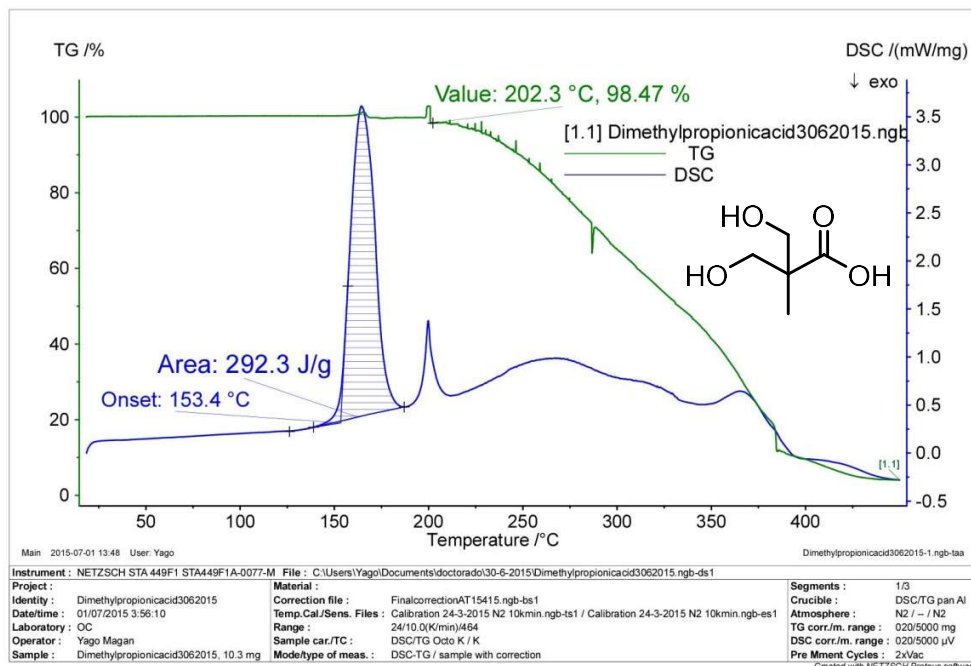
## N,N'-dioctadecyloxalamide



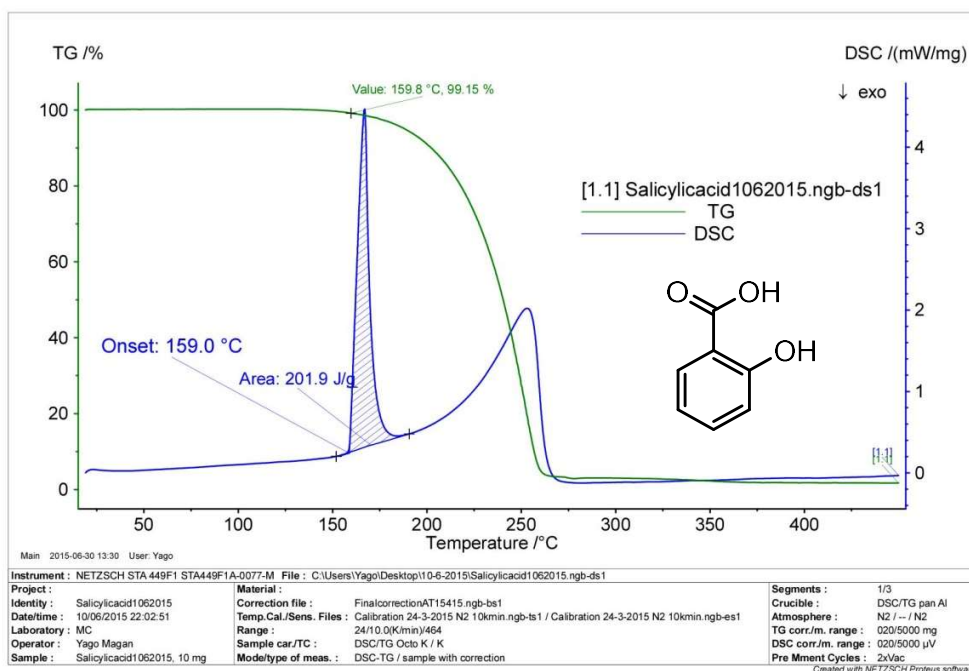
## Diaminopimelic acid



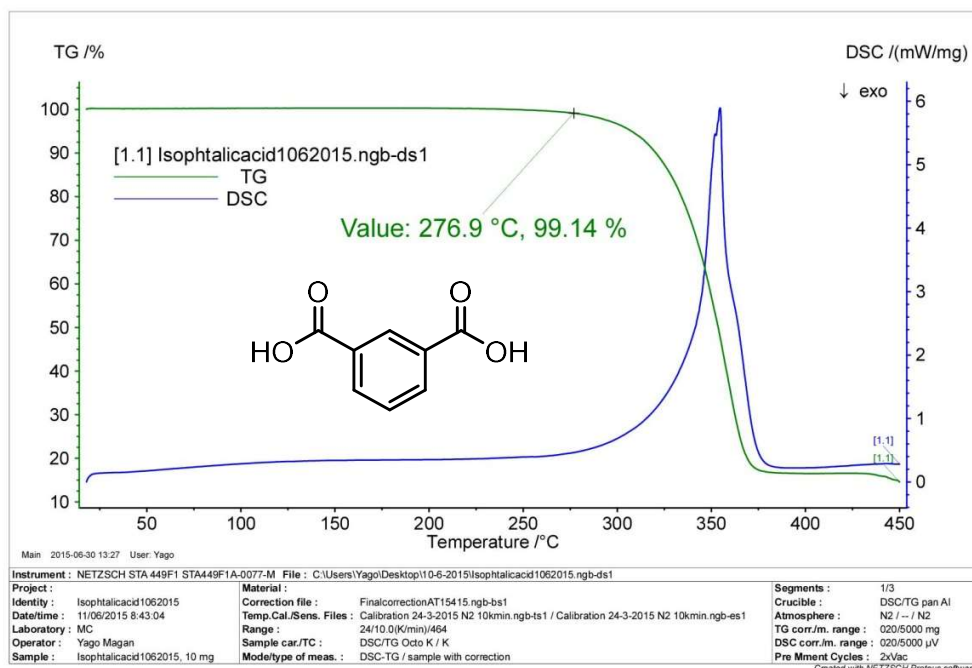
## Dimethylpropionic acid



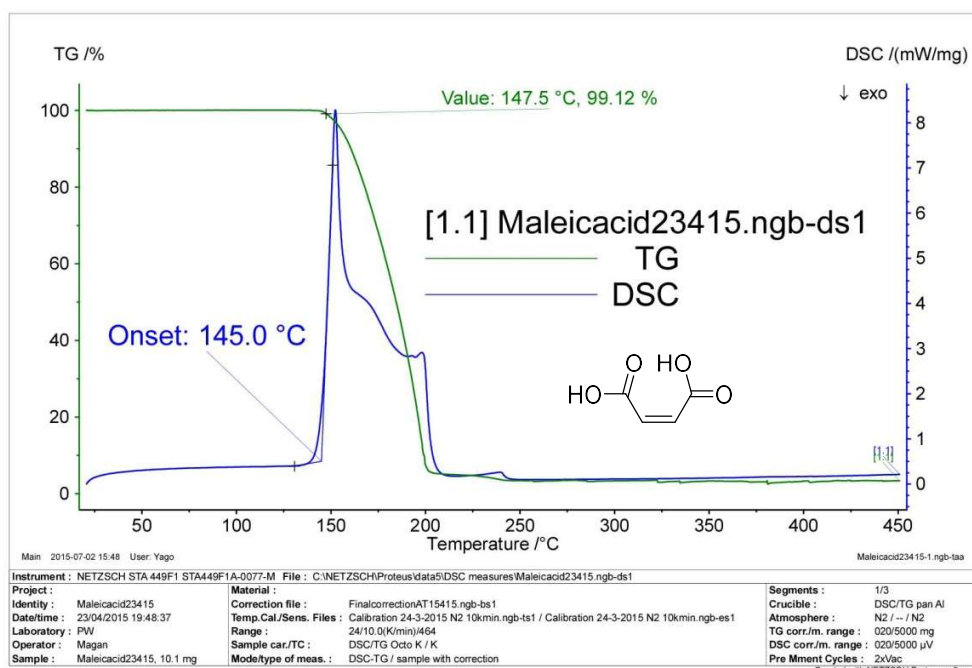
## Salicylic acid



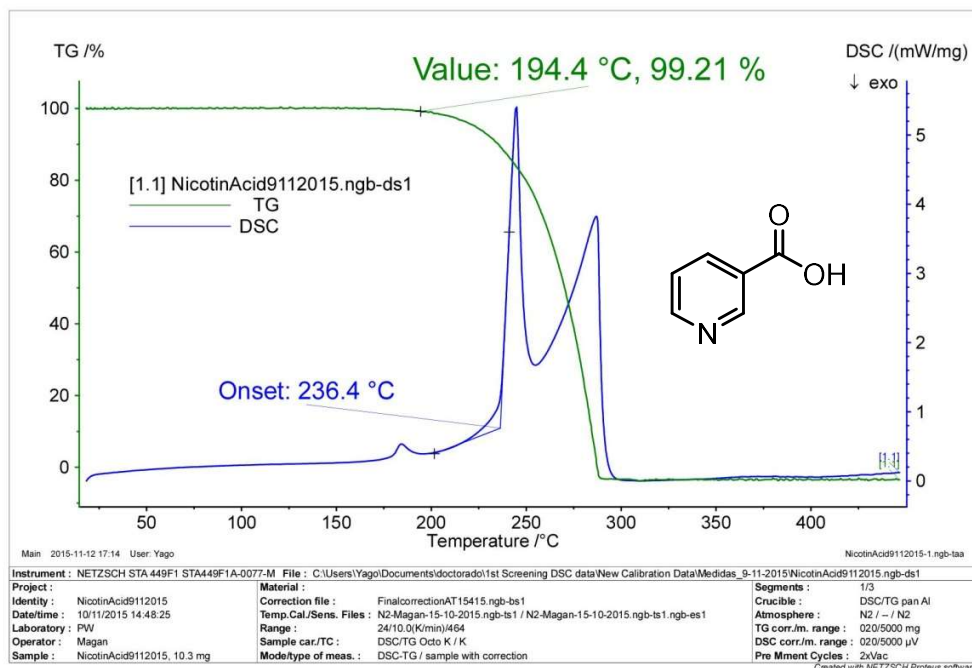
## Isophthalic acid



## Maleic acid

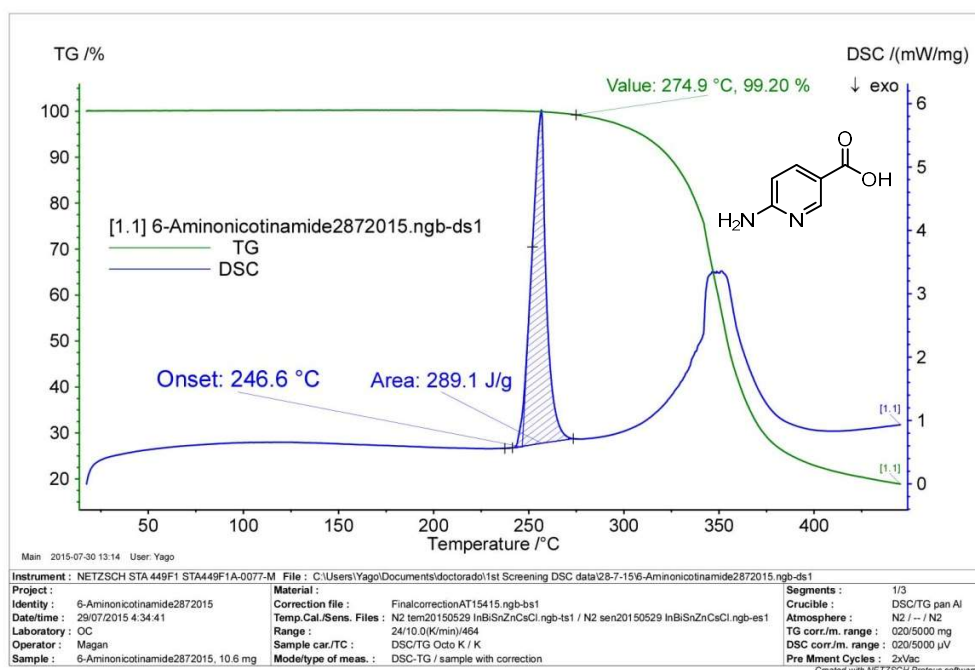


## Nicotinic acid

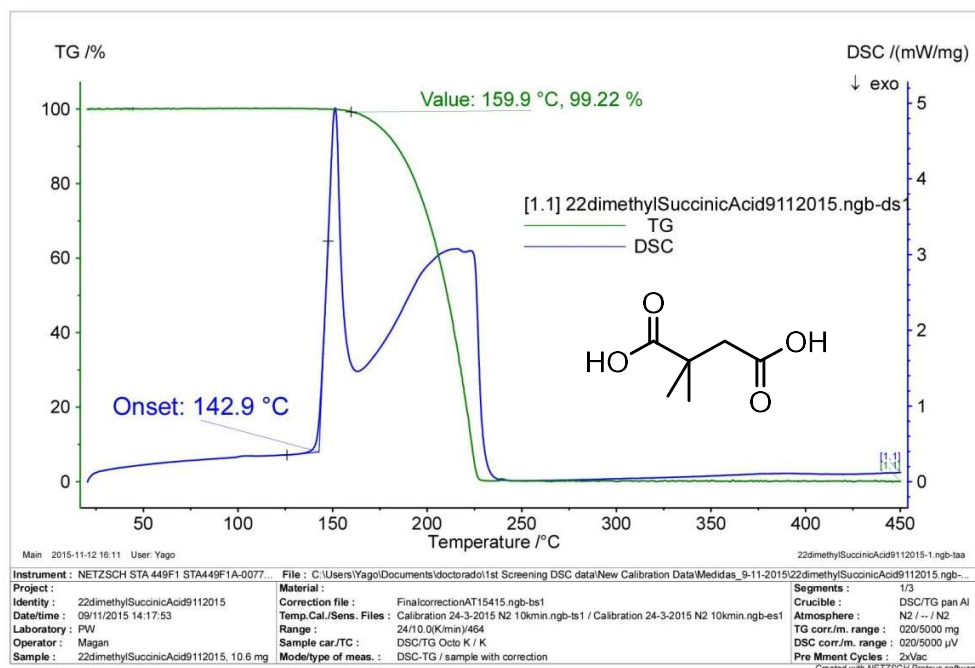




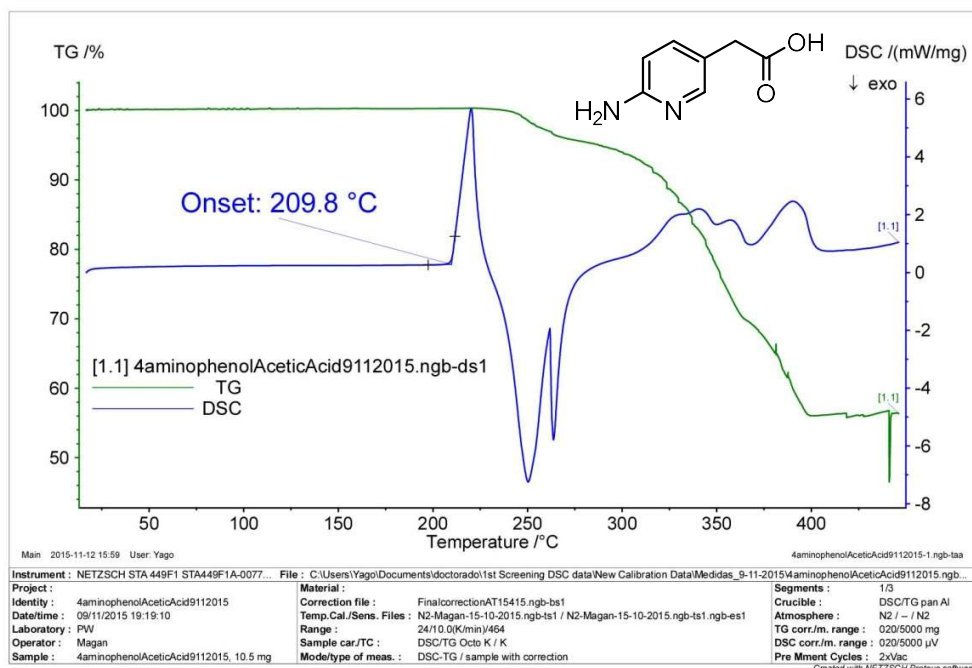
## 6 – Aminonicotinamide



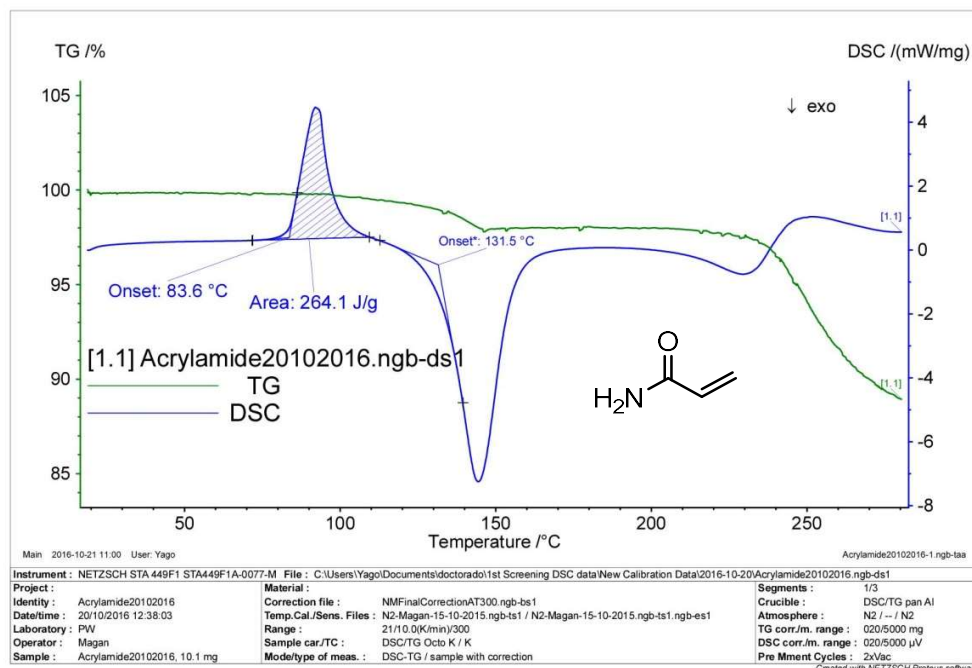
## 2,2 Dimethyl succinic acid



## 4-Aminophenylacetic acid

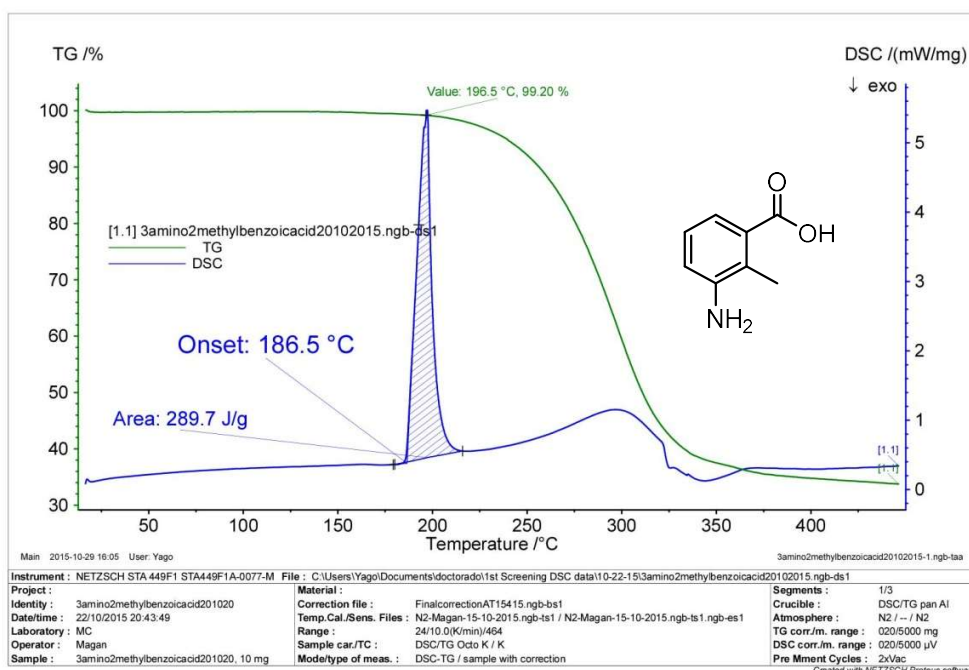


## Acrylamide

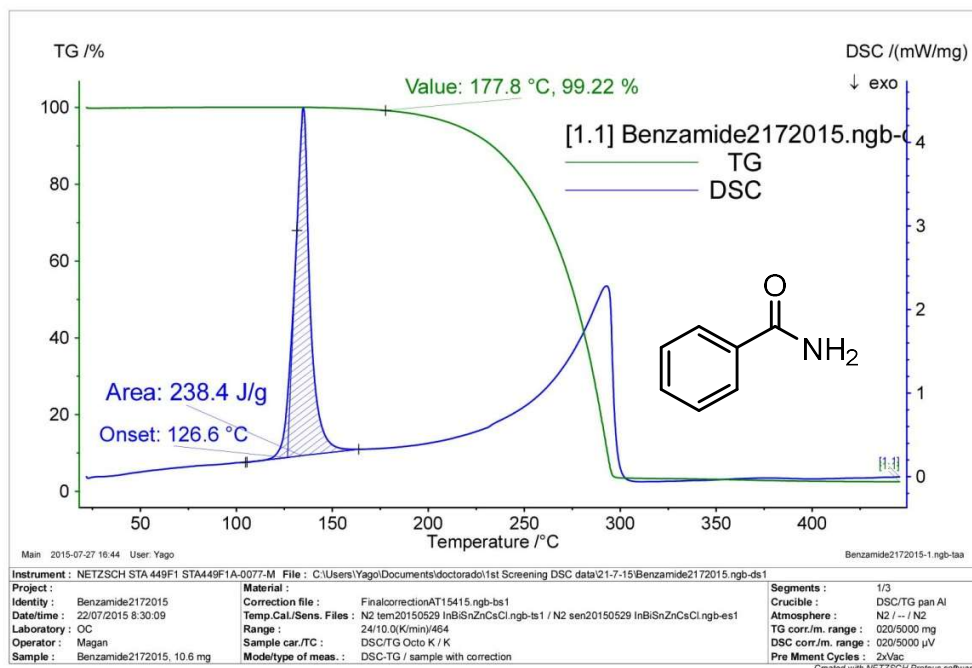




## 3-Amino-2-methylbenzoic acid

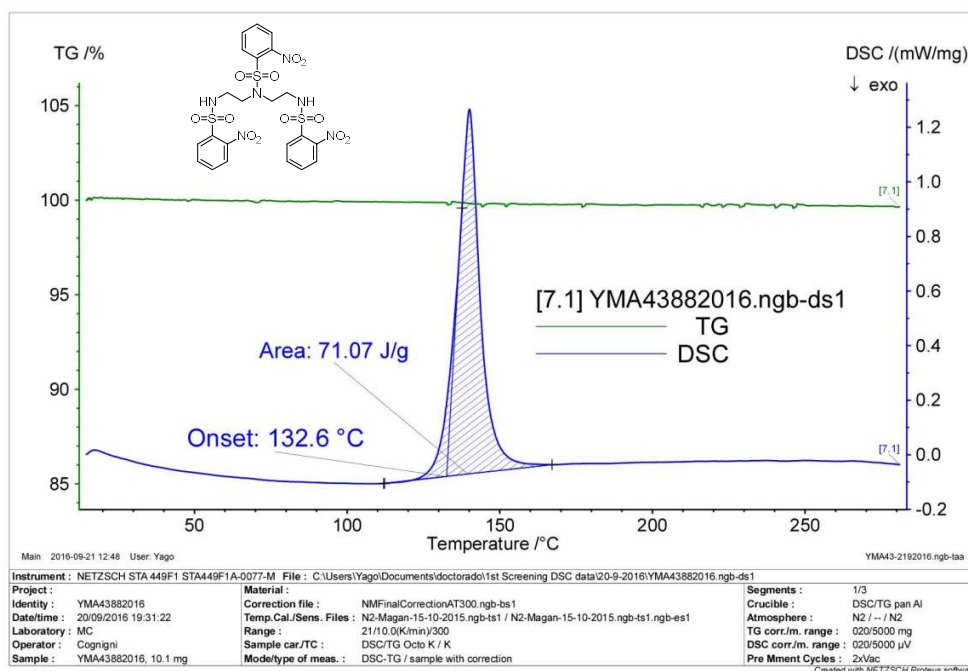


## Benzamide

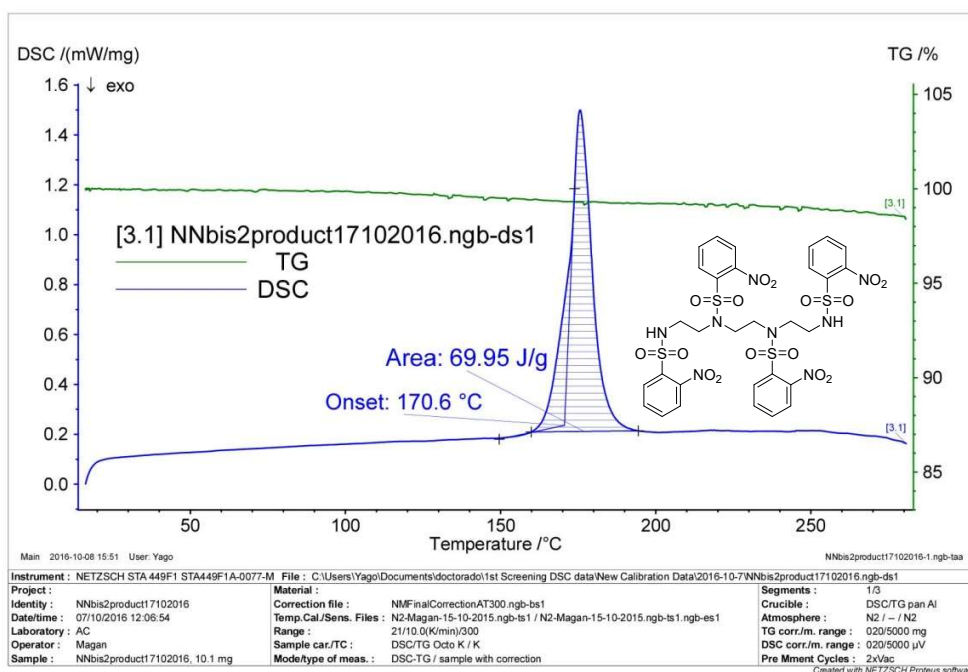


### 5.1.9 3,6-diazaoctane-1,8-diol and derivatives

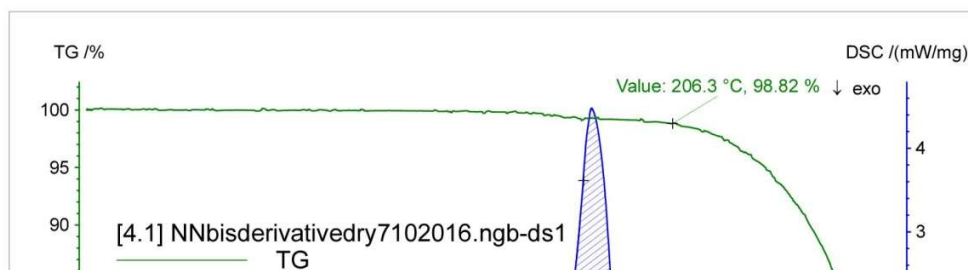
#### 1,4,7-Tris(2-nitrobenzenesulfonyl)-1,4,7-triazaheptane

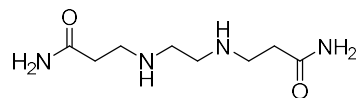


#### 1,4,7,10-tetrakis(2-nitrobenzenesulfonyl)-1,4,7,10-tetraazadecane

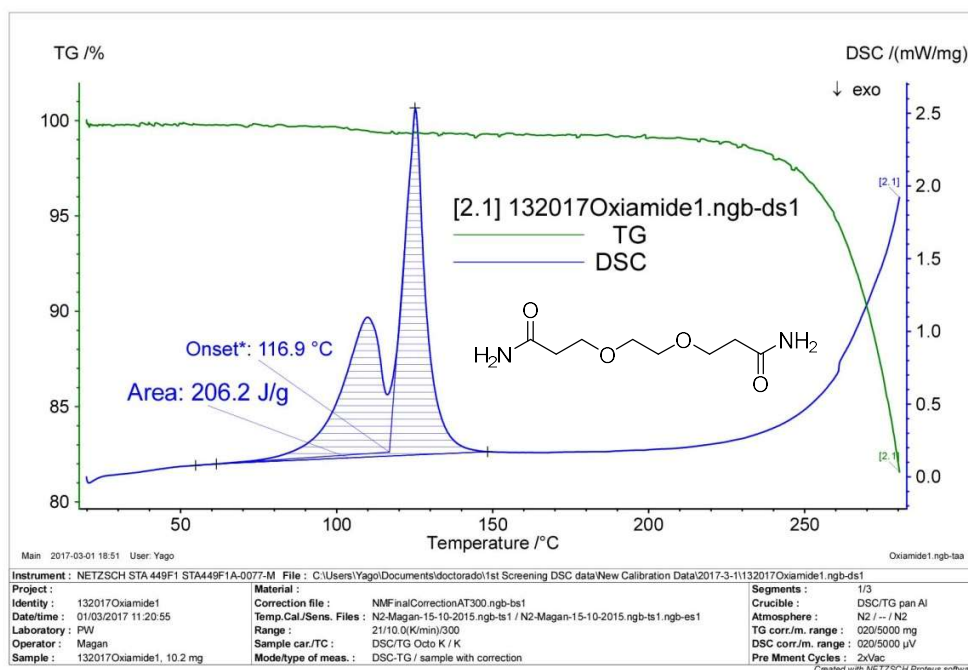


#### 4,7-diazadecanediamide

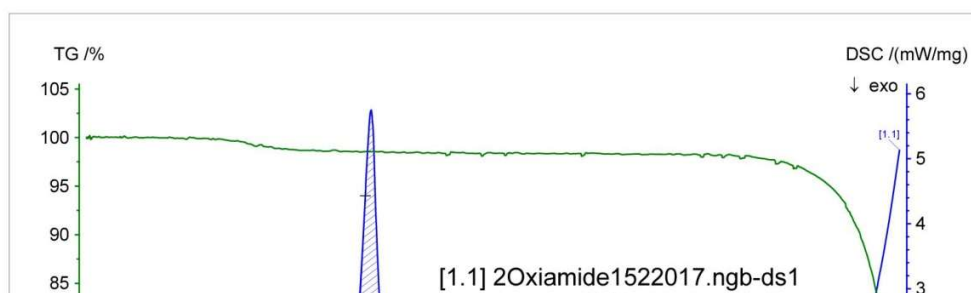


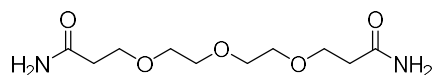


## 4,7-dioxa-1,10-octanedicarboxamide

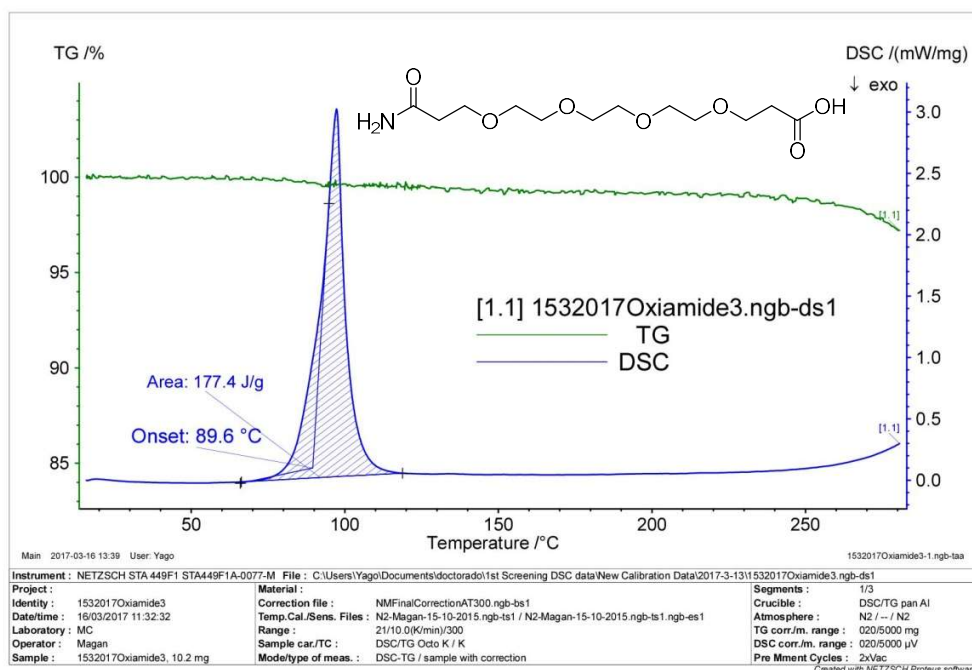


## 4,7,10-trioxa-1,13-undecanedicarboxamide

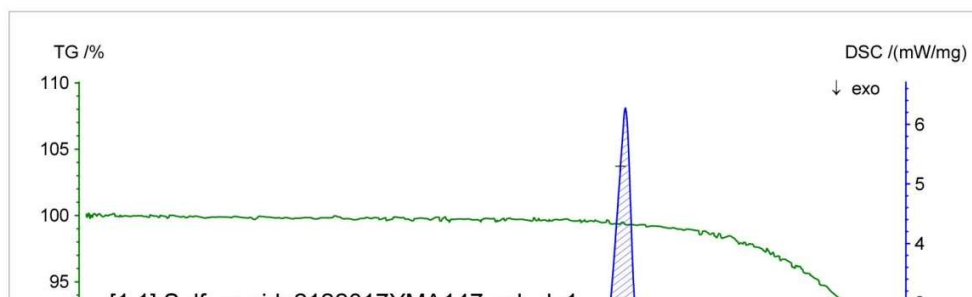


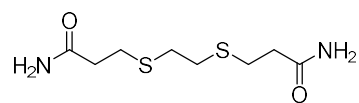


4,7,10,13-tetraoxa-1,16-hexadecanedicarboxamide



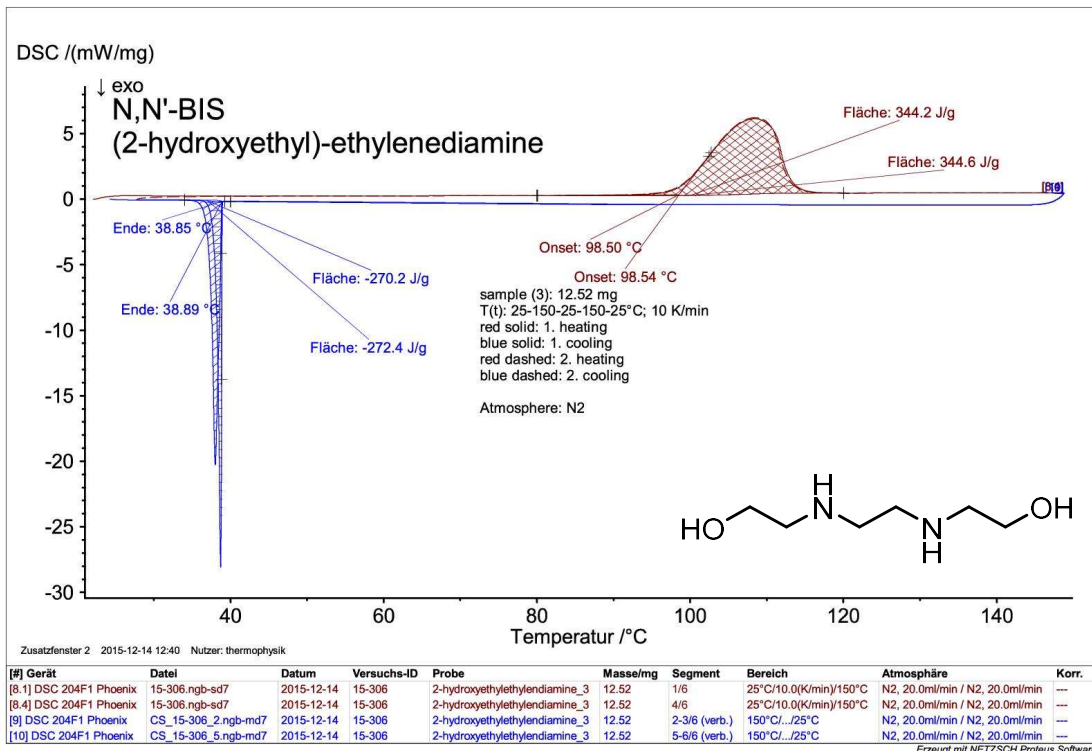
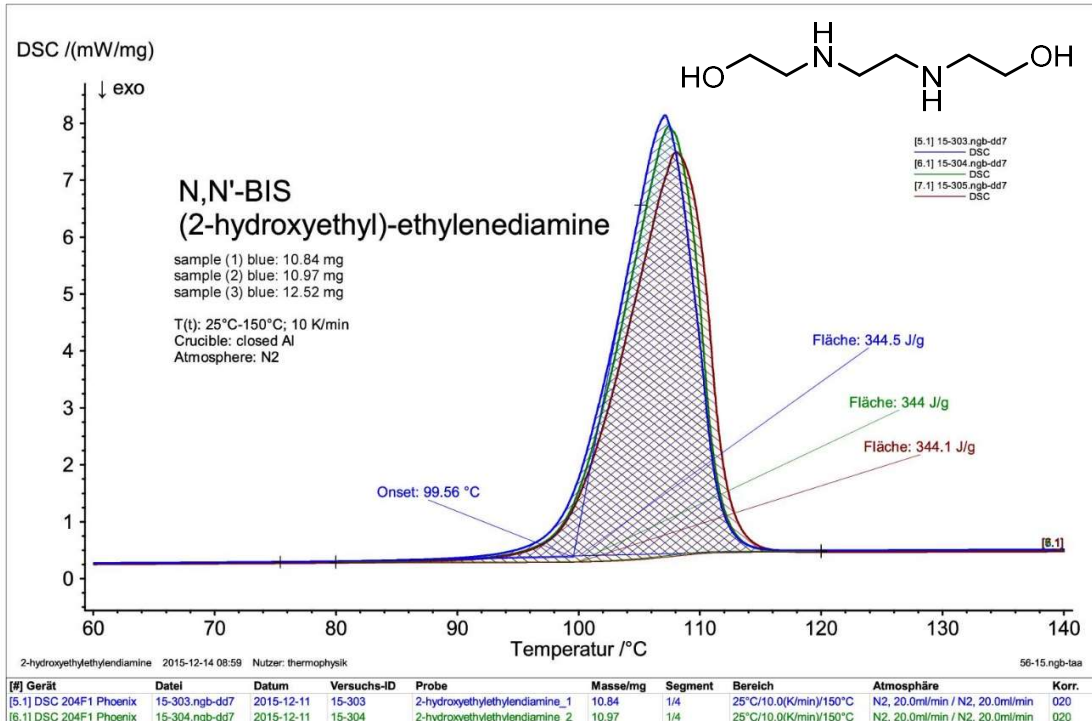
3-[2-(2-carbamoyl ethylsulfanyl)ethylsulfanyl]propionamide



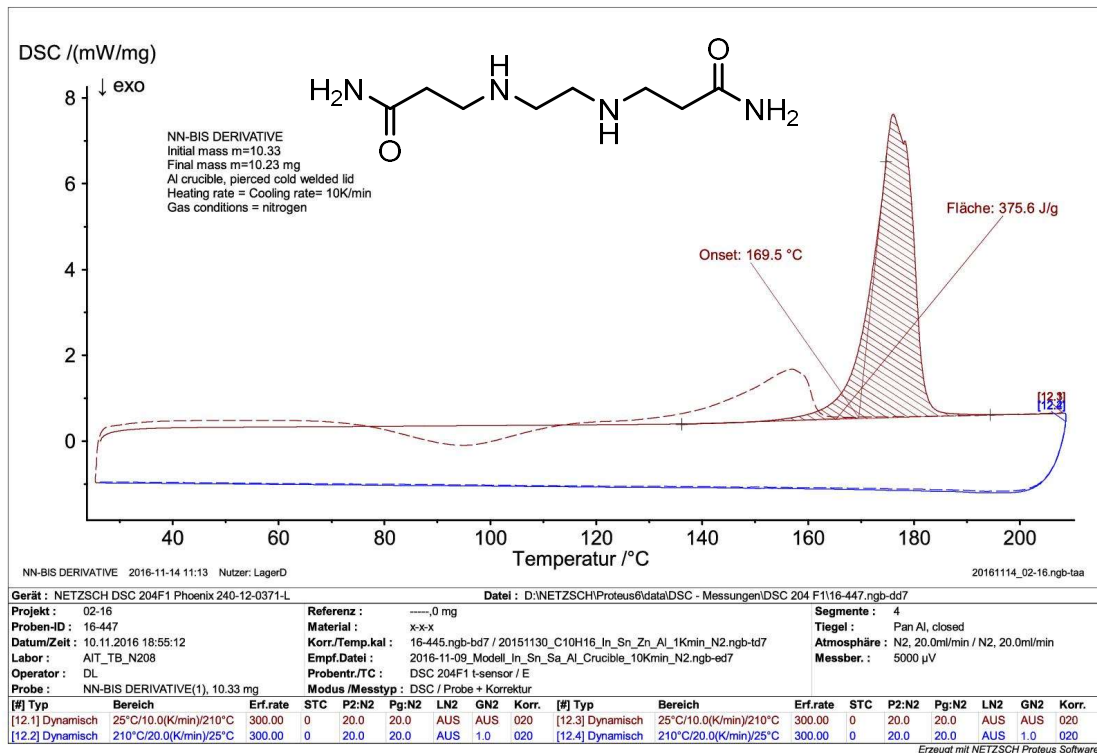


## 5.2 AIT DSC graphics

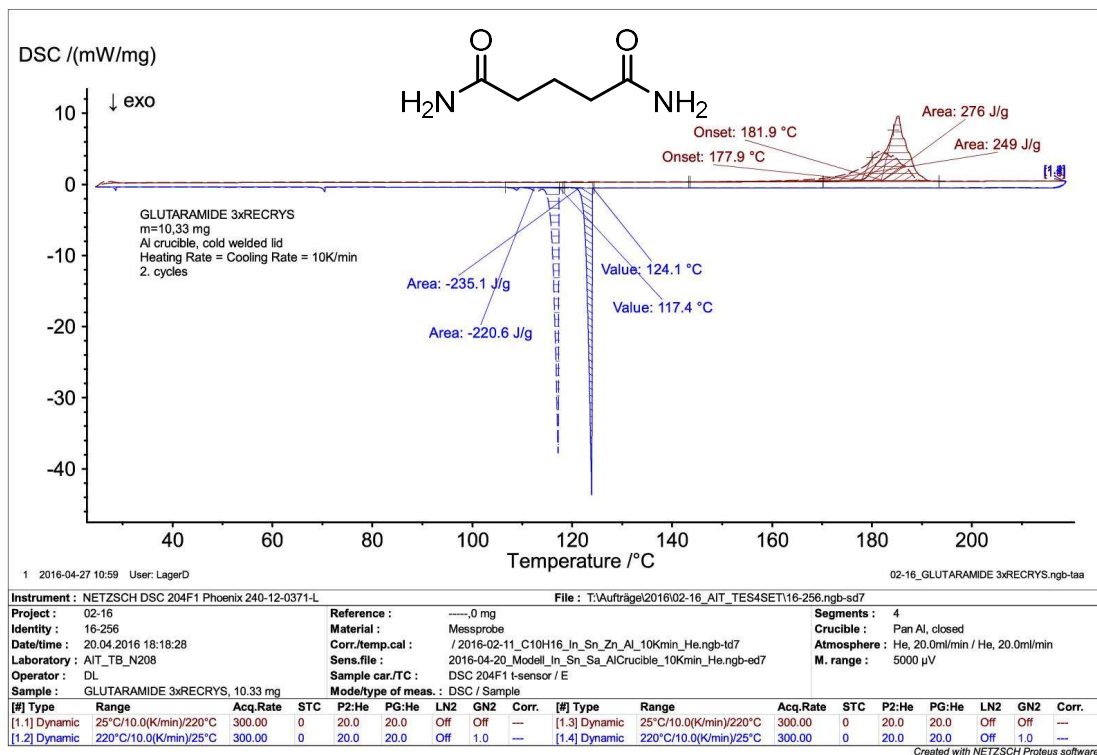
### N-N'-BIS(2-hydroxyethyl)-ethylenediamine



## 4,7-diazadecanediamide

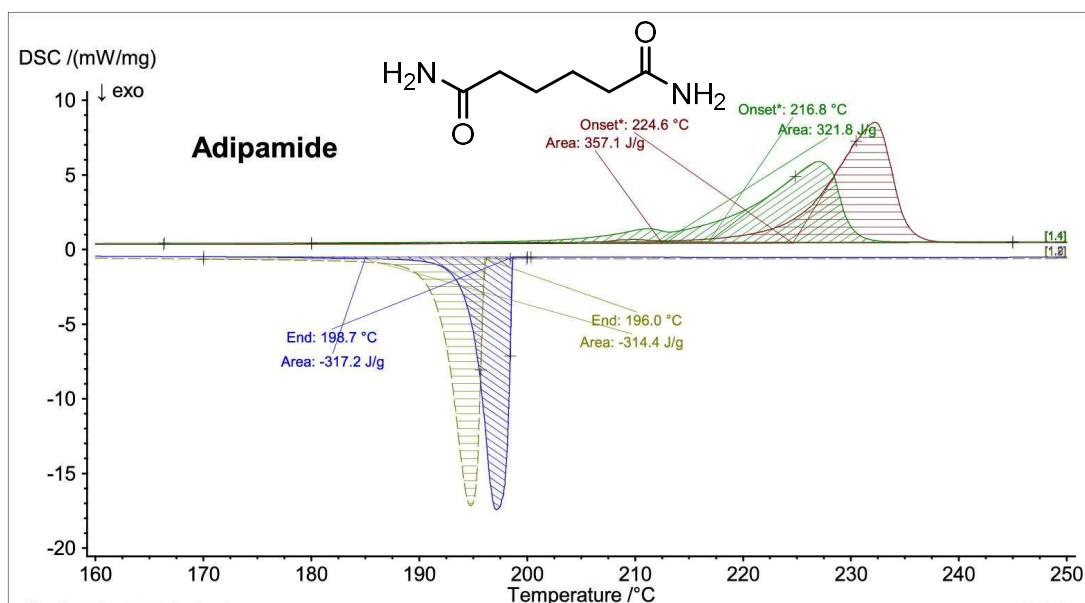


## Glutaramide





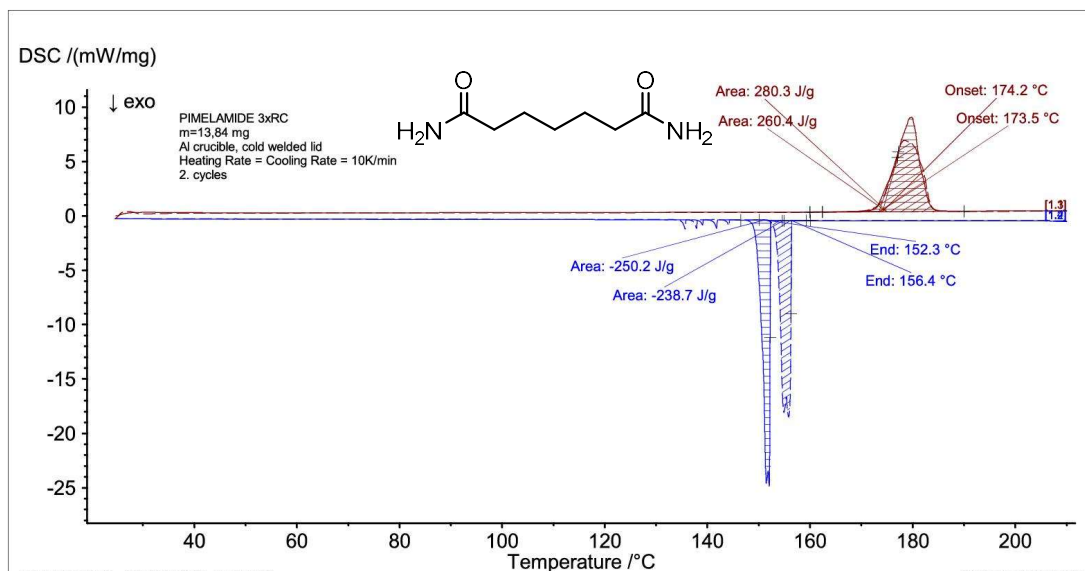
## Adipamide



Instrument : NETZSCH DSC 204F1 Phoenix 240-12-0371-L										File : D:\NETZSCH\Proteus\data\15-164.ngb-ed7									
Project : 20-15					Operator : DL					Corr./temp.cal : / 20150519_N2_Al_2Kmin.ngb-td7					Segments : 5				
Identity : 15-164					Sample : Adipamide_1, 9.17 mg					Sens.file : 39-15.ngb-ed7					Crucible : Pan Al, pierced lid				
Date/time : 21.07.2015 12:56:54					Reference : ----, 0 mg					Sample car./TC : DSC 204F1 t-sensor / E					Atmosphere : N2, 20.0ml/min / N2, 20.0ml/min				
Laboratory : AIT					Material : Dicarbonsäuren					Mode/type of meas. : DSC / Sample					M. range : 5000 µV				
[#] Type	Range	Acq.Rate	STC	P2:N2	PG:N2	LN2	GN2	Corr.	[#] Type	Range	Acq.Rate	STC	P2:N2	PG:N2	LN2	GN2	Corr.		
[1.1]	Dynamic	20°C/10.0(K/min)/270°C	150.00	0	20.0	20.0	Off	Off	[1.4]	Dynamic	155°C/10.0(K/min)/270°C	300.00	0	20.0	20.0	Off	Off	---	
[1.2]	Dynamic	270°C/10.0(K/min)/155°C	150.00	0	20.0	20.0	Off	1.0	[1.5]	Dynamic	270°C/10.0(K/min)/20°C	300.00	0	20.0	20.0	Off	1.0	---	

Created with NETZSCH Proteus software

## Pimelamide

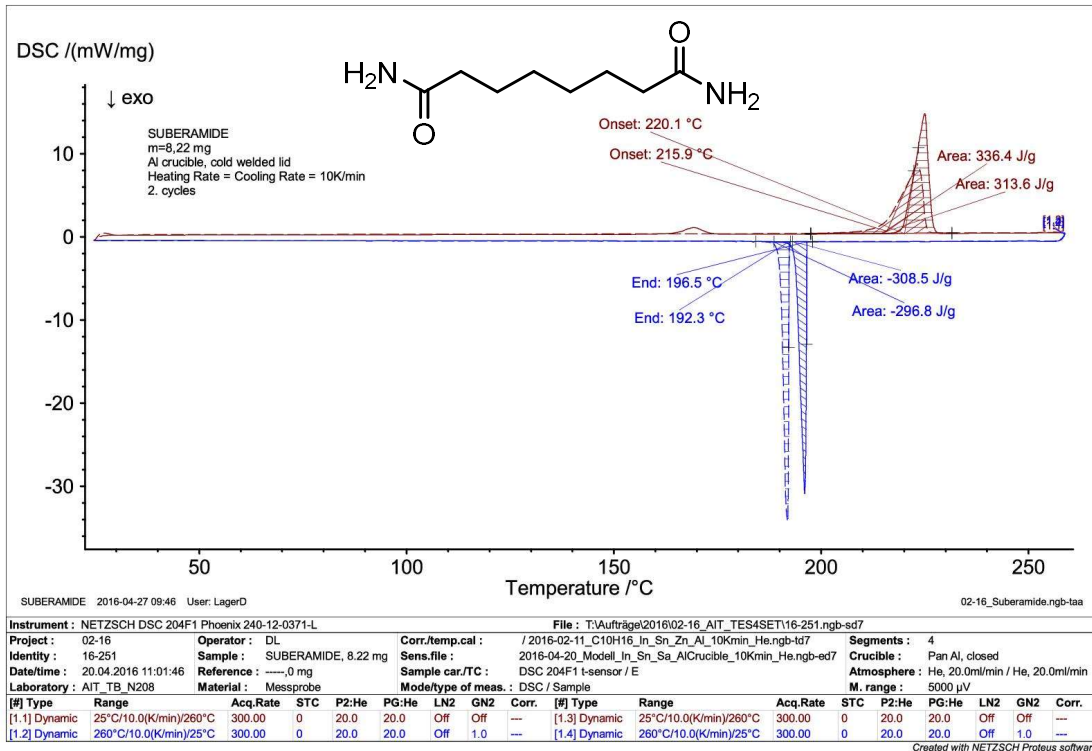


Instrument : NETZSCH DSC 204F1 Phoenix 240-12-0371-L										File : D:\NETZSCH\Proteus\data\Aufträge\DSC\DSC 204 F1\2016\02-16_F1-DSC_AIT-TE54SET16-250.ngb-sd7									
Project : 02-16					Reference : ----, 0 mg					Segments : 4									
Identity : 16-250					Material : Messprobe					Crucible : Pan Al, closed									
Date/time : 20.04.2016 09:41:37					Corr./temp.cal : / 2016-02-11_C10H16_In_Sn_Zn_Al_10Kmin_He.ngb-td7					Atmosphere : He, 20.0ml/min / He, 20.0ml/min									
Laboratory : AIT_TB_N208					Sens.file : 2016-04-20_Modell_In_Sn_Sa_AlCrucible_10Kmin_He.ngb-ed7					M. range : 5000 µV									
Operator : DL					Sample car./TC : DSC 204F1 t-sensor / E					Mode/type of meas. : DSC / Sample									
Sample : PIMELAMIDE 3xRECRY, 13.84 mg																			
[#] Type	Range	Acq.Rate	STC	P2:He	PG:He	LN2	GN2	Corr.	[#] Type	Range	Acq.Rate	STC	P2:He	PG:He	LN2	GN2	Corr.		
[1.1]	Dynamic	25°C/10.0(K/min)/215°C	300.00	0	20.0	20.0	Off	Off	[1.3]	Dynamic	25°C/10.0(K/min)/215°C	300.00	0	20.0	20.0	Off	Off	---	
[1.2]	Dynamic	215°C/10.0(K/min)/25°C	300.00	0	20.0	20.0	Off	1.0	[1.4]	Dynamic	215°C/10.0(K/min)/25°C	300.00	0	20.0	20.0	Off	1.0	---	

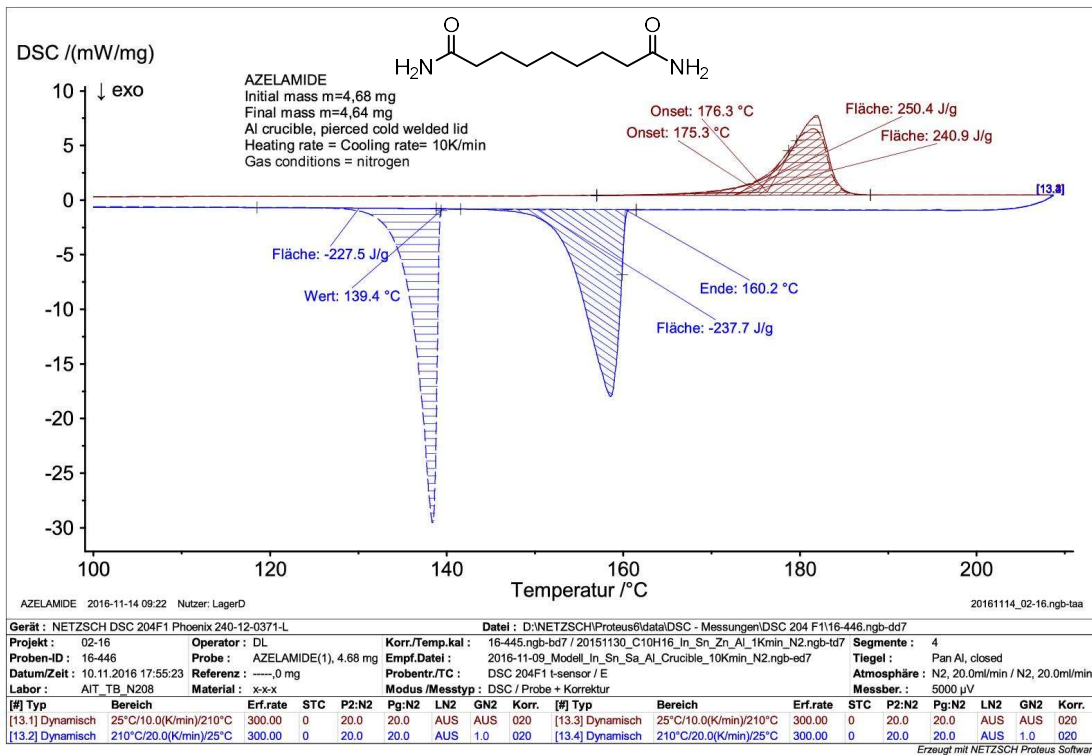
Created with NETZSCH Proteus software



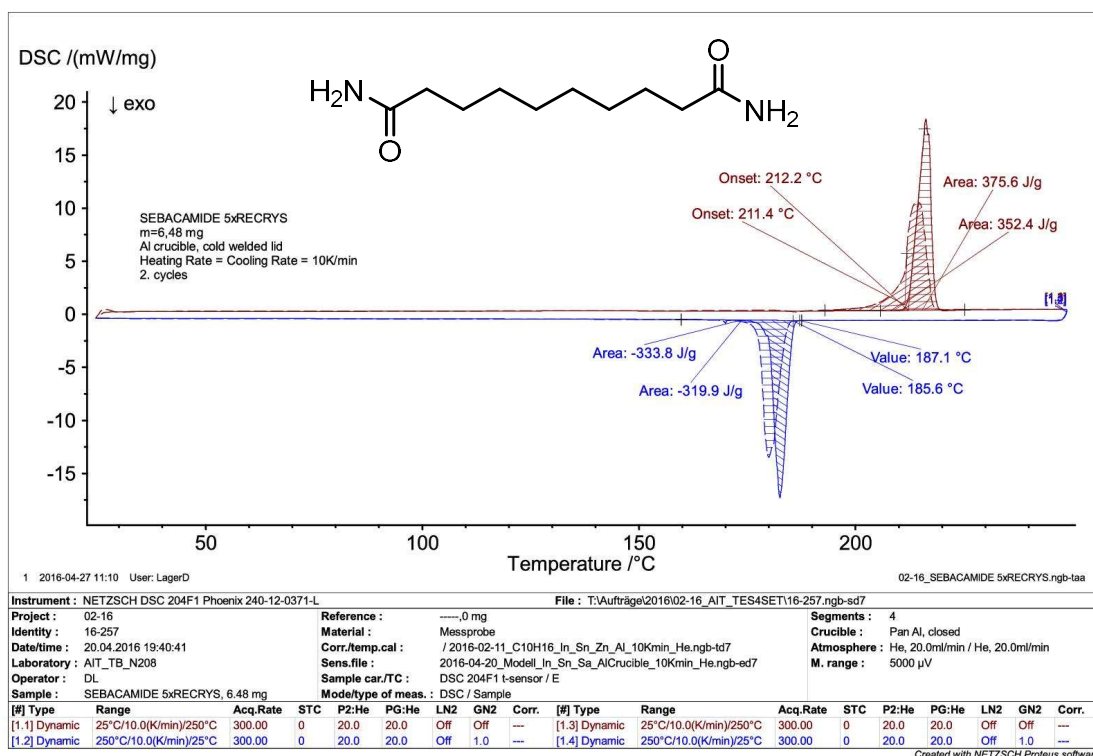
### Suberamide



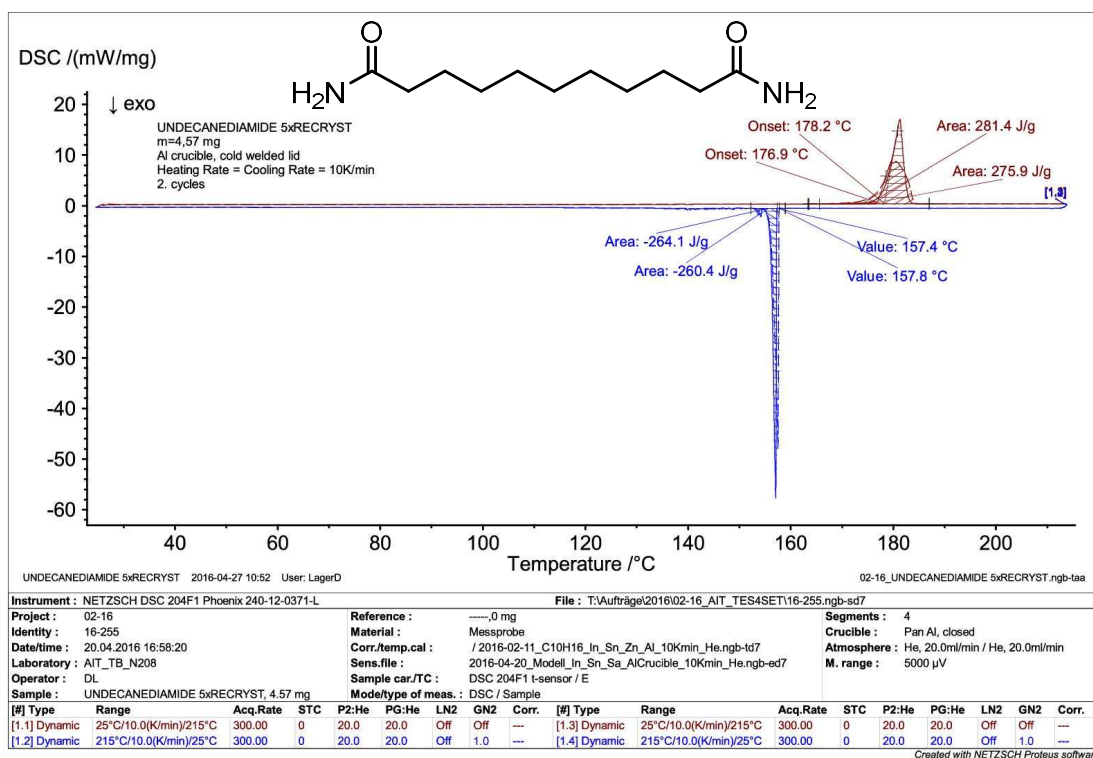
### Azelamide



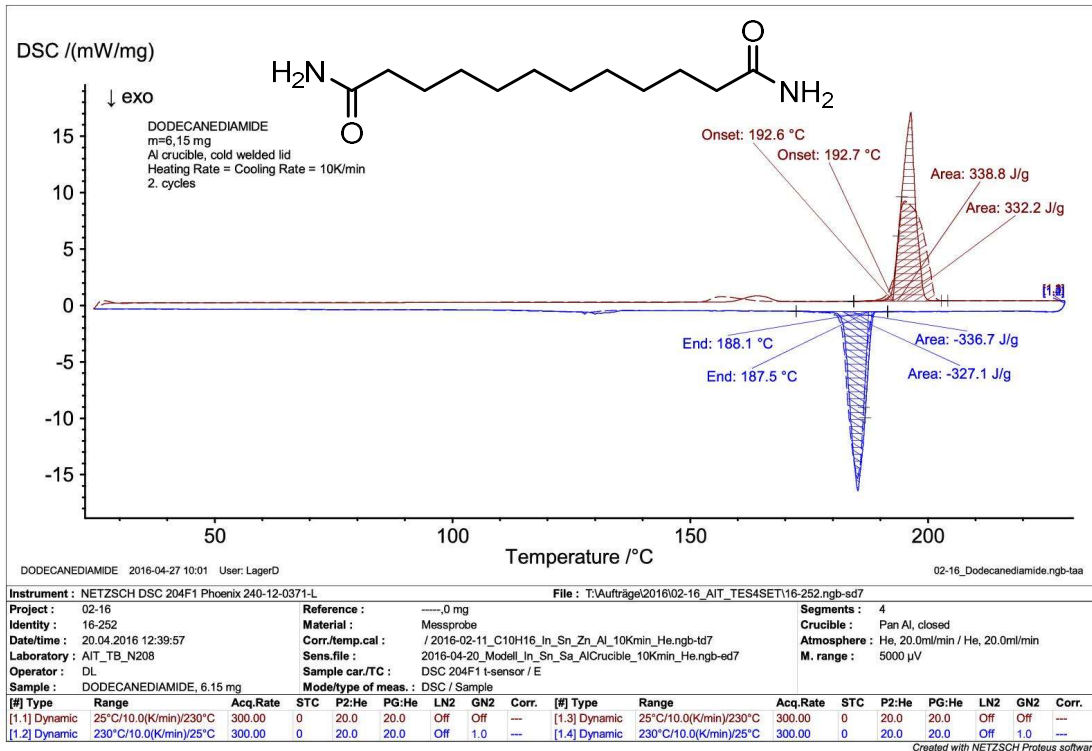
## Sebacamide



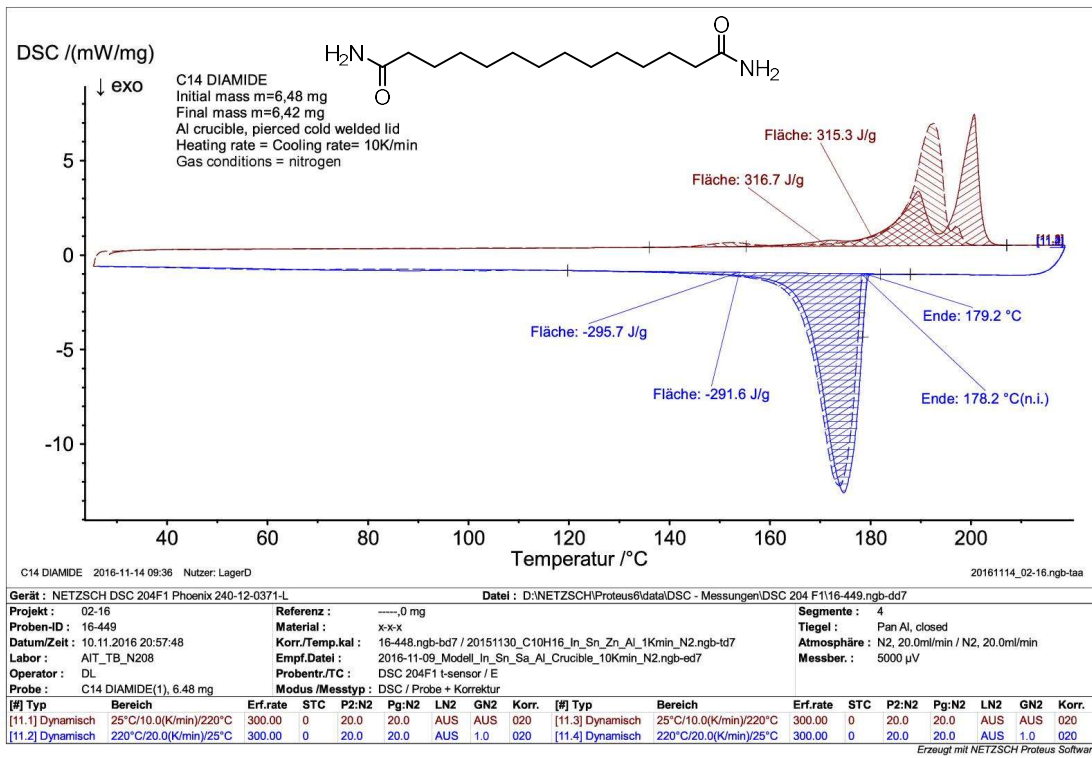
## Undecanediamide



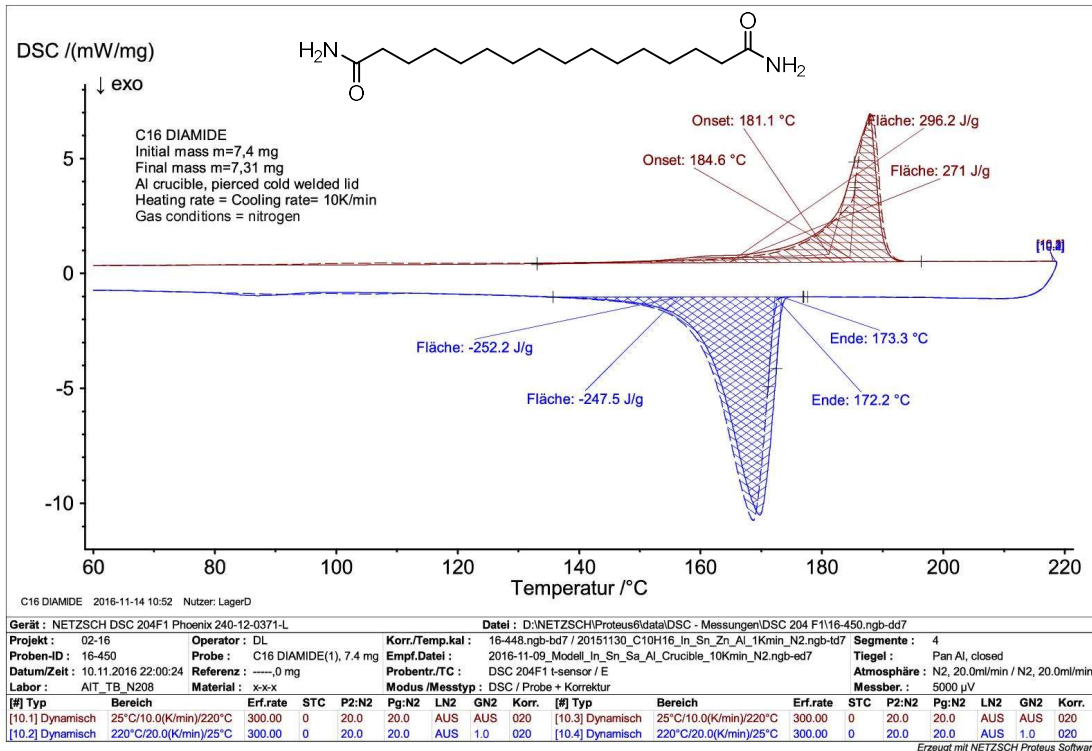
### Dodecanediamide



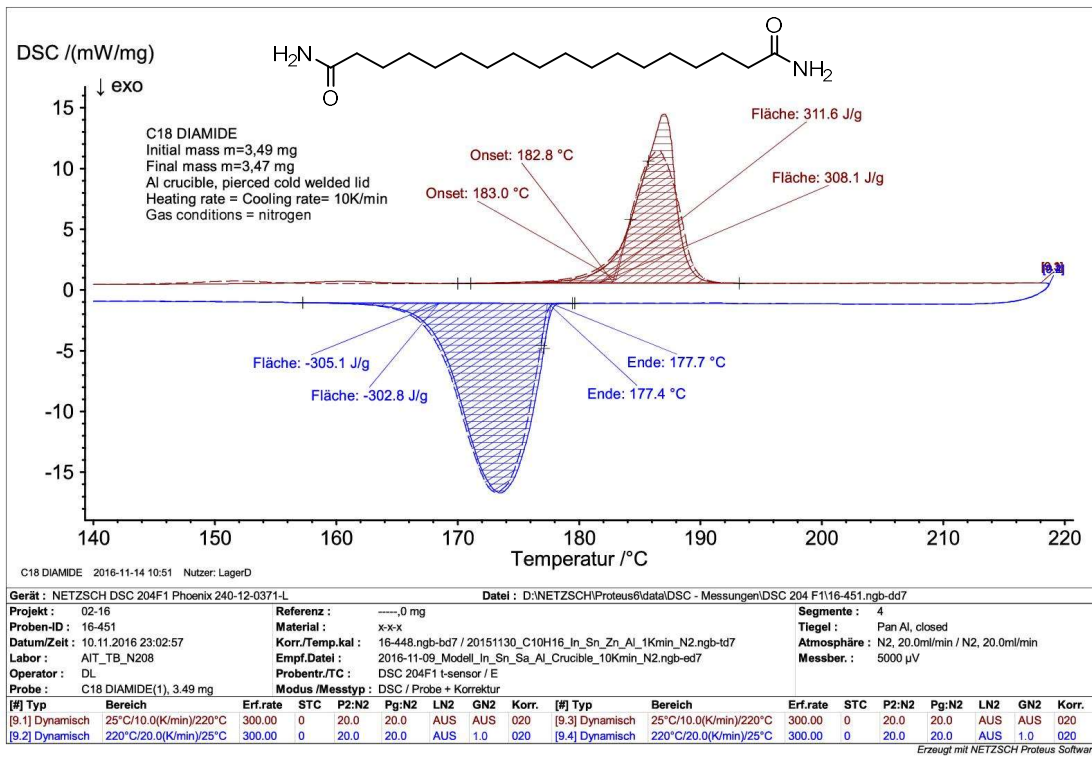
### Tetradecanediamide



### Hexadecanediamide

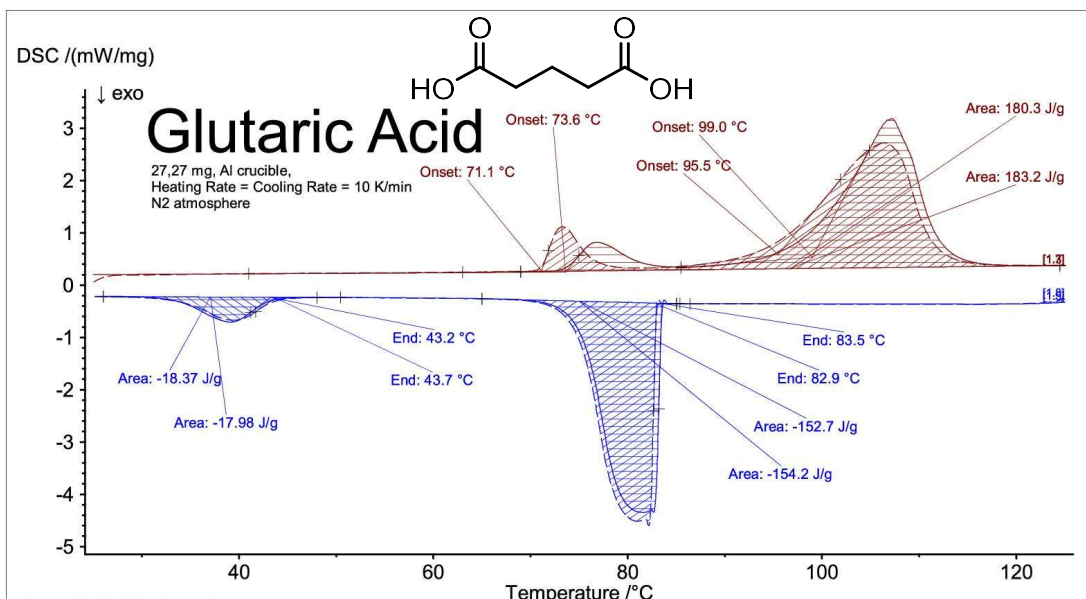


### Octadecanediamide





### Glutaric acid



Glutaric 2015-10-13 10:38 User: LagerD

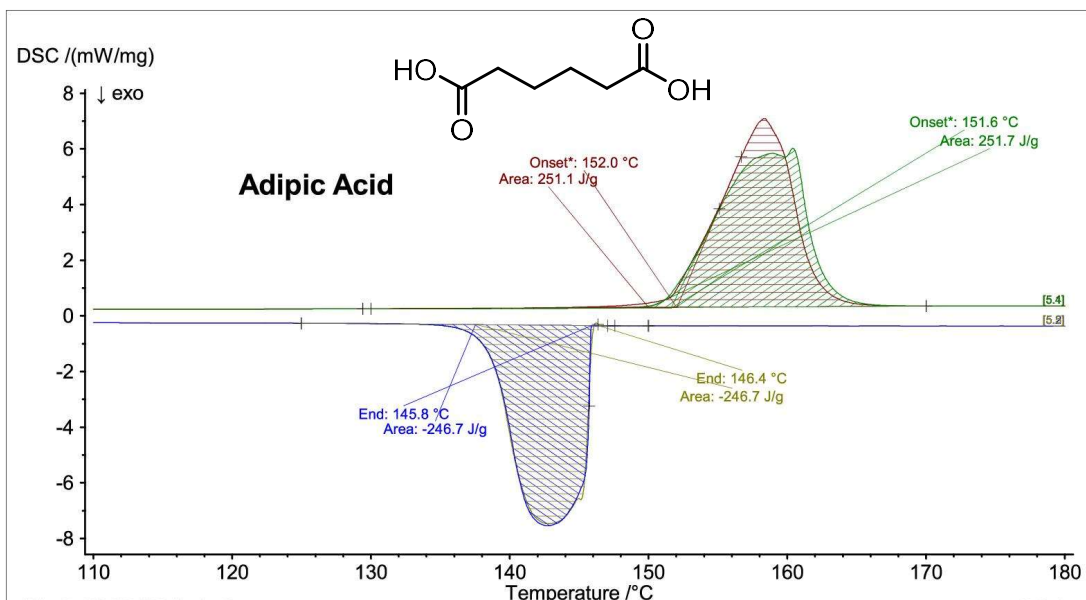
Instrument : NETZSCH DSC 204F1 Phoenix 240-12-0371-L File : T:\Aufträge\2015\49-15\_AIT-Tes4Set\49-15\_DSC\_TES4SET15-235.ngb-dd7

Project : 49-15	Operator : DL	Corr./temp.cal : 15-234.ngb-bd7 / 20150519_N2_AI_2Kmin.ngb-td7	Segments : 8
Identity : 15-235	Sample : Glutaric_acid, 27,27 mg	Sens.file : 39-15.ngb-ed7	Crucible : Pan Al, pierced lid
Date/time : 08.10.2015 20:54:09	Reference : ---,0 mg	Sample car./TC : DSC 204F1 t-sensor / E	Atmosphere : N2, 20.0ml/min / N2, 20.0ml/min
Laboratory : AIT_TB_N208	Material : Messprobe	Mode/type of meas. : DSC / sample with correction	M.range : 5000 µV

[#] Type	Range	Acq.Rate	STC	P2:N2	PG:N2	LN2	GN2	Corr.	[#] Type	Range	Acq.Rate	STC	P2:N2	PG:N2	LN2	GN2	Corr.
[1.3] Dynamic	-50°C/10.0(K/min)/130°C	300.00	0	20.0	20.0	Off	Off	020	[1.7] Dynamic	25°C/10.0(K/min)/130°C	300.00	0	20.0	20.0	Off	Off	020
[1.5] Dynamic	130°C/10.0(K/min)/25°C	300.00	0	20.0	20.0	Off	50.0 %	020	[1.8] Dynamic	130°C/10.0(K/min)/25°C	300.00	0	20.0	20.0	Off	50.0 %	020

Created with NETZSCH Proteus software

### Adipic acid



Adipic\_acid 2015-08-19 11:15 User: LagerD

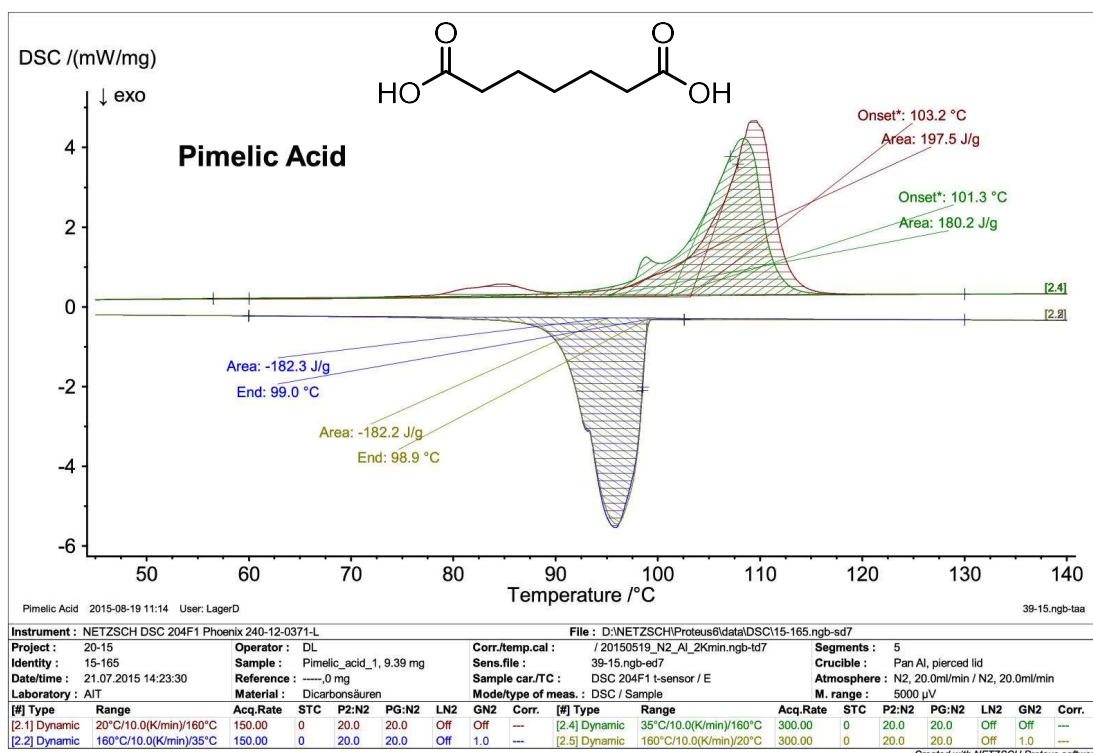
Instrument : NETZSCH DSC 204F1 Phoenix 240-12-0371-L File : D:\NETZSCH\Proteus\data\DSC\15-168.ngb-sd7

Project : 20-15	Operator : DL	Corr./temp.cal : / 20150519_N2_AI_2Kmin.ngb-td7	Segments : 5
Identity : 15-168	Sample : Adipic_acid_1, 11,24 mg	Sens.file : 39-15.ngb-ed7	Crucible : Pan Al, pierced lid
Date/time : 21.07.2015 17:31:39	Reference : ---,0 mg	Sample car./TC : DSC 204F1 t-sensor / E	Atmosphere : N2, 20.0ml/min / N2, 20.0ml/min
Laboratory : AIT	Material : Dicarbonsäuren	Mode/type of meas. : DSC / Sample	M.range : 5000 µV

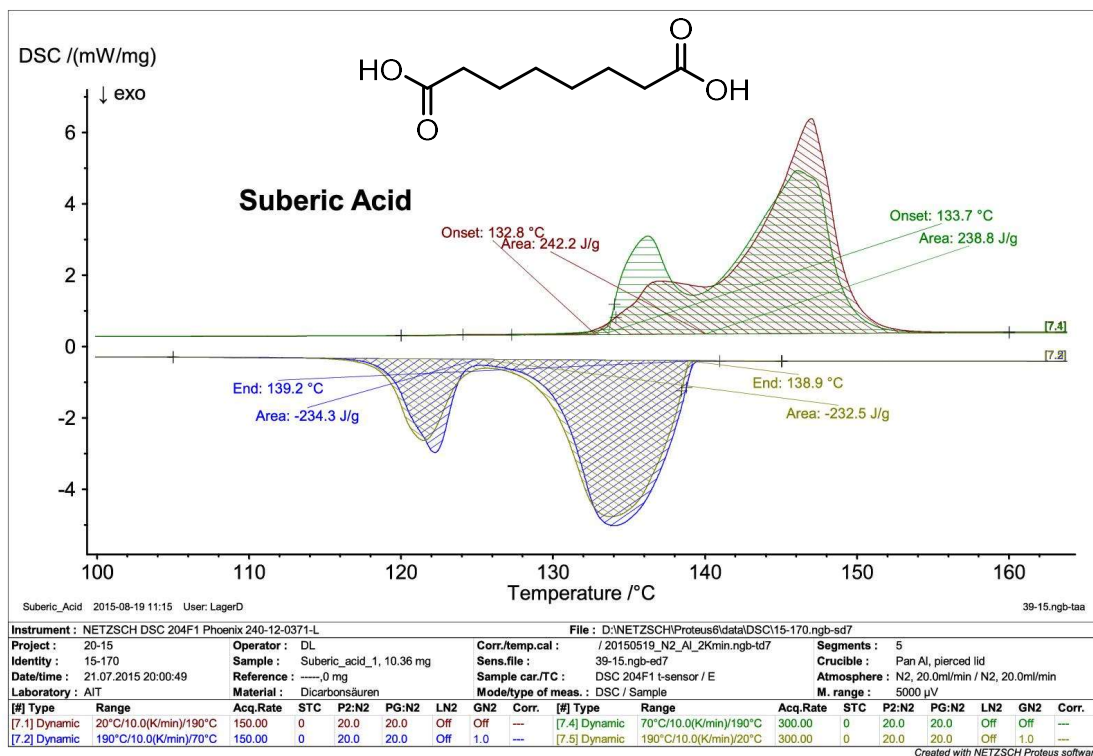
[#] Type	Range	Acq.Rate	STC	P2:N2	PG:N2	LN2	GN2	Corr.	[#] Type	Range	Acq.Rate	STC	P2:N2	PG:N2	LN2	GN2	Corr.
[5.1] Dynamic	20°C/10.0(K/min)/200°C	150.00	0	20.0	20.0	Off	Off	---	[5.4] Dynamic	80°C/10.0(K/min)/200°C	300.00	0	20.0	20.0	Off	Off	---
[5.2] Dynamic	200°C/10.0(K/min)/80°C	150.00	0	20.0	20.0	Off	1.0	---	[5.5] Dynamic	200°C/10.0(K/min)/20°C	300.00	0	20.0	20.0	Off	1.0	---

Created with NETZSCH Proteus software

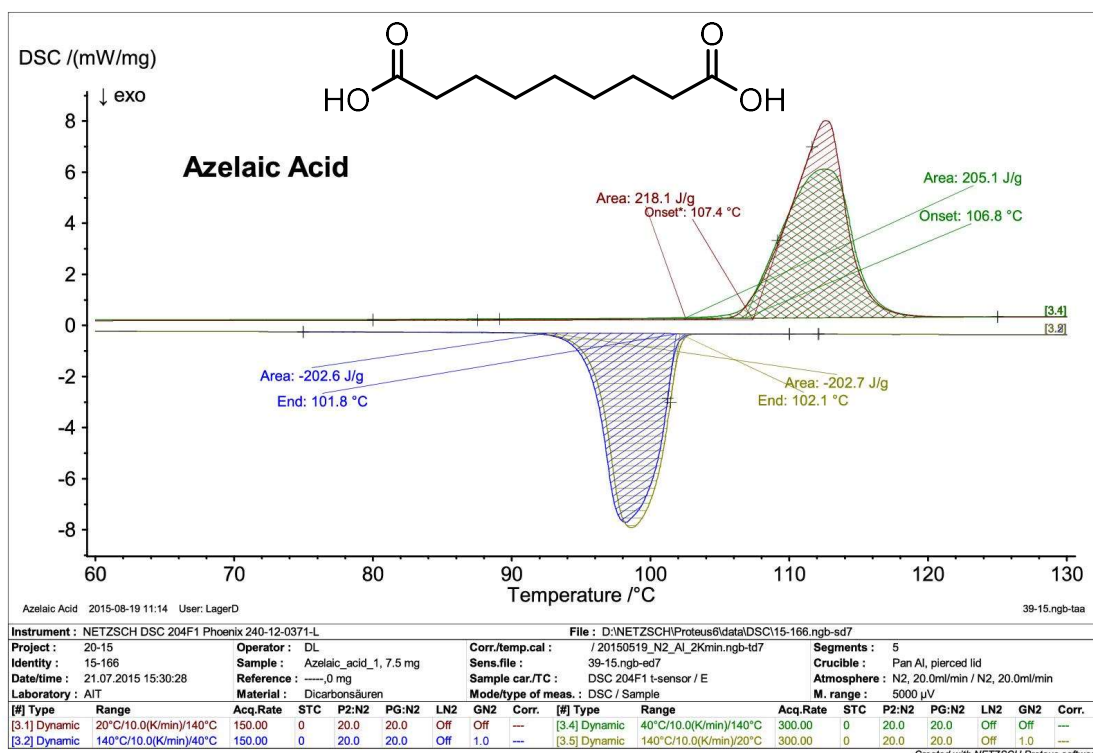
## Pimelic acid



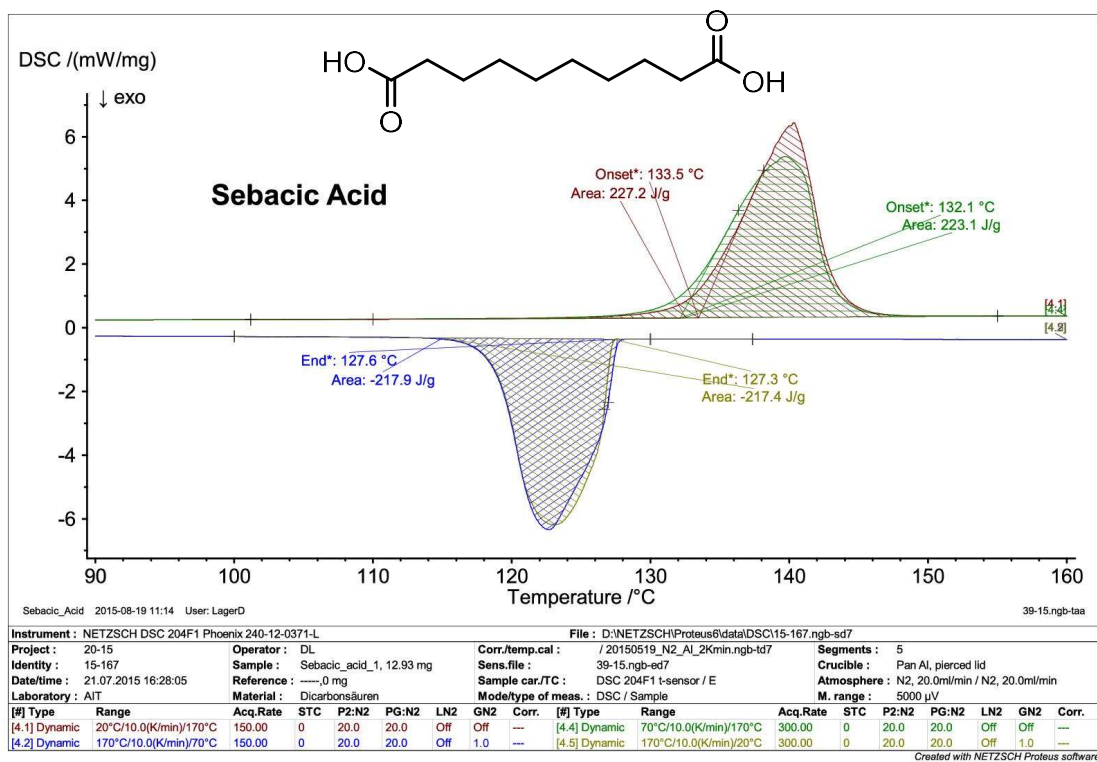
## Suberic acid



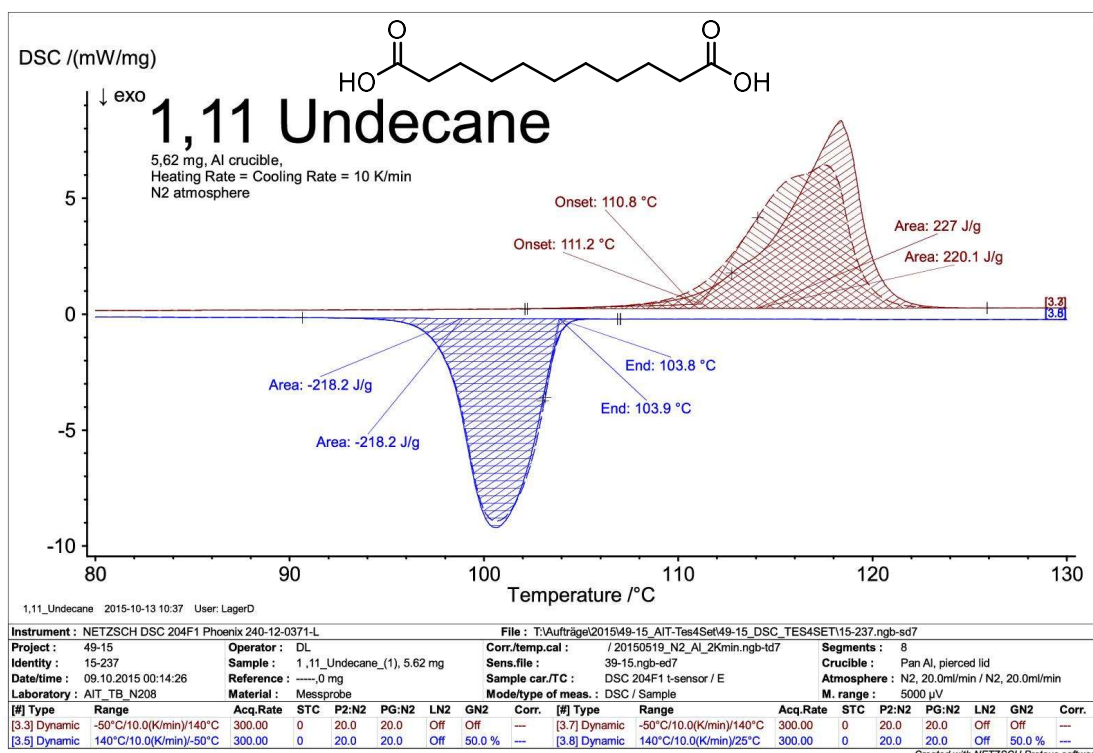
## Azelaic acid



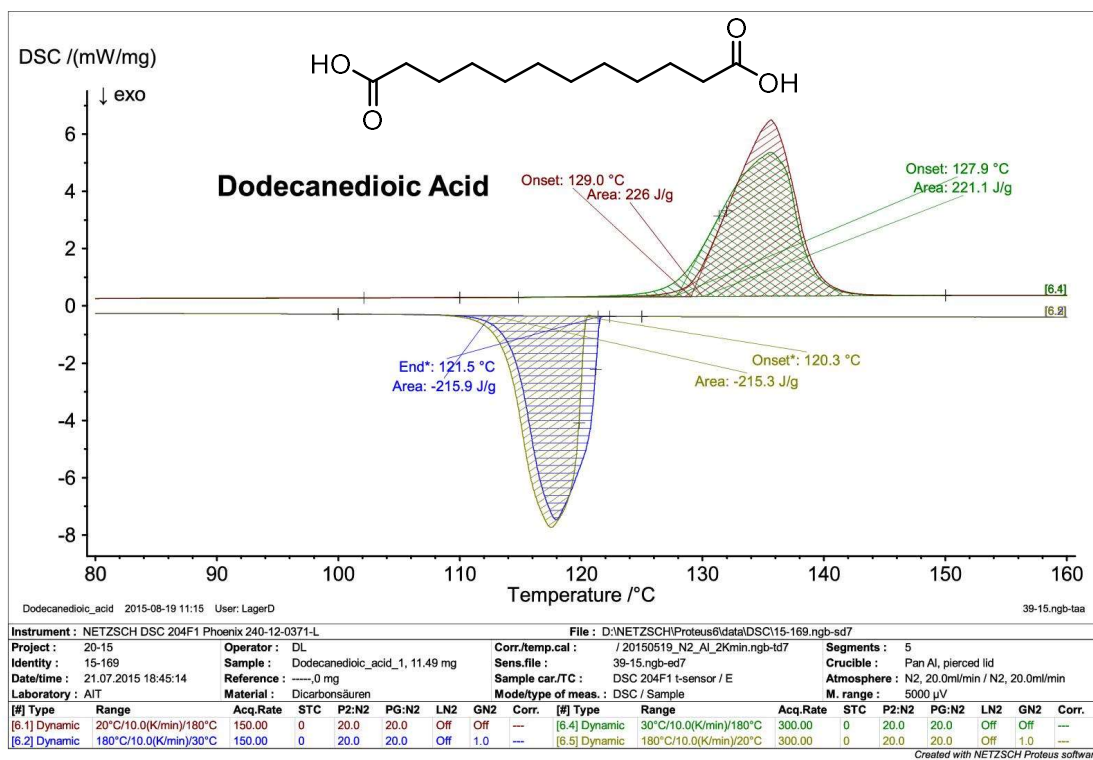
## Sebacic Acid



## Undecanedioic acid

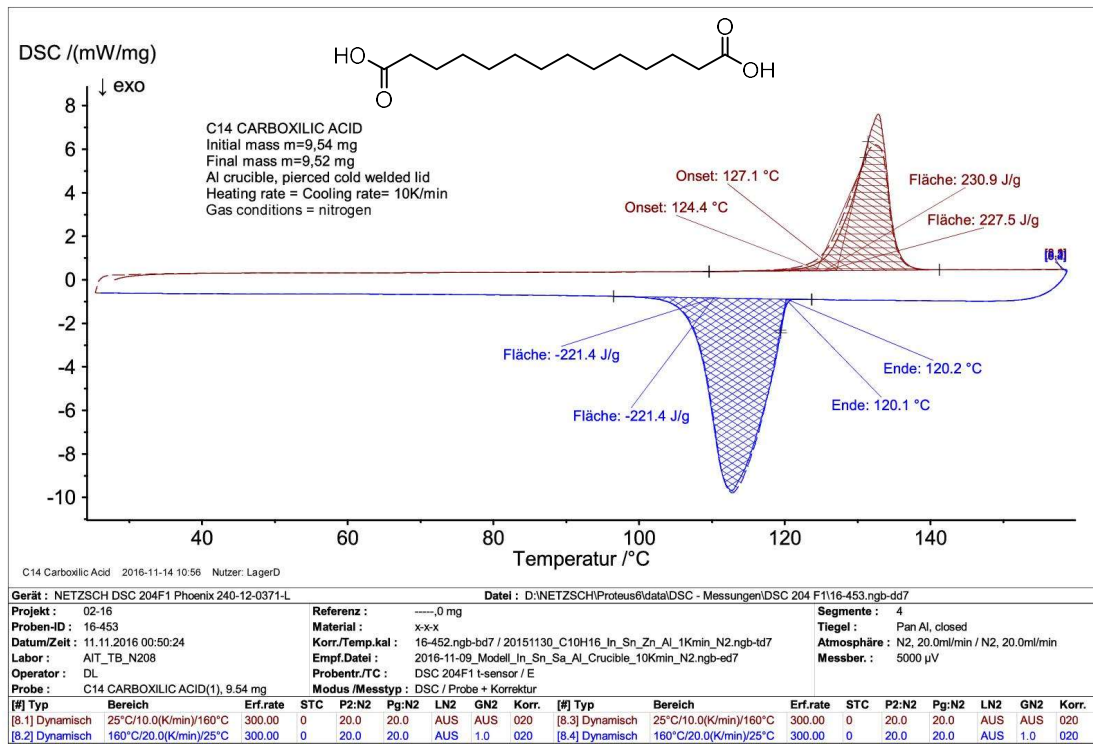


## Dodecanedioic acid

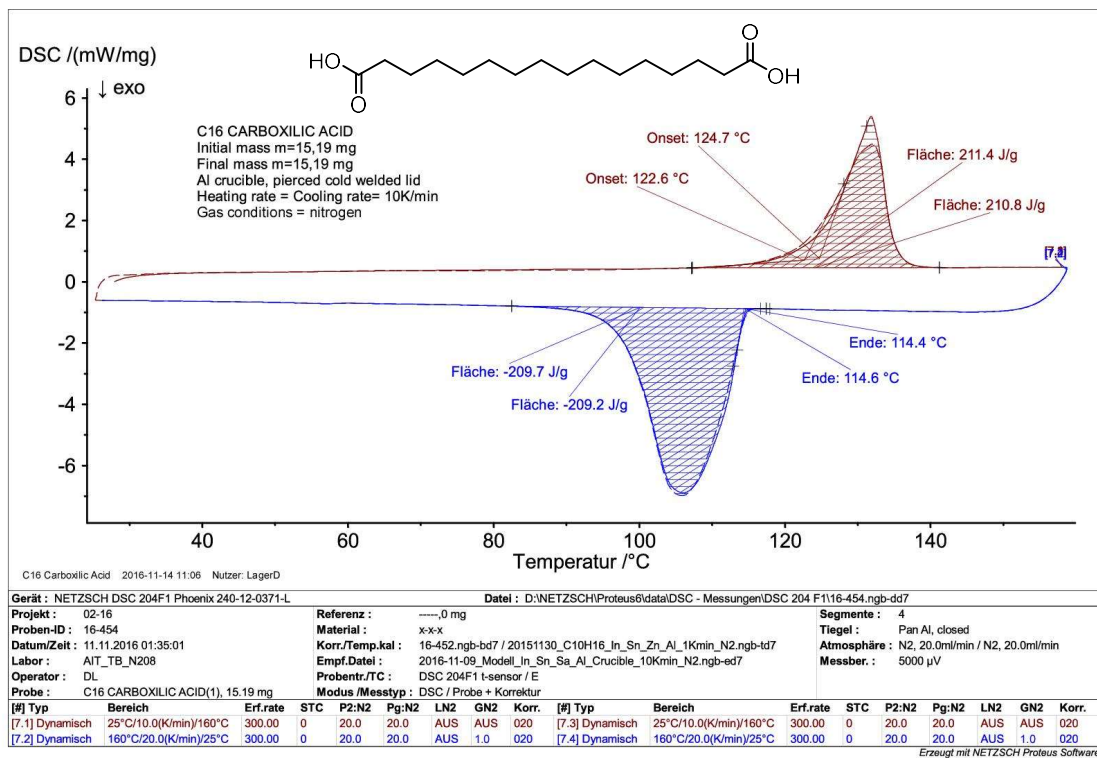




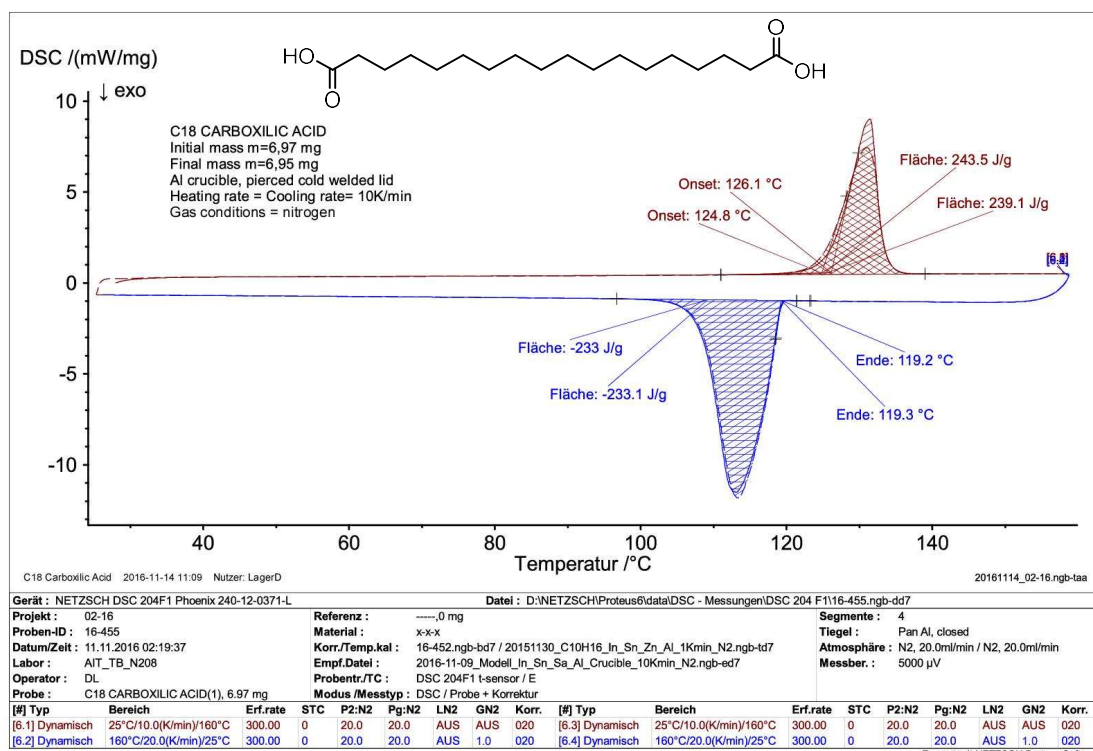
## Tetradecanedioic acid



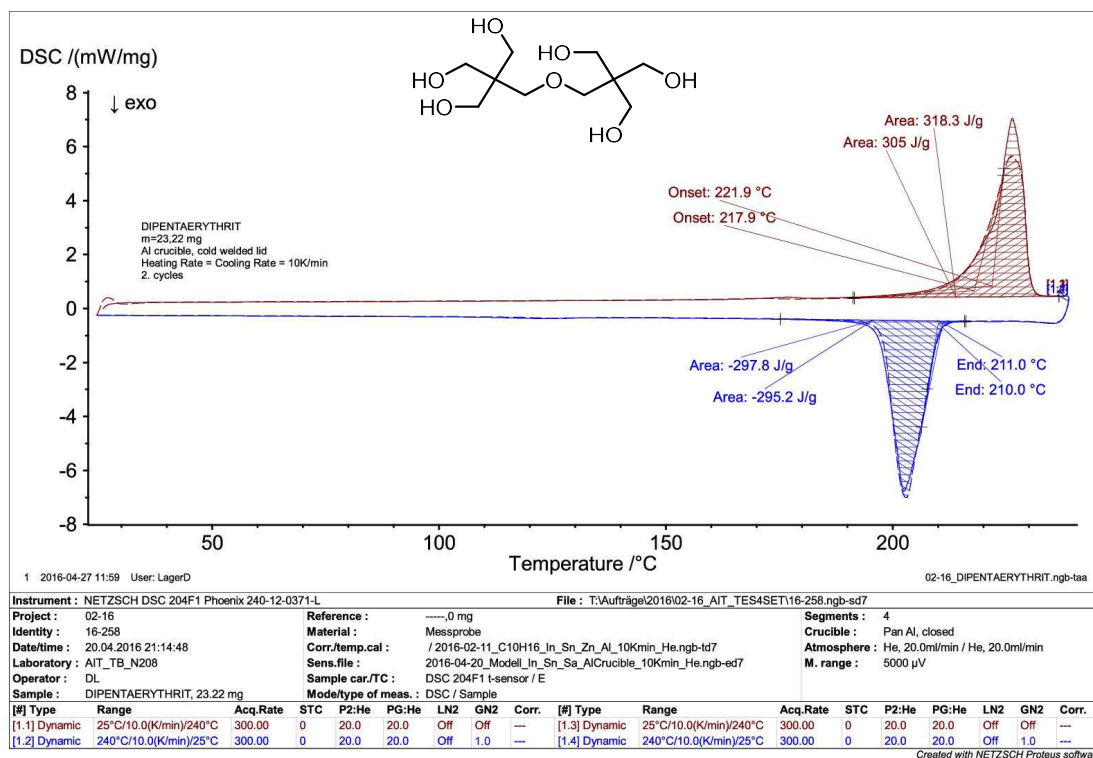
## Hexadecanedioic acid



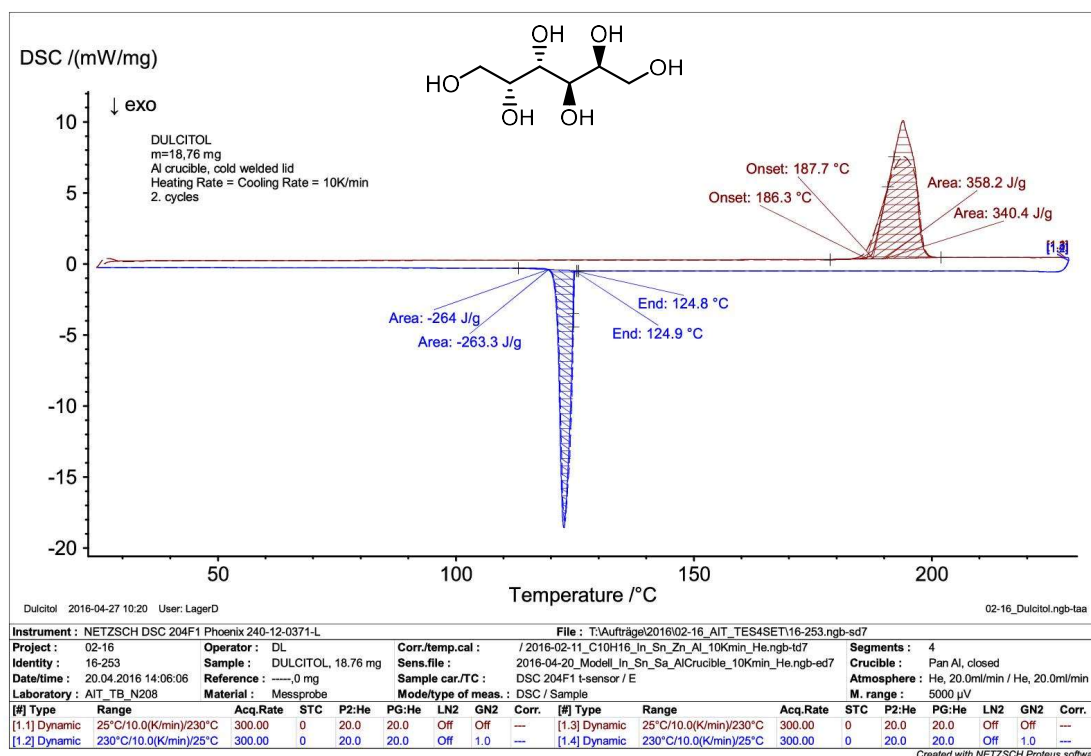
## Octadecanedioic acid



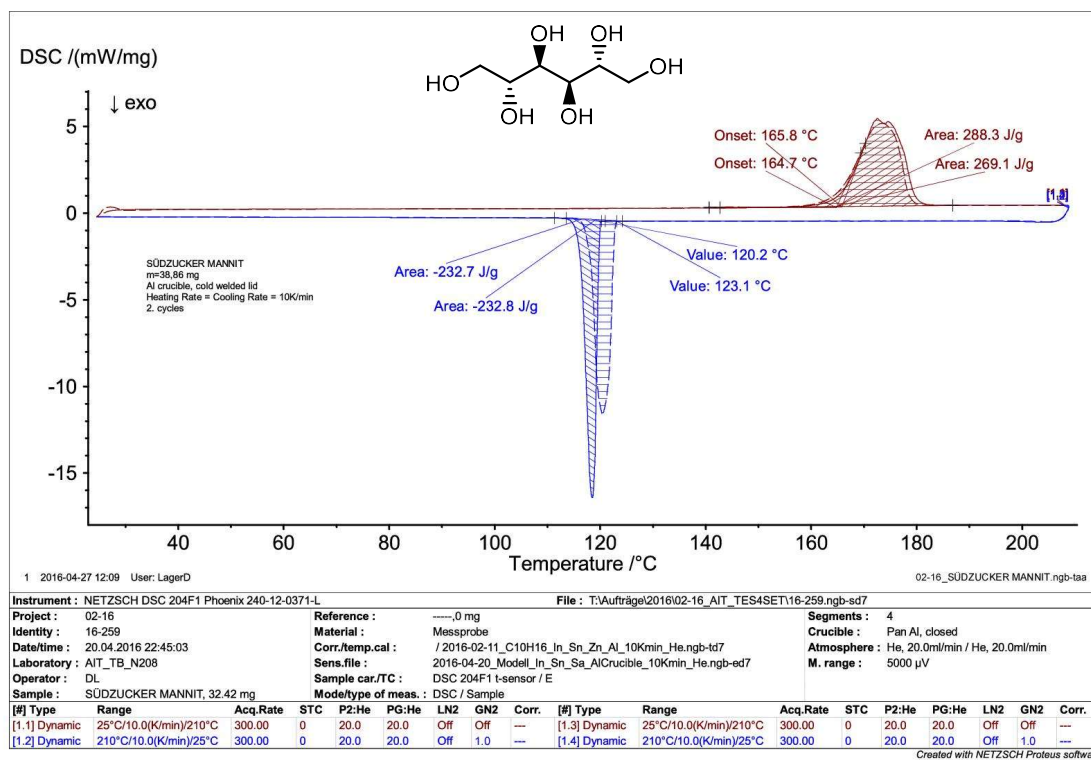
## Dipentaerythritol



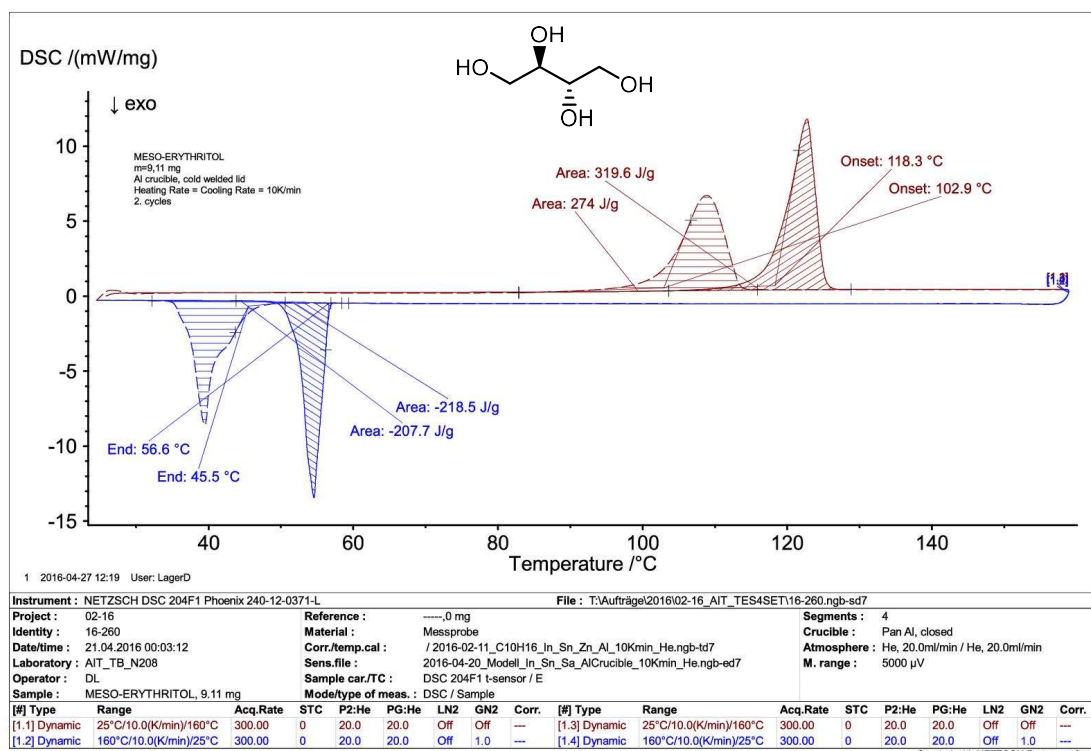
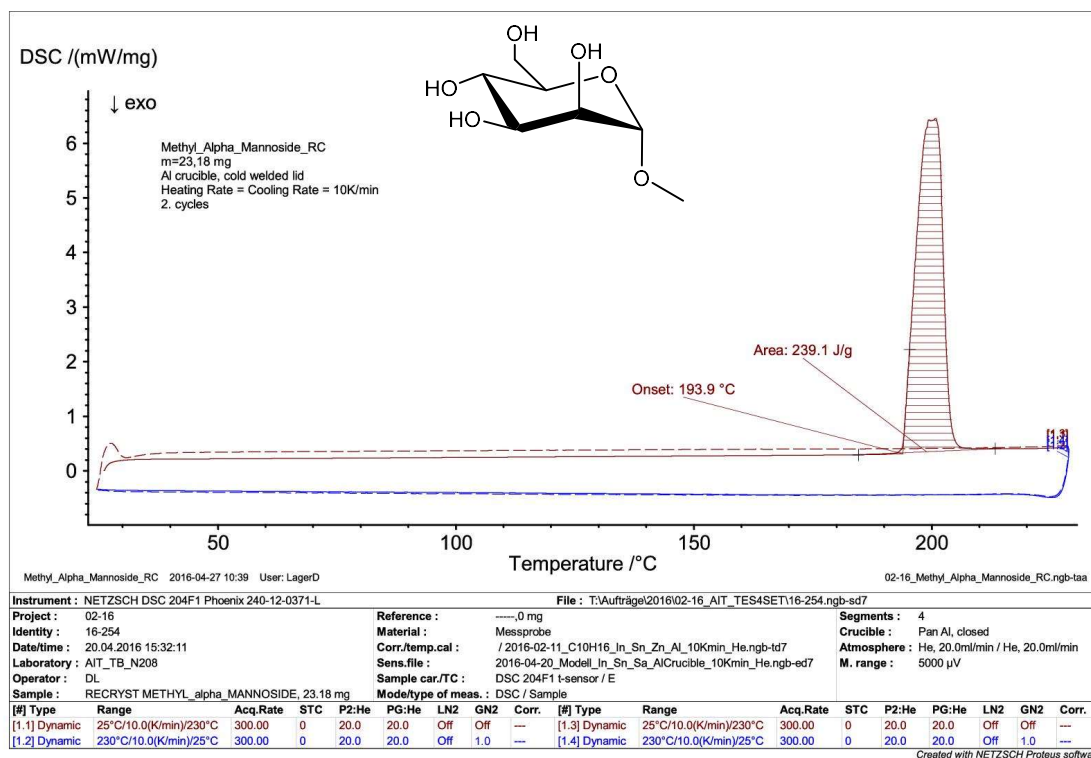
## Dulcitol



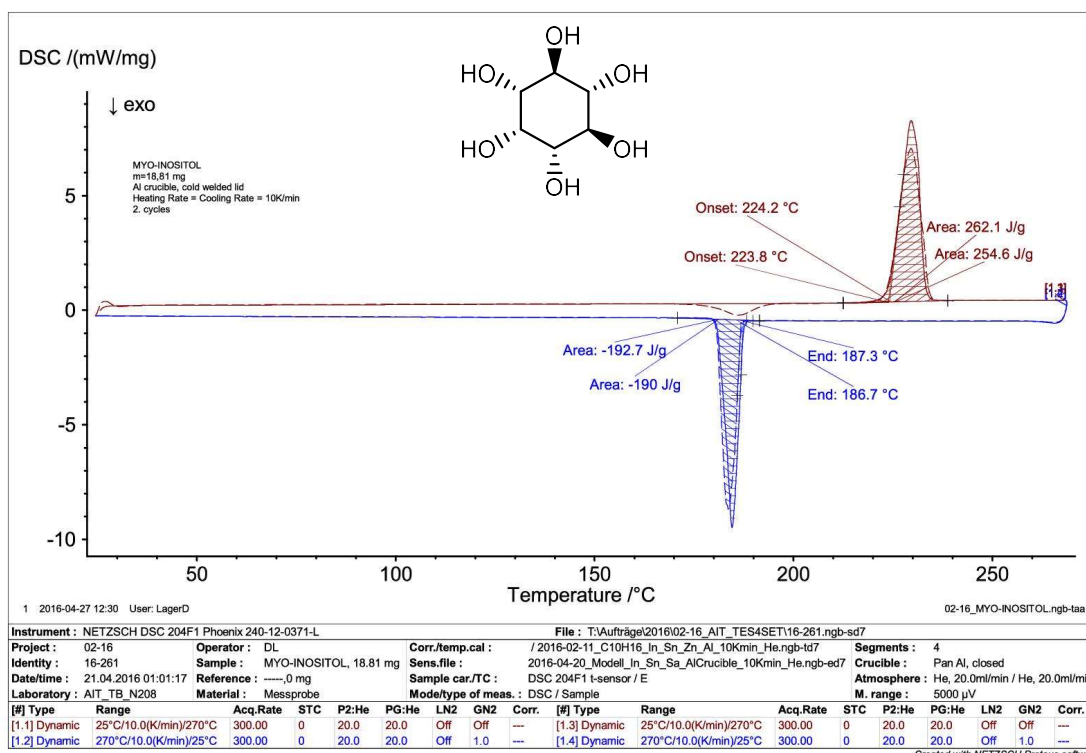
## Mannitol



## Erythritol

Methyl- $\alpha$ -mannoside

## Myo-inositol



## 5.3 References

- [1] Parameshwaran, R., S. Kalaiselvam, S. Hari Krishnan, and A. Elayaperumal. 'Sustainable Thermal Energy Storage Technologies for Buildings: A Review'. *Renewable and Sustainable Energy Reviews* 16, no. 5, pp 2394–2433, 2012.
- [2] D. Aydin, S. P. Casey and S. Riffat. 'The Latest Advancements on Thermochemical Heat Storage Systems'. *Renewable and Sustainable Energy Reviews* 41, pp 356–67, 2015.
- [3] BP, Statistical Review of World Energy (annual). Accessed 17 November 2017.
- [4] F. Trausel, A. de Jong, R. Cuypers "A Review on The Properties of Salt Hydrates for Thermochemical Storage" *Energy Procedia*, 48, pp 447-452, 2014.
- [5] A. de Jong, F. Trausel, C. Finck, L. van Vliet, R. Cuypers "Thermochemical Heat Storage – System Design Issues" *Energy Procedia*, 48, pp 309-319, 2014.
- [6] G.A. Lane "Solar Heat Storage – Latent Heat Materials", vol. I. Boca Raton, FL: CRC Press, Inc. 1983
- [7] A. Sharma, V.V. Tyagi, C.R. Chen, D. Buddhi "Review on Thermal Energy Storage with Phase Change Materials and Applications" *Renewable and Sustainable Energy reviews*, vol. 13, pp 318-45, 2009.
- [8] B. Cárdenas, N. León "High Temperature Latent Heat Thermal Energy Storage: Phase Change Materials, Design Considerations and Performance Enhancement Techniques" *Renewable and Sustainable Energy reviews*, 27, pp 724-737, 2013.
- [9] T. Nomura, N. Okinaka, T. Akiyama "Technology of Latent Heat Storage for High Temperature Application: A Review". *Journal of the Iron and Steel Institute of Japan*. 50, 1229-39, 2010.
- [10] Y. Jiang, E. Ding and G. Li "Study on Transition Characteristics of PEG/CDA Solid-Solid Phase Change Materials" *polymer*, 43, 117-22, 2002.
- [11] J.C. Su and P.S. Liu "A Novel Polymeric Solid-Solid Phase Change Heat Storage Material (PCM) with Polyurethane Block Co-Polymer Structure" *energy convers. manag.*, 47, 3185-91, 2009
- [12] Q. Cao and P. Liu "Hyperbranched Polyurethane as Novel Solid–Solid Phase Change Material for Thermal Energy Storage". *Eur. Polym. J.*, 42, 2931, 2006.
- [13] J. Hu, H. Yu, Y. Chen and M. Zhu "Study on Phase Change Characteristics of PET-PEG Copolymers" *J. macromol. Sci. Phys.*, 45, 615, 2006.
- [14] W.D. Li and E. Y. Ding "Preparation and Characterization of Coss-Linking PEG/MDI/PE Copolymer as Solid-Solid Phase Change Heat Storage Material" *Solar Energy Mater. Solar Cells*, 91. 764, 2007



- [15] L. F. Cabeza, A. Castell, C. Barreneche, A. de Gracia, A. I. Fernández "Materials Used as PCM in Thermal Energy Storage in Buildings: A Review" *Renewable and Sustainable Energy Reviews*, vol. 15, pp 1675-1695. 2011
- [16] H. Mehling, L.F. Cabeza "Heat and Cold Storage with PCM. An up to Date Introduction into Basics and Applications" Springer. 2008
- [17] H. Mehling, L.F. Cabeza "Phase Change Materials and Their Basic Properties". In: Paksoy H.Ö. (eds) Thermal Energy Storage for Sustainable Energy Consumption. NATO Science Series (Mathematics, Physics and Chemistry), vol 234. Springer, Dordrecht 2007.
- [18] S.D. Sharma and K. Sagara "Latent Heat Storage Materials and Systems: A Review" *International Journal of Green Energy*, 2:1, 1-56, 2005.
- [19] A. Abhat "Low Temperature Latent Heat Thermal Energy Storage: Heat Storage Materials" *Solar Energy*, 30, 313-32, 1981.
- [20] G.A. Lane et al. "Macro-encapsulation of PCM" *Report no. ORO/5117-8*, Midland, Michigan, Dow Chemical Company, p. 152, 1978
- [21] G.A. Lane, H.E. Rossow "Encapsulation of Heat of Fusion Storage Materials" *In: Proceedings of the second south eastern conference on application of solar energy*, p. 442-55, 1976
- [22] M. Telkes "Thermal Storage for Solar Heating and Cooling" *In: Proceedings of the workshop on solar energy storage sub-systems for heating and cooling of buildings*, University of Virginia, Charlottesville; 1975.
- [23] T. Akiyama, Y. Ashizawa, J. Yagi "Storage and Release of Heat in a Single Spherical Capsule Containing Phase Change Material with a High Melting Point" *Heat Transfer Japanese Research*, 21, p. 199-217, 1992.
- [24] A.M. Gasanealiev, B.Y. Gamataeva "Heat-Accumulating Properties of Melts" *Russian Chemical Reviews*, 69, p. 179-86, 2000.
- [25] D. Farkas, C.E. Birchenall "New Eutectic Alloys and Their Heats of Transformation" *Metallurgical and Material Transactions*, 16, p. 323-8, 1985.
- [26] J.Q. Sun, R.Y. Zhang, Z.P. Liu, G.H. Lu "Thermal Reliability Test of Al-34%Mg-6%Zn Alloy as Latent Heat Storage Material and Corrosion of Metal with Respect to Thermal Cycling" *Energy Conversion and Management*, 48, p. 619-24, 2007.

- [27] R.J. Petri, E.T. Ong "High Temperature Composite Thermal Energy Storage (TES) Systems for Industrial Applications" In: *Proceedings of the 21st intersociety energy conversion engineering conference*, 2, p. 873–80, 1986.
- [28] A. George "Hand Book of Thermal Design" In: Guyer C, editor. *Phase change thermal storage materials*. McGraw Hill Book Co., chapter 1, 1989
- [29] D. Buddhi, R. L.Sawhney "Proceedings on Thermal Energy Storage and Energy Conversion" 1994
- [30] G.A. Lane, D.N. Glew "Heat of Fusion System for Solar Energy Storage" In: *Proceedings of the workshop on solar energy storage subsystems for the heating and cooling of buildings*, Virginia, Charlothensville, p. 43– 55, 1975.
- [31] S. Herrick, D.C. Golibersuch "Quantitative Behavior of a New Latent Heat Storage Device for Solar Heating/Cooling Systems" In: *General International Solar Energy Society Conference*, 1978.
- [32] A. Solé, H. Neumann, S. Niedermaier, I. Martorell, P. Schossig, L. F. Cabeza "Stability of Sugar Alcohols as PCM for Thermal Energy Storage" *Solar Energy Materials & Solar Cells*, Vol. 126, pp. 125-134, 2014.
- [33] C. Rathgeber, L. Miró, L. F. Cabeza, S. Hiebler "Measurement of Enthalpy Curves of Phase Change Material Via DSC T-History: When Are Both Methods Needed to Estimate the Behaviour of the Bulk Material in Applications?" *Thermochimica Acta*, Vol. 596. pp. 79-88. 2014.
- [34] H. Neumann, S. Niedermaier, A. Solé, P. Schossig "Thermal Stability of D-Mannitol as Phase Change Material (PCM)" *Eurotherm Seminar*, #99.
- [35] A. Solé, H. Neumann, S. Niedermaier, L.F. Cabeza, E. Palomo "Thermal Stability Test of Sugar Alcohols as Phase Change Materials for Medium Temperature Energy Storage Application" *Energy Procedia*, Vol. 48. pp. 436-439. 2014.
- [36] S.N. Gunasekara, R. Pan, J. N. Chiu, V. Martin "Polyols as Phase Change Materials for Surplus Thermal Energy Storage" *Applied Energy*, Vol. 162. pp. 1439-1452. 2016.
- [37] G. Ferrer, A. Solé, C. Barreneche, I. Martorell, L.F. Cabeza "Review on the Methodology Used in Thermal Stability Characterization of Phase Change Materials" *Renewable and Sustainable Energy Reviews*, vol. 50, pp 665-685. 2015.
- [38] V.L. Peterson and E.S. West "The Volumetric estimation of hydroxyl groups in Sugars and other Oorganic compounds" *The Journal of biological chemistry*, vol. 74(2), pp. 379-383. 1927.
- [39] A.F. Regin, S.C. Solanki, J.S. Saini "Heat transfer characteristics of thermal energy storage system using PCM capsules: a review" *Renew Sustain EnergyRev*, 12, p. 2438 – 58, 2008.



- [40] H. Koizumi "Time and spatial heat transfer performance around an isothermally heated sphere placed in a uniform, downwardly directed flow (in relation to the enhancement of latent heat storage rate in a spherical capsule)" *Appl. Therm. Eng.*, 24, p. 2583-600, 2004.
- [41] L. Bilir and Z. Ilken "Total solidification time of a liquid phase change material enclosed in cylindrical/spherical container" *Appl Therm Eng*, 25, p. 1488–1502, 2005.
- [42] C. Arkar and S. Medved "Influence of accuracy of thermal property data of a phase change material on the result of a numerical model of a packed bed latent heat storage with spheres" *Thermochim. Acta*, 438, p. 192-201, 2005.
- [43] H. Ettouney, I. Alatiqi, M. Al-Sahali and K. Al-Hajirie "Heat transfer enhancement in energy storage in spherical capsules filled with paraffin wax and beads" *Energy Conversion and Management*, 47, p. 211–228, 2006.
- [44] S. Kalaiselvam, M. Veerappan, A.A. Aaronb and S. Iniyan "Experimental and analytical investigation of solidification and melting characteristics of PCMs inside cylindrical encapsulation" *Int. J. Therm. Sci.*, 47, p. 858-874, 2008.
- [45] M.N.A. Hawlader, M.S. Uddin and M.M. Khin "Microencapsulated PCM thermal-energy storage system" *Applied Energy*, 74, p. 195-202, 2003.
- [46] C. Liang, X. Lingling, S. Hongbo and Z. Zhibin "Microencapsulation of butyl stearate as a phase change material by interfacial polycondensation in a polyurea system" *Energy Conversion and Management*, 50, p.723-729, 2009.
- [47] J. Giro-paloma, M. Martínez, L.F. Cabeza and A.I. Fernández "Types, methods, techniques and applications for microencapsulated phase change materials (MPCM): A review" *Renawable and sustainable energy reviews*, 53, p. 1059-75, 2016.
- [48] S. Pincemin, X. Py, R. Olives, M. Christ, O. Oettinger "Elaboration of conductive thermal storage composites made of phase change materials and graphite for solar plant" *Journal of Solar Energy Engineering*, 130, p. 1-5, 2008.
- [49] K. Lafdi, O. Mesalhy and A. Elgafy "Graphite foams infiltrated with phase change materials, as alternative materials for space and terrestrial thermal energy storage applications" *Carbon*, 46, p. 159-168. 2008.
- [50] H. Yin, X. Gao, J. Ding and Z. Zhang "Experimental research on heat transfer mechanism of heat sink with composite phase change materials" *Energy Convers. Manag.*, 49, p. 1740-46, 2008.
- [51] Y. Shiina and T. Inagaki "Study on the efficiency of effective thermal conductivities on melting characteristics of latent heat storage capsules" *Int. J. Heat. Mass Trans.*, 48, p. 373-83, 2005.

- [52] A. Siahpush, J. O'Brien and J. Crepeau "Phase change heat transfer enhancement using copper porous foam" *ASME J. Heat Transf.*, 130, art. no. 082301, 2008.
- [53] Y. Zhang, J. Ding, X. Wang, R. Yang and K. Lin "Influence of additives on thermal conductivity of shape-stabilized phase change material" *Solar Energy Mater. Solar Cells*, 90, p. 1692-702, 2006.
- [54] P.D. Dalton, D. Grafahrend, K. Klinkhammer, D. Klee and M. Möller "Electrospinning of polymer melts: Phenomenological observations" *Polymer*, 48, p. 6823-33, 2007.
- [55] T. Steiner "The Hydrogen Bond in the Solid State" *Angew. Chem. Int. Ed.*, 41, p. 48–76, 2002.
- [56] J. Emsley "Very Strong Hydrogen Bonds" *Chemical Society Reviews*, 9 (1), p. 91–124. 1980.
- [57] J.W. Larson and T.B. McMahon "Gas-phase bihalide and pseudobihalide ions. An ion cyclotron resonance determination of hydrogen bond energies in XHY- species (X, Y = F, Cl, Br, CN)" *Inorganic Chemistry*, 23 (14), p. 2029–2033, 1984.
- [58] A.C. Legon and D.J. Millen "Angular geometries and other properties of hydrogen-bonded dimers: a simple electrostatic interpretation of the success of the electron-pair model" *Chemical Society Reviews*, 16, p. 467-98. 1987.
- [59] Chemical Bonding Ms Shethi and M. Satake
- [60] G.S. Tschumper "Reliable electronic structure computations for weak noncovalent interactions in clusters" *Reviews in Computational Chemistry. John Wiley & Sons*, p. 39–90, 2008.
- [61] D.A. Skoog, F.J. Holler and T.A. Nieman "Principles of instrumental analysis" p. 805–808, 1998.
- [62] A.W. Coats and J.P. Redfern "Thermogravimetric analysis: a review" *Analyst*, 88 (1053), p. 906–924, 1963.
- [63] X. Liu and W. Yu "Evaluating the thermal stability of high performance fibers by TGA". *Journal of Applied Polymer Science*, 99, p. 937–944, 2006.
- [64] Z. Tao, J. Jin, S. Yang, D. Hu, G. Li and J. Jiang "Synthesis and characterization of fluorinated PBO with high thermal stability and low dielectric constant" *Journal of Macromolecular Science, Part B*, 48:6, p. 1114-1124, 2009.
- [65] T. Inagaki and T. Ishida "Computational design of non-natural sugar alcohols to increase thermal storage density: beyond existing organic phase change materials" *J. Am. Chem. Soc.*, 138 (36), p. 11810–11819, 2016

- [66] C. Stanetty and I.R. Baxendale "Large-scale synthesis of crystalline 1,2,3,4,6,7-hexa-O-acetyl-L-glycero- $\alpha$ -D-manno-heptopyranose" *European Journal of Organic Chemistry*, 12, p. 2718-26, 2015.
- [67] Z. Hricovíniová "Rapid, one pot preparation of d-mannose and d-mannitol from starch: the effect of microwave irradiation and MoVI catalyst" *Tetrahedron: Asymmetry*, 22, p. 1184-1188, 2011.
- [68] K. Kraehenbuehl, S. Picasso and P. Vogel "Synthesis of C-Linked Imino Disaccharides (= Aza-C-disaccharides) with a Pyrrolidine-3,4-diol Moiety Attached at C(3) of Galactose via a Hydroxymethylene Linker and of a 7-(1,2,3-Trihydroxypropyl)-octahydroxyindolizine-1,2,6,8-tetrol" *Helvetica Chimica Acta*, 81, p. 1439-1479, 1998.
- [69] T. Prange, M.S. Rodriguez and E. Suarez . "Synthesis of phytuberin. 4-endo-tet acid-catalyzed cyclization of  $\alpha$ -hydroxy epoxides" *J. Org. Chem.*, 68 (11), p. 4422-4431, 2003.
- [70] D.E. Kiely, L. Chen and T. Lin "Synthetic polyhydroxypolyamides from galactaric, xylaric, D-glucaric, and D-mannaric acids and alkylenediamine monomers—some comparisons" *Journal of Polymer Science: Part A: Polymer Chemistry*, 38, p. 594-603, 2000.
- [71] E. Badea, G. Della Gatta, D. D'Angelo, B. Brunetti and Z. Recková "Odd-even effect in melting properties of 12 alkane- $\alpha,\omega$ -diamides" *J. Chem. Thermodynamics*, 38, p. 1546-1552, 2006.
- [72] A.R. Katritzky, B. Pilarski, L. Urogi "Efficient Conversion of Nitriles to Amides with Basic Hydrogen Peroxide in Dimethyl Sulfoxide" *Synthesis*, p. 949-951, 1989
- [73] C. Freudenreich, J. Samama, J. Biellmann "Design of inhibitors from the three-Dimensional Structure of Alcohol Dehydrogenase. Chemical Synthesis and Enzymatic Properties" *J. Am. Chem. Soc.*, 106, p. 3344-3353, 1984.
- [74] G.F. D'Alelio and E.E. Reid "Preparation of amides" United States Patent Office, 2109941, patented 5th June 1936.
- [75] M.S. Abaee, E. Akbarzadeh, R. Sharifi et al. "Environmentally friendly transesterification and transacylation reactions under LiBr catalysis" *Monatsh Chem*, 141, p. 757-61, 2010.
- [76] B. Larisch, M. Pischetsrieder and T. Severin "Reactions of Dehydroascorbic Acid with Primary Aliphatic Amines Including N $\alpha$ -Acetyllysine" *J. Agric. Food Chem.*, 44 (7), p. 1630-34, 1996
- [77] L.M. Rice, C.H. Grogan and E.E. Reid "N,N'-Dialkyloxamides" *J. Am. Chem. Soc.*, 75, p. 242-43, 1953
- [78] W. Acree Jr., J.S. Chickos "Phase Transition Enthalpy Measurements of Organic and Organometallic Compounds. Sublimation, Vaporization and Fusion Enthalpies From 1880 to 2010"

- [79] H. Maeda, S. Furuyoshi, Y. Nakatsuji and M. Okahara "Synthesis of N-Unsubstituted Di- and Triaza Crown Ethers" *Bull. Chem. Soc. Jpn.*, 56, p. 3073-77, 1983.
- [80] J.M. Wilson, F. Giordani, L.J. Farrugia, M.P. Barrett, D.J. Robinsa and A. Sutherland "Synthesis, characterisation and anti-protozoal activity of carbamate-derived polyazamacrocycles" *Org. Biomol. Chem.*, 5, p. 3651-56, 2007.
- [81] S. Aime, M. Botta, L. Frullano, S. Geninatti Crich, G.B. Giovenzana, R. Pagliarin, G. Palmisano, M. Sisti "Contrast Agents for Magnetic Resonance Imaging: A Novel Route to Enhanced Relaxivities Based on the Interaction of Gd<sup>III</sup> Chelate with Poly- $\beta$ -cyclodextrins" *Chem. Eur. J.*, 5, No 4, p. 1253-60, 1999.
- [82] F. Cardullo, D. Donati, G. Merlo, A. Paio, M. Salaris, M. Taddei "Deprotection of o-Nitrobenzensulfonyl (Nosyl) Derivatives of Amines Mediated by a Solid-Supported Thiol" *Synlett*, No. 19, p. 2996-98, 2005.
- [83] M.S. Chao, H.H. Lu, M.L. Tsai, S.L. Huang and T.H. Hsieh "Reversible switching of coordination modes of nickel (II) complexes using a hemilabile 4,7-diazadecanediamide ligand" *Inorganica Chimica Acta*, 362(10), p. 3835-39, 2009.
- [84] C. Chen "Catalysis by exchange resins. Improved cyanoethylation and carbamoylethylation of diols" *Journal of Organic Chemistry*, 27, p. 1920-1, 1962.
- [85] G. Chaput and G. Jeminet "Constantes d'association de quelques éthers de polyethylene glycols avec Na<sup>+</sup>, K<sup>+</sup>, Cs<sup>+</sup> et Tl<sup>+</sup>" *Can. J. Chem.*, 53, p. 2240-9, 1975 .
- [86] H.A. Bruson "Esters of poly- $\beta$ -carboxyalkyl ethers of polyhydric Alcohols" United States Patent Office, 2372808, patented 30<sup>th</sup> July 1941.
- [87] H. A. Bruson "Aliphatic Polyether Polyamides" United States Patent Office, 2359708, patented 3rd October 1944.
- [88] H. Veisi, B. Maleki, M. Hameliana and S.S. Ashrafi "Chemoselective hydration of nitriles to amides using hydrated ionic liquid (IL) tetrabutylammonium hydroxide (TBAH) as a green catalyst" *RSC Adv.*, 5, p. 6365-71, 2015.
- [89] F. Brustolin, M. Surin, V. Lemaure, G. Romanazzi, Q. Sun, J. Cornil, R. Lazzaroni, N. Sommerdijk, P. Leclère and E. Meijer "The Self-Assembly of Amphiphilic Oligothiophenes: Hydrogen Bonding and Poly(glutamate) Complexation" *Bull. Chem. Soc. Jpn.*, 80, No. 9, 1703-15, 2007.
- [90] S. Hussain, S.K. Bharadwaj, M. Chaudhuri and H. Kalita "Borax as an efficient metal-free catalyst for hetero-Michael reactions in an aqueous medium" *Eur. J. Org. Chem.*, p. 374-378, 2007.

- [91] A. Sonousi and D. Crich "Selective Protection of Secondary Amines as the N-Phenyltriazenes. Application to Aminoglycoside Antibiotics" *Org. Lett.*, 17 (16), p. 4006–9, 2015.
- [92] M. Ramanathan and S.T. Liu "Preparation of Quinazolines via a 2+2+2 Annulation from Aryldiazonium Salts and Nitriles" *J. Org. Chem.*, 82 (15), p. 8290–5, 2017.
- [93] T.E. Pou, S. Fouquay "Polymethylenepolyamine dipropionamides as environmentally safe inhibitors of the carbon corrosion of iron" United States Patent Office, 6365100, patented 2<sup>nd</sup> April 2002.
- [94] R. Neelapapu and P.A. Petukhov "A one-pot selective synthesis of N-Boc protected secondary amines: tandem direct reductive amination/N-Boc protection" *Tetrahedron*, 68, p. 7056-62, 2012.
- [95] J. Weisell, M.T. Hyvönen, J. Vepsäläinen, L. Alhonen, T.A. Keinänen, A.R. Khomutov and P. Soininen "Novel isosteric charge-deficient spermine analogue--1,12-diamino-3,6,9-triazadodecane: synthesis, pK(a) measurement and biological activity." *Amino Acids*, 38, p. 501-7, 2010.
- [96] S. Kahwaji, M.B. Johnson, A.C. Kheirabadi, D. Groulx and M.A. White "Fatty acids and related phase change materials for reliable thermal energy storage at moderate temperatures" *Solar Energy Materials and Solar Cells*, 167, P. 109-20, 2017.
- [97] V.R. Thalladi, M. Nusse, R. Boese, "The Melting Point Alternation in  $\alpha,\omega$ -Alkanedicarboxylic Acids" *J. Am. Chem. Soc.*, 122, p. 9227–9236, 2000.
- [98] J. Bernstein, R.E. Davis, L. Shimoni, L.N. Chang, "Patterns in Hydrogen Bonding: Functionality and Graph Set Analysis in Crystals" *Angew. Chem. Int. Engl.*, 34, p. 1555–1573, 1995.
- [99] R. Boese, H.C. Weiss, D. Bläser, "The Melting Point Alternation in the Short-Chain n-Alkanes: Single-Crystal X-Ray Analyses of Propane at 30 K and of n-Butane to n-Nonane at 90 K" *Angew. Chem. Int.*, 38/7, p. 988–992, 1999.
- [100] E.L.Charsley, P.G. Laye, H.M. Markham, "The use of organic calibration standards in the enthalpy calibration of differential scanning calorimeters" *Thermochimica Acta*, 539, p. 115-117, 2012.
- [101] T.W. Green, P.G.M. Wuts, "Protective Groups in Organic Synthesis", *Wiley-Interscience*, 150-160, 712-715, 1999.
- [102] V.L. Peterson, E.S. West, "The volumetric estimation of hydroxyl groups in sugars and other organic compounds", *The Journal of biological chemistry*, 74(2), p. 3358-3359, 1927.
- [103] S. Amslinger, A. Hirsch, F. Hampel, "Synthesis of a biotinated amphiphile", *Tetrahedron*, Volume 60, Issue 50, P. 11565-11569, 2004

- [104] X. Li, D. Wu, T. Lu, G. Yi, H. Su, Y. Zhang, "Highly Efficient Chemical Process To Convert Mucic Acid into Adipic Acid and DFT Studies of the Mechanism of the Rhenium-Catalyzed Deoxydehydration" *Angew. Chem. Int.*, 53, p. 4200–4204, 2014
- [105] A. Palmelund, R. Madsen, "Chain Elongation of Aldoses by Indium-Mediated Coupling with 3-Bromopropenyl Esters", *J. Org. Chem.*, 70 (20), p. 8248–8251, 2005.
- [106] M. Lombardo, R. Girotti, S. Morganti, C. Trombini, "A New Protocol for the Acetoxyallylation of Aldehydes Mediated by Indium in THF", *Org. Lett.*, 3 (19), p. 2981–2983, 2001
- [107] N.K. Nkosana, D.J. Czyzyk, Z.S. Zarek, J.M. Cote, E.A. Taylor "Synthesis, kinetics and inhibition of *Escherichia coli* Heptosyltransferase I by monosaccharide analogues of Lipid A", *Bioorganic & Medicinal chemistry letters*, 28 (4), p. 594–600, 2018
- [108] J.C. Irvine, *Chemistry & Industry (London, United Kingdom)* 1928, V47, P494-5 CAPLUS
- [109] S.Y. Ko, A.W. Lee, S. Masamune, L.A. Reed III, K.B. Sharpless, F.J. Walker; *Tetrahedron*, vol. 46 (1), p. 245 - 264, 1990
- [110] K. Weinges, H. Schick, G. Schilling, H. Irngartinger, T. Oeser; *European Journal of Organic Chemistry*, 1, p. 189 – 192, 1998
- [111] Kopf, Morf, Zimmer, Bischoff, Koll; *Carbohydrate Research*, vol. 229 (1), p. 17 – 32, 1992
- [112] B. Kang, Y. Wang, S. Kuwano, Y. Yamaoka, K. Takasu, K. Yamada, *Chemical Communications*, vol. 53 (32), p. 4469 – 4472, 2017
- [113] A. Kamal, M.A. Khan, K.S. Reddy, K. Srikanth, *Tetrahedron Letters*, vol. 48 (22), p. 3813 – 3818 2007
- [114] J. Liang, M. Sun - EP1559703, 2005, A1

# YAGO MAGAN MONTOTO



**Burggasse 102/6, 1070 Vienna (Austria)**



**[yagomagan@hotmail.es](mailto:yagomagan@hotmail.es)**



**0043 680 143 3374**



**22.04.85 in A Coruña (Spain)**



## PROFESSIONAL EXPERIENCE

**1) January 2019 – Present**

**Researcher**

Kao corporation, Darmstadt (Germany)

**Mission -**

**Tasks:**

-

**2) October 2014 – July 2018**

**Project Research Assistant**

TU Wien, Vienna (Austria)

**Mission -** Search of suitable compounds for phase change material applications

**Tasks:**

- Lab machines/techniques such as: Chromatography columns (MPLC), Recrystallization, GC-MS, NMR.
- Data acquisition, interpretation and compound design.
- Thermal analysis of promising materials, using techniques such as differential scanning calorimetry (DSC) and thermogravimetric analysis (TG).
- Synthesis of new materials in collaboration with Südzucker and AIT.

**3) April 2014 – September 2014**

**Research Assistant**

Ludwig Boltzmann Institute, Vienna (Austria)

**Mission -** Macromolecular analysis of different types of Silk among others

**Tasks:**

- Lab machines/techniques such as: FPLC, SDS-PAGE Electrophoresis, Electron-spin resonance, dialysis.
- Automation sample collection.

- Preparing solvents and solution for FPLC.
- Search and deal with sample suppliers.

**4) February 2013 – October 2013**  
Jugendzentrum Atoll, Amstetten (Austria)





## EVS Social Worker

**Mission** – Advise and support young visitors of an Austrian youth center.

**Tasks:**

- Organizing, coordinate and manage events. Leading groups. Technical support and assistance.
- 

## EDUCATION

- **2014 - 2019**  **PhD in Organic Chemistry**  
"Sugar alcohols and other organic compounds as phase change materials" - Development of materials for thermal energy storage in cooperation with AIT (Austrian institute of Technology) and Südzucker TU Wien – Vienna, Austria
- **2010 - 2012**  **Degree in Chemistry "Licenciatura en Químicas"**  
University of Coruña – Galicia, Spain
- **2009 - 2010**  **Master Thesis in Organic Chemistry**  
"Glycosylation of phenolic compounds promoted by HMCM-22 zeolite catalyst" - Carbohydrate chemistry synthesis  
University of Lisbon – Lisbon, Portugal
- **2003 - 2009**  **Degree in Chemistry**  
University of Coruña – Galicia, Spain

## SKILLS

### COMPUTER

- Microsoft Office Word  
■ ■ ■ ■ □
- Microsoft Office Excel  
■ ■ ■ □ □
- Microsoft Office PowerPoint  
■ ■ ■ ■ □
- Adobe Photoshop CS3  
■ ■ ■ □ □
- OTHER**
- Adobe Lightroom  
■ ■ ■ ■ □
- Chemdraw  
■ ■ ■ □ □

### LANGUAGES

